FLUIDIZED BED UTILIZATION OF SOUTH AUSTRALIAN COALS

Anna Elisabeth Wildegger-Gaissmaier

Department of Chemical Engineering

University of Adelaide

Submitted for the degree of PhD on 30. September 1988

Table of Contents

ABSTRACT

South Australia has large reserves of low rank coal. These coals contain an appreciable amount of water in their 'as-mined' state. Fluidized bed combustion or gasification is an economic and environmentally acceptable way to utilize low rank coals. The main advantages of fluidized bed technology are high heat transfer coefficients, low SO_2 and NO_x emissions and independence of feed stock.

Most previous research has focused on the conversion of dry coal and char. However low rank coals contain an appreciable amount of volatiles and water in their 'as-mined' state. Complete water removal prior to combustion or gasification is not economical. The volatiles of the low rank coals can contribute for more than 50% of the energy released during combustion. Experimental data reported on devolatilization under pyrolysis and combustion conditions of wet coal are limited.

For the design of a fluidized bed combustor/gasifier, it is important to understand the interactive processes which occur during combustion/gasification of wet coals. The processes include drying, devolatilization, combustion of volatile matter in the gas phase followed by combustion of char. This thesis reports the results of an experimental as well as modelling investigation aimed at an improved understanding of these interactive processes.

The experimental investigation includes overall weight loss experiments for drying, coupled drying and devolatilization under pyrolysis conditions and coupled drying and devolatilization under combustion conditions for single particles. The shrinkage of particles during drying has been established. The evolution of volatiles species during the pyrolysis of wet and dry Bowmans coal particles has also been investigated. A novel experimental set-up has been developed which allows accurate measurement of the time

dependent histories for drying and devolatilization under pyrolysis as well as under combustion conditions. A wide range of experiments using different particle diameters, temperature and initial moisture contents have been carried out.

A model for the drying and devolatilization of a single coal particle has been developed. The model includes shrinkage of the particle. The interactive influence of volatile combustion on drying has also been investigated. The model assumes heat transfer to and through the coal particle and chemical reaction as rate limiting steps for coupled drying and devolatilization. A shrinking core model describing the drying and a moving particle radius due to shrinkage has been included in the overall concept. In a separate modelling approach volatile combustion has been related for the first time with fluidized bed design parameters. The flame temperature was estimated using a modified Shwab-Zeldovic approach to the fuel droplet combustion problem. Comparisons of experimental data obtained using the experimental system mentioned above and data obtained from literature are seen to be in good agreement with the model predictions.

STATEMENT

This thesis contains no material which has been accepted for the award of any other degree or diploma in any University and the thesis contains no material previously published or written by another person, except where due reference is made in the text of the thesis.

The author consents to the thesis being made available for photocopying and loan if applicable if accepted for the award of the degree.

ACKNOWLEDGMENTS

I wish to thank the following organizations and individuals for their contribution during the course of this project:

- The University of Adelaide for the financial assistance of a Postgraduate Research Award.
- The Department of Chemical Engineering University of Adelaide, special research grants University of Adelaide and University C.S.I.R.O. grants for the financial support of the project.
- Dr. P.K. Agarwal for his help and guidance during the course of this investigation.
- Mr. P. Wallis, Mr. V. Rendall and Mr. C. Tipper for the help in the construction of the experimental set-up.
- Mr. A. da Silva and Mr. A. Marshall for volatile species analysis on the gas chromatograph.
- Mr. R. Weimann for the assistance in the drying and devolatilization experiments.
- My husband Rudi for his support.

LIST OF TABLES

LIST OF FIGURES

1 INTRODUCTION

96% of the energy consumed in Australia (Department of Energy and Mining, 1982) is obtained from three sources, oil, coal and natural gas. However, there is a mismatch between reserves and demands for the forms of energy. As can be seen in Figure 1.1, 95% of the non-renewable energy sources in Australia are composed of coal whereas crude oil represents only 1%. On the other hand, 45% of the energy consumed is in the form of oil and only 40% in the form of coal.

Since the oil crisis in the early seventies, coal as an abundant alternative fuel source has become the focus of new research and development efforts. Coal is expected to bridge the gap between the receding supplies of oil and the emergence of future energy technologies such as nuclear fusion and solar (photovoltaic) energy. With improved conversion technologies like fluidized bed combustion and gasification, a high efficiency as well as pollution control and operational reliability can be obtained. Despite the intensive research efforts in this area there are several fundamental aspects which are not well understood.

1.1 COAL

Coal is formed from the accumulation and decomposition of plant substances which originated in vast primeval swamps. Thick beds of concentrated organic matter called peat were formed by partial decay of trees and plants. The organic matter was buried before it was completely oxidized to carbon dioxide by micro-organisms. The plant material underwent drastic physical and chemical changes through the attack of

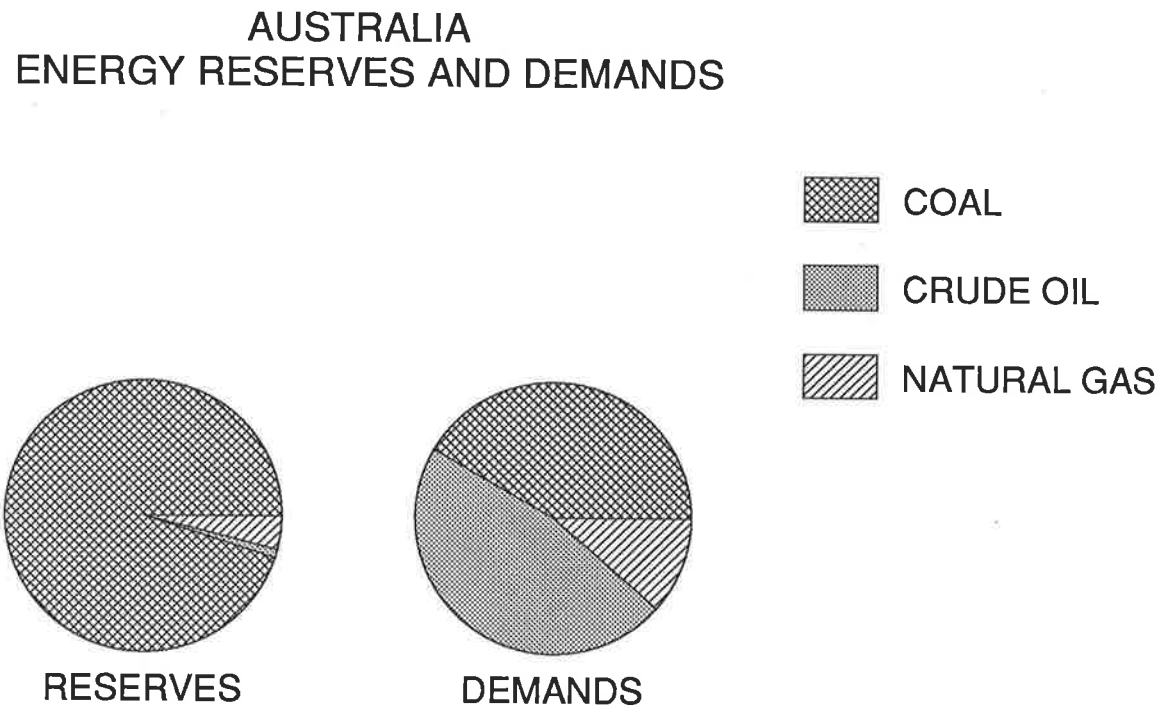

Fig. 1.1 Australia energy reserves and demands

bacteria and fungi as well as through increasing temperature and pressure, as peat became buried under layers of younger sediments. During the coalification process the chemical and physical properties of coal change considerably. Coal varies widely in composition from source to source which is due to the complexity of the source materials, geological circumstances, climatic conditions and the degree of coalification. Strong heterogeneity can be observed even within a given coal seam (Damberger et al., 1984).

Coal research has gone on for more than a hundred year (van Krevelen, 1982) and various attempts have been made to classify coals (Ergun, 1979). One of the most widely used classification systems has been developed by the ASTM (American Society of Testing Materials). It is based on amounts of fixed carbon, volatile matter, heat value and agglomerating character. As can be seen from Table 1.1 fixed carbon and heating value increase with coal rank, whereas volatile matter decreases with increase in rank.

The recoverable coal reserves in South Australia, in view of current mining technology, are all low-rank (sub-bituminous and lignite) coals. Bowmans coal deposit is the largest known tertiary deposit in South Australia (Department of Energy and Mining, 1984) containing 1.25 million tonnes of lignite. The depth of the seams are between 55 and 100 m below the surface and the individual seam thickness ranges from 0.5 to 15 m, which makes the deposit attractive for open cut mining. However the high sulphur, chlorine and sodium content could cause problems if burned in conventional power stations. Fluidized bed technology seems to be an economic and environmentally acceptable way to utilize this coal.

Table 1.1 ASTM CLASSIFICATION OF COALS BY RANK

Class & Group	Fixed Carbon (DAF Basis)	Volatile Matter (DAF Basis)	Heating Value (DAF Basis)	
	%	%	MJ/kg	
Lignite				
- B			< 14.6	
- A			14.6 - 19.3	
Sub-bituminous				
- C			19.3 - 22.1	
- B			22.1 - 24.4	
- A			24.4 - 26.7	*
Bituminous				
- High volatile C			24.4 - 26.7	**
- High volatile B			26.7 - 30.2	***
- High volatile A	< 69	> 31	30.2 - 32.5	***
- Med. volatile	69 - 78	22 - 31	32.5	
- Low volatile	78 - 86	14 - 22		
Anthracite				
- Semi-anthracite	86 - 92	8 - 14		*
- Anthracite				
- Meta-anthracite				

* non-agglomerating ** agglomerating *** commonly agglomerating

1.2 COAL CONVERSION IN FLUIDIZED BEDS

For obtaining energy out of coal several techniques can be applied:

- combustion
- pyrolysis
- gasification
- liquefaction

The major methods of coal combustion have been fixed bed firing, where mechanical strokers are used and suspension firing using pulverized coal.

In recent years, fluidized bed combustion and gasification are receiving increased attention. Fluidized bed technology offers several advantages over conventional techniques:

a) Heat transfer coefficients in a fluidized bed can be up to 5 times greater than the heat transfer to a conventional tube bank. The high transfer coefficients allow a more compact design (Corey, 1978; Essenhigh, 1979). Due to rapid and complete mixing of the solids in the bed, a uniform temperature can be achieved in a fluidized bed, which in turn minimizes temperature control problems. Furthermore, an operation efficiency (overall efficiency of a power station) of about 40% can be achieved using a pressurised Fluidized Bed Combustor (PFBC) or a combined cycle atmospheric FBC power generator (Young et al., 1987). The efficiency of a conventional pulverized coal combustor is about 37%.

b) The emissions of SO_2 and NO_x can be lowered. By using a chemically active sulphur sorbent (limestone or dolomite) as bed material, sulphur dioxide (Chen and Saxena, 1977) is absorbed 'in-situ' without the need of expensive additional scrubbing equipment. NO_x emissions (Cowley and Roberts, 1981) are significantly lower at operating temperatures typical of a FBC. Lower operating temperatures also minimize ash fusion and problems related to agglomeration.

c) A fluidized bed combustor (FBC) is essentially independent of coal ash characteristics. That means FBC technology is largely independent of feedstocks (Damberger et al., 1984). A variety of low-rank fuels such as low-rank coal, peat, crop residue and municipal solid waste can be burnt or gasified.

1.3 STATEMENT OF THE PROBLEM

Australia has large reserves of low-rank coal, the estimated deposits exceed 68,800 million tonnes (A.I.E., 1983). These coals contain a considerable amount of moisture, volatile matter, sulphur, sodium and minerals. South Australian lignite, for example, contains up to 60% moisture in its 'as-mined' state. Complete moisture removal prior to coal conversion is not economical. The volatiles in the low-rank coals contribute more than 50% of the energy released during combustion. It is, then, important to understand the interactive processes which take place during the conversion of wet coal. However, most research efforts have been focussed on the conversion of pre-dried coal. Very few attempts have been made to study the fundamental

phenomena of drying, shrinkage, devolatilization, combustion of volatiles and combustion of residual char of 'as-mined' low-rank coals in FBC (Potter and Keogh, 1981; Agarwal, 1984).

In this study, a detailed experimental and theoretical approach has been undertaken to understand some of the phenomena which occur during pyrolysis and combustion of wet coal. The following phenomena have been studied:

- drying with shrinkage for single coal particles in a convective environment;
- coupled drying and devolatilization under pyrolysis conditions for single coal particles in a convective environment;
- coupled drying and devolatilization under combustion conditions for single coal particles in a convective environment;
- volatile combustion of dry coal in fluidized beds.

Chapter 2 summarizes the results of previous investigations relevant to this study.

The experimental set-up and the experimental methods are described in Chapter 3.

The mathematical models developed to analyse the relevant phenomena are described in Chapter 4. The results of parametric studies are discussed.

Chapter 5 discusses the experimental results in comparison with the prediction of the models. Model results are also compared with the experimental data reported in the literature.

Chapter 6 outlines the conclusions drawn of the present study and makes recommendations for further investigations.

The computer programs and raw data are included as Appendices.

2 LITERATURE SURVEY

2.1 DRYING

Drying is an important unit operation in the process industry. Considerable research on drying has been done over the years, however drying is still not well understood. In several literature reviews (Keey, 1980; van Brakel, 1980), the existence of large discrepancies between science and application have been pointed out.

In general, drying problems have been solved mathematically using differential equations for heat and mass transfer with phase change on a moving boundary. Several reviews (Wilson et al., 1978; Ockendon et al., 1975; Fasano and Primicerio, 1983; Rubinstein, 1967) deal with the analytical and numerical techniques available to solve moving boundary problems.

The following mechanisms for the drying of capillary porous bodies have been reported in literature (Fortes and Okos, 1980; Peck and Wasan, 1974):

- liquid diffusion due to differences in moisture concentrations;
- vapour diffusions in partly air filled pores due to partial pressure gradients;
- liquid movement due to capillary forces;
- liquid or vapour movement due to differences in total pressure, originated by shrinkage or high temperature inside the moist material;
- surface diffusion;
- liquid movement due to gravity.

Mathematical models are based on mass, energy and momentum transport equations for the solid, liquid and vapour phases. The physical properties of the phases in the bulk material can change with varying temperatures and concentrations. Therefore, appropriate boundary conditions for the different physical situations must be applied (Whitaker, 1980). However, most of the models proposed are limited to specific conditions. Previous models are summarized in Table 2.1.

As already pointed out physical properties and transport coefficients are dependent on temperature and concentration within the bulk of the drying medium. Linear variation of properties (Whitaker, 1977; Kansa, 1982) and power variation of the diffusion coefficient (Ashworth, 1977) have been considered. Schoeber and Thijssen (1977) proposed a short-cut method for the calculation of drying rates for slabs with concentration-dependent diffusion coefficient. The method was based on the numerical solution of the diffusion equation for a slab. The main application was for materials in which the diffusion coefficient decreases strongly with decreasing concentration below the critical concentration.

Fluidized bed drying (Perry et al., 1984; Kunii and Levenspiel,1969) is an economic way for drying large tonnages of solids. Particularly solids like coal, cement, rock and limestone are dried in fluidized beds. The effect of fluidization has to be incorporated in the drying model by defining suitable boundary conditions and using the appropriate heat and mass transfer coefficients at the external surface of the drying specimen. However, unusual temperature changes not found in classical convective drying have been reported for materials with large porosities (Sugiyama et al., 1974) during drying in fluidized beds.

Table 2.1 SUMMARY OF REPORTED THEORETICAL INVESTIGATIONS ON DRYING

Ref.	Model	Comments
Luikov and Mikhailov, 1961	- slow diffusive transport of moisture in pores and capillaries	
Kumar and Narang, 1965	- slow diffusive transport of moisture in pores and capillaries; - moisture migration at constant velocity	
Krisher, 1963	- capillary and diffusional moisture transfer (two coefficients relating moisture movements to the diffusional and capillary driving forces)	- coefficients dependent on material, temperature and pore structure;
Berger and Pei, 1973	- coupled capillary flow of liquids and vapour diffusion including heat transfer and Clausius-Clapeyron relation	- theoretical approach - no experimental verification
Mikaheilov, 1975	- moving evaporation front in a porous half space; - solutions for temperature and moisture distribution - two drying stages: period of decreasing rate and intensive drying in the presence of molar transfer	- compares well with experimental data, however, parameters have to be evaluated by experiments
Peck et al. 1977	- diffusional mass transfer, heat transfer and capillarity; - permeability equation as a function of water concentration developed	- experimental information required for pore distribution of solid - numerical solution
Whitaker, 1980; 1977	- mass, momentum and energy conservation equations for the gas, liquid and solid phase	- transport coefficients estimated theoretically;

Keey (1977) discussed the use of a so called 'characteristic' drying curve as process design tool in determining local drying rates in fluidized bed dryers.

Several experimental studies have been undertaken in fluidized bed drying. Vanecek et al. (1970) tested 21 different mainly inorganic materials, in 12 different continuous fluidized bed dryers. Ziesing et al. (1979), using existing vendor equipment including batch and continuous fluidized bed dryers, obtained drying data for Rosebud seam semi-bituminous coal.

There are major differences between drying as processing step prior to combustion and drying in a FBC. Operating temperatures in a FBC are much higher than in a fluidized bed dryer. Therefore it could be expected that drying, devolatilization and combustion take place simultaneously. The interaction of these processes can well influence the drying rates. Also, the amount of coal in a FBC is only about 1-2% of the total bed material in comparison with a fluidized bed dryer where the entire bed material would be the coal itself.

2.1.1 Drying of Coal

Low-rank coals contain a considerable amount of moisture in their 'as-mined' state. Moisture in coal can be bounded chemically and physically. Experimental results obtained by Stewart and Evans (1967) with Yallourn brown coal show that different types of water can be associated with brown coal. They distinguished between four different moisture zones:

- water from 2 down to about 0.8 g / g dry coal is not bonded and is associated with the coal as bulk water;

- 0.8 to 0.2 g water / g dry coal is present in the capillary structure of the coal;

water from 0.2 g to 0.08 g / g dry coal is physically absorbed;

-

the remaining moisture is chemisorbed.

-

Very little work has been reported on rapid drying of brown coals. McIntosh (1976a,b) studied the convective drying of Australian brown coal in a mill drying system. He proposed the empirical correlation

$$\frac{C(t)}{C_0} = \exp(-nt) \tag{1}$$

where C(t) is the moisture content at any given time and

$$n = \frac{6h(T_a - T_{wb})}{\lambda \rho_c [C_0/(1+C_0)]d} \tag{2}$$

T_{wb} is the wet bulb temperature and ρ_c is the density of the wet coal. A shrinking core model using a pseudo-steady state formulation of the heat conduction equation was also derived:

$$t = \frac{\lambda d \rho_c}{2} \frac{C_0/(1+C_0)}{h(T_a - T_{wb})} [1/3(1-Bi)(1-C/C_0) + Bi/2(1-(C/C_0)^{2/3}] \tag{3}$$

Mass transfer was assumed to be virtually instantaneous in view of the high porosity in the dried shell. Experiments showed substantial cracking of the particles and temperature measurements by a thermo-couple inserted into the particle were found to be significantly different from the postulated wet-bulb temperature.

Agarwal et al. (1984a) extended the model of McIntosh to include the effect of shrinkage during drying. The model predictions seemed to be in reasonable agreement with the reported data. The model predictions showed dimensionless drying curves were largely independent of shrinkage.

The inability of this model to predict the drying time accurately was overcome by Agarwal et al. (1984e) by including the transient effects in the modelling of drying. The model was based on a unsteady state heat conduction equation with convective boundary. Heat transfer to and through the coal particle was assumed to be the rate limiting step. Excellent agreement has been obtained with the limited data for drying of Mississippi lignite. However, shrinkage of the particle during drying was not considered.

2.1.2 SHRINKAGE

Drying of low-rank coals with high moisture content can result in considerable shrinkage of the coal particles. Several studies have been reported in the past few years on the evolution of the pore structure during drying. Evans (1973) using Australian Yallourn coal which contains 2 g moisture/g dry coal, showed that shrinkage occurs in several stages. In the initial drying process pores larger than 1200 Å were emptied with little contraction of the coal cylinders. In the next step the water was removed from smaller capillaries which collapsed. Removal of the multilayer water caused the collapse of the open gel structure with disproportionate-

ly larger shrinkage. Drying of the last two water layers around each micelle entailed no further shrinkage, some swelling in this stage has even been observed. Androutsopoulos and Linardos (1986) found that the drying of Greek lignite was accompanied by a considerable particle contraction. A slight decrease in the macro- and mesopore volume and marked increase in the relevant surface area occurred particularly in the area of high weight losses. Their measurements with mercury porosimetry on raw or partially dried samples indicated the formation of pores in the size range +75 -1500 Å at the expense of pores in the range +1500 -10,0000 Å. This observation was attributed to pore shrinkage and pore emptying as counter action of particle contraction and moisture removal respectively. Changes in pore structure as a result of drying have also been observed by Bale et al. (1986) using small-angle X-ray scattering. Deevi and Suuberg (1987), in their study on the physical properties of North Dakota lignites, concluded that irreversible shrinkage is mainly associated with the collapse of macro and transitional porosities. It may be these investigations have been performed at temperatures and heating rates substantially lower in comparison with the operating temperatures for fluidized bed combustion. Additionally, until the time the details of the pore structure evolution can be included in model descriptions, it is of importance to determine the macroscopic particle contraction of the operating conditions of interest in FBC.

To include shrinkage in the modelling of drying Das (1983) proposed the following empirical correlation for shrinkage:

$$\left(\frac{d}{d_0}\right)=\left(\frac{C}{C_0}\right)^{0.158} \tag{4}$$

by analysing drying data obtained by Jung (1979) to justify the empirical correlation.

Agarwal et al. (1984a) included shrinkage in their pseudo steady state receding core model. Shrinkage was evaluated using the following expression

$$\varepsilon = \frac{R_p}{R_{p0}} = \left[1 - \overline{F} x_v \left(1 - \left(\frac{C}{C_0} \right) \right) \right]^{1/3} \tag{5}$$

where x_v is the initial volume fraction of water in the particle and $0 < \overline{F} < 1$ is a proportionality constant with the limiting values corresponding to no shrinkage and complete collapse of the pore structure respectively. Parametric studies revealed that the influence of shrinkage on the dimensionless drying curves are small. To obtain the time dependent drying behaviour, however, the total drying time had to be used as an input parameter.

2.2 DEVOLATILIZATION

Research efforts world wide have been focused on pyrolysis over the years. Extensive literature reviews dealing with pyrolysis (Anthony and Howard, 1976; Wen and Dutta 1979; Juntgen and van Heek, 1979; Gavalas, 1982) have been published. The most important aspects will be discussed in the following.

2.2.1 KINETICS OF COAL DECOMPOSITION

Coal pyrolysis involves a large number of chemical reactions and physical transformations. Consequently, its understanding, in spite of intensive research remains incomplete. Simple first order decomposition kinetic models had been used

most often in earlier studies to model the overall process.

$$\frac{dV}{dt} = k'(V^o - V) \tag{6}$$

where $V \rightarrow V^o$ as $t \rightarrow \infty$

k = ko exp (-E/RT)

These models are now considered inadequate since they cannot predict the dependence of the yield on the peak temperature. Moreover, the predicted activation energies are much lower than expected from model compound studies (Anthony and Howard, 1976; Gavalas, 1982; Suuberg et al., 1978). Kinetic parameters - for overall weight loss as well as individual species evolution - obtained by different investigators using these models varied widely. These discrepancies have been attributed to the difference in coal type as well as the experimental technique employed (Anthony and Howard, 1976; Felder et al., 1982). Distributed activation energy (DAE) models (Pitt, 1962) are now gaining rapid acceptance. The overall decomposition of coal as well as the evolution of individual species are described by a large number of independent parallel first order reactions. The activation energies are assumed to follow a statistical distribution; most often a Gaussian function is used (Juntgen and van Heek, 1979; Gavalas, 1982), though other forms including a modified Rosin-Rammler distribution (Suuberg et al., 1978) have also been used. The common pre-exponential factor can be fixed before hand (Anthony and Howard, 1976; Agarwal et al., 1984b), seen as an adjustable parameter (Weimer et al., 1979; Solomon and Hamblen, 1983) or a Gaussian distribution can also be employed (Juntgen and van Heek, 1979). Anthony and Howard (1976) derived the following expression for the kinetics of coal decomposition

$$\frac{V^o - V}{V^o} = \int_0^\infty \exp - \left[\int_0^t (k_o \exp(-E/RT)dt) \right] f(E)dE \qquad (7a)$$

for non-isothermal particle

$$\frac{V^o - V}{V^o} = \int_0^\infty \exp(-k_o t \exp(-E/RT)) f(E)dE \qquad (7b)$$

for isothermal particle

where the Gaussian distribution of activation energies is given by

$$f(E) = [\sigma(2\pi)^{1/2}]^{-1} \exp\left[-\frac{(E - E_o)^2}{2\sigma^2} \right] \qquad (8)$$

This approach overcomes the shortcomings of simple reaction schemes without introducing a much larger set of adjustable parameters. The application of this model appears to have brought a semblance of order in coal pyrolysis kinetics.

Solomon and Hamblen (1983) examined their experimental data for species evolution from heated grid and entrained flow pyrolysis of pulverized coal particles based on the DAE model. They concluded that the kinetic parameters were largely insensitive to coal rank; the maximum yield however, was found to depend on the type of coal.

2.2.2 DEVOLATILIZATION OF LARGE COAL PARTICLES

Relatively fewer studies have been conducted on the devolatilization of large coal particles - mainly due to the greater interest in pulverized coal combustion.

Fluidized bed technology employs coal particles > 1 mm in size. Consequently, besides the kinetics of the chemical reactions, transport phenomena will also become increasingly important in determining the rate of coal decomposition.

The pyrolysis of coking coal particles - size range 1.0 - 1.5 mm - have been studied by Peters and Bertling (1965). They found out, that for high external heat transfer (as applicable to fluidized beds) large temperature gradients could be expected within a particle. They assumed, that the devolatilization process is of zero reaction order and proposed the following prediction of the dependence of the rate of pyrolysis on the temperature and particle size

$$\frac{V}{V^o} = 0.0003(T_a - 330)d^{-0.26}t \tag{9}$$

Berkowitz (1960) developed a model for devolatilization where mass transfer was assumed to be the rate limiting mechanism. He justified that with the argument that low-rank coal does not reach the zero weight loss rate significantly faster at 523 K (total weight loss may not be greater than 3%) than at 873 K (total weight loss may exceed 30%). Low activation energies as predicted by first order decomposition kinetics were assumed.

Devanathan and Saxena (1987) developed a transport model for the devolatilization of large nonplastic coal particles. Heat and mass transfer phenomena as well as first-order kinetics for the pyrolysis reaction have been considered. An empirical correlation for devolatilization time has been proposed

$$t_v = k'd^n \tag{10}$$

The constants k' and n were fitted using a least square regression. The value of n was 1.88. It was found that pressure and particle size have strong influence on devolatilization time. Bed temperature has a strong influence on volatile yield.

The models summarized above show that the devolatilization time is approximately proportional to the square of the particle diameter. However, the transient transport of heat as well as mass is presented in terms of $Fo = \alpha t/d^2$.

Gokhale and Mahalingam (1985) conducted an experimental investigation on the influence of particle size on lignite devolatilization in a fixed-bed reactor. It was concluded that a simple first-order model fitted the weight loss data well and the activation energies were not particularly sensitive to the particle size range (1 - 4 mm) studied.

Agarwal et al. (1984b) have proposed a general non-isothermal coal particle model which assumed that heat transfer (both to and through the coal particle) and chemical reaction (represented by DAE kinetics) were the rate controlling mechanisms for the pyrolysis of coal. Additionally a second model for large particles (> 1 mm), where heat transfer was assumed to be the rate limiting step with chemical reaction controlling only the residual amount of volatiles was reported (1984c).

The general model has been used recently (Agarwal et al., 1987; Agarwal, 1985) to simulate the release of gaseous volatiles from pulverized as well as large coal particles in fluidized beds. The investigation concluded, in agreement with Solomon and Hamblen (1983), that the kinetic parameters for the evolution of C_1 - C_3 hydrocarbons, carbon oxides and hydrogen were largely insensitive to coal type. Kinetic parameters obtained from heated grid, entrained flow and slow heating

techniques were found to be applicable also to fluidized bed data; the maximum yield however, was found to depend on coal type and on the experimental apparatus. The need for additional experiments on large particle pyrolysis was stressed.

Bliek et al. (1985) have made a detailed examination of the effects of intra-particle heat and mass transfer during devolatilization of a single coal particle. Their mathematical model includes a transient devolatilization kinetics description, intra-particle mass and heat transfer and secondary deposition reactions for the tarry volatiles. Model parameters included coal type, coal particle size and heating rate. A kinetically controlled devolatilization rate for small coal particles and a heat transfer controlled regime for large particles was predicted. Model predictions and experimental data from this work and various literature sources were in good agreement.

Additionally, low-rank coals contain appreciable amounts of moisture in their 'as-mined' state. Since complete moisture removal prior to utilization is from the economic point of view not practical,the need to study the effect of coal moisture on the pyrolysis behaviour has been pointed out (Agarwal et al., 1986). No data appear to have been reported on the influence of moisture on the pyrolytic evolution of volatile species from large wet coal particles.

2.3 IGNITION

The ignition process of propane/air mixtures and liquid fuel droplets (Dennis et al., 1986; Kanury, 1975; Rah et al., 1986a,b; Hallett, 1986; Brzustowski, 1983) has received wide attention.

Ignition phase for coal however remains a vexing problem (Gomez and Vastola, 1985). Howard and Essenhigh (1967) have suggested that for particle sizes greater than 0.065 mm, homogeneous ignition is expected to take place as the surface flux of volatiles would be large enough to prevent oxygen from reaching the surface. Thomas et al. (1968) have, however, pointed out that the ignition phase would depend also on coal char reactivity. Annamalai and Durbetaki (1977) have proposed a detailed model for the transition of ignition phase, however, they have made the questionable assumptions (Agarwal et al., 1984b) of a uniform particle temperature and first order pyrolysis kinetics. Bandyopadhyay and Bhaduri (1972) outline an analytical method, based upon Semenov's thermal ignition theory for evaluation of the ignition temperature for a single coal particle. An equation describing the temperature-time history of the particle has also been developed. They found out, that the ignition temperature was dependent on particle size and type of coal. The model prediction seemed to be in good agreement with data obtained for anthracite, bituminous and lignite coals. However volatile ignition has not been taken into account. Ahluwalia and Chung (1978) developed a model for surface ignition of fuel particles in radiative and diffusive environment. The results of the theory have been applied to study ignition characteristics of coal particles under the conditions prevailing in magneto-hydrodynamics combustors. Gomez and Vastola (1983) reported an experimental investigation in ignition and combustion of coal particles. The occurrence of two different mechanisms of ignition could be seen using light intensity measurements. It was observed, when a particle ignites homogeneously, that the combustion of the volatile matter produced an initial flash of light followed by the glowing of the remaining particle as heterogeneous combustion proceeds. When the combustion mechanism was purely heterogeneous, no initial flash of light was observed only the final glowing was detected. Karcz et al.

(1983) solved the problem of heterogeneous and homogeneous ignition of coal particles numerically using the Delta - Dirac approximation of the source terms and the Vant Hoff criterion for volatile ignition. A particle parameter dependent on coal type which separated the two regimes of ignition was obtained. The separating diameter for bituminous coal was 0.350 mm.

2.4 COMBUSTION OF VOLATILES

Experimental studies on coal volatile combustion have been reported using single coal particles in both stagnant (Essenhigh, 1963; Ivanova and Babii, 1966; Stambuleanu, 1976; Carabogdan, 1965; Carabogdan, 1967) and convective oxidizing (Ragland and Weiss, 1979) environments as well as in fluidized beds (Pillai, 1981; Yates et al., 1980). Though experimental results could be correlated with the expression of the form

$$\tau_v = k_v d^n \tag{11}$$

the variations (or the lack of variation) in the values of k_v and n for different coal types and operating conditions have not been well understood. The results of the previous experimental investigations are summarized in Table 2.2.

Essenhigh (1963) developed a formula for devolatilization time by studying the devolatilization of particles in the size range of 0.295 to 4.76 mm in a non-fluidized bed combustion system where mass transfer was assumed to be the rate limiting step. The devolatilization time was predicted by

$$\tau_v = \left(\frac{\rho_d \eta}{8p'c}\right)\left(\frac{V^o}{100}\right)d^2 \tag{12}$$

Table 2.2 SUMMARY OF REPORTED EXPERIMENTAL INVESTIGATIONS ON DEVOLATILIZATION UNDER COMBUSTION CONDITIONS

Ref.	d(mm)	Exp. Conditions O_2 conc.(%)	Gas Temp(K)	Other	k_v (sec/mm^n)	n	Results influenced by Coal Type	Gas Temp
Ivanova and Babii (1966)	0.15-0.8	5 10 21	1200-1600	Re = 1 single particle	0.45	2	-	NO
Essenhigh (1963)	0.3-4.75	21		Re = 1 single particle ten coals	0.44 - 1.31 recommended value $(0.9 + 0.1)/s^2$	2	NO (taken into account by s)	-
Carabogdan (1965)*	0.5-3.0		973-1473	Re = 1 single particle ten coals	0.46 - 1.18	1.88	YES	NO
Carabogdan (1967)*				continuous flow	k_v drops 40 - 60 %			
Ragland and Weiss (1979)	2.0-12.0	10.5 21	978-1090	Re = 10 - 1000 single particle three coals	1.5	1.5	NO	NO
Pillai (1981)	0.25-8.0	13	1043-1283	fluidised bed, twelve coals	$1/T_a^m$ m = 1.5-6	0.3-1.8	YES	YES

* as reviewed by Stambuleanu (1976)

A similar model with mass transfer as rate controlling step has been proposed by LaNauze (1982). The estimation of devolatilization time was expressed as

$$\tau_v = \frac{\rho_v d^2}{24Dc} \tag{13}$$

Experimental data on devolatilization and combustion of wet Australian brown coal have been reported by Jung and Stanmore (1980). It was found, that the total burn-out time, that is, the time for drying, devolatilization and combustion, was largely independent of a wide range of water contents. Asay et al. (1983) reported similar experimental results.

Since coal is a partially pyrolysing substance, the detailed modelling of single particle devolatilization under oxidizing conditions would require the consideration of several phenomena including (a) pyrolysis (devolatilization under inert conditions prior to ignition) - chemical reaction with associated internal and external transport phenomena; (b) ignition of coal - heterogeneous (on the particle surface) or homogeneous (in the gas phase) (c) combustion of coal volatiles and its feedback effect on subsequent devolatilization.

The effect of the combustion of volatiles on subsequent devolatilization is not well understood. The models based on mass transfer limitations for the evolution of coal volatiles (Essenhigh, 1963; LaNauze, 1982) would not directly distinguish between devolatilization under inert and oxidizing conditions. Borghi et al. (1977) proposed a model in which heat transfer to the coal particle and chemical reaction were assumed to be the rate limiting mechanisms. The effect of the heat transmitted back from the flame, assumed to be at a constant adiabatic flame temperature, was taken into account. However the isothermal particle assumption is questionable (Agarwal et al., 1984b,c).

Ragland and Yang (1985) developed a non-isothermal volatile combustion model, where the devolatilization rate was presented by the DAE model and the temperature profile was obtained using a spherical unsteady state heat conduction equation with a radiation boundary condition. They assumed that at the particle surface the radiation heat transfer was much greater than convective heat transfer since the rapid volatile release screens the surface from convective heat transfer.

Choi and Kruger (1985) developed a Spherical Translucent and Radiation (STaR) cloud model, where the volatile cloud was modelled as a radiatively and conductively participating medium between the coal particle and the flame shield. The model, however, is limited to the calculation of the steady state heat transfer rate when the particle surface temperature, flame sheet radius and temperature, and other environmental conditions are given.

Saito et al. (1987) recently conducted experiments in devolatilization characteristics of single coal particles under combustion and pyrolysis conditions. They found out, that the volatile evolution rate under combustion conditions was 2 - 3 times higher than under pyrolysis conditions. They also obtained a higher weight loss in volatile matter for combustion. This result could be explained with the higher ambient temperature from the volatile flame resulting in a higher particle temperature, which in turn influences the evolution rate and the final volatile yield.

The effects of the combustion of volatiles on subsequent devolatilization were recently taken into account by Agarwal (1986). The evolution of coal volatiles was modelled using coupled heat transfer (both to and through the coal particle) and chemical reaction (represented by the distributed activation energy model (Anthony and Howard, 1976) limited formulation. The analysis was divided into pre-ignition and

post-ignition stages. The flame temperature was estimated from a modified Schvab-Zeldovich approach. In the post-ignition stage, the heat transmitted from the volatile flame around the coal particle was taken into account. The model results were applied with success to the devolatilization (under oxidizing conditions) data for single coal particles in both stagnant as well as convective environments.

2.5 COUPLED DRYING AND DEVOLATILIZATION UNDER PYROLYSIS AND COMBUSTION CONDITIONS

Few studies have been reported on the interaction of drying on subsequent devolatilization and volatile combustion.

Kansa (1982) proposed a model for drying of wood under intensive heating conditions. Mass, energy and momentum equations for the gaseous and liquid species in one-dimensional rectilinear coordinates have been used to describe the problem. A moving drying front has been assumed. The resulting non-linear partial differential equations have been solved numerically. Comparisons of the model predictions and data obtained by Lee and Diehl (1981) agreed qualitatively. The differences between model and data was attributed to the existence of recondensation (not taken into account by the model) and the formation of cracks in the wood specimen during experiments.

Tsang and Edgar (1983a,b) proposed a model for drying, pyrolysis and gasification of large blocks of coal (as applicable in underground coal gasification). One dimensional moisture and heat transfer equation on either side of a drying front were set up. Pyrolysis was modelled by simultaneous independent first order reactions and the

dusty gas model was used to calculate the concentration profiles. Reasonable agreement was obtained by comparing the model with data reported by Westmoreland and Forrester (1977).

Few investigations have been reported on devolatilization of wet coal. Jones et al. (1964) reported data on the fluidized pyrolysis of wet (20% moisture) and pre-dried sub-bituminous coal in nitrogen and steam at around 780°C. It was found that the tar yield was slightly higher for moist coal. Gavalas (1982) thought that the differences are due to the change in the pore and chemical structure which occurs in the coal during drying.

Agarwal et al. (1984d) reported an experimental and theoretical study for coupled drying and devolatilization of low-rank coals in fluidized beds. The analysis was divided in two stages. Stage I (drying and devolatilization) was modelled using the transient drying model as mentioned earlier and incorporating the drying particle temperature profile in the non-isothermal DAE kinetics model. Stage II (devolatilization when drying is completed) was modelled by solving the unsteady state heat conduction equation in one-dimensional spherical coordinates for a convective boundary condition. The resulting temperature profile has been incorporated in the non-isothermal DAE kinetics model. A good agreement between model calculations and experimental data has been obtained.

Experimental studies on fluidized bed combustion of wet brown coal have been reported by Jung and Stanmore (1980). They found out, that the total burnout time changed little over a wide range of water content, and that the char from wetter coals burnt faster than from nearly dry material. However the data for coupled drying and

devolatilization indicates a time lag for the commencement of the devolatilization process. Das (1983) developed a mathematical model for the combustion of moist brown coal particles, however, the burning of volatiles was not taken into account.

Prins (1987) conducted an experimental investigation on devolatilization, ignition and combustion phenomena in a 'two-dimensional' fluidized bed. Coal samples differing in rank (lignite, bituminous, anthracite) and particle size (4 - 9 mm) have been used. The experiments have been recorded using TV video techniques. Visual observations on the release, ignition and combustion of volatiles and char as well as measurements on volatiles and char ignition times have been reported. It was found that the length of devolatilization period was dependent on size and moisture content of the particle.

Massaquoi and Riggs (1983a,b,c) extended the model of Tsang and Edgar (1983a,b) to take combustion as well as drying and devolatilization into account. The model predicts the flame position, flame temperature, combustion rate and temperature on the coal surface for underground coal gasification.

Agarwal and Pedler (1986) investigated the effect of drying on the evolution and combustion of coal volatiles. The pseudo steady state model as already outlined in the drying section and the devolatilization model for large particles as already described in the devolatilization section have been used to model the processes. Model prediction and experimental data were in good agreement. This model, however, requires the specification of the drying time determined experimentally. The pseudo steady state approach would also suggest, that the drying time and the time required for the removal of the volatiles are the same.

2.6 COMBUSTION OF VOLATILES IN FLUIDIZED BEDS

The potential of fluidized bed combustion as an economic and environmentally acceptable technology for burning low grade coals has drawn wide research attention. Extensive reviews dealing with fluidized bed combustion of char and volatiles are available in literature (La Nauze, 1985; Turnbull and Davidson, 1984). Major research efforts have been focused on the combustion of carbon/char in fluidized beds (Avedesian and Davidson, 1973; Ross and Davidson, 1979; Chakraborty and Howard, 1978; Rhemat et al., 1980). Low-rank coals contain a substantial amount of volatile material which contributes a significant portion of the total energy released during combustion. Moreover, volatile combustion would also play a significant role in the formation and emission of CO and NO_x . Consequently the importance of including devolatilization as a rate process in the overall modelling of fluidized bed combustion is now being rapidly recognized (Agarwal et al., 1984b; LaNauze, 1982; Pillai, 1981; Borghi et al., 1977; Park et al., 1981). Few investigations have, however, been reported on the detailed process of evolution and combustion of coal volatiles and the impact of these phenomena on the subsequent combustion of residual char (Pillai, 1981; Pyle, 1975; Atimay, 1980).

In fluidized beds, the situation is more complex due to the bubble induced disturbances and solid circulation patterns. Aoyagi and Kunii (1974) have shown that combustion of char takes place predominantly when the particles are in the bubble phase. Similarly, Cowley and Roberts (1981), using high resolution slow motion video analysis, confirm that ignition and burning of volatile matter occurred preferentially in the bubbles. Flames attached to the coal particles were observed to extinguish when the particle entered the bubble cloud regions and no evidence was found for volatile matter

combustion in the emulsion phase. Their findings on the manifestation of volatile flames were confirmed by the more extensive work conducted by Prins (1987). Depending on the momentary location of the coal particle, different volatile flames were observed: as a yellow diffusion flame around the coal particle, when the coal particle was above the bed surface or in the bubble phase and as a blue pre-mixed flame straight above but apart from the coal particle which was then situated several centimetres below the bed surface in the emulsion phase. At no time volatile flames were observed in the dense phase of the fluidized bed. The extinction of the volatile flame in the emulsion phase may be attributed to combined effects of thermal losses as well as free radical quenching. Moreover oxygen partial pressure measurements (Boiarski et al., 1984 ; Minchener and Stringer, 1984) inside fluidized bed combustors showed high fluctuations, which could be attributed to the two phases in a fluidized bed. Low oxygen content in the emulsion phase would be not favourable for burning volatiles. LaNauze (1985) pointed out at the present stage of development that neither the evolution of the volatiles nor the solid circulation is known with sufficient accuracy to predict volatiles combustion from basic principles.

Agarwal (1986), as a preliminary estimate, suggested the introduction of phase residence time factors p and q such that

$$\tau_{vfb} = p\tau_{ve} + p\tau_{vg} \tag{14}$$

$$p + q = 1 \tag{15}$$

where τ_{ve} was the devolatilization time if the particle was in the emulsion phase (corresponding to pyrolysis) and τ_{vg} was the devolatilization time if the particle was in the bubble phase. The factors p and q were to be determined from the hydrodynamics of the fluid bed though no method was outlined to make such calculations. Prins (1987)

obtained volatile flame history pictures for 33s, where the flame periods were up to 1.5 seconds long interrupted by time intervals of no flames of maximal 2 seconds. The interruptions were thought to be caused by packets of bed materials extinguishing the flame and possibly by discontinuities in the volatiles escape. The flame frequency in bubbles seemed to be relatively low and it was concluded, that most of the volatile combustion occurred in the freeboard region.

Only few system models incorporating fluidized bed hydrodynamics and volatile combustion are available. Park et al. (1980; 1981) developed a plume model presenting a ABFC with large particles. It was assumed, that instantaneous devolatilization occurs at the feed entry point where plumes of unburnt combustible gases are evolved. It was assumed that a diffusion controlled combustion occurs at the boundary between volatiles and the surrounding oxygen rich gas. Bywater (1980) developed a similar model and included the effect of solids dispersion. The model identifies three distinct combustion regimes: external flame, embedded flame (discrete diffusion flame around individual particles) and instantaneous devolatilization limit. The particle and bed temperatures were assumed to be uniform, implying instantaneous heating up of the coal particle. This, however, does not apply for large particles as commonly used in FBC. The calculations performed imply a significant impact of solids dispersion and circulation upon flame structure and volatiles escape.

3 EXPERIMENTAL INVESTIGATION

The experimental investigation was conducted with the following objectives:

- measure moisture/volatile loss versus time for single particles under pyrolysis and combustion conditions (weight loss experiments) to obtain time dependent histories for drying and devolatilization;

- estimate the particle diameter as a function of moisture content to establish the influence of shrinkage;

- collect data on the evolution of gaseous species from large wet and predried coal particles (gas analysis experiments).

The experimental conditions of the different experiments are shown in Table 3.1 and Table 3.2.

3.1 EXPERIMENTAL SYSTEM

A schematic diagram of the experimental apparatus is shown in Figure 3.1. Air or nitrogen flows through a 750 mm long by 100 mm diameter stainless steel fluidized bed (1 mm sand bed particles) heated by twelve Silicon Carbide heating rods. Each of these electrical heating rods can deliver a maximum of 666 W. A reducer on top of the

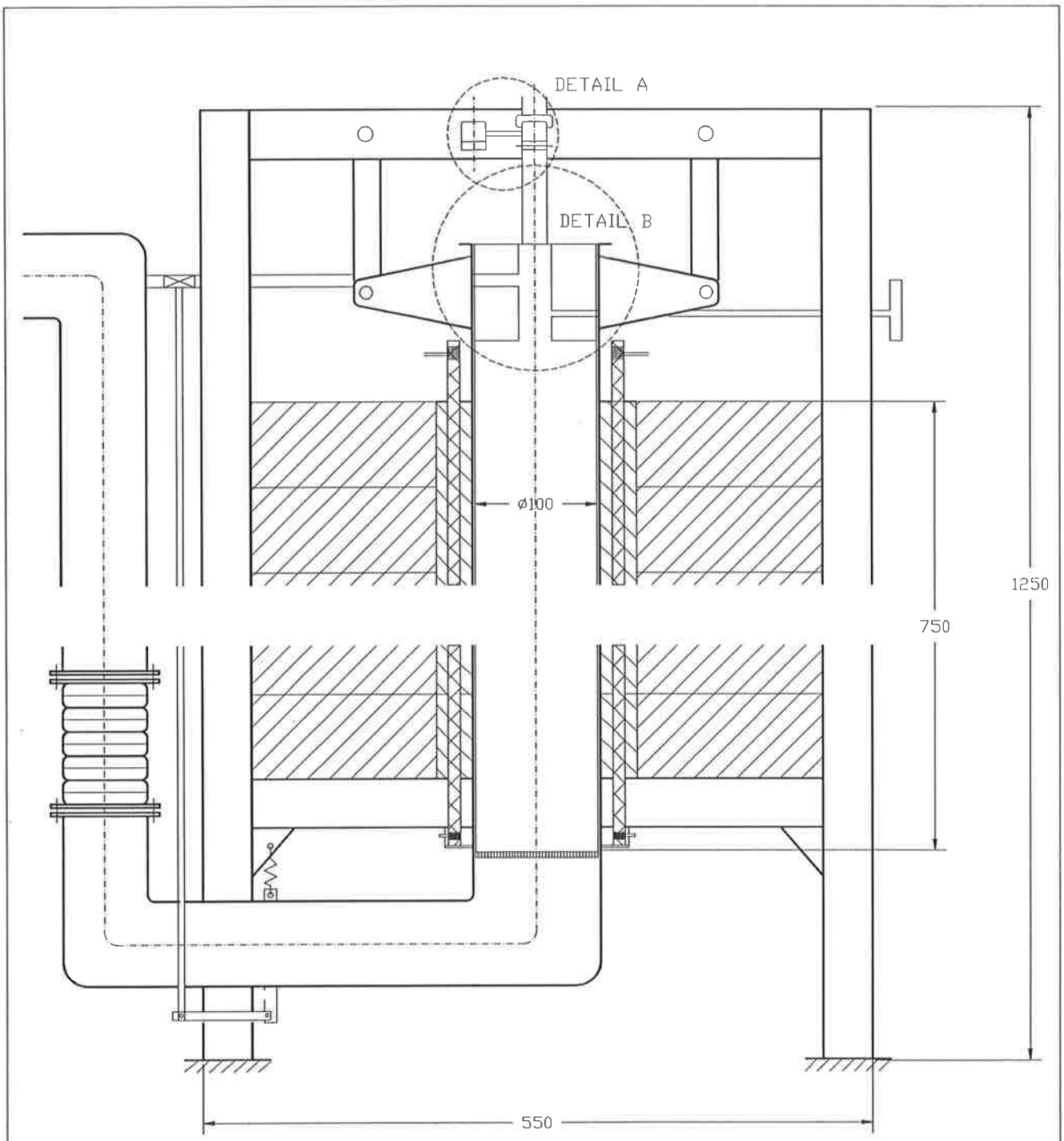

EXPERIMENTAL SET-UP SCALE 1:5

DETAIL A

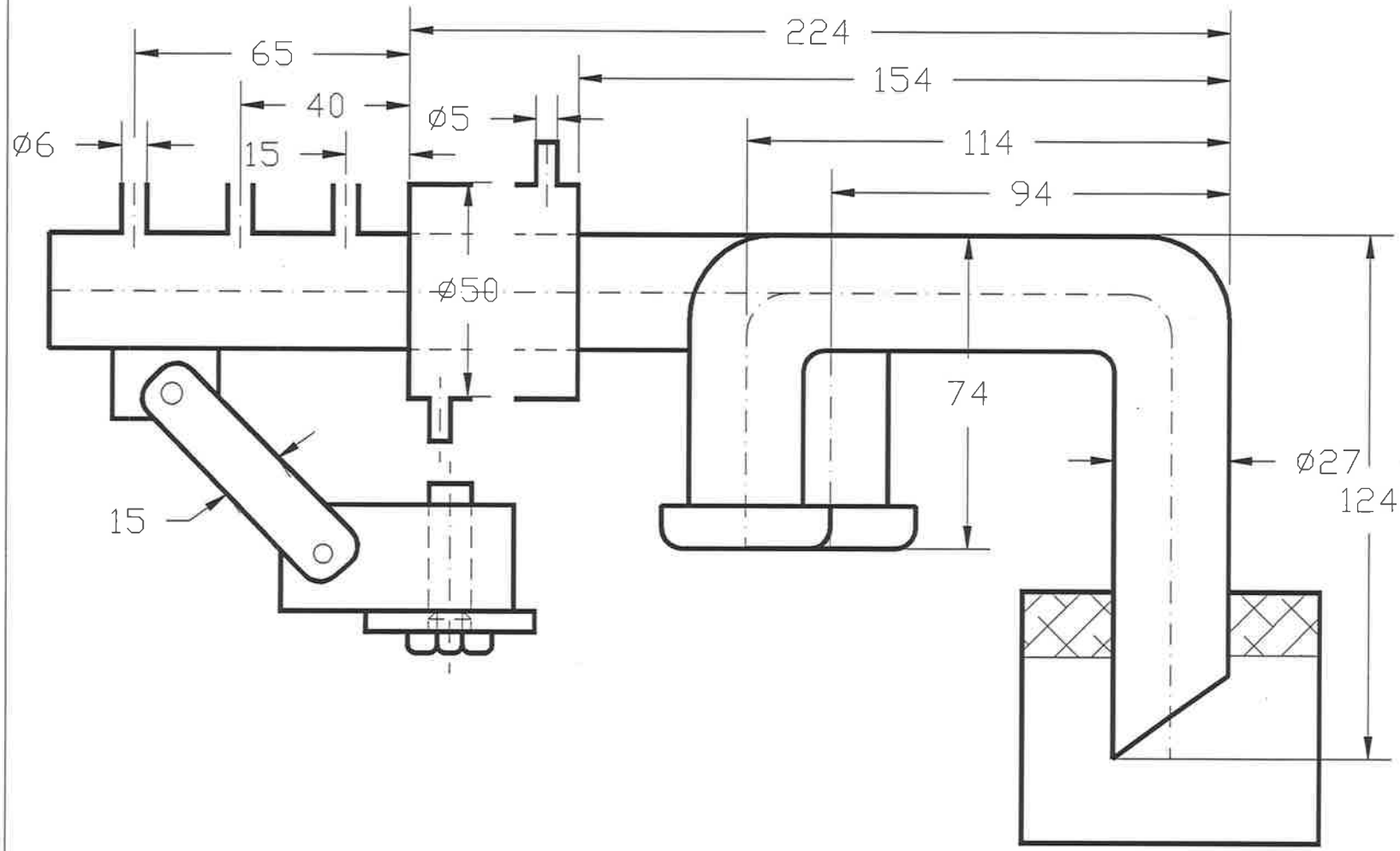

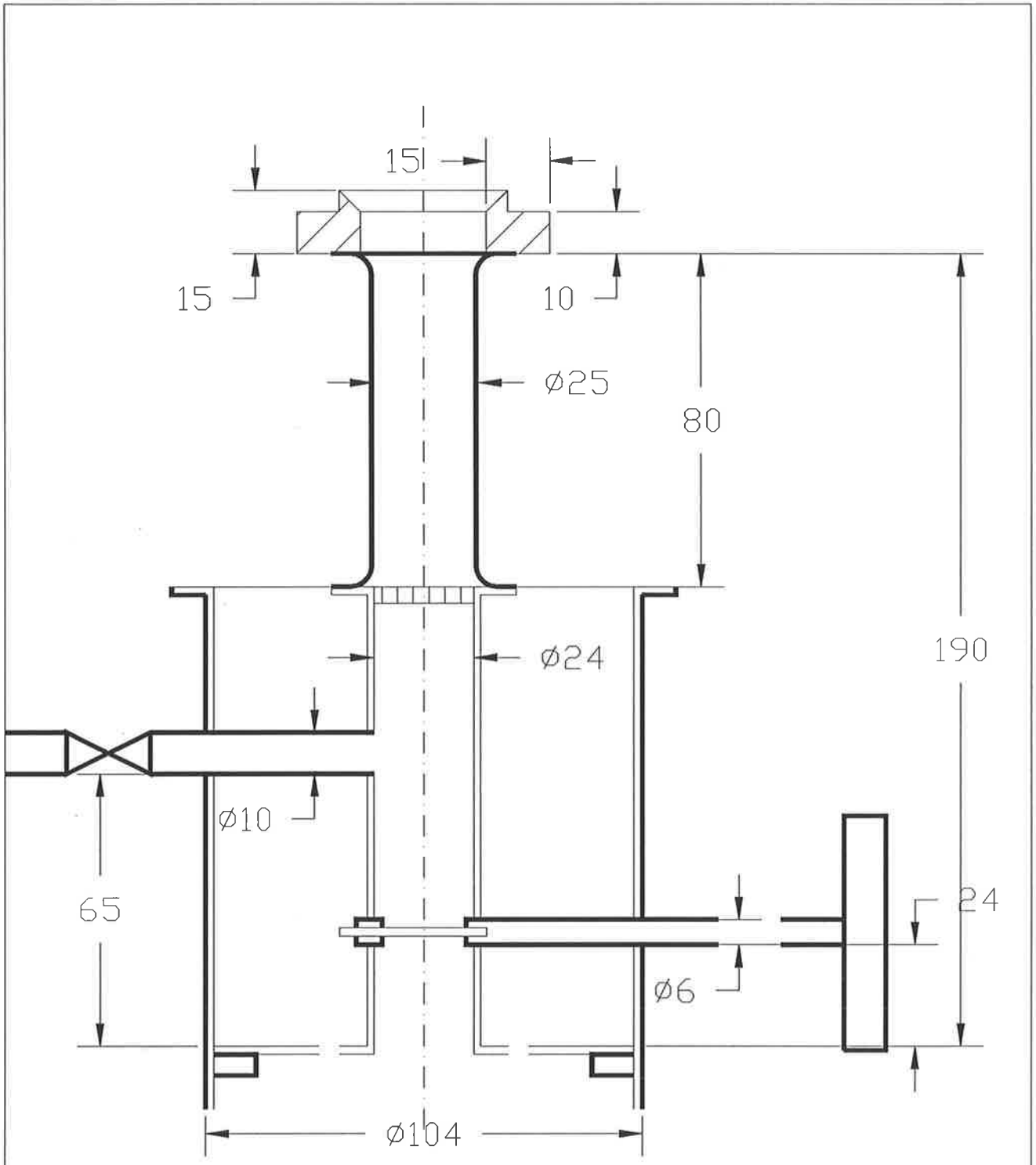

DETAIL B

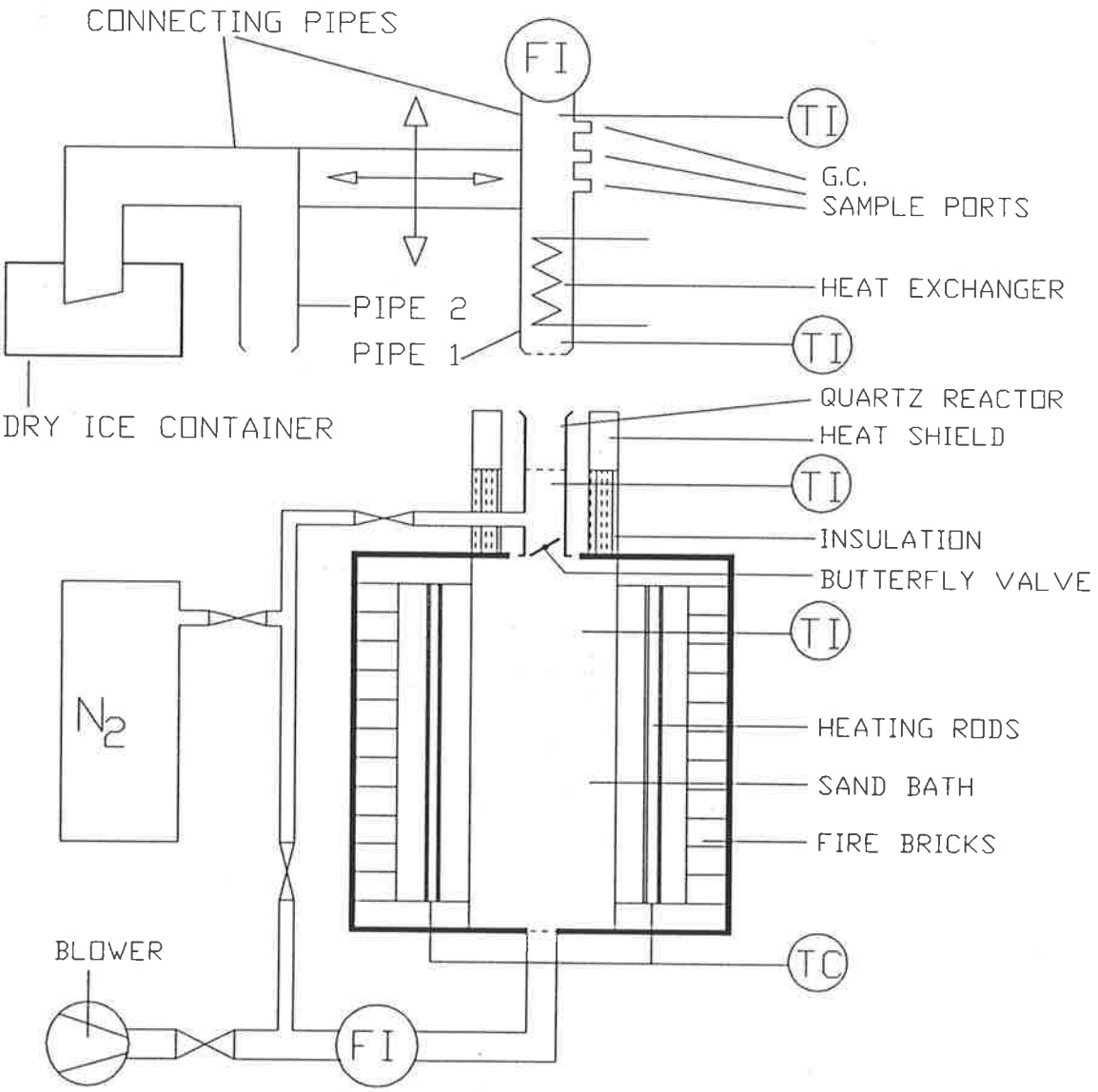

Fig. 3.1 Experimental system

Table 3.1 EXPERIMENTAL CONDITIONS FOR WEIGHT LOSS EXPERIMENTS

Temp.	Particle size	Gas velocity	Initial moist. content	Conditions	
(K)	(mm)	(m/s)	(g/g dry coal)	Air	Nitrogen
423	10	4.2	1.10	NO	YES
573	10	4.2	1.10	NO	YES
823	10	4.2	1.10	YES	YES
923	10	4.2	0.00	NO	YES
923	10	4.2	0.47	YES	NO
923	10	4.2	0.64	NO	YES
923	10	4.2	1.10	YES	YES
1023	10	4.2	1.10	YES	YES
923	5	1.2	1.10	YES	YES
423	1.8	0.5	1.10	NO	YES
423	1.8	0.5	0.68	NO	YES
573	1.8	0.5	1.10	NO	YES
823	1.8	0.5	1.10	YES	YES
923	1.8	0.5	0.00	YES	NO
923	1.8	0.5	0.59	YES	NO
923	1.8	0.5	0.68	NO	YES
923	1.8	0.5	1.10	YES	YES
1023	1.8	0.5	1.10	YES	YES

Table 3.2 EXPERIMENTAL CONDITIONS FOR VOLATILE SPECIES EXPERIMENTS

Temperature (K)	Particle size (mm)	Moisture content (g/g dry coal)
673	5	0.0
673	5	1.1
773	5	0.0
773	5	1.1
873	5	0.0
873	5	1.1
873	10	0.0
873	10	1.1

fluid bed decreases the diameter of the tube to the diameter of the quartz reactor. A screen on the bottom of the quartz tube prevents particles from falling into the fluidized bed. Holes on the lower end of the reducer enable a part of the nitrogen stream to flow outside the quartz reactor and minimize heat loss. A heat shield, insulated with rockwool is also fitted around the reactor. A gap in the shield makes it possible to observe the experiment visually. Two different outlet pipes can be swivelled onto the top end of the quartz combustor. Pipe 1 is fitted with a screen, which prevents coal particles from being blown out with the air/nitrogen stream, followed by a heat exchanger, three gas sample ports and a rotameter. The gas sample ports are fitted with special gas sampling cylinders mounted on quick connects. Pipe 2 is fitted with a dry ice container for quenching the coal particle after the experiment.

3.2 COAL PREPARATION

Chunks of Bowmans coal (proximate and ultimate analysis are given in Table 3.3) were carved, using a sharp knife, into a roughly spherical shape. The smaller particles size 1.8 mm were obtained by crushing and sieving the coal. Some of the moisture has been lost through handling the coal. To obtain an equilibrium moisture content of about 1.1 g moisture per g dry coal, the coal has been stored for at least 12 hours in a desiccator in a water saturated atmosphere under vacuum (app. 4 MPas).

3.3 EXPERIMENTAL PROCEDURE AND VISUAL OBSERVATIONS

3.3.1 WEIGHT LOSS EXPERIMENTS

The butterfly valve was closed, the coal particle introduced into the quartz reactor and Pipe 1 swivelled onto the top of the combustor. The air flow was adjusted with the butterfly valve allowing the coal particles to float in the quartz tube. At the end of the required time the valve was closed, the connecting pipes on top of the quartz combustor changed and the particles blown out into the dry ice container using nitrogen. The particles were weighed and analysed for moisture and volatile content. Five readings were taken for each time interval to ensure reproducible results.

The following visual observations have been made during the combustion experiments:

After an initial heating up period, the coal particles started to glow. Shortly there after volatile flames were established around the coal particle. Two different coloured flames were observed visually. The first, bright yellow in colour, is thought to be due to the burning of aromatics/tars released in the earlier phase of devolatilization. In the course of time, the bright yellow flame was replaced by a relatively less dense whitish flame.

3.3.2 VOLATILES ANALYSIS EXPERIMENTS

The butterfly valve was closed, the coal particles introduced into the quartz reactor and pipe 1 fitted on to the top of the quartz reactor. The nitrogen flow was adjusted to 2.2 l/min using the butterfly valve. The gas sampling cylinders were evacuated prior to connection with the gas sampling ports. Samples were obtained at pre-determined time intervals. The gas samples wer analysed using a Shimadzu gas chromatograph.

The extent of non-ideality (deviation from plug flow of gases from the micro-reactor to the sampling ports was characterized by tracer experiments. A pulse input of the tracer gas CO_2 was injected by a syringe into the reactor - the nitrogen flow being maintained at 2.2 l/min - and the off-gas was analyzed (Figure 3.2). The exit age distribution (Figure 3.3) obtained from the tracer experiments was used for the interpretation of experimental results.

3.4 ANALYTICAL PROCEDURE

3.4.1 MOISTURE CONTENT

The samples were weight and dried at 108° C for 3 hours in a drying oven according to Standard ASTM D 3392.

3.4.2 VOLATILES CONTENT

Volatiles content was analyzed by subjecting the samples to a temperature of 950° C for 10 minutes under nitrogen atmosphere in crucibles with a closed lid. Samples were purged using nitrogen prior to heating up.

Table 3.3 ANALYSIS OF BOWMANS COAL

Proximate Analysis (wt%)	
Total moisture (wet basis)	57
Ash (dry basis)	11.6
Volatile matter (dry basis)	49.2
Fixed Carbon (dry basis)	39.2
Ultimate Analysis (VM and FC Fraction) (%daf)	
C	69.4
H	4.6
N	0.5
S	4.6
O (by difference)	20.9
Ash Characteristics (kg/kg)	
Sodium/Ash	0.11
Chlorine/Ash	0.11
Heating Value (MJ/kg)	
Higher Heating Value (dry basis)	23.9

3.4.3 GAS ANALYSIS

The gas analysis has been conducted using a Shimadzu gas chromatograph under the following conditions:

flow rate: 30 ml/min

column 1: Carbosphere

temperature: 65° C

detection of: CO, CH_4

column 2: Poropak

temperature: 75° C

detection of: CO_2, C_2H_4, C_2H_6

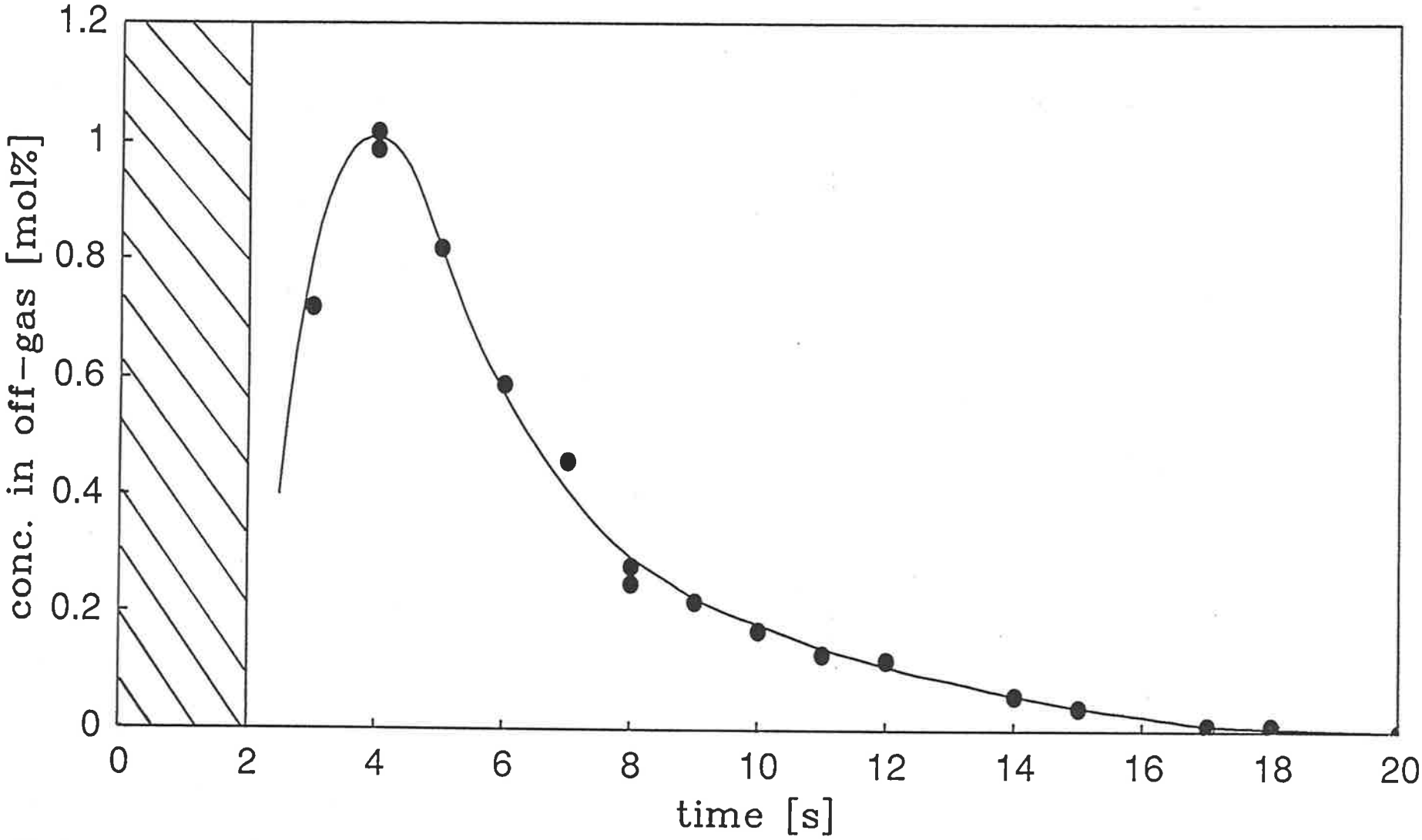

Fig. 3.2 Experimental data for CO_2 tracer studies

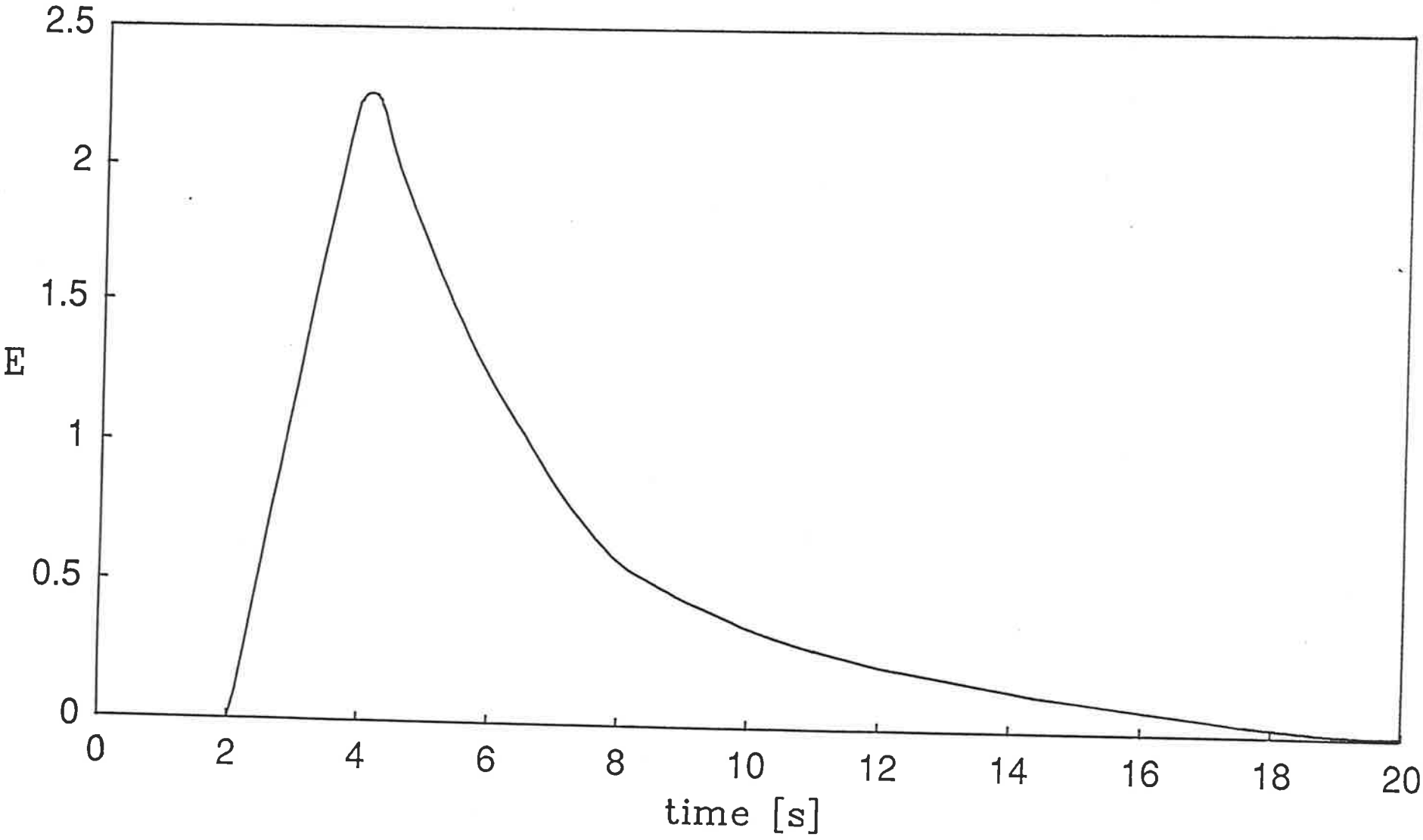

Fig. 3.3 Exit age distribution

4 MATHEMATICAL MODELLING

Considering the inevitable presence of moisture in the fluidized bed combustion of coal, a stagewise approach is being undertaken for the detailed study of the several interactive processes. The various components of the overall study are depicted in Figure 4.1. The problems of drying without devolatilization (pseudo steady-state model (Agarwal et al., 1984a) and transient model without shrinkage (Agarwal et al., 1984e)), devolatilization of predried coal under pyrolysis (Agarwal et al., 1984b), as well as combustion conditions (Agarwal, 1986), coupled drying and devolatilization (without shrinkage) under pyrolysis conditions (Agarwal et al., 1984d) and combustion conditions (pseudo steady-state model (Agarwal and Pedler, 1986)) have already been treated. The problems considered in the present thesis have also been considered.

In this chapter mathematical models were developed to analyse the phenomena of

- coupled drying and devolatilization under pyrolysis conditions with particle shrinkage taken into account
- coupled drying and devolatilization under combustion conditions.

The results of parametric studies are also discussed.

4.1 DEVOLATILIZATION

All of the following sections involve devolatilization. For clarity of presentation, the devolatilization model used is outlined first. Heat transfer to and through the coal particle and chemical reaction are assumed to be the rate limiting steps for devolatilization.

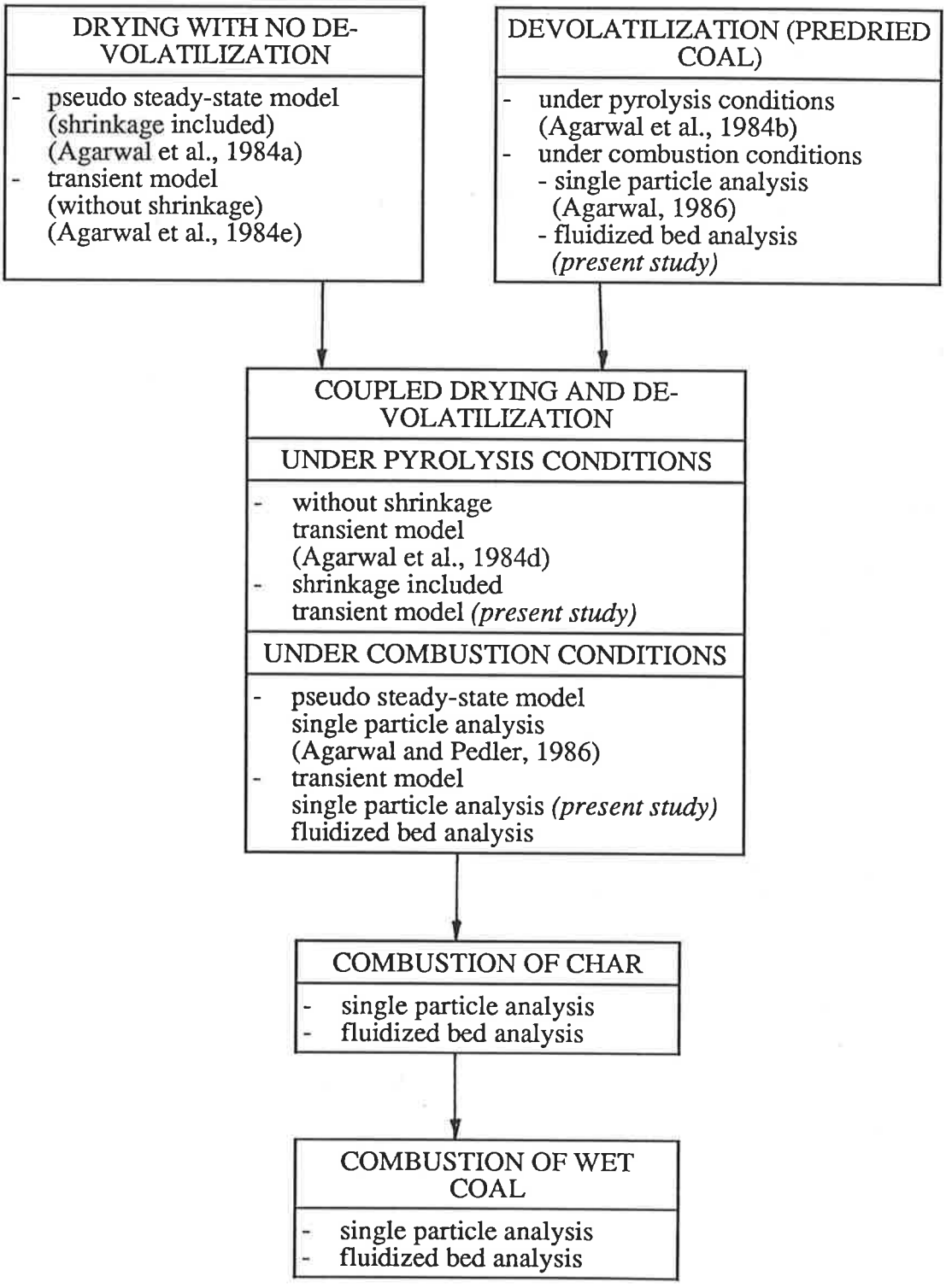

Fig. 4.1 Stagewise modelling approach

Representing the chemical reactions by the distributed activation energy kinetics (Anthony and Howard, 1976), the volumetric average devolatilization for a spherical particle of initial radius R_p can then be expressed as:

$$X_{avg} = \frac{3}{R_p^3}\int_0^{R_p}\int_0^{\infty} \exp\left(-k_0\int_0^{t} e^{-E/RT(r,t)}dt\right) f(E)dE\,r^2dr \qquad (16a)$$

The Gaussian distribution of activation energies, f(E), has a mean E_0 and a standard deviation σ,

$$f(E) = (\sigma(2\pi)^{1/2})^{-1}\exp\left(-\frac{(E-E_0)^2}{2\sigma^2}\right) \qquad (16b)$$

X_{avg} was calculated by numerical integration using Gaussian quadrature (of order 12) at each of three nested levels.

Equation (16a) may also be easily modified to account for contributions from different clustered volatiles sources

$$X_{avg} = \frac{3}{R_p^3}\left[\sum_{i=1}^{n} V_i^*\left(\int_0^{R_p} X r^2 dr\right)\right] \qquad (16c)$$

where V_i^* is the fractional maximum yield from the i^{th} cluster of sources.

To solve equations (16a-c) the temperature profile of the particle, T(r,t) has to be estimated. It can be obtained from the analytical solution of the unsteady state heat conduction equation in spherical co-ordinates with the appropriate convective boundary and initial temperature conditions.

4.2 EFFECT OF SHRINKAGE DURING COUPLED DRYING AND DEVOLATILIZATION UNDER PYROLYSIS CONDITIONS

In several literature reviews (Wilson et al., 1978; Ockendon et al., 1975; Fasano and Primicerio, 1983; Rubinstein, 1967) the analytical and numerical techniques available to solve moving boundary problems have been pointed out. Differential equations for heat and mass transfer have been applied to solve drying problems.

The procedure for the development of the model equations is similar to coupled drying and devolatilization for single particles as reported by Agarwal et al. (~~Agarwal et al.~~, 1986). In the following only the major steps are outlined and the principal differences are identified. Drying, assumed to be controlled by the rate of heat transfer to and through the coal particle, is modelled on a moving wet core formulation. The effect of chemical reaction during devolatilization is modelled using the non-isothermal distributed activation energy formulation (Anthony and Howard, 1976).

In Table 4.1 the relevant heat conduction equation for the dry shell region and the appropriate boundary conditions are listed.

where $\lambda' = (T_e - T_0)(c_{pw} + c_{pc}/C_0) + \lambda$, is the sum of sensible heat and latent heat of vaporization.

Transformation of the spherical coordinate system in Equation (17) to a rectilinear coordinate system by substituting v = Tr yields

$$\frac{\partial v}{\partial t} = \alpha \frac{\partial^2 v}{\partial r^2} \tag{19}$$

Table 4.1 HEAT CONDUCTION EQUATION AND BOUNDARY CONDITIONS

Dry shell heat conduction equation: $\frac{\partial T}{\partial r}=\frac{\alpha}{r^2}\frac{\partial}{\partial r}\left(r^2\frac{\partial T}{\partial r}\right)$ $r_e \le r \le R_p$	(17)
convective boundary condition at particle surface: $k\frac{\partial T}{\partial r}\Big\|_{r=R_p}=q(t)$	(18*a*)
heat balance at the receding wet-dry interface $k\frac{\partial T}{\partial r}\Big\|_{r=r_e}=\lambda' C_0 \rho_c \frac{dr_e}{dt}$	(18*b*)

Application of integration results in

$$\int_{R_p}^{r_e} \frac{\partial v}{\partial t} dr = \alpha \frac{\partial v}{\partial r}|_{r=r_e} - \alpha \frac{\partial v}{\partial r}|_{r=R_p} \tag{20}$$

Applying Leibnitz's rule

$$\frac{d}{dt}\int_{R_p}^{r_e} v\,dr - v_e \frac{dr_e}{dt} + v_s \frac{dR_p}{dt} = \alpha \frac{\partial v}{\partial r}|_{r=r_e} - \alpha \frac{\partial v}{\partial r}|_{r=R_p} \tag{21}$$

It may be noted, that the inclusion of shrinkage results in an additional term on the LHS of Equation (21) in comparison with the non-shrinking formulation reported by Agarwal et al. (~~Agerwal et al.~~, 1984e). The individual terms in Equation (21) may now be evaluated as in Table 4.2.

The moving boundary in Equation (21) is immobilized by redefining the space variable $\phi' = (r - r_e)/(R_p - r_e)$. Also a quadratic temperature profile is assumed in the dry shell (Agarwal et al., 1984e)

$$T = T_e + (T_s - T_e)(2\phi' - \phi'^2) + q(t)\frac{(R_p - r_e)}{k}(\phi'^2 - \phi') \tag{22}$$

incorporation of shrinkage as per Equation (5), yields:

$$\frac{d}{dt}\int_{R_p}^{r_e} v\,dr = \frac{d}{dt} R_{p0}^2 \{ \frac{q(t)R_{p0}}{12k}(\varepsilon^3 - \phi_T\varepsilon^2 - \phi_T^2\varepsilon + \phi_T^3)$$

$$-\frac{T_e + 5T_s}{12}(\varepsilon^2 - \phi_T\varepsilon) - \frac{T_e + T_s}{4}(\phi_T\varepsilon - \phi_T^2)\} \tag{23}$$

where ε is the volumetric shrinkage, R_{p0} the initial particle radius, r_e the wet core radius, $\phi = r_e/R_p$, T_s the surface temperature and T_e wet-dry interface temperature.

Table 4.2 TERMS OF EQUATION (21)

$v_e \frac{dr_e}{dt} = T_e r_e \frac{dr_e}{dt}$	(24*a*)
$v_s \frac{dR_p}{dt} = T_s R_p \frac{dR_p}{dt}$	(24*b*)
$\alpha \frac{\partial v}{\partial r}\|_{r=r_e} = L r_e \frac{dr_e}{dt} + \alpha T_e$	(25*a*)
$\alpha \frac{\partial v}{\partial r}\|_{r=R_p} = \frac{R_p}{\rho_c c_{pc}} q(t) + \alpha T_s$	(25*b*)

Table 4.3 COEFFICIENTS OF DRYING EQUATION (29)

$$\frac{q(t)R_{p0}}{k}=\frac{Bi_{d0}\phi_{ps}(T_a-T_e)}{2\phi_{ps}-Bi_{d0}\varepsilon(\phi_{ps}-\varepsilon)} \tag{31}$$

$$\frac{T_s-T_e}{T_a-T_e}=Bi_{d0}\varepsilon^2\frac{1-\phi_{ps}/\varepsilon}{2\phi_{ps}-Bi_{d0}\varepsilon(\phi_{ps}-\varepsilon)} \tag{32}$$

$$L=\frac{\lambda' C_0}{c_{pc}} \tag{33}$$

$$A=\frac{q(t)\,|_{\theta=1}R_{p0}}{12k}(1-\overline{F}x_v)-\frac{T_e+5T_s\,|_{\theta=1}}{12}(1-\overline{F}x_v)^{2/3}+\frac{L+T_e}{2}-T_s\frac{(1-(1-\overline{F}x_v)^{2/3})}{2} \tag{28}$$

$$F=\frac{\phi_{ps}^2-1}{\phi_{ps}^2\,|_{\theta=1}-1} \tag{34}$$

Substitution of Equations (24a), (24b), (25a), (25b) and (23) into Equation (21) and subsequent integration results in:

$$\frac{q(t)R_{p0}}{12k}(\varepsilon^3-\phi_T\varepsilon^2-\phi_T^2\varepsilon+\phi_T^3)-\frac{T_e+5T_s}{12}(\varepsilon^2-\phi_T\varepsilon)$$

$$-\frac{T_e+T_s}{4}(\phi_T\varepsilon-\phi_T^2)+\frac{L+T_e}{2}(1-\phi_T^2)-T_s\frac{\varepsilon^2-1}{2}$$

$$=-\frac{\alpha}{R_{p0}}\left\{\int_0^t\frac{T_s-T_e}{R_{p0}}dt+\int_0^t\frac{\varepsilon q(t)}{k}dt\right\} \tag{26}$$

The time required for the particle to dry or for the moving boundary to reach the centre of the particle ($\phi_T = 0$) is defined τ and incorporating $\theta = t / \tau$ as dimensionless time yields:

$$\frac{q(t)R_{p0}}{12k}(\varepsilon^3-\phi_T\varepsilon^2-\phi_T^2\varepsilon+\phi_T^3)-\frac{T_e+5T_s}{12}(\varepsilon^2-\phi_T\varepsilon)$$

$$-\frac{T_e+T_s}{4}(\phi_T\varepsilon-\phi_T^2)+\frac{L+T_e}{2}(1-\phi_T^2)-T_s\frac{\varepsilon^2-1}{2}$$

$$=A\frac{\int_0^\theta\frac{T_s-T_e}{R_{p0}}d\theta+\int_0^\theta\frac{\varepsilon q(t)}{k}d\theta}{\int_0^1\frac{T_s-T_e}{R_{p0}}d\theta+\int_0^1\frac{\varepsilon q(t)}{k}d\theta} \tag{27}$$

where

$$A=\frac{q(t)|_{\theta=1}R_{p0}}{12k}(1-\overline{F}x_v)-\frac{T_e+5T_s|_{\theta=1}}{12}(1-\overline{F}x_v)^{2/3}+\frac{L+T_e}{2}-T_s\frac{(1-(1-\overline{F}x_v)^{2/3})}{2} \tag{28}$$

The resulting equation for drying may be solved if an appropriate estimate of the particle surface temperature, T_s, as a function of time is available. In the absence of experimental information the pseudo steady-state model may be used (Agarwal et al., 1984e) to estimate the time dependent behaviour of the particle surface temperature T_s and the heat flux at the

surface q(t). The drying equation can then be written as:

$$\frac{q(t)R_{p0}}{12k}(\varepsilon^3-\phi_T\varepsilon^2-\phi_T^2\varepsilon+\phi_T^3)-\frac{T_e+5T_s}{12}(\varepsilon^2-\phi_T\varepsilon)-\frac{T_e+T_s}{4}(\phi_T\varepsilon-\phi_T^2)$$

$$+\frac{L+T_e}{2}(1-\phi_T^2)-T_s\frac{(1-\varepsilon^2)}{2}-A*F=0 \qquad (29)$$

The coefficients of Equation (29) are tabulated in Table 4.3

The total drying time can be obtained by a trial and error solution to satisfy the equality

$$A=L(\frac{1-\phi_{ps}^2|_{\theta=1}}{2}+\frac{(1-\overline{F}x_v(1-\phi_{ps}^3|_{\theta=1}))^{2/3}-(1-\overline{F}x_v)^{2/3}}{2\overline{F}x_v}$$

$$-\bar{\varepsilon}_T\frac{(1-\overline{F}x_v(1-\phi_{ps}^3|_{\theta=1}))^{1/3}-(1-\overline{F}x_v)^{1/3}}{(\overline{F}x_v)} \qquad (30a)$$

where

$$\bar{\varepsilon}_T=(1+(1-\overline{F}x_v)^{1/3})/2 \qquad 30b$$

The devolatilization occurs only in the dry shell and the particle temperature profile required for the solution of equation (16a) can be evaluated from equation (22) during the drying stage. When the particle is dry, devolatilization however will still occur. Agarwal et al. (1986) used the heat conduction equation with a convective boundary and the temperature profile of the particle at the end of drying as initial condition to obtain the temperature profile of the particle as

$$T(r,t')=T_a-\sum_{i=1}^{\infty}N_i\frac{\sin\beta_i r/R_p}{\beta_i r/R_p}\exp(-\beta_i^2\alpha t'/R_p^2) \qquad (35)$$

Since no shrinkage is assumed to take place on account of devolatilization, equation (35) applies. However the particle radius at the end of drying has to be used in equation (35). The coefficients of equation (35) are listed in Table 4.4.

Table 4.4 COEFFICIENTS OF EQUATION (35)

$$N_i = 2(C_1A_1 - (2C_2 - C_3)A_2 - (C_3 - C_2)A_3)/A_4 \tag{36a}$$

$$A_1 = \sin\beta_i - \beta_i\cos\beta_i \tag{36b}$$

$$A_2 = \cos\beta_i\left(\frac{2}{\beta_i} - \beta_i\right) + 2\sin\beta_i - \frac{2}{\beta_i} \tag{36c}$$

$$A_3 = \cos\beta_i\left(\frac{6}{\beta_i} - \beta_i\right) + 3\sin\beta_i\left(1 - \frac{2}{\beta_i^2}\right) \tag{36d}$$

$$A_4 = \beta_i - \sin\beta_i\cos\beta_i \tag{36e}$$

$$C_1 = (T_a - T_e) \tag{36f}$$

$$C_2 = (T_s|_{t'=0} - T_e) = Bi_{d0}\varepsilon^2\frac{(1-\phi_{ps}/\varepsilon)(T_a - T_e)}{2\phi_{ps} - Bi_{d0}\varepsilon(\phi_{ps} - \varepsilon)} \tag{36g}$$

$$C_3 = q(t)|_{t'=0}\frac{R_p}{k} = \frac{Bi_{d0}\phi_{ps}(T_a - T_e)}{2\phi_{ps} - Bi_{d0}\varepsilon(\phi_{ps} - \varepsilon)} \tag{36h}$$

$$t' = t - \tau \tag{36i}$$

Results of the parametric studies made with the model are presented to study the effect of shrinkage on drying and evolution of volatiles.

To demonstrate the influence of shrinkage, a set of standard parameters are chosen. The standard parameters are C_0 = 1.1 g moisture/g dry coal, Bi_{d0} = 5, T_a = 423 K, $R_{p0} = 5mm$, c_{pc} = 1.25 kJ/kgK, ρ_c = 1250 kg/m³ and α = 0.2 mm²/s.

In Figure 4.2 sample calculations are shown to demonstrate the effect of shrinkage proportionality factor on drying time and behaviour. As one might expect for lower shrinkage proportionality factors the drying times are higher.

Figure 4.3 shows the influence of initial moisture content on shrinkage plotted as volumetric shrinkage ε^3 against dimensionless moisture content (C/C_0). As can be seen higher initial moisture content results in more shrinkage of the particle.

4.3 GENERAL MODEL DESCRIPTION FOR COMBUSTION OF WET COAL

The systematic modelling approach for combustion of a wet coal particle has been outlined in Figure 4.4. When the cold coal particle is introduced into the hot combustion environment, drying will commence as soon as enough latent heat of vaporization can be supplied to the surface moisture. Due to the higher permeability of the vapour phase, the wet core will recede with time towards the centre of the coal particle. The dry shell will start heating up and devolatilization will commence with the break-up of the thermal bonds in the coal structure. As the volatile release becomes more rapid, ignition of volatiles will take place in the gas phase for particle sizes > 0.065 mm (Howard and Essenhigh, 1967). The volatiles will prevent any oxygen from approaching the surface of the coal. The energy from the volatiles flame will increase the

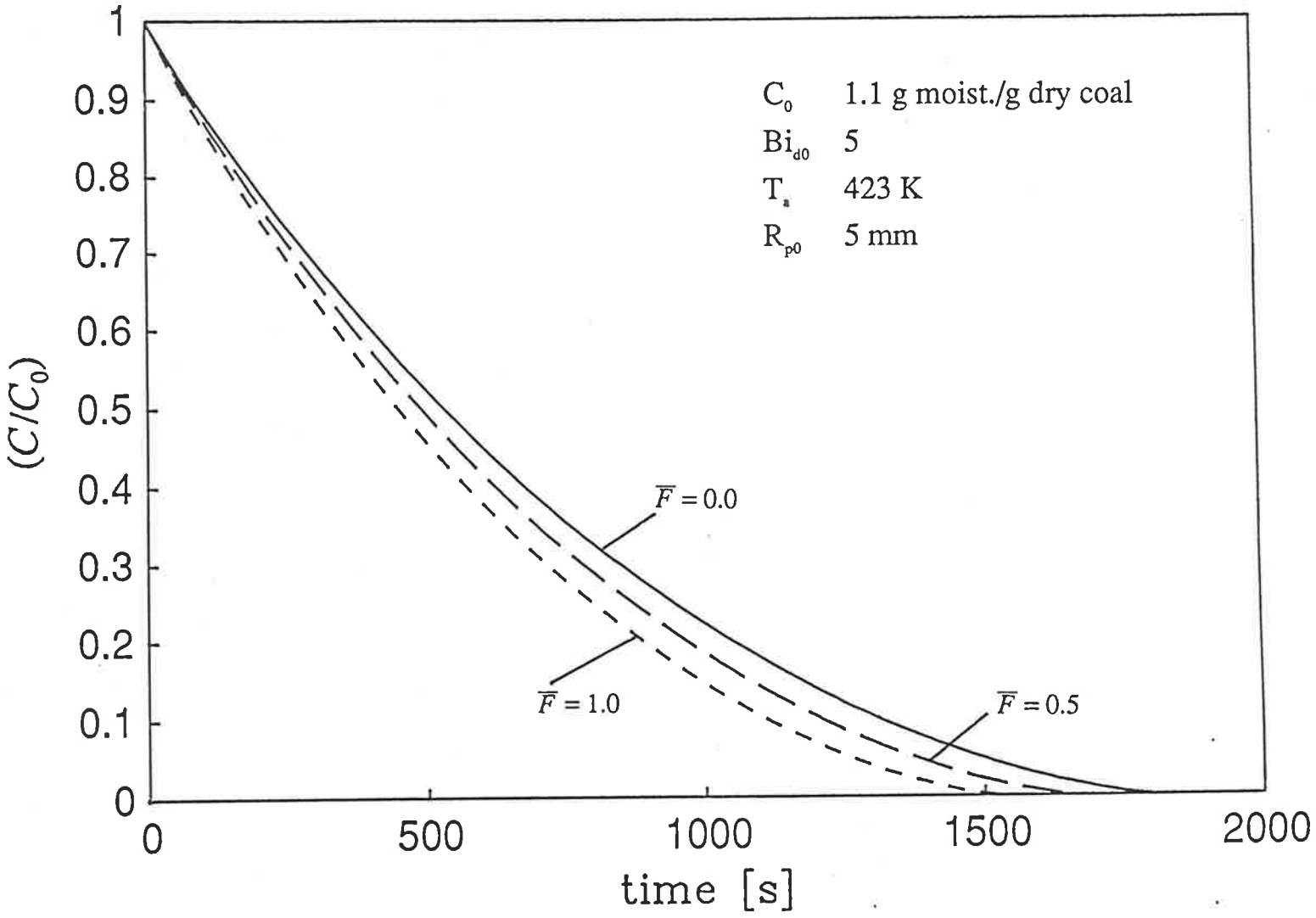

Fig. 4.2 Influence of shrinkage proportionality constant on drying time

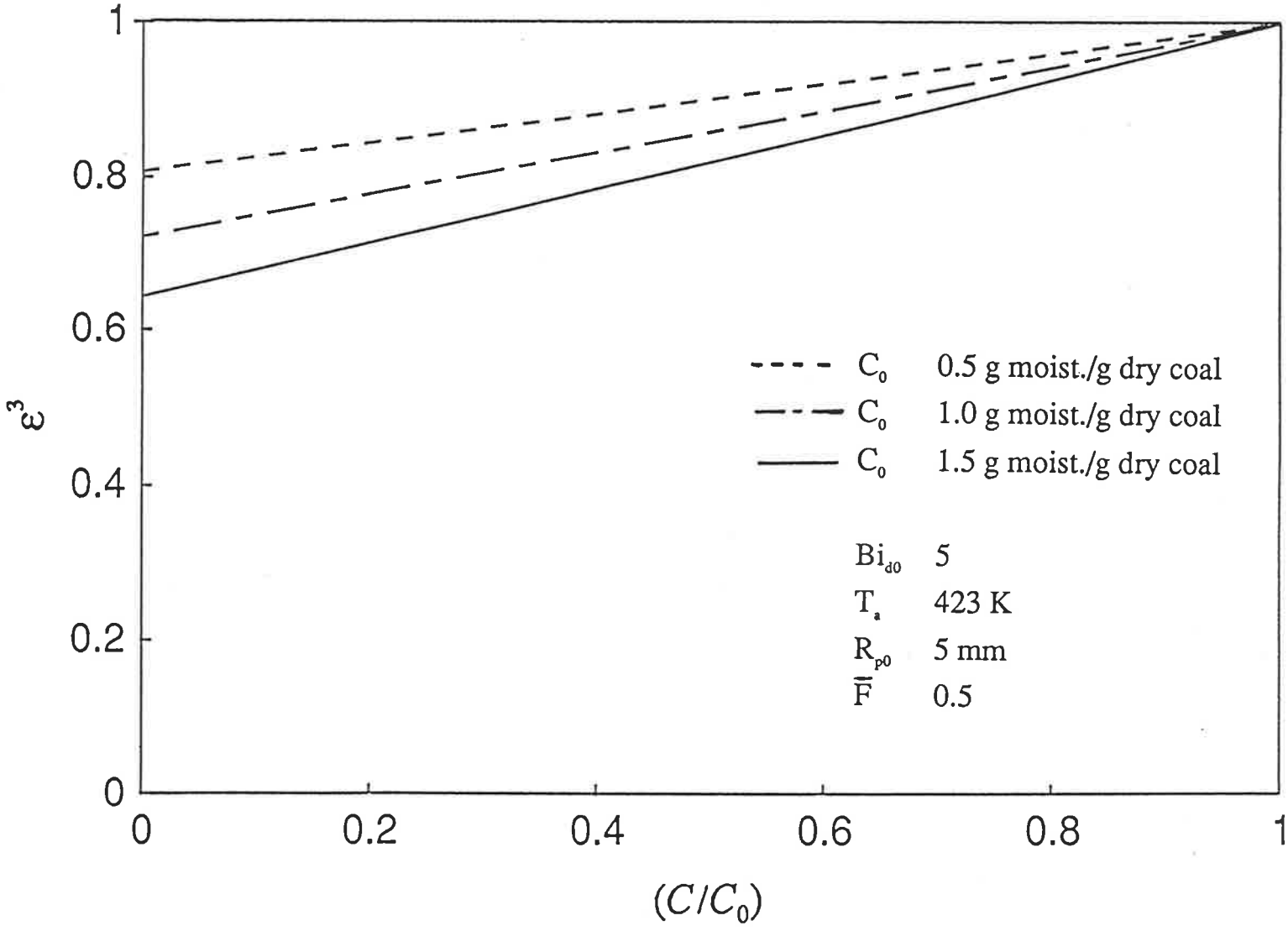

Fig. 4.3 Influence of initial moisture content on volumetric shrinkage

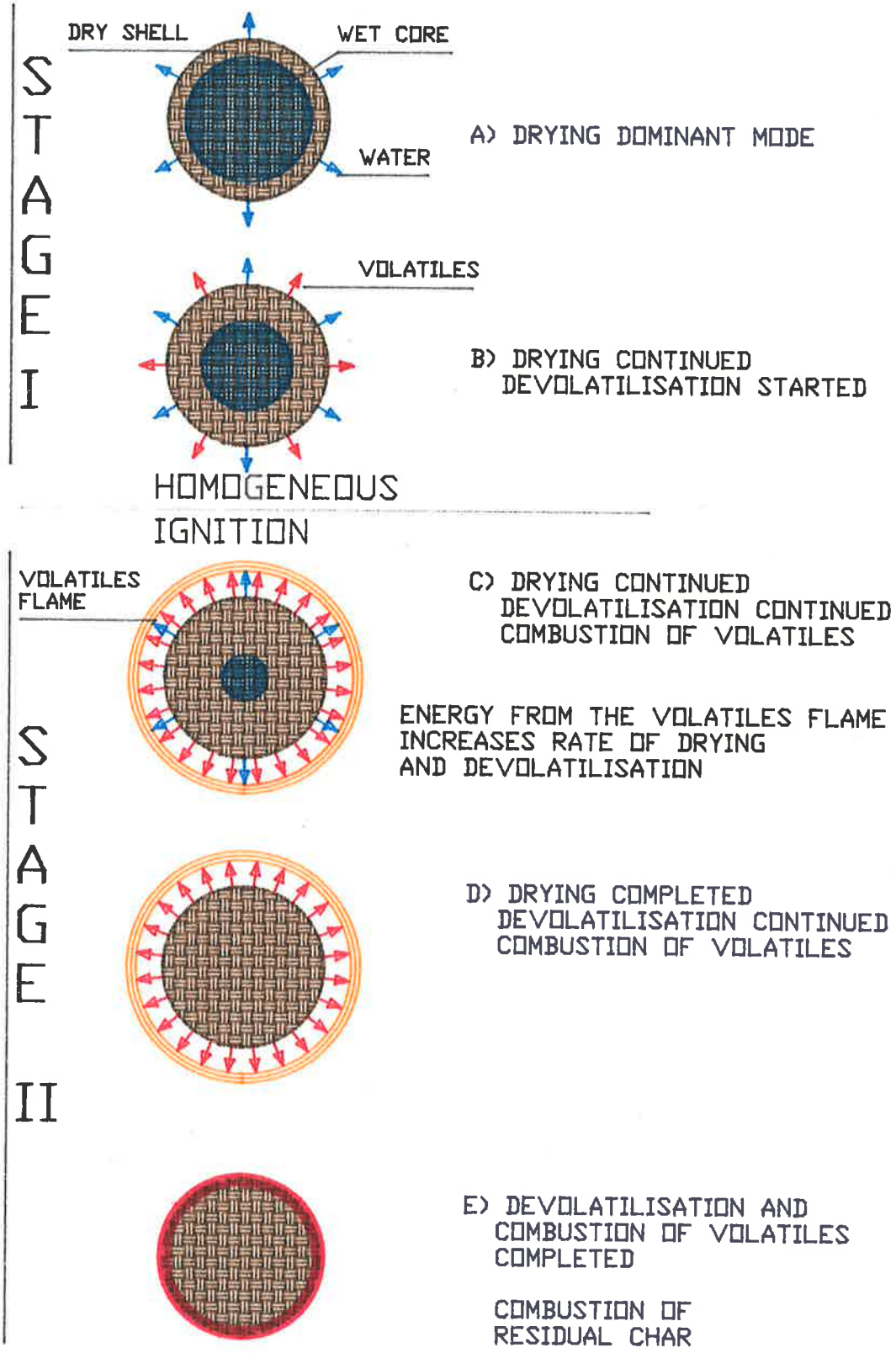

Fig. 4.4 General model description for combustion of a wet particle

rate of drying and devolatilization which in turn can alter the location of the flame front and the flame temperature. Finally, the volatiles will be depleted from within the coal particle, the flame will collapse permitting oxygen to attack the residual char.

4.4 ESTIMATION OF FLAME TEMPERATURE

For the modelling of drying and devolatilization under combustion conditions it is necessary to calculate the flame temperature. To estimate the flame temperature, the Schwab Zeldovich approach applied to the fuel droplet combustion problem is adapted to coal volatile combustion to obtain an estimate of the flame temperature T_f. The development is based on the solution as presented by Kanury (1975). The following development is valid for dry coal particles (Agarwal, private communication).

The steady state conservation equations and the definition of the conserved variable, b, leads to the following differential equation

$$\rho_g \alpha_g \frac{d}{dr}\left(r^2 \frac{db}{dr}\right) - (\dot{w} r^2)\,|_{R_p} \frac{db}{dr} = 0 \qquad (37a)$$

for $R_p \le r \le R_p + \delta$ which has to be solved with the boundary conditions

$$\dot{w}\,|_{R_p} = \rho_g \alpha_g \frac{db}{dr}\,|_{R_p}$$

$$b\,|_{R_p+\delta} = 0 \qquad (37b)$$

To obtain an expression for δ,

$$k_g \frac{dT}{dr}\,|_{R_p} = h(T_a - T_s) \qquad (38a)$$

Assuming that the temperature profile in the thermal boundary layer is linear,

$$k_g(T_a - T_s)/\delta_h = h(T_a - T_s) \qquad (38b)$$

Further assuming that the momentum boundary layer thickness and the conduction thickness are equal prior to ignition,

$$\delta \sim \delta_h = k_g/h = 2k_g R_p/(k_s Bi_d) \qquad (38c)$$

The flame radius, in general, may be assumed to be $r_f = R_p + \delta/i$ where i may vary from one to infinity (corresponding to the flame sitting at the edge of the momentum boundary layer and the particle surface respectively). Then after ignition,

$$k_g \frac{dT}{dr}|_{R_p} = h_f(T_f - T_s) \qquad (39a)$$

Retaining the assumption of a linear temperature profile in the thermal boundary layer,

$$k_g(T_f - T_s)/\delta_{hf} = h_f(T_f - T_s) \qquad (39b)$$

Since $r_f = R_p + \delta/i$, then $\delta_{hf} = \delta/i$. Consequently

$$Bi_f = k_g R_p/(k_s \delta_{hf}) = iBi \qquad (39c)$$

Using equation (38c), the solution of equation (37) leads to an expression for the Mass Transfer number

$$\ln(1+B) = \frac{(iBi_d + 2k_g/k_s)}{(i-1)Bi_d} \ln(1 + fY_{oa}) \qquad (40)$$

where B is the mass transfer number, f is the stochiometric coefficient and Y_{oa} is the oxygen concentration of the combustion environment. It has been assumed that all the volatiles released are combustible. It may be seen that the value of B is most sensitive to the flame location for lower values of Bi_d and that the value of B increases as the value of i decreases (corresponding to flame radius moving away from the particle).

As pointed out by Agarwal (1986), the movement of the flame front with time is expected to be complex. The simplifying assumption made in the text leads to $r_f = R_p + \delta/2$ and

$$Bi_f = 2Bi \tag{41a}$$

$$\ln(1+B) = 2\frac{(Bi_d + k_g/k_s)}{Bi_d}\ln(1+fY_{oa}) \tag{41b}$$

It may also be shown that

$$\left(\frac{T_f - T_s}{Q}\right) = \frac{B - fY_{oa}}{c_{pg}(1+fY_{oa})} \tag{42a}$$

In the fuel droplet combustion problem, Q, a constant is the sum of the sensible heat required to raise the temperature of the droplet surface to its evaporation temperature and the latent heat of vaporization. In the case of coal, the temperature of the whole solid changes with time. This changing temperature profile results in the thermal break-up of bonds; the reactions themselves being thermally neutral. Hence, the value of Q is expected to be time dependent.

To obtain an estimate for T_f, Q' is defined as the average amount of sensible heat required for the per gram release of volatiles and T_s' as the average surface temperature. If T_2 is defined as a temperature at which devolatilization is complete (Agarwal et al., 1984c), then the particle may be considered to be depleted of all volatiles when the temperature at the particle center reaches T_2. Pyrolysis data for different coals (Wen and Dutta, 1979) indicates that T_2 may vary between 900 - 1200 K. Assuming a linear temperature profile in the particle with its center at T_2,

$$Q' \sim c_{pc}\frac{(T_s' + T_2 - 2T_0)}{2V^0} \tag{42b}$$

where V^0 is the volatile content of the coal. T_s' may be estimated from the definition of the mass transfer number and equation (42) as

$$T_s' = \frac{\Delta H f Y_{oa} + c_{pg} T_a - A'(T_2 - 2T_0)}{A' + c_{pg}} \qquad (43a)$$

$$A' = B c_{ps}/(2V^0) \qquad (43b)$$

T_f may be obtained from equations (41-43)

$$T_f = \frac{\left(\frac{\Delta H f Y_{oa}}{c_{pg}} + T_a\right)\left(1 + \frac{\left(B - f Y_{oa}\right) c_{pc}}{2V^0 c_{pg}(1 + f Y_{oa})}\right)}{(A' c_{pg} + 1)}$$

$$- \left(\frac{\frac{c_{pc}}{2V^0}(T_2 - 2T_0)}{(A' + c_{pg})}\right)\left(\frac{f Y_{oa}(1+B)}{1 + f Y_{oa}}\right) \qquad (44)$$

The effects of the various terms in the expression obtained was tested numerically. In the absence of other information, the flame temperature may be approximated, for oxygen concentration less than that of air, by

$$T_f \sim 0.95\left(\frac{\Delta H f Y_{oa}}{c_{pg}} + T_a\right) \qquad (45)$$

The results of a parametric study to consider the effect of the assumptions made regarding the flame locations are shown in Figure 4.5 and 4.6. The values for the parameters chosen are $\Delta H = 2465 kJ/kg$, f = 0.3 kg fuel/kg oxygen, V^0 = 0.36, E_0 = 236 kJ/mol, σ = 36 kJ/mol, Bi = 1, T_a = 1000 K, Y_{oa} = 0.15, R_p = 1.5 mm, $k_0 = 1.67*10^{13}$ s^{-1} and α = 0.1 mm^2/s. In Figure 4.5, the effect of the variation in the assumed value of i (related to flame location as discussed earlier) on the estimation of the flame temperature is examined. Results using the detailed equation (44) as well as the approximation equation (45), are

shown. The flame temperature appears to be fairly insensitive to the value of i for i ≥ 1.5. In Figure 4.6, the time dependent devolatilization structure is shown for a convective oxidizing environment with i as a parameter. As expected, pre-ignition behaviour does not depend on flame location. Post-ignition behaviour is different for various values of i, but i = 2 appears to be a reasonable average.

The procedure for the estimation of the flame temperature for wet coal particles may be developed along similar lines. For estimation of Q, the average heat required per gram release of volatiles, the initial moisture content of the coal particle has to be considered. Q can be approximated as

$$Q \sim \frac{c_{pc}(T_s + T_2 - 2T_0) + 2C_0\lambda}{2V^0} \tag{46}$$

T_f may then be obtained as

$$T_f = \left(\frac{\frac{\Delta H f Y_{oa}}{c_{pg}} + T_a}{1 + \frac{c_{pc}B}{2c_{pg}V^0}} \right) \left(1 + \frac{\left(B - \frac{fY_{oa}}{Y_{FR}} \right) c_{pc}}{2V_{pg}^0 \left(1 + f\frac{Y_{oa}}{Y_{FR}} \right)} \right)$$

$$- \frac{f\frac{Y_{oa}}{Y_{FR}}(1+B)}{1 + f\frac{Y_{oa}}{Y_{FR}}} \left(\frac{\frac{c_{pc}}{2V^0}(T_2 - 2T_0) - C_0\frac{\lambda}{V^0}}{c_{pg} + \frac{Bc_{pc}}{2V^0}} \right) \tag{47}$$

The effect of the various parameters in equation (47) has been tested numerically. The following simpler approximation may be used.

$$T_f \cong 0.95 \left(\frac{\Delta H f Y_{oa}}{c_{pg}} + T_a \right) (1 + C_0)^{-0.17} \tag{48}$$

for $0.08 \le Y_{oa} \le 0.23$, $0.4 \le V^0 \le 0.6$, $0.1 \le C_0 \le 2.5$, $700 \le T_a \le 1200$ K.

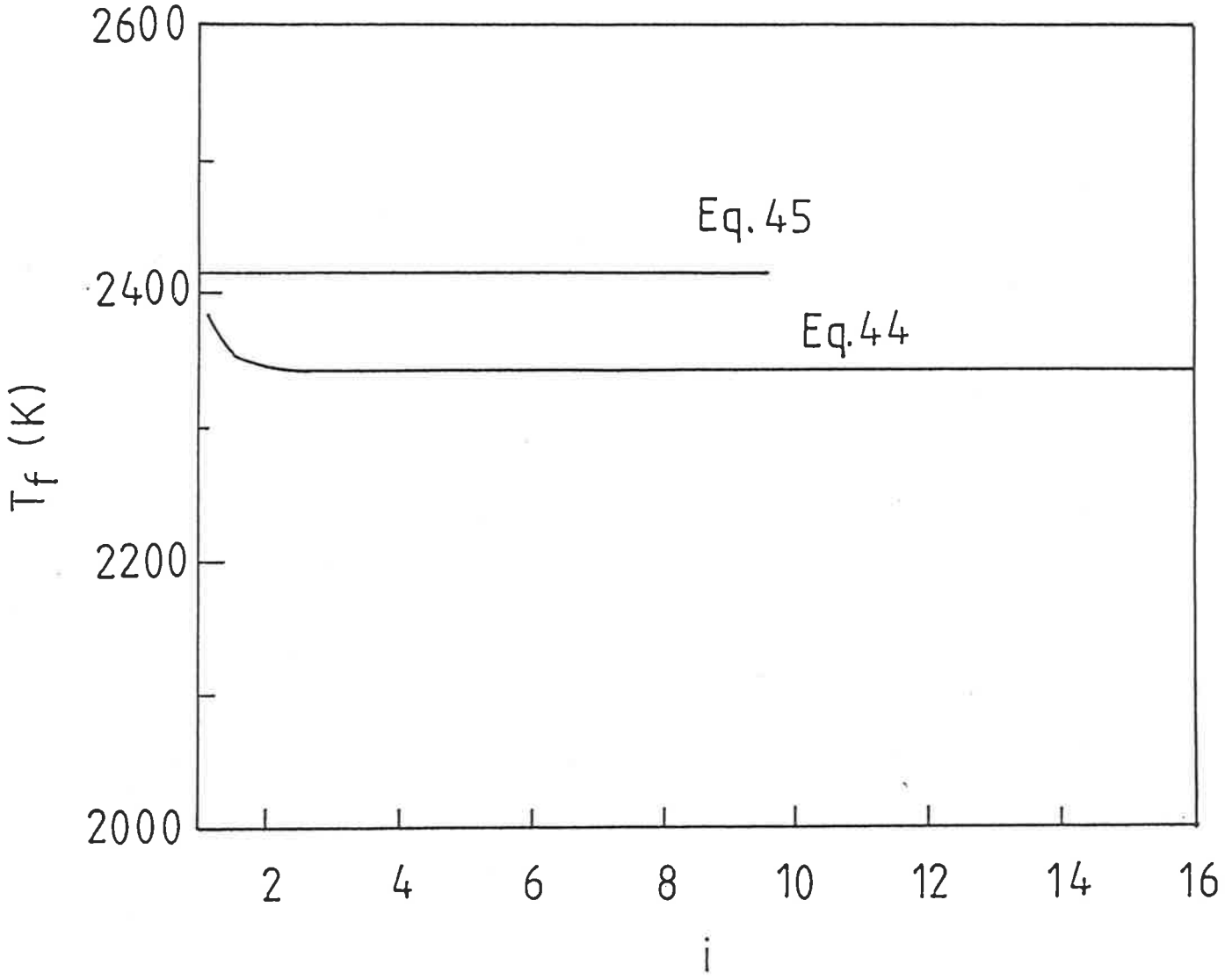

Fig. 4.5 Flame temperature as a function of the flame front position

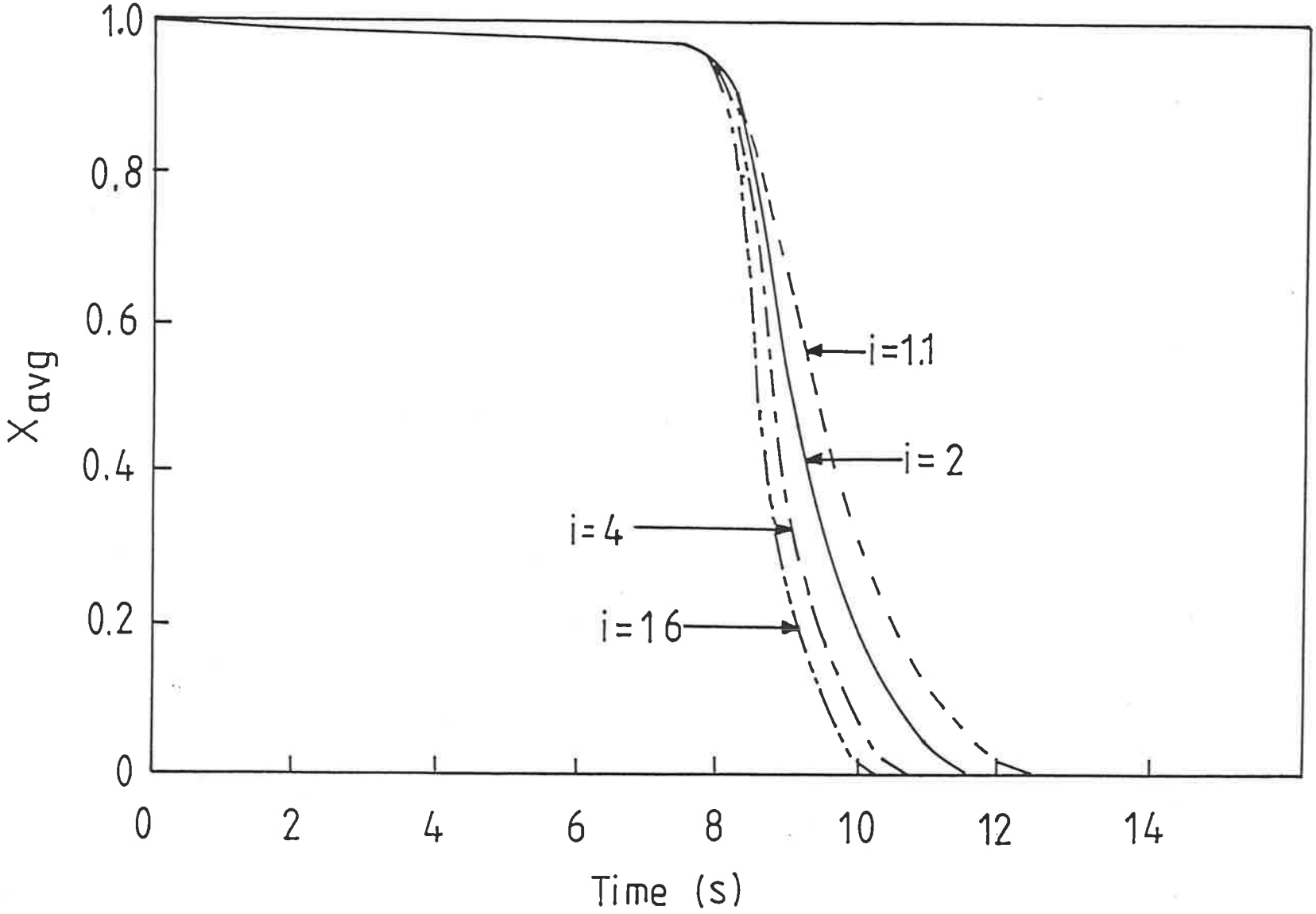

Fig. 4.6 Time dependent devolatilization structure in a convective oxidizing environment with flame front position as a parameter

Admittedly, the procedure for estimating the flame temperature is crude and more rigorous theoretical as well as experimental work is required. Kanury (1975) notes that the major restriction in the analysis involves the unity Lewis number assumption. Also, a more detailed analysis should consider the time-dependent movement of the flame front which would require the consideration of the transient conservation equations in the gas phase. Moreover, the presence of non-combustibles in the volatiles released, like CO_2, must be taken into account.

4.5 COUPLED DRYING AND DEVOLATILIZATION UNDER COMBUSTION CONDITIONS

The mathematical analysis for coupled drying and devolatilization under combustion conditions is divided into pre-ignition and post-ignition stages. The pre-ignition stage corresponds to drying and devolatilization under pyrolysis conditions as developed by Agarwal et al. (1986). Post-ignition stage is characterized by the formation of a diffusion flame around the coal particle.

The procedure for the development of the model equations is similar to coupled drying and devolatilization under pyrolysis conditions. For clarity of presentation, the major steps are outlined in the following; principal differences from earlier work have been identified. The model assumes that drying takes place from the surface of a receding wet core of radius r_c within the coal particle of initial radius R_p. Devolatilization has been modelled using the DAE kinetics as developed by Anthony and Howard (1976). The heat conduction equation, boundary conditions and devolatilization model for pre- and post-ignition stages are shown in Figure 4.7.

Using equation (20) and applying Leibnitz's rule for non-shrinking particles yields

$$\frac{d}{dt}\int_{R_p}^{r_e} v\,dr - v_e\frac{dr_e}{dt} = \alpha\frac{\partial v}{\partial r}\Big|_{r=r_e} - \alpha\frac{\partial v}{\partial r}\Big|_{r=R_p} \tag{49}$$

To solve the above equation for combustion conditions the integral has to be divided into two parts

$$\frac{d}{dt}\int_{R_p}^{r_e} v\,dr = \frac{d}{dt}\left(\int_{R_p}^{r_{e_i}} Tr\,dr + \int_{r_{e_i}}^{r_e} Tr\,dr\right) \tag{50}$$

By redefining the space variable for the pre-ignition part as $\phi' = (r - r_{e_i})/(R_p - r_{e_i})$ and the post-ignition part as $\phi' = (r - r_e)/(r_{e_i} - r_e)$ of the integral, the moving boundary in equation (49) is immobilized. Incorporating a quadratic temperature profile equation (22) and estimating an appropriate surface temperature using pseudo steady-state formulation (Agarwal and Pedler, 1986) yields the drying equation as:

$$\left(\frac{T_e + 5T_{sc}}{12}\phi_{T_i} - \frac{T_e + T_{sc}}{4}\phi_{T_i} - \frac{q(t)_c R_p}{12k}\phi_{T_i}^2\right)\phi_T$$

$$-\left(\frac{q(t)_c R_p}{12k}\phi_{T_i} - \frac{T_e + T_{sc}}{4} + \frac{T_e + L}{2}\right)\phi_T^2 + \frac{q(t)_c R_p}{12k}\phi_T^3$$

$$-A(F-1) = 0 \tag{51}$$

The coefficients of equation (51) are listed in Table 4.5

The indices i always indicate the value of the particular variable at ignition time.

The value of the total drying time can be obtained by a trial and error solution to satisfy the equality

$$A = \frac{3\alpha}{R_p^2}\left(Bi_f\frac{(T_f - T_e)}{(Bi_f + 4)}\tau_c(1-\theta_i) + Bi\frac{(T_a - T_e)}{(Bi + 4)}\tau_i\right)(1 - \phi_{ps}^2) \tag{55}$$

Table 4.5 COEFFICIENTS OF DRYING EQUATION (51)

$$\frac{q(t)R_p}{k}=\frac{Bi_{df}\phi_{ps}(T_f-T_e)}{2\phi_{ps}-Bi_{df}(\phi_{ps}-1)} \tag{52}$$

$$\frac{T_{s_c}-T_e}{T_f-T_e}=\frac{Bi_{df}(1-\phi_{ps})}{2\phi_{ps}-Bi_{df}(\phi_{ps}-1)} \tag{53}$$

$$L=\frac{\lambda' C_0}{c_{pc}} \tag{32}$$

$$A=\frac{q(t)_i R_p}{12k}\left(1-\phi_{T_i}\right)\left(1-\phi_{T_i}^2\right)-\frac{T_e+5T_{s_i}}{12}\left(1-\phi_{T_i}\right)-\frac{T_e+T_{s_i}}{4}\phi_{T_i}\left(1-\phi_{T_i}\right)$$
$$+\frac{q(t)_c\,|_{\theta=\theta_{dry}} R_p}{12k}\phi_{T_i}^3-\frac{T_e+5T_{s_c}\,|_{\theta=\theta_{dry}}}{12}\phi_{T_i}^2+\frac{T_e+L}{2} \tag{54}$$

$$F=\frac{\phi_{ps}^2-1}{\phi_{ps}^2\,|_{\theta=\theta_{dry}}-1} \tag{33}$$

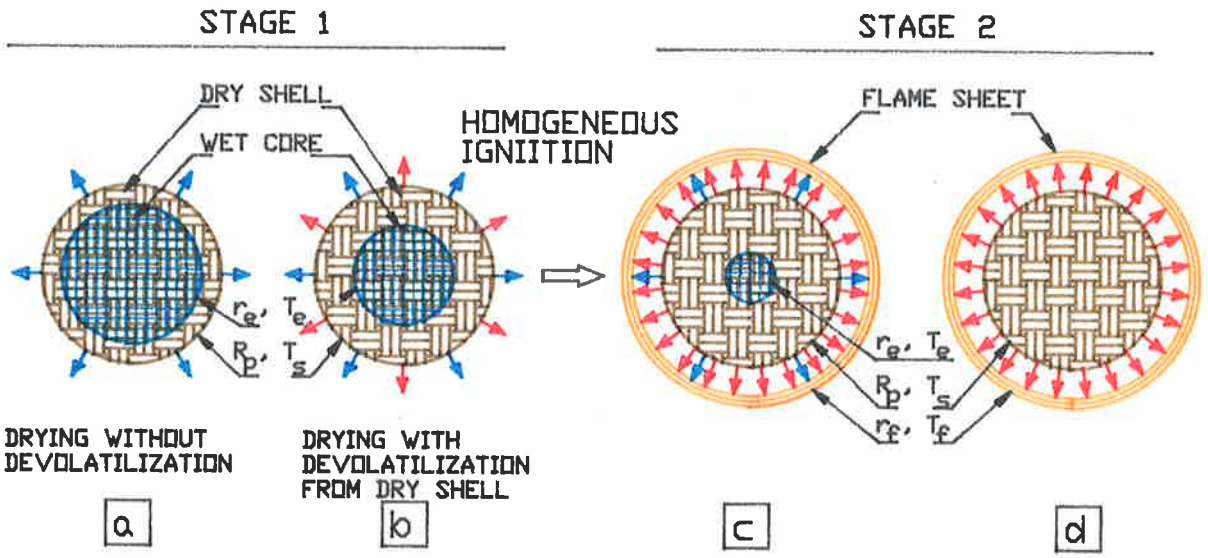

DRYING (a,b,c)	
$\frac{\partial T}{\partial r}=\frac{\alpha}{r^2}\frac{\partial}{\partial r}\left(r^2\frac{\partial T}{\partial r}\right)$	$r_e \le r \le R_p$ (17)
boundary conditions	
$k\frac{\partial T}{\partial r}\Big\|_{r=r_e}=\lambda' C_0 \rho_c \frac{dr_e}{dt}$	(18*b*)
$k\frac{\partial T}{\partial r}\Big\|_{r=R_p}=h(T_a-T_s)$ (18*c*) (a,b)	$k\frac{\partial T}{\partial r}\Big\|_{r=R_p}=h(T_f-T_s)$ (*c*) (18*d*)

DEVOLATILIZATION (b,c,d)
$X_{avg}=\frac{3}{R_p^3}\int_0^{R_p}\int_0^{\infty}\exp\left(-k_0\int_0^t e^{-E/RT(r,t)}dt\right)f(E)dE\,r^2dr$ (16*a*)
$f(E)=(\sigma(2\pi)^{1/2})^{-1}\exp\left(-\frac{(E-E_0)^2}{2\sigma^2}\right)$ (16*b*)

TEMPERATURE PROFILE	
(a,b,c) $T(r,t)=T_e+(T_s-T_e)(2\phi'-\phi'^2)+q(t)\frac{(R_p-r_e)}{k}(\phi'^2-\phi')$ (24)	(d) $T(r,t)=T_f-\sum_{i=1}^{\infty}N_i\frac{\sin\beta_i r/R_p}{\beta_i r/R_p}\exp\left(-\frac{\beta_i^2 t'}{R_p^2}\right)$ (56)

Figure 4.7 Mathematical model for drying and devolatilization under combustion conditions

The devolatilization model and the respective temperature profiles for the different stages is depicted in Figure 4.7. When the particle is dry, devolatilization will still occur. The initial temperature condition for this case will be the temperature profile of the dry particle where $r_e = 0$. Then

$$T(r,t=\tau) = T_e + \left(T_s|_{\theta=\theta_{dry}} - T_e\right)\left(2\left(\frac{r}{R_p}\right) - \left(\frac{r}{R_p}\right)^2\right) + q(t)|_{\theta=\theta_{dry}}\left(\frac{R_p}{k}\right)\left(\left(\frac{r}{R_p}\right)^2 - \left(\frac{r}{R_p}\right)\right) \qquad (56)$$

Using the heat conduction equation with a convective boundary and initial condition equation (56), the temperature profile can be written as

$$T(r,t') = T_f - \sum_{i=1}^{\infty} N_i \frac{\sin \beta_i r/R_p}{\beta_i r/R_p} \exp\left(-\frac{\beta_i^2 t' \alpha}{R_p^2}\right)$$

$$0 < r < R_p \qquad (57)$$

The coefficients of equation (57) are listed in Table 4.6

In Figures 4.8 - 4.13 the results of the parametric studies for drying, devolatilization and volatiles combustion are shown. Ignition is assumed to take place when 5% of the volatiles are released. As can be seen in the figures as soon as ignition takes place the drying devolatilization rates increase rapidly. To demonstrate the influence of the operating conditions , a set of standard parameters are chosen. Each parameter is varied in turn. The standard parameters are C_0 = 1.1 g moisture/g dry coal, Bi_d = 4, R_p = 4 mm, T_g = 1000 K, Y_{oa} = 0.23.

In Figure 4.8 sample calculations are shown to demonstrate the effect of the heat transfer Biot number. For lower Biot numbers, the heat-up time a for the particle is larger and therefore the times required for complete drying and devolatilization are larger too. For Bi_d = 1 the particle could be considered as isothermal, there is almost no devolatilization as long as the moisture content, acting as a heat sink, is present. Therefore for low Biot numbers drying and devolatilization may be treated as sequential. For large Biot

Table 4.6 COEFFICIENTS OF EQUATION (57)

$$N_i = 2(D_1F_1 - (2D_2 - D_3)F_2 - (D_3 - D_2)F_3)/F_4 \tag{58a}$$

$$D_1 = (T_f - T_e) \tag{58b}$$

$$D_2 = (T_s|_{t'=0} - T_e) = \frac{Bi_{fd}(T_f - T_e)(1 - \phi_{ps})}{2\phi_{ps} + Bi_{fd}(1 - \phi_{ps})} \tag{58c}$$

$$D_3 = q(t)|_{t'=0} = \frac{\phi_T Bi_{fd}(T_f - T_e)}{2\phi_{ps} + Bi_{fd}(1 - \phi_{ps})} \tag{58d}$$

$$F_1 = \sin\beta_i - \beta_i \cos\beta_i \tag{58e}$$

$$F_2 = \cos\beta_i\left(\frac{2}{\beta_i} - \beta_i\right) + 2\sin\beta_i - \frac{2}{\beta_i} \tag{58f}$$

$$F_3 = \cos\beta_i\left(\frac{6}{\beta_i} - \beta_i\right) + 3\sin\beta_i\left(1 - \frac{2}{\beta_i^2}\right) \tag{58g}$$

$$F_4 = \beta_i - \sin\beta_i \cos\beta_i \tag{58h}$$

$$t' = t - \tau \tag{58i}$$

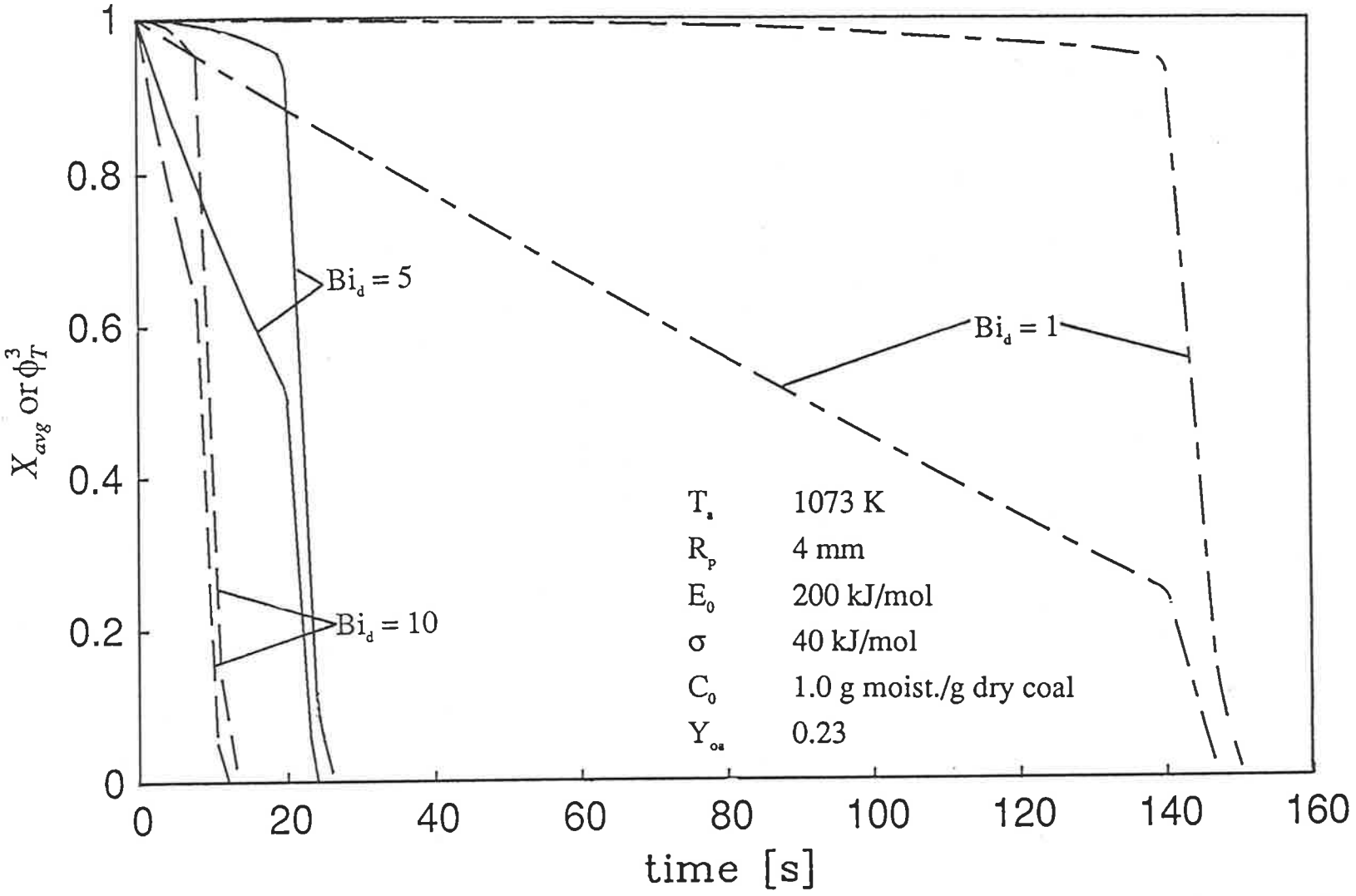

Fig. 4.8 Effect of Biot number on drying and devolatilization under combustion conditions

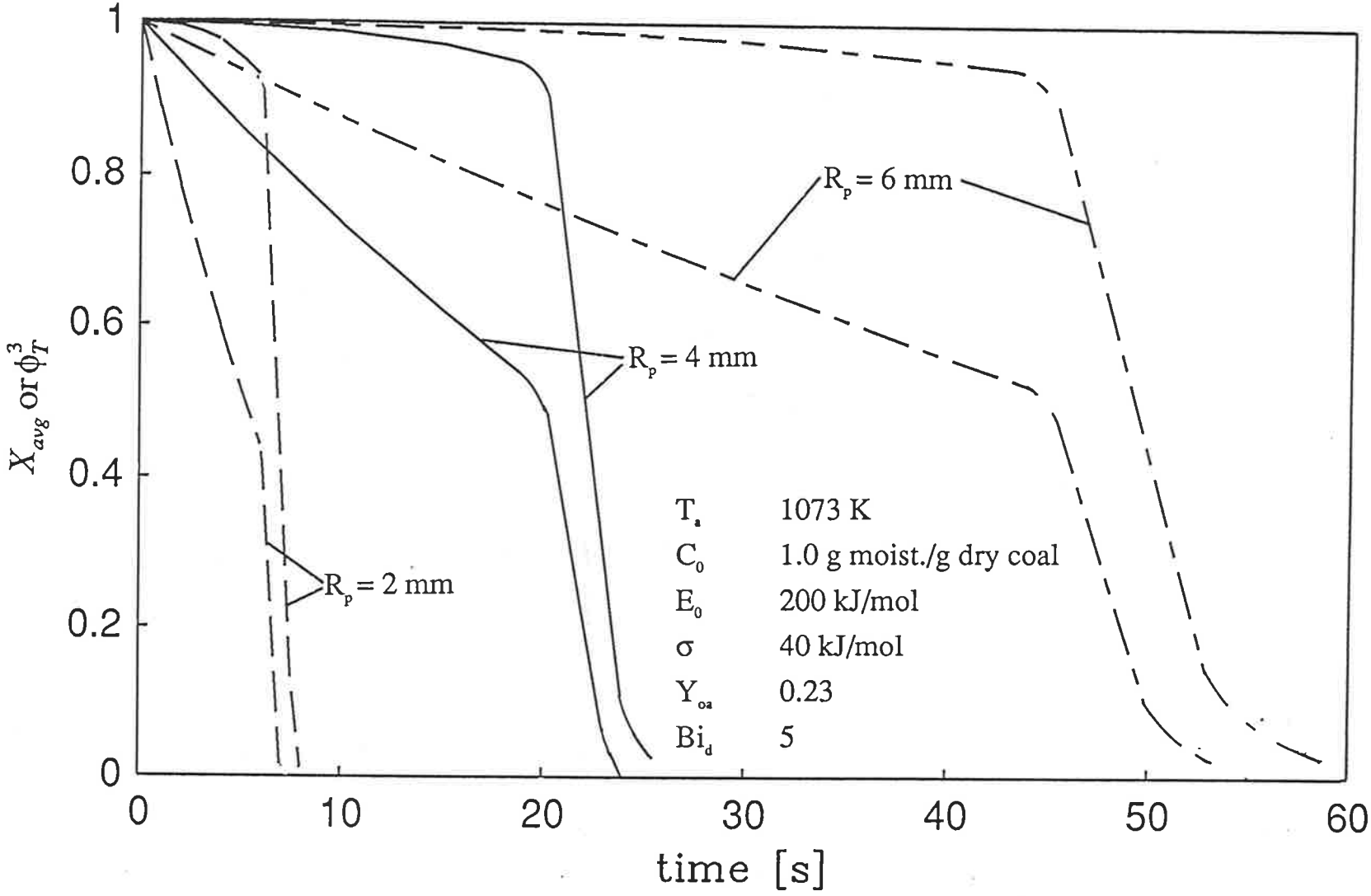

Fig. 4.9 Effect of particle radius on drying and devolatilization behaviour under combustion conditions

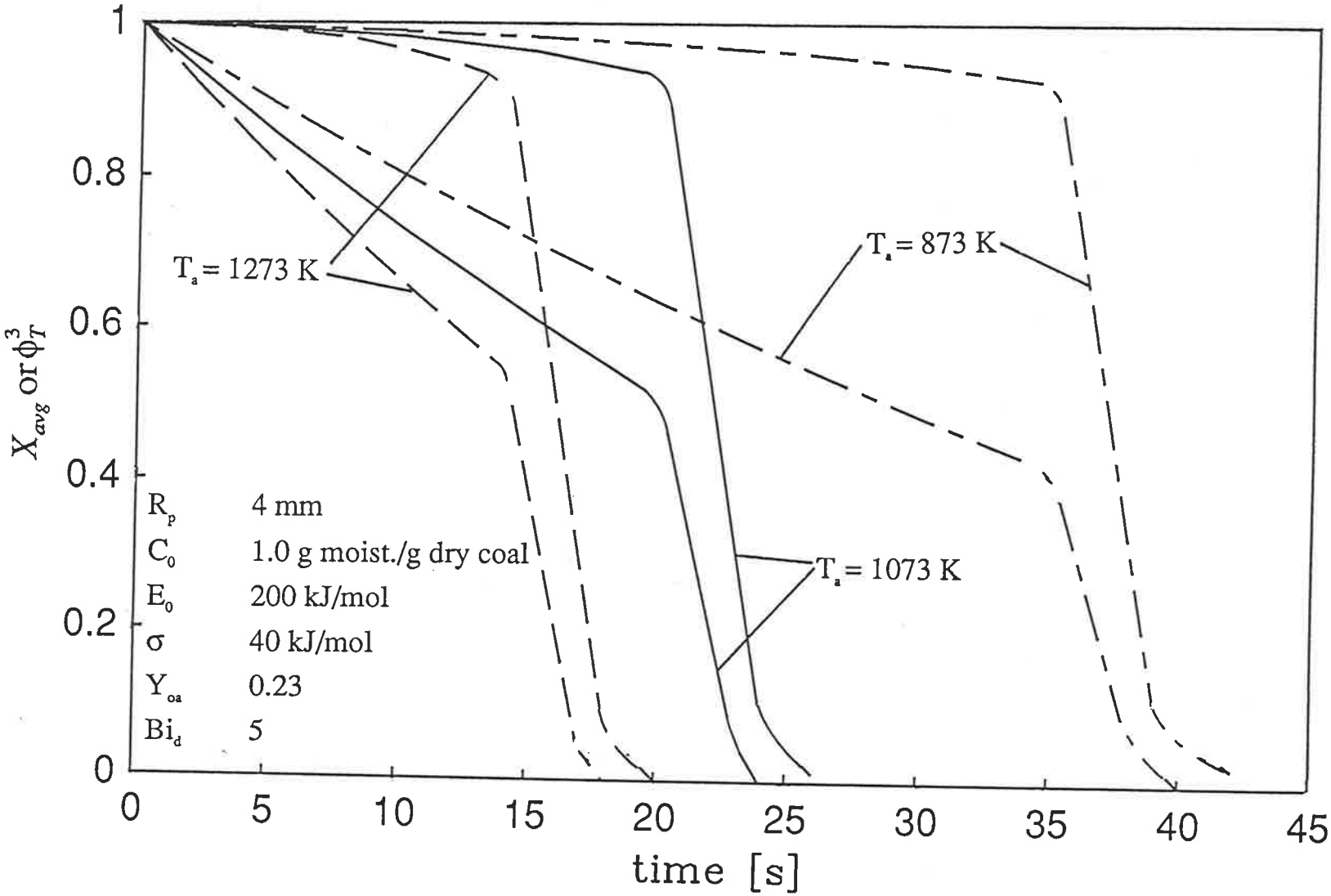

Fig. 4.10 Effect of ambient temperature on drying and devolatilization behaviour under combustion conditions

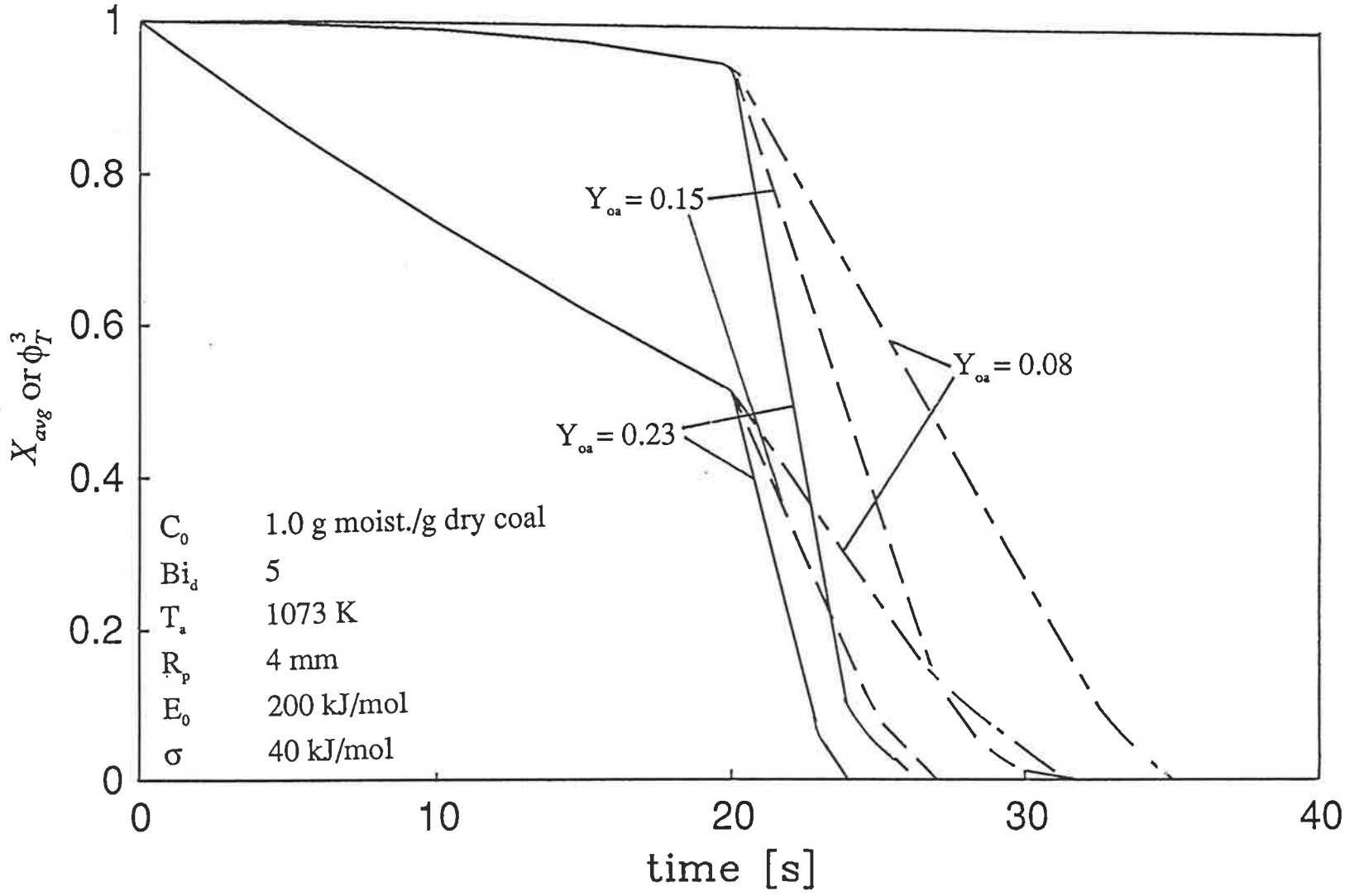

Fig. 4.11 Effect of oxygen mass concentration on drying and devolatilization behaviour under combustion conditions

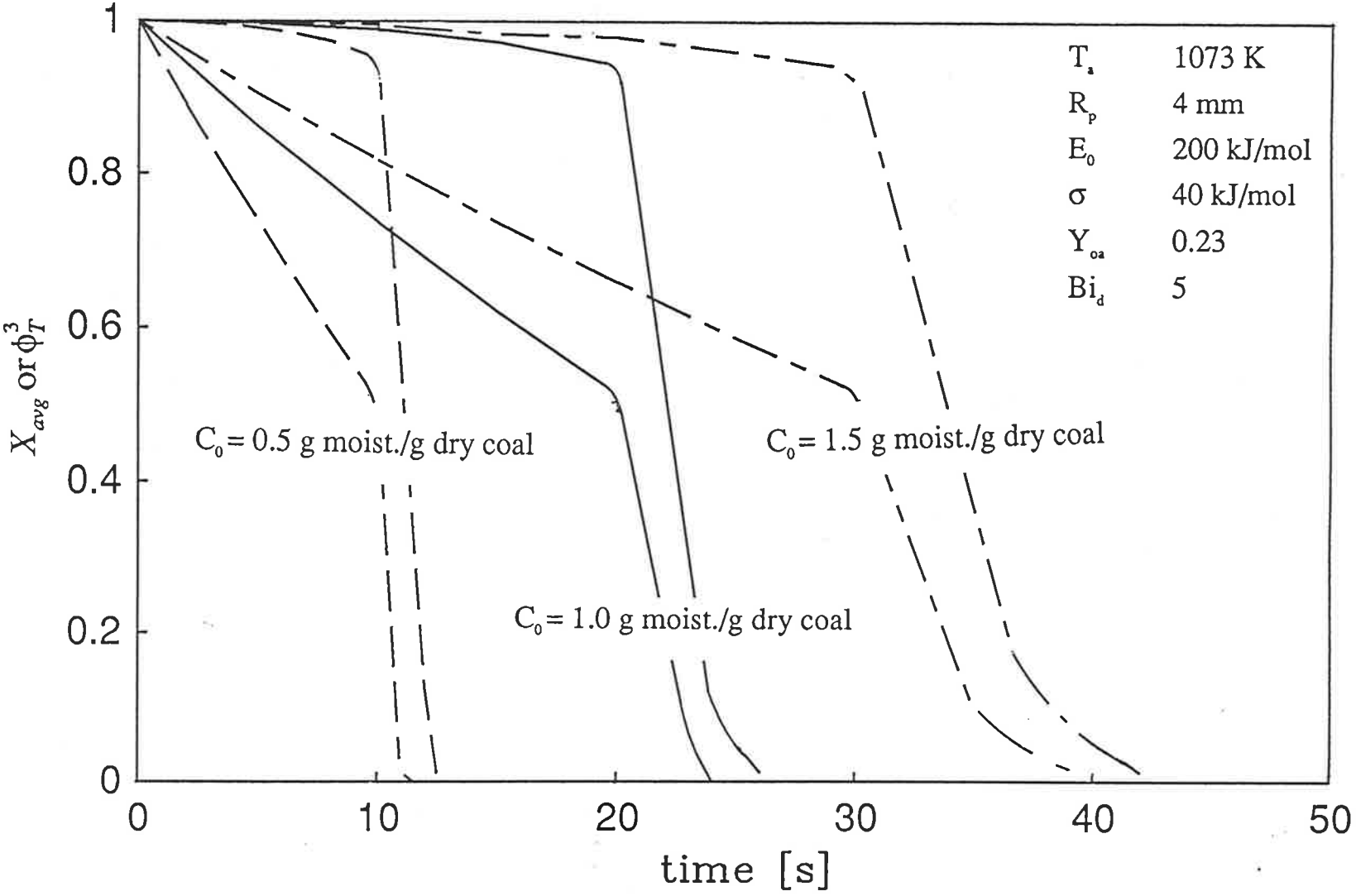

Fig. 4.12 Effect of initial moisture content on drying and devolatilization behaviour under combustion conditions

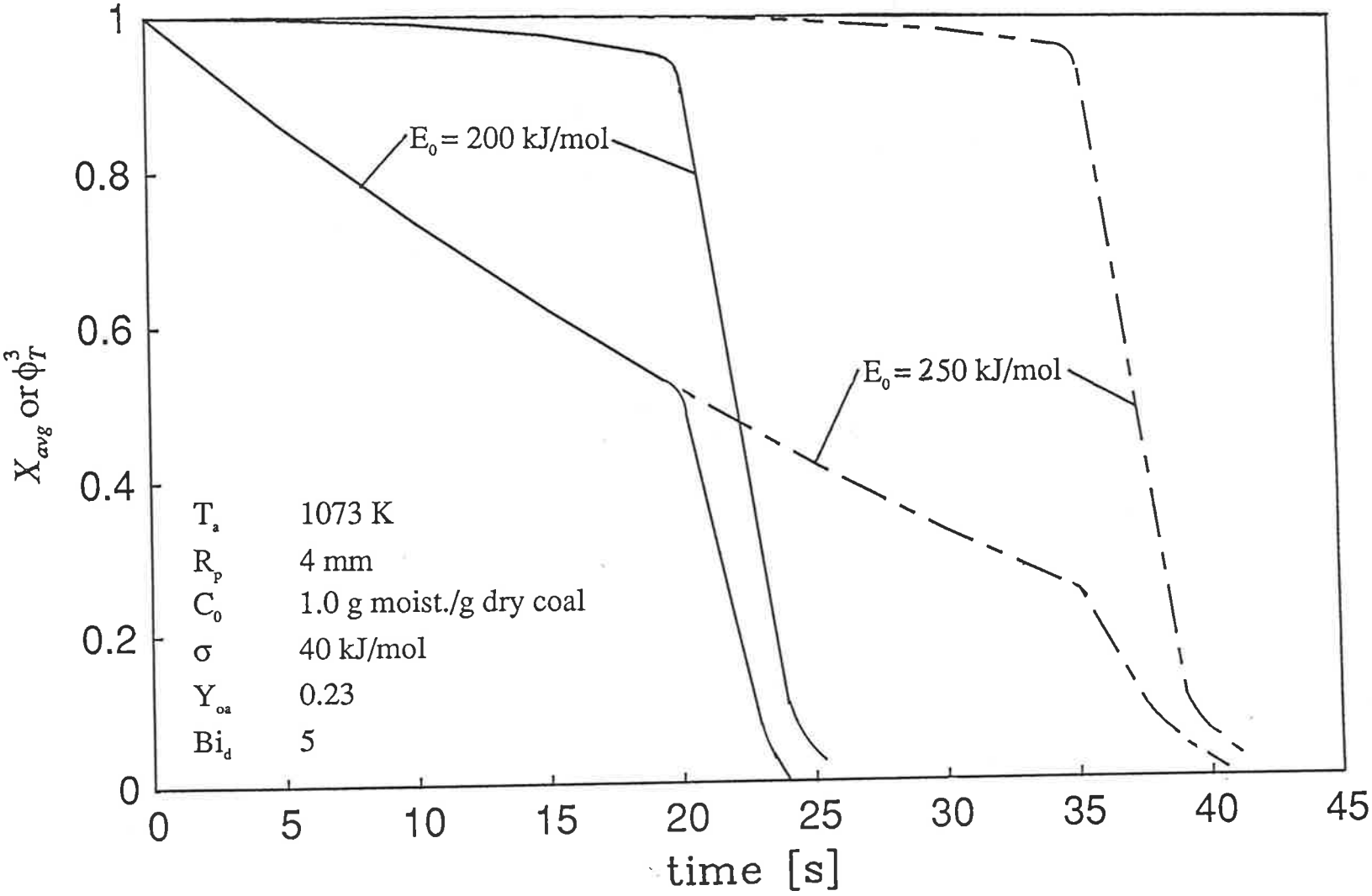

Fig. 4.13 Effect of coal type on drying and devolatilization behaviour under combustion conditions

numbers, a coupled approach is more reasonable. In Figure 4.9 the effect of the variation of particle size is shown. As expected smaller particle dry and devolatilize much more rapidly. In Figure 4.10 the effect of the variation of ambient temperature is considered. As expected, for lower ambient temperatures, the drying and devolatilization times are much larger. A larger ignition delay is also predicted. Figure 4.11 shows the effect of variation in oxygen concentration of the combustion environment. As would be expected the pre-ignition stage is not affect by the flame temperature. It can be seen that, for the conditions simulated, changing oxygen concentration from 8% to 23% results in ~ 20% reduction of the drying and devolatilization times. The effect of change in the initial moisture content is shown in Figure 4.12. Higher moisture contents result in a larger ignition delay as well as drying and devolatilization times. In Fig. 4.13 different coal types are simulated by different mean activation energies. As expected the initial drying stage prior to ignition is not effected by coal type. However the total drying time for coal with lower values of mean activation energy is smaller due to earlier ingition time.

4.6 COMBUSTION OF VOLATILES IN GAS FLUIDIZED BEDS

The schematic representation of the model is shown in Figure 4.14. It is assumed that the coal particle moves alternatively between bubble and the emulsion phases. Such mobility for char particles, at least in shallow beds, has been visually observed by Chakraborty and Howard (1978). The characteristic frequency describing this particle mobility between the phases as well as the relative amounts of time spent in each phase for the bubble-emulsion cycle depend on the hydrodynamics of the bed.

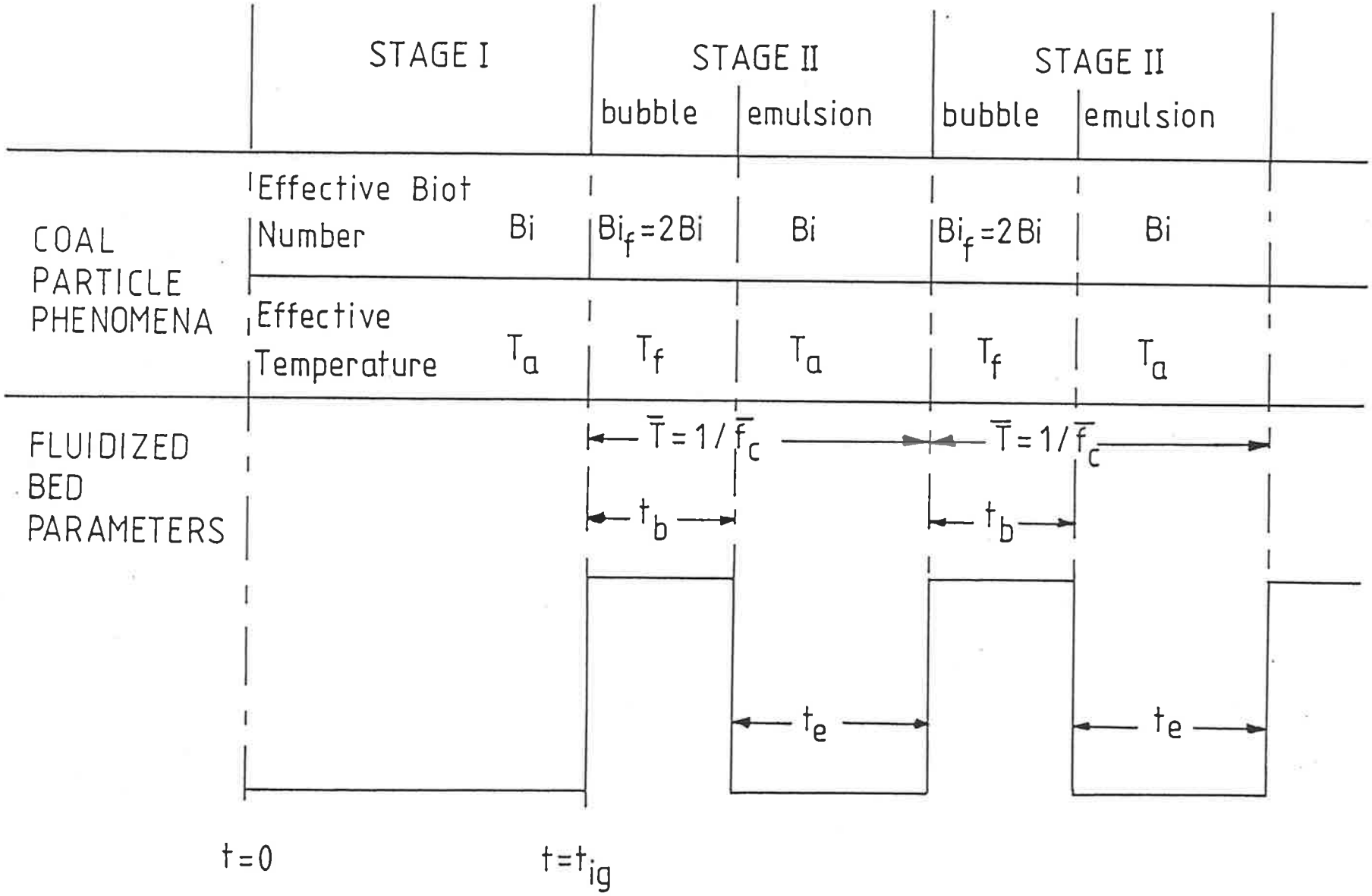

Fig. 4.14 Schematic presentation of the model

Based on the visual evidence of Aoyagi and Kunii (1974), Cowley and Roberts (1981) as well as Prins (1987), it is assumed that homogeneous combustion of volatiles takes place (in a diffusion flame mode) when the coal particle is in the bubble phase. Pyrolysis like conditions are assumed to prevail in the pre-ignition period as well as in each time interval the coal particle is in the emulsion phase. It may be noted that probe measurements of oxygen concentrations in fluidized bed combustors (Boiarski et al., 1984; Minchener and Stringer, 1984) have indicated sharp fluctuations - the lows corresponding to the emulsion phase and the highs corresponding to the bubble phase. From this point of view, under steady combustor operating conditions, char or volatile combustion in the emulsion phase appears to be less likely. The devolatilization behaviour for the two stages and in each phase depends on the chemical reaction and transport phenomena associated with the coal.

The mathematical description for the coal related phenomena and the fluidized bed parameter estimation can thus be 'decoupled' and is presented in the following:

4.6.1 COAL PARTICLE PHENOMENA

The volatile combustion analysis, for the purpose of mathematical description, can be divided into two major stages: the pre-ignition stage and the post-ignition stage which includes two minor stages representing the particle being in the bubble or in the emulsion phase. The volumetric average fractional amount of volatiles retained within a non-isothermal, spherical, non-swelling particle of radius R_p can be expressed (Agarwal et al., 1984b) by using the non-isothermal distributed activation energy formulation of Anthony and Howard (1976) for the overall decomposition of coal (equations (16a-b)).

The calculation for the devolatilization history within each of the above stages then depends on the estimation of the spatial and temporal temperature distribution within the

coal particle for each stage. In the following, the derivation of the temperature profiles for the stages (pre-ignition, post-ignition: bubble phase, emulsion phase) are presented. These profiles may then be used in conjunction with equations (16a-b) to obtain the time resolved devolatilization characteristics. Nested numerical integration is required - the basic technique for such integration has been discussed by Agarwal et al. (1984b).

The reactions leading to the production of volatiles from coal are thermally neutral (Anthony and Howard, 1976). Then the required temperature profile is obtained from the solution of the unsteady state heat conduction equation, in one-dimensional spherical co-ordinates for a convective boundary condition, as (Jacob, 1959)

$$T(r,\theta) = T_{eff} - \sum_{k=1}^{\infty} N_k \frac{\sin \beta_k r/R_p}{\beta_k r/R_p} \exp\left(-\frac{\beta_k^2 \alpha \theta}{R_p^2}\right) \qquad (59a)$$

where θ is the time interval under consideration, T_{eff} is the temperature of the exterior source of heat to the particle and β_k are the roots of the transcendental equation

$$\beta \cos \beta = (1 - Bi_r) \sin \beta \qquad (59b)$$

N_k are the coefficients which depend on the initial temperature condition $T(r, \theta = 0)$ and Bi_r is the heat transfer Biot number based on the particle radius.

In the first stage - before the initial ignition takes place - whether the coal particle is in the emulsion or in the bubble phase, pyrolysis like conditions prevail. During this particle heat-up period, the temperature profile may be obtained as

$$T(r,\theta) = T_a - \sum_{i=1}^{\infty} A_i \frac{\sin \beta_i r/R_p}{\beta_i r/R_p} \exp\left(-\frac{\beta_i^2 \alpha \theta}{R_p^2}\right) \qquad (60a)$$

where

$$A_i = 2(T_a - T_o)\left[\frac{\sin\beta_i - \beta_i\cos\beta_i}{\beta_i - \sin\beta_i\cos\beta_i}\right] \qquad (60b)$$

recognizing that $T_{eff} = T_s$ for $0 < \theta < t_{ig}$ and $T(r,\theta=0) = T_o$. β_i 's are the roots obtained from equation (59b) with $Bi_r = Bi$.

For a single particle in convective flow, the heat transfer Biot number can be estimated using available correlations (Agarwal, 1988). For a fluidized bed, however the heat transfer is affected by gas convection as well as particle-particle interaction and radiation. Correlations are available for gas-particle heat transfer in beds of monosize particles. Heat transfer to and from cylinders or spherical objects, large in comparison with bed particle size and immersed at a fixed in-bed location, has also been studied extensively (Kunii and Levenspiel, 1969). However, transfer from a freely moving large particle in a bed of smaller and more dense particles has received scant attention and the estimation of Biot number is difficult. Due to the current lack of information the correlations summarized by Kunii and Levenspiel (1969) for estimating the particle Nusselt number in fluidized beds has been used

$$\mathrm{Nu} = 0.03Re^{1.3} \qquad Re < 80 \qquad (61a)$$

for $Re \geq 80$, the fluidized bed gas-particle heat transfer has been found to lie between the correlations for fixed bed and single particles. Hence,

$$\mathrm{Nu} = 2.0 + 1.2Re^{1/2}Pr^{1/3} \qquad Re \geq 80 \qquad (61b)$$

$$Bi_d = \mathrm{Nu}\,k_g/k_s \qquad (61c)$$

Using these correlations and the reported values for thermophysical properties, it may be shown that the Biot number may range from 1 to 20 for particle sizes and operating conditions of interest in fluidized bed combustion (Agarwal et al., 1984b).

Initial ignition is assumed - for the particle sizes, bed temperatures and oxygen concentrations of interest in fluidized bed combustion - to take place when app. 5% of the initial volatile content of the coal has been removed. Though this serves as a simplifying assumption for the present analysis - more detailed calculations would obviously be preferable - the importance of ignition phase criterion increasing with decreasing particle sizes.

As visualized in the model description, homogeneous ignition of coal volatiles would take place when the coal particle is in the bubble phase. To formulate the heat conduction problem, the flame temperature and the flame radius have to be specified to obtain the requisite convective boundary condition. The initial condition may be derived as the temperature profile at the time of ignition or when the particle enters the bubble phase. A detailed outline for the estimation of flame temperature has been discussed in a earlier section.

The solution of the heat conduction equation leads to

$$T(r,\theta) = T_f - \sum_{j=1}^{\infty} N_j \frac{\sin \beta_j r/R_p}{\beta_j r/R_p} \exp\left(-\frac{\beta_j^2 \alpha \theta}{R_p^2}\right) \qquad (62a)$$

where

$$N_j = 2.0(T_f - T_a)\left[\frac{\sin\beta_j - \beta_j \cos\beta_j}{\beta_j - \sin\beta_j \cos\beta_j}\right]$$

$$+ \sum_{i=1}^{\infty}\left(N_i \exp\left(-\frac{\beta_i^2 \alpha t_e}{R_p^2}\right)\right)\frac{\beta_j^2}{\beta_i}\left(\frac{\sin(\beta_i - \beta_j)}{\beta_i - \beta_j} - \frac{\sin(\beta_i + \beta_j)}{\beta_i + \beta_j}\right)$$

$$/(\beta_j - \sin\beta_j \cos\beta_j) \qquad (62b)$$

recognising that $T_{eff} = T_f$ for $t_e < \theta < t_e + t_b$. β_j's are the roots of equation (59b) obtained with $Bi_r = Bi_f = 2Bi$. it may be noted that for the period $t_{ig} < \theta < t_{ig} + t_b$ as shown in Figure 4.14, the term $N_i \exp(-\beta_i^2 \alpha t_e / R_p^2)$ in equation (62) is equivalent to $A_i \exp(-\beta_i^2 \alpha t_e / R_p^2)$. The coefficient N_i in general, are defined from the consideration of the behaviour in the emulsion phase as following.

At the end of its residence time in the bubble phase, the coal particle is transferred to the emulsion phase resulting in volatile combustion becoming negligible. The solution to the heat conduction equation may then be obtained with the initial temperature condition obtained from the previous stage. The temperature profile may be derived as

$$T(r,\theta) = T_a - \sum_{i=1}^{\infty} N_i \frac{\sin \beta_i r/R_p}{\beta_i r/R_p} \exp\left(-\frac{\beta_i^2 \alpha \theta}{R_p^2}\right) \qquad (63a)$$

where

$$N_i = 2.0(T_a - T_f)\left[\frac{\sin\beta_i - \beta_i \cos\beta_i}{\beta_i - \sin\beta_i \cos\beta_i}\right]$$

$$+ \sum_{j=1}^{\infty}\left(N_j \exp\left(-\frac{\beta_j^2 \alpha t_b}{R_p^2}\right)\right)\frac{\beta_i^2}{\beta_j}\left(\frac{\sin(\beta_j - \beta_i)}{\beta_j - \beta_i} - \frac{\sin(\beta_j + \beta_i)}{\beta_j + \beta_i}\right)$$

$$/(\beta_i - \sin\beta_i \cos\beta_i) \qquad (63b)$$

for $T_{eff} = T_a$, $t_b < \theta < t_b + t_e$

The solutions for the devolatilization in each stage of the bubble-emulsion cycle may then be obtained using equations (16a-b), (59) - (63). A computational flow chart is shown in Figure 4.15.

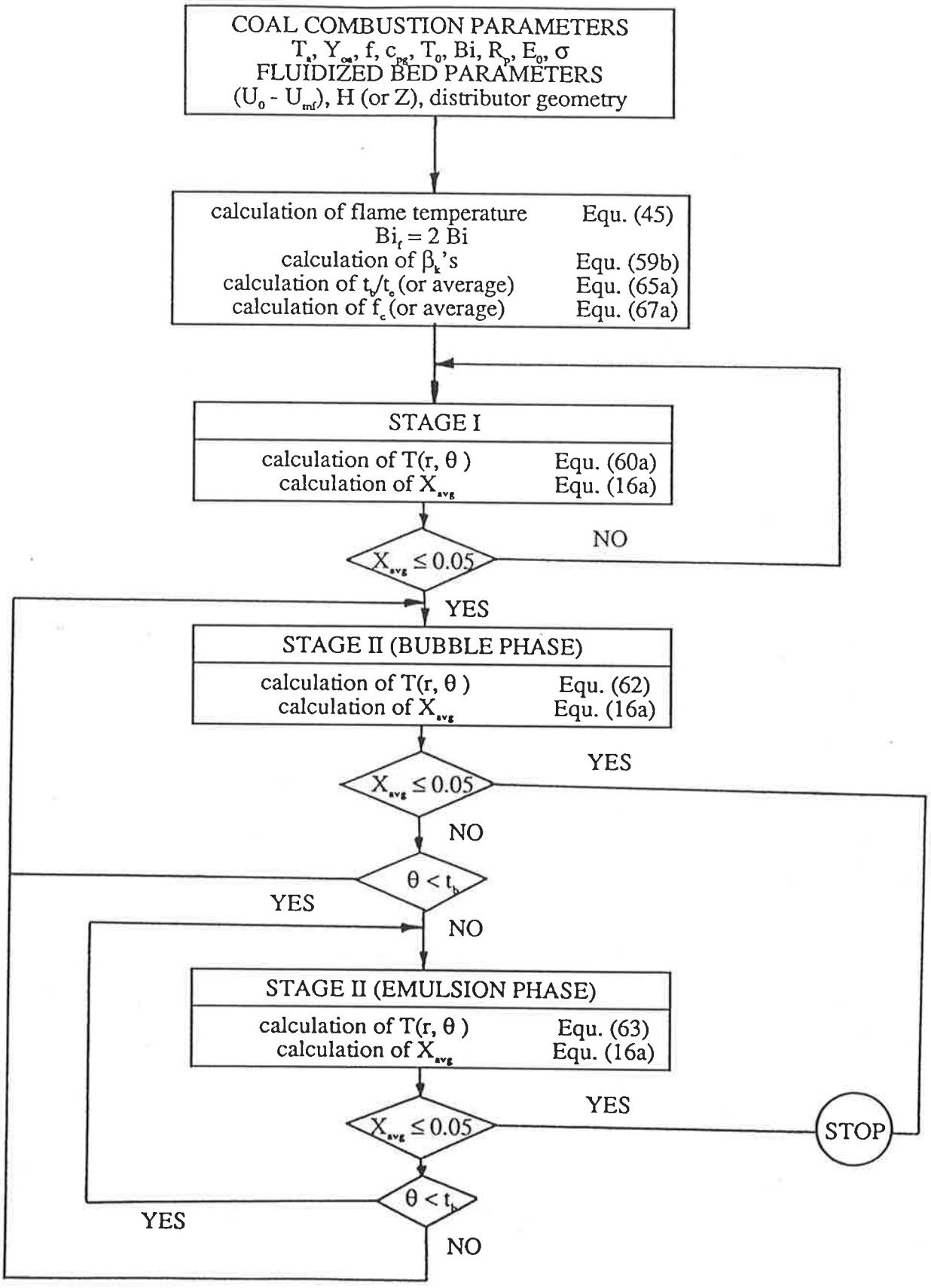

Fig. 4.15 Computational flow-sheet for combustion of coal volatiles in fluidized beds

4.6.2 INTERACTION OF VOLATILE COMBUSTION WITH FLUIDIZED BED PARAMETERS

As visualised by the model, after the initial ignition the coal particle goes through a sequence of volatile combustion (bubble) and pyrolysis (emulsion phase) steps. The fluidized bed parameters determine the frequency at which these transitions take place as well as the relative amount of time spent between the two phases for each cycle. Agarwal (1985) has been developed a model for bubble coalescence and growth in non-slugging gas fluidized beds based on the population balance approach. The model was used to obtain distributions and averages of bubble characteristics. The model was also used to obtain expressions for bubble point and level frequencies; and in conjunction with the two-phase theory, for number concentration and bed expansion. From the model expressions, the height dependent local volume fraction constituting the bubble phase is obtained as

$$\varepsilon_b = \frac{U_o - U_{mf}}{\bar{v}'} \qquad (64a)$$

where $\bar{v}'$ is the average of the bubble velocity density function and is expressed in terms of the initial bubble diameter d_{bo} and local height above the distributor , Z, as

$$\bar{v}' = (U_o - U_{mf}) + 22.26 d^{1/2} + 8.2 Z^{0.4} \qquad (64b)$$

the initial bubble diameter may be estimated for the geometry of the distributor under consideration using the correlations of Miwa et al. (1972).

Assuming that the relative amount of time spent between the two phases is equal to the relative fractions of each phase at any specific height within the bed, it can be shown that

$$\frac{t_b}{t_e} = \frac{(U_o - U_{mf})}{22.26 d_{bo}^{1/2} + 8.2 Z^{0.4}} \tag{65a}$$

The average value over the total bed height, H, may then be obtained

$$\left[\frac{t_b}{t_e}\right]_{avg} = 0.61\left[\frac{(U_o - U_{mf})}{H^{0.4}\Phi^{1.5}}\right]\left(\frac{\Phi^{1.5}}{3} - \Phi^{0.5} + \tan^{-1}\Phi^{0.5}\right) \tag{65b}$$

where

$$\Phi = 0.37 H^{0.4}/d_{bo}^{1/2} \tag{65c}$$

the frequency of the bubble-emulsion cycle would depend on the frequency with which bubbles strike/envelope the coal particle. The level frequency of bubbles (the number of bubbles passing a level per second) is given by (Agarwal, 1985)

$$f_l = \frac{13.1}{\overline{d}_b{}' Z^{0.6}} \tag{66a}$$

where

$$\overline{d}_b{}' = (d_{bo}^{1/2} + 0.37 Z^{0.4})^2 \tag{66b}$$

Then multiplying the level frequency with the projected area of the coal particle ($= \pi d^2/4$) yields the required cycle frequency as

$$f_c = \frac{10.3 d^2}{(d_{bo}^{1/2} + 0.37 Z^{0.4})^4 Z^{0.6}} \tag{67a}$$

The average value over the total bed height may also be calculated

$$\overline{f}_c = \frac{23.3 d^2}{H d_{bo}^{1.5}}\left[\frac{(1+\Phi)^3 - 1}{(1+\Phi)^3}\right] \tag{67b}$$

It may be noted that the local expressions for frequencies would be more appropriate for constrained coal particles as in the experiments of Yates et al. (1980). The average values computed here are rigidly applicable if it can be assumed that, during the entire devolatilization process, the coal particle could be at any location with an equal probability. It is obvious, that solid circulation patterns and the location of the coal injection ports would influence the frequency values. It is felt, however, that the present technique provides a fairly reasonable method for the determination of devolatilization characteristics of individual coal particles in fluidized beds as well as assessing the influence of the fluidized bed design parameters on volatile combustion.

In the following, the results of parametric studies made with the model are presented to study the effect of fluidized bed variables on volatile combustion. The complete computational flowchart is shown in Figure 4.15. In all cases, a porous distributor is simulated using (Miwa et al., 1972)

$$d_{bo} = 0.00376(U_0 - U_{mf})^2 \qquad (68a)$$

Calculations may be performed analogously for perforated plate distributors using (Agarwal, 1985)

$$d_{bo} = 0.347(A_t(U_0 - U_{mf})/n_d)^{0.4} \qquad (68b)$$

In Figure 4.16a, the local residence time ratio t_v/t_c is plotted as a function of height within the bed with the excess gas velocity as a parameter. It may be seen that the values are sensitive to bed height only for Z < 20 cm.

In Figure 4.16b, the average values (using equation (65b)) are plotted with total bed height as a parameter. It may be seen that for larger values of excess gas velocity, the average value does not depend strongly on the total bed height.

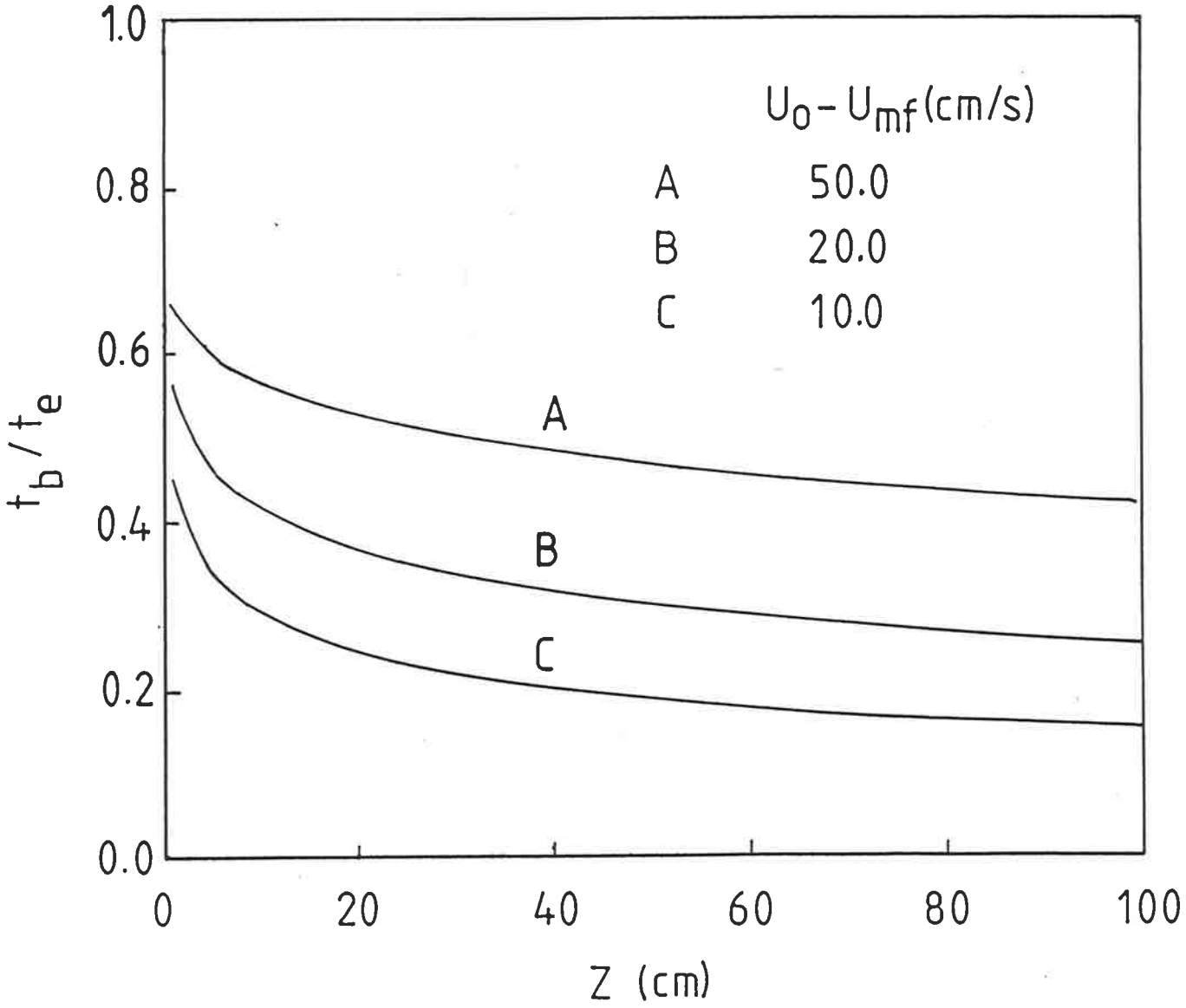

Fig. 4.16a Dependence of the phase residence time ratio on height within the fluidized bed

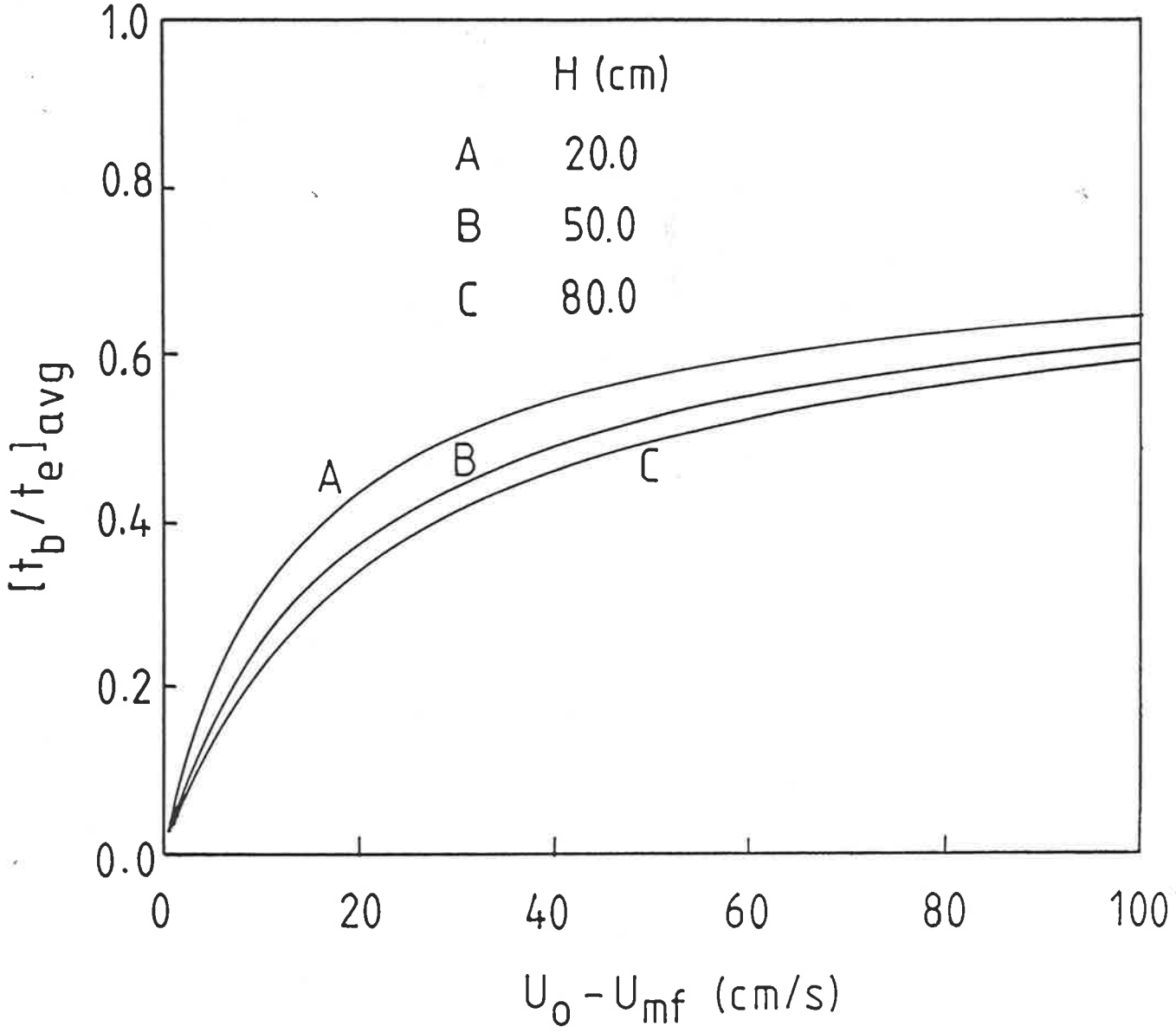

Fig. 4.16b Dependence of the height averaged phase residence time ratio on excess gas velocity

In Figures 4.17a-d, local and average frequency values of the bubble-emulsion cycle are plotted. From Figures 4.17a-b, it may be seen that the local frequency increases with the size of the coal particle and decreases with increasing values of d_{bo} (reflecting the excess gas velocity through equations (68a-b)). A similar trend is observed for the average values of the frequency (Figures (4.17c-d).

In Figures 4.18 and 4.19, sample calculations are presented to demonstrate the effect of operating variables and bed parameters on the devolatilization history of the coal particle. The values chosen for the estimation of the flame temperature are $\Delta H = 2464$ kJ/kg, $f = 0.3$, and $Y_{oa} = 0.08$. In Figure 4.18, results are presented for the devolatilization characteristics for constrained coal particles with height within the bed as a parameter. It may be seen that the total devolatilization time is larger for a particle constrained to be near the distributor. In Figure 4.19a-c, unconstrained coal particles are simulated and the expressions averaged over the total bed height (equations (65b) and (67b)) have been used. In Figure 4.19a, the amount of volatiles retained are plotted as a function of time . Three different coals are simulated by using different values of the mean of the activation energy distribution. It may be ascertained that the total time between initial flame ignition and final extinction is virtually the same for the three coals. This would suggest that for coals of similar physical properties, the devolatilization time as defined above would not depend strongly on the type of coal. The experimental investigations of Pillai (1981) suggest a similar conclusion as the values of k_v and n, for coals with similar swelling numbers, were found to be similar. This suggest that effects of coal swelling may erroneously be understood as differences due to coal rank and type. It is noteworthy that Essenhigh (1963) found that the scatter in values of k_v for different coals was substantially reduced once the swelling aspect was taken into account (Table 2.2). However, the duration of the pre-ignition stage depends on the type of coal. Thus to evaluate the complete devolatiliza-

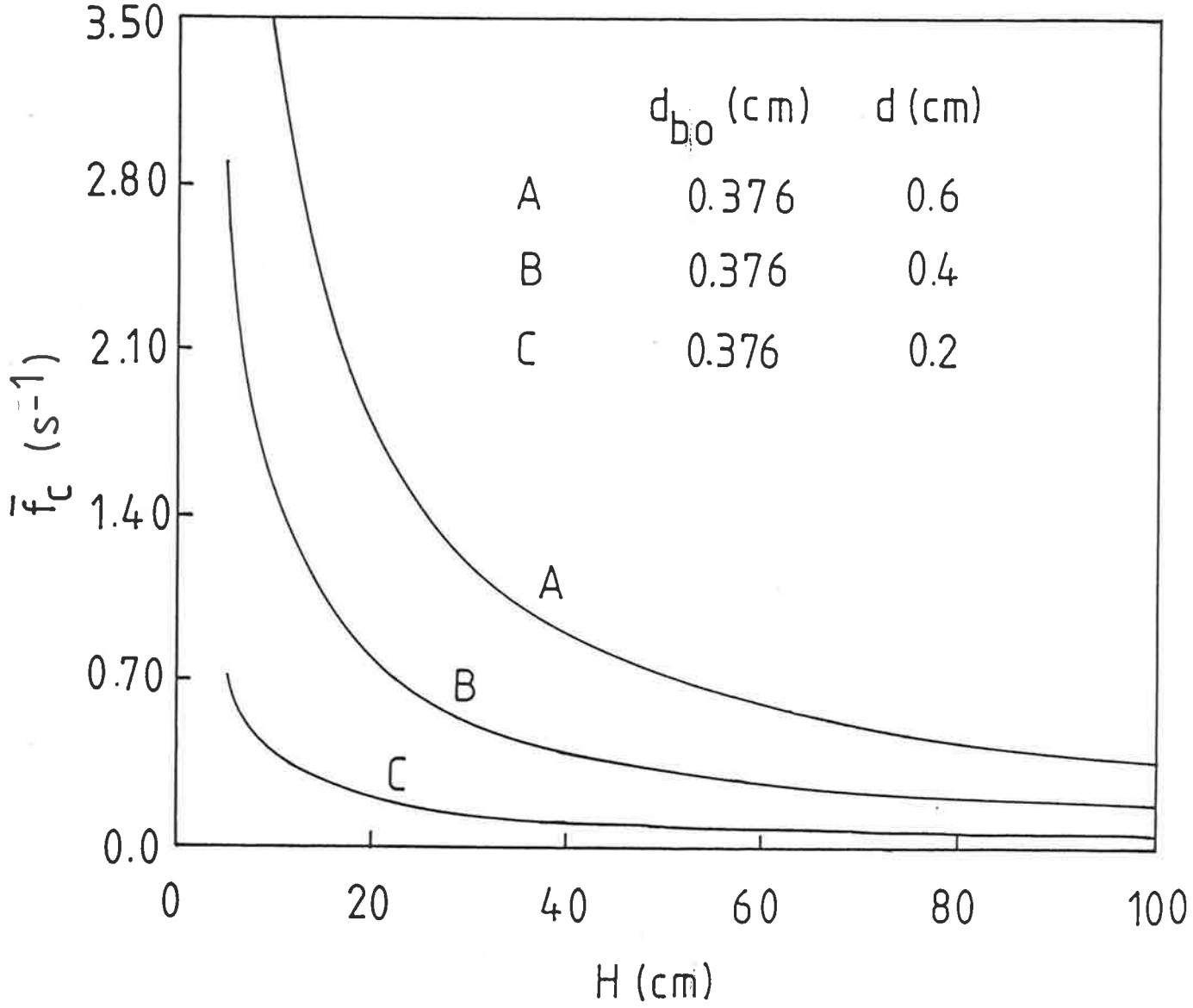

Fig. 4.17a Bubble-emulsion cycle frequency at any height within the bed with $d_{bo} = 0.376$ cm

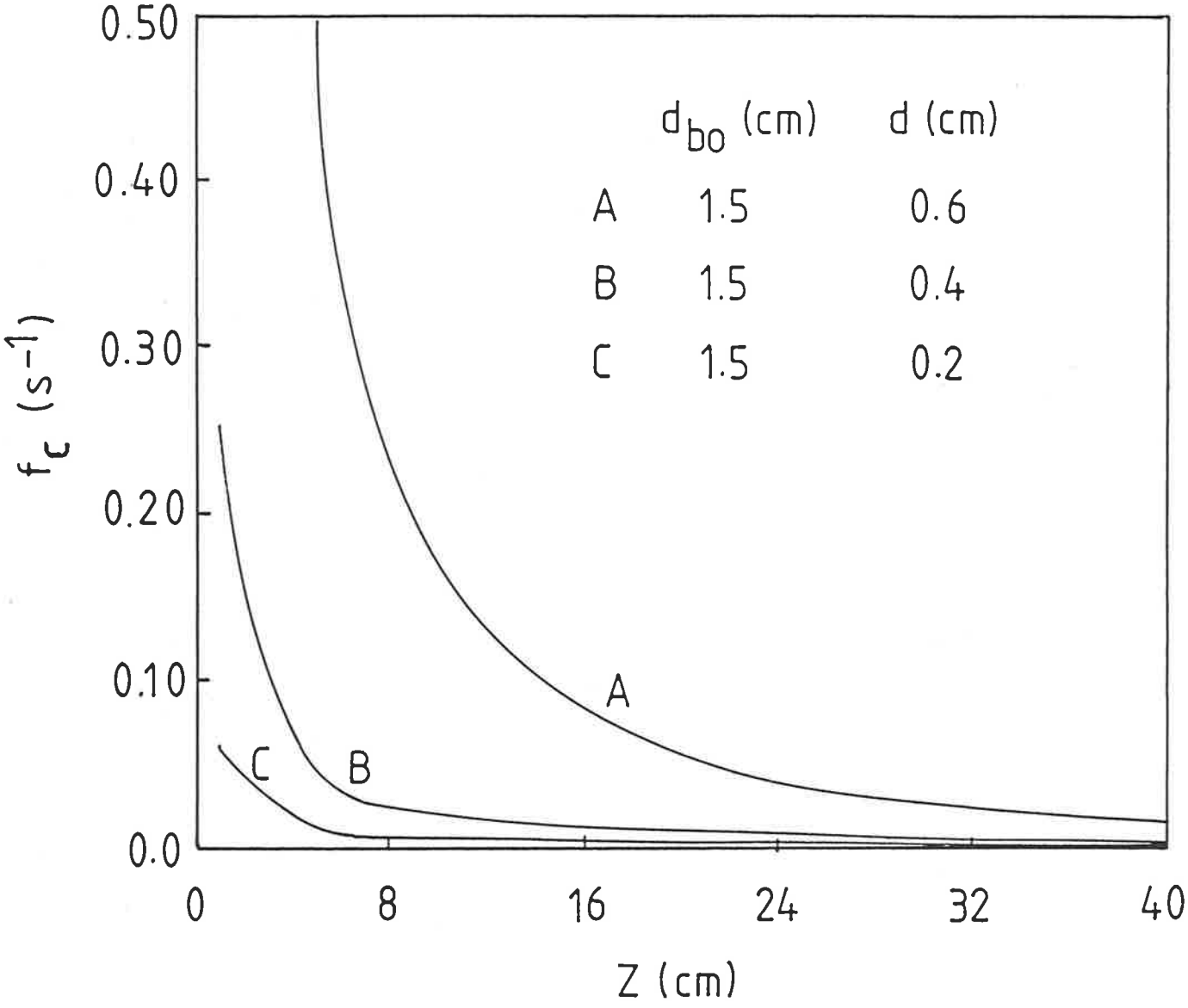

Fig. 4.17b Bubble-emulsion cycle frequency at any height within the bed with d_{bo} = 1.5 cm

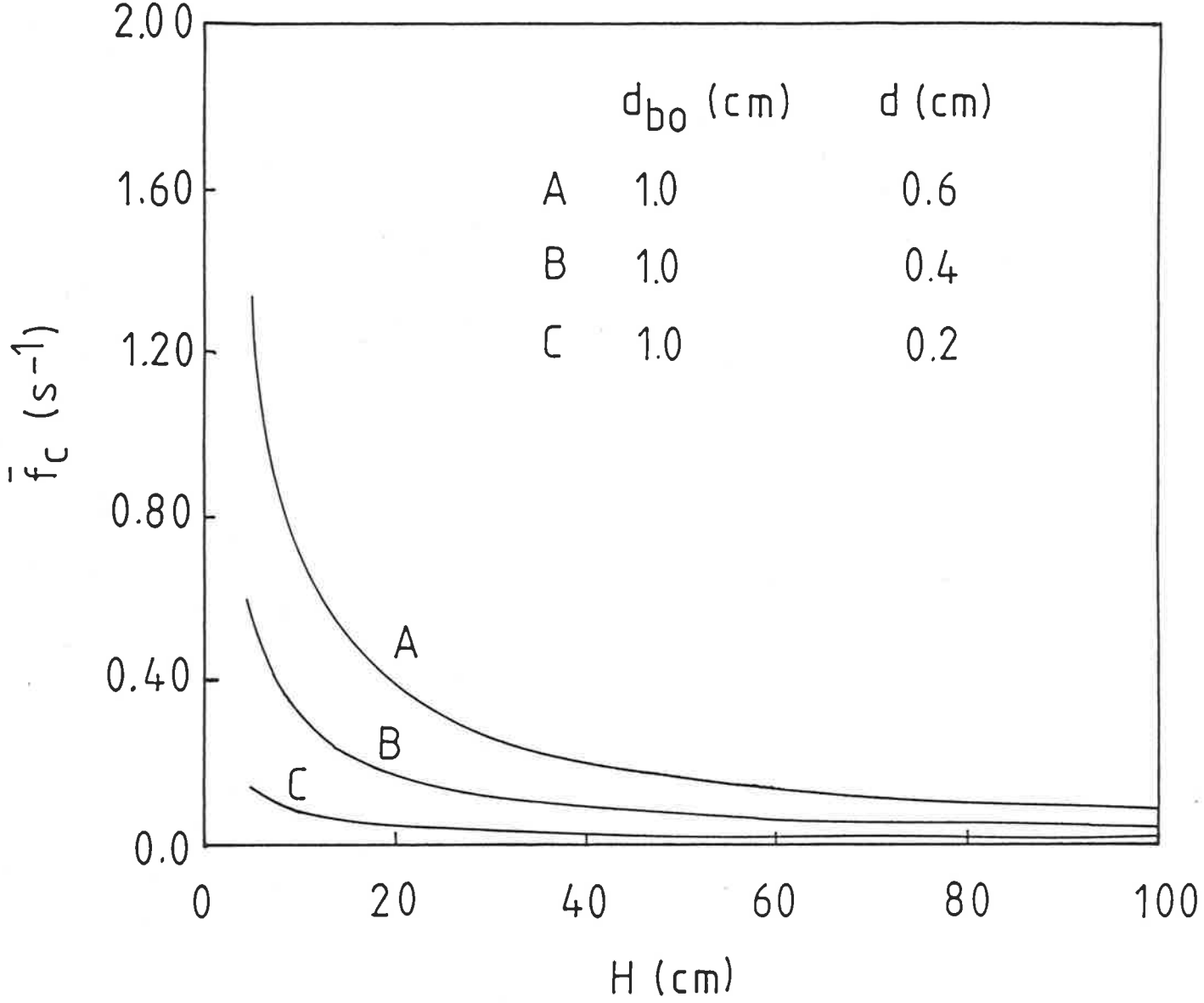

Fig. 4.17c Average bubble-emulsion cycle frequency as a function of total bed height with d_{bo} = 0.367 cm

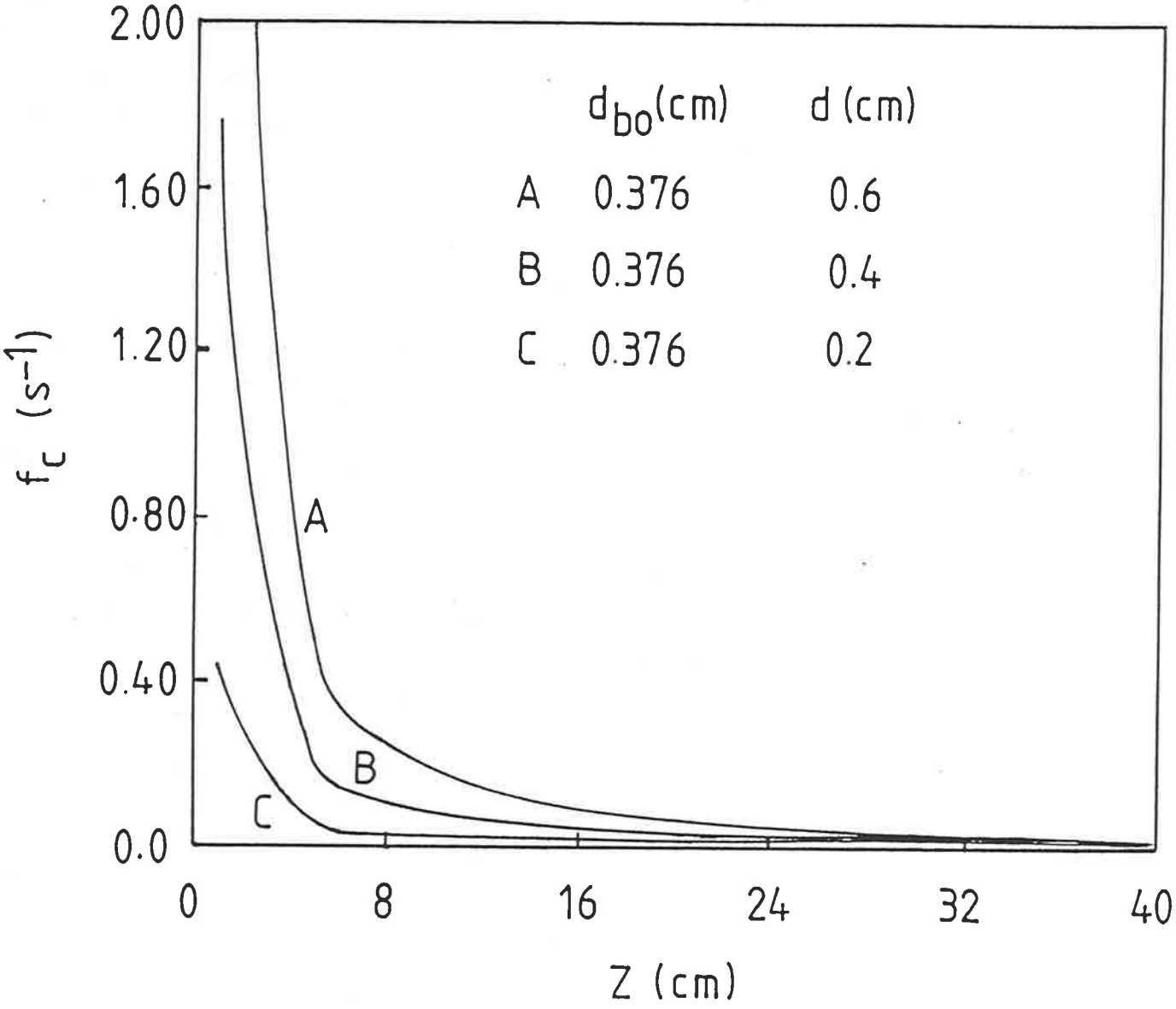

Fig. 4.17d Average bubble-emulsion cycle frequency as a function of total bed height with d_{bo} = 1.0 cm

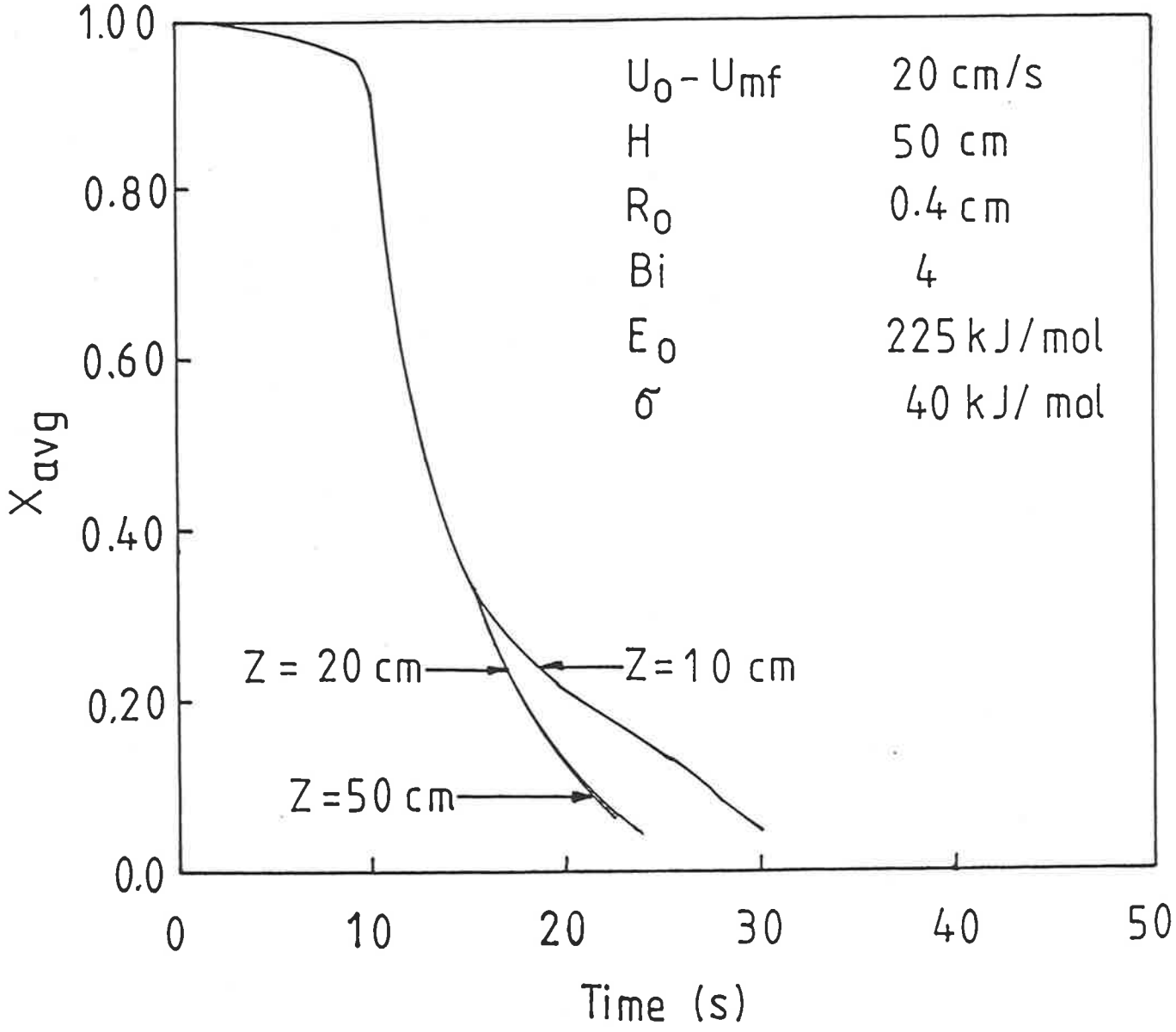

Fig. 4.18 The effect of height within the bed on the devolatilization history of a constrained coal particle

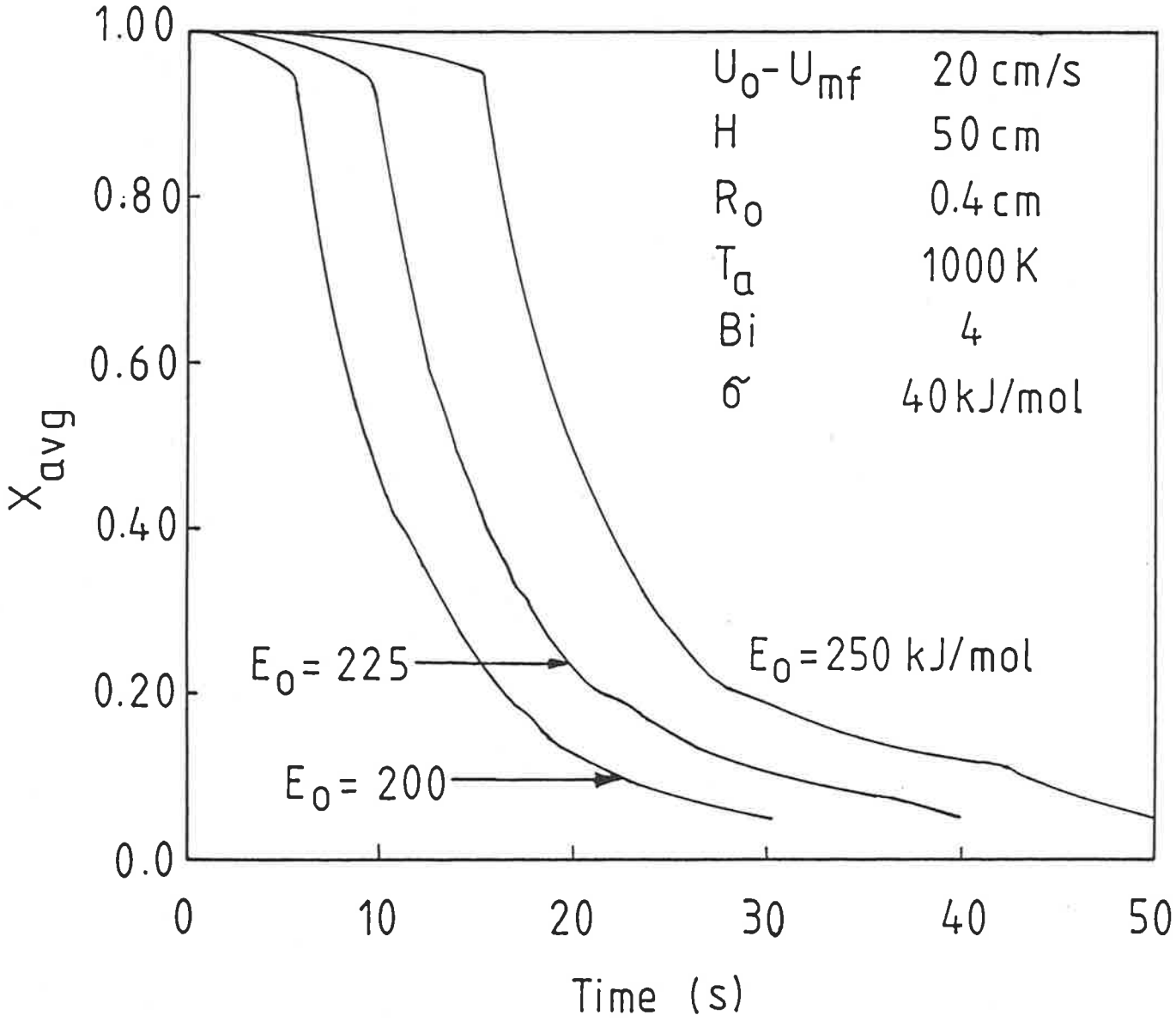

Fig. 4.19a The effect of the type of coal on the devolatilization history of the coal particle

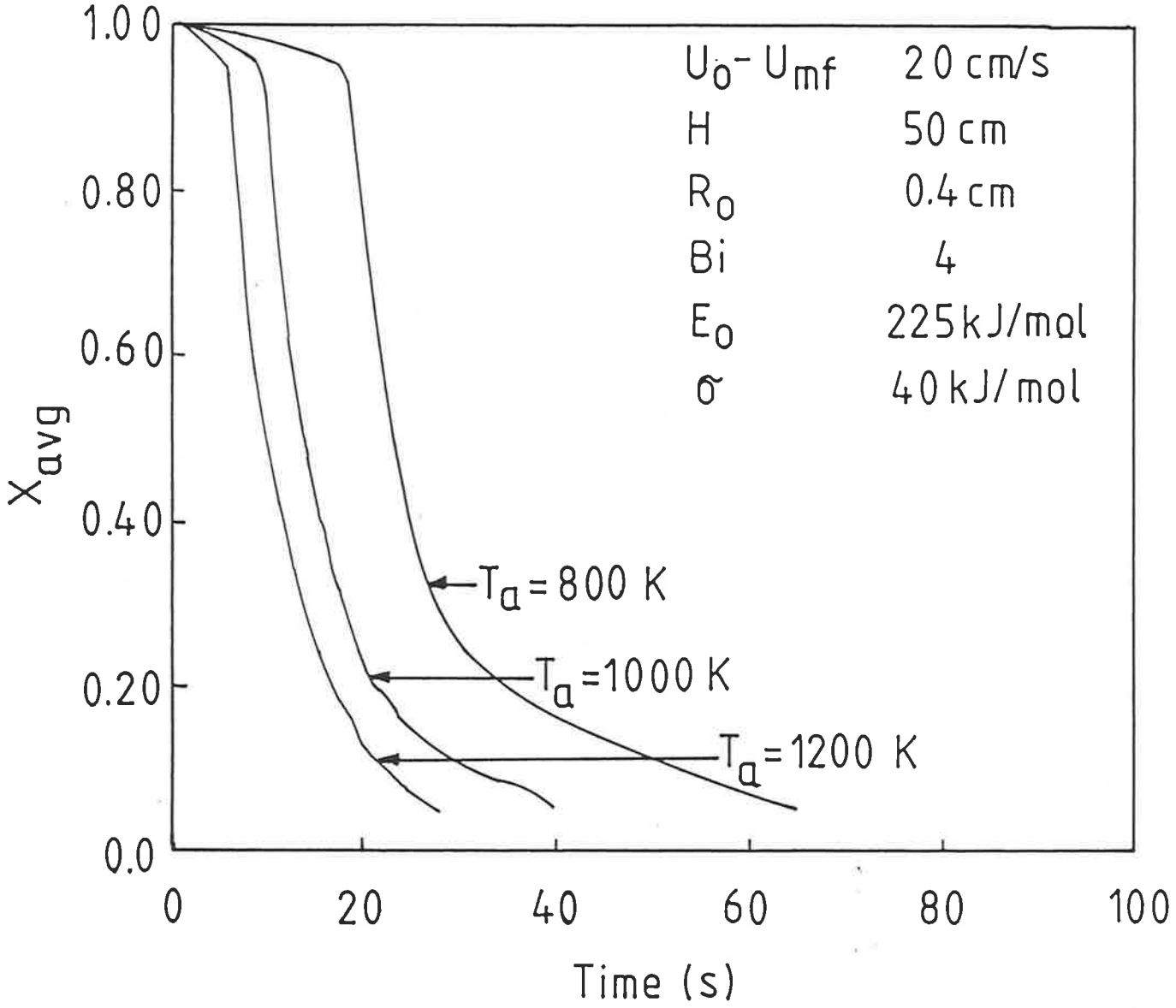

Fig. 4.19b The effect of bed temperature on the devolatilization history of the coal particle

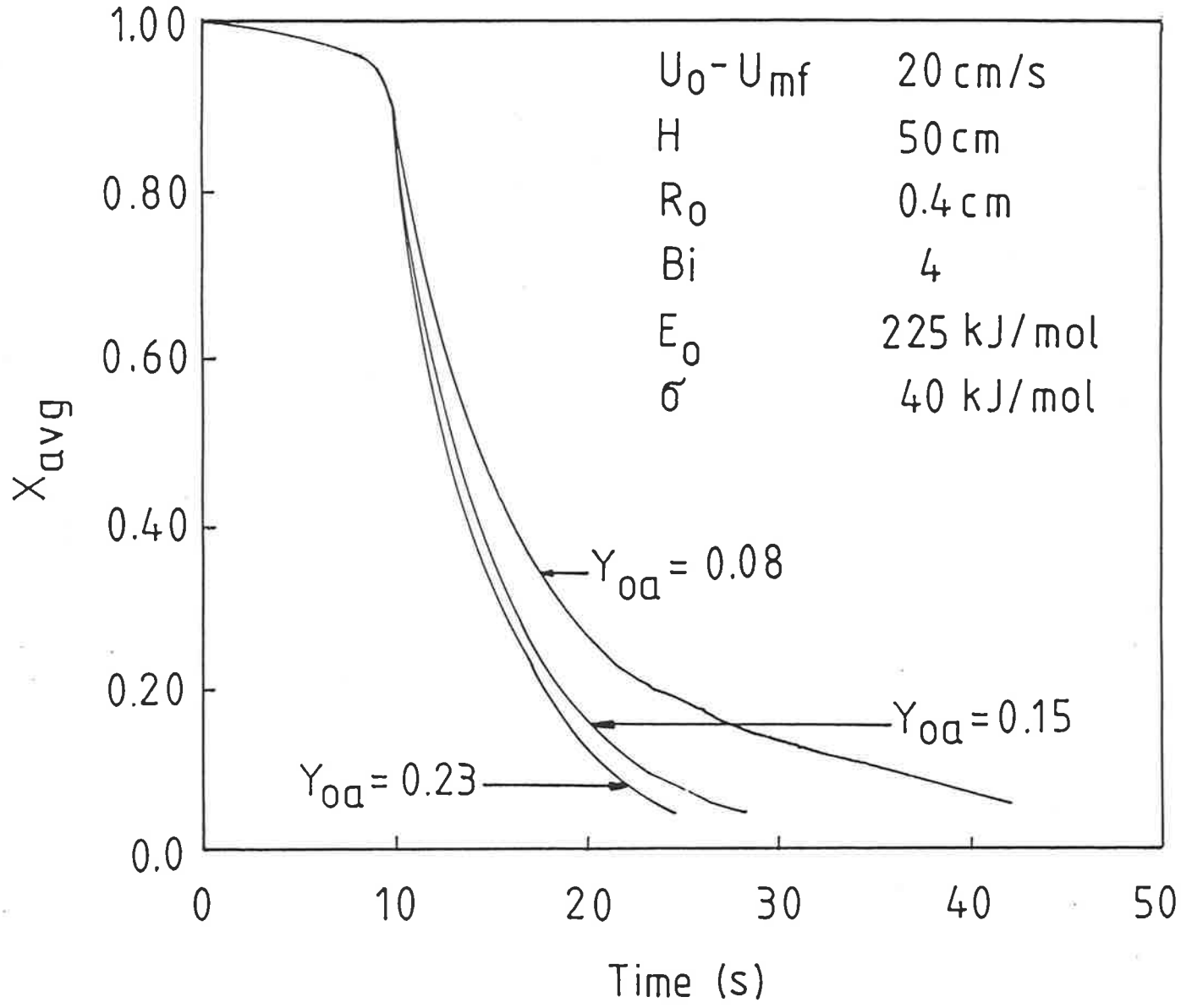

Fig. 4.19c The effect of oxygen mass fraction on the devolatilization history of the coal particle

tion characteristics, kinetic parameters obtained in pyrolysis studies should also be reported with combustion results. Moreover, the influence of kinetics is expected to become stronger as the size of the coal particle decreases (> 0.5mm). In Figure 4.19b, the effect of bed temperature is examined. As may be seen, the devolatilization time depends more on the bed temperature than on the type of coal. The importance of bed temperature is also confirmed by experimental results of Pillai (1981). In Figure 4.19c, the effect of oxygen mass concentration has been shown. As expected the devolatilization times are larger for lower oxygen mass fractions.

In Figures 4.20a and b, sample results of the interaction of fluidized bed design parameters with volatile combustion have been presented. From Figure 4.20a, it may be seen that higher values of excess gas velocity result in quicker combustion of coal volatiles due to the increased value of $(t_b/t_c)_{avg}$ and lower values of f_c. For lower values of the excess gas velocity, the value of $(t_b/t_c)_{avg}$ decreases rapidly leading to predominance of pyrolysis like conditions. Thus for lower values of $(U_0 - U_{mf})$, as employed by Yates et al. (1980), the devolatilization is expected to lead to formation of volatile bubbles detaching from the coal particle in preference over diffusion flame mode of volatile combustion as observed by Pillai (1982). In Figure 4.20b, the effect of total bed height is considered. As may be seen, though the devolatilization rates may differ on time resolved basis, the total devolatilization time is fairly independent of bed heights greater than 20cm.

In Figure 4.21, predicted spatial and temporal temperature profiles are plotted for a coal particle with R_p = 4mm. Fluctuating temperatures are predicted at the surface of the coal particle; the fluctuations are damped out in the inner core. The temperature profiles and the fluctuations are expected to have an important bearing on the fragmentation aspects of the coal as well as the subsequent combustion of char. Moreover, sufficiently high temperatures may result in ash fusion and consequently decrease combustion efficiency.

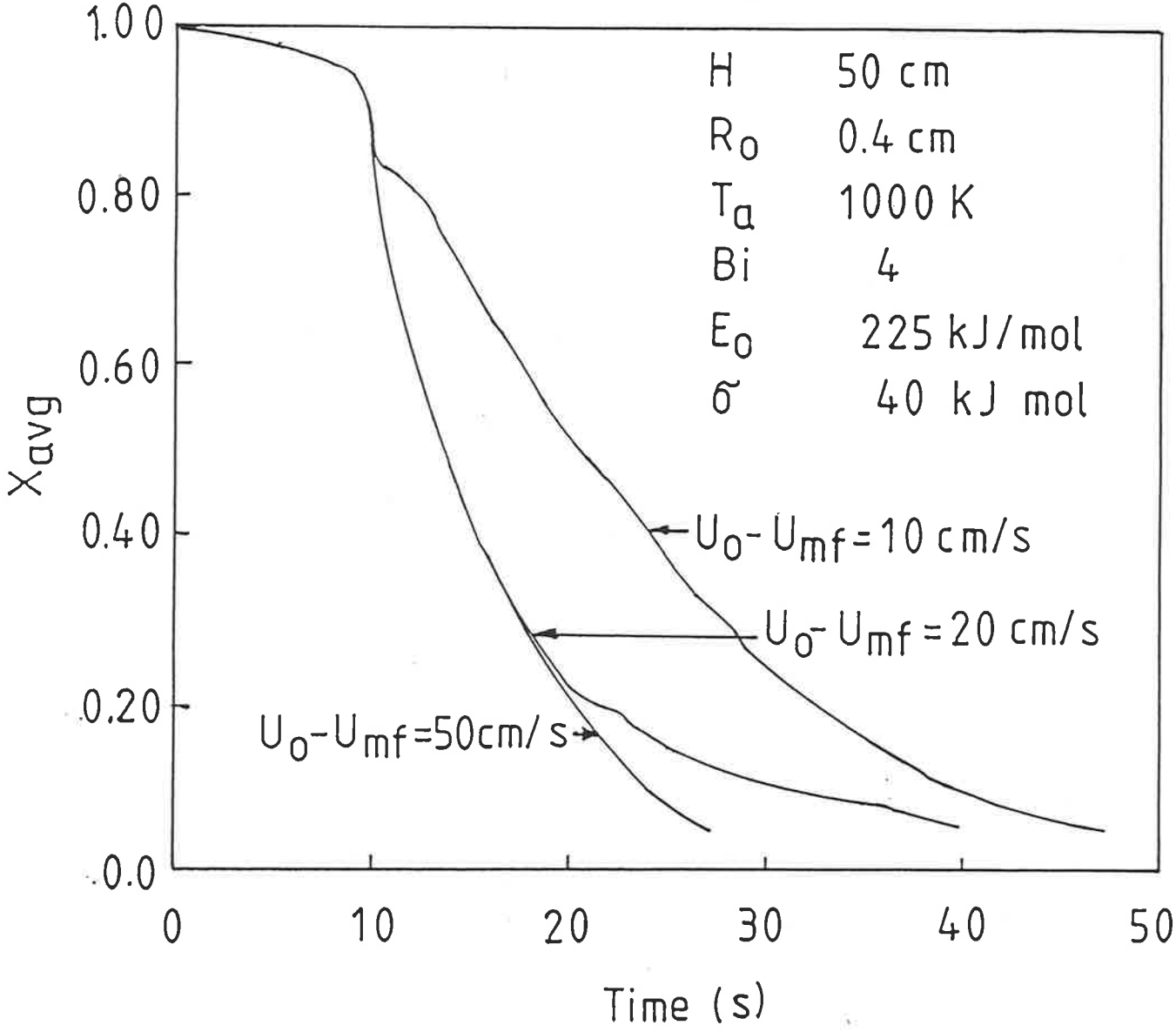

Fig. 4.20a The effect of the excess gas velocity on the devolatilization history of the coal particle

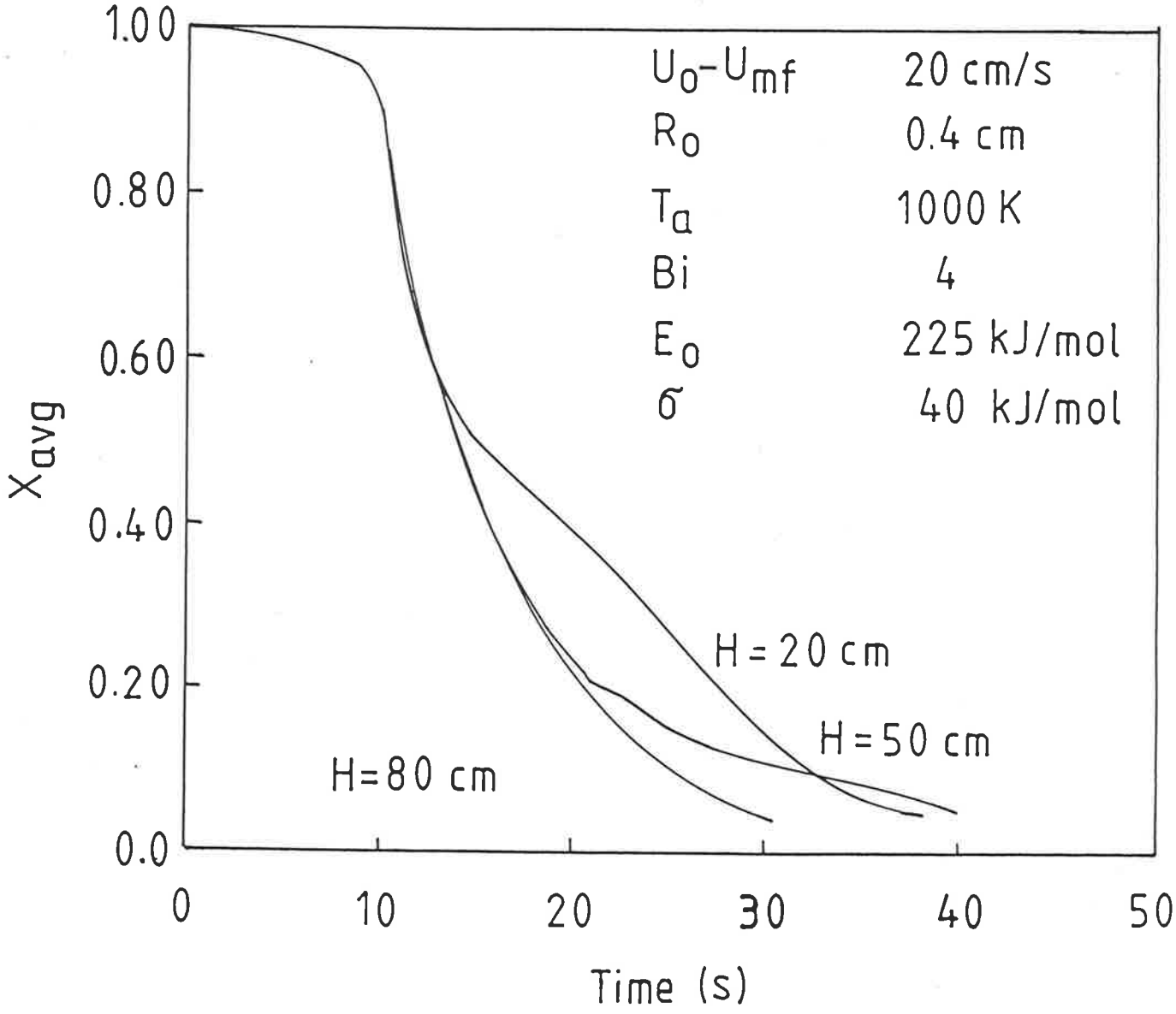

Fig. 4.20b The effect of the total bed height on the devolatilization history of the coal particle

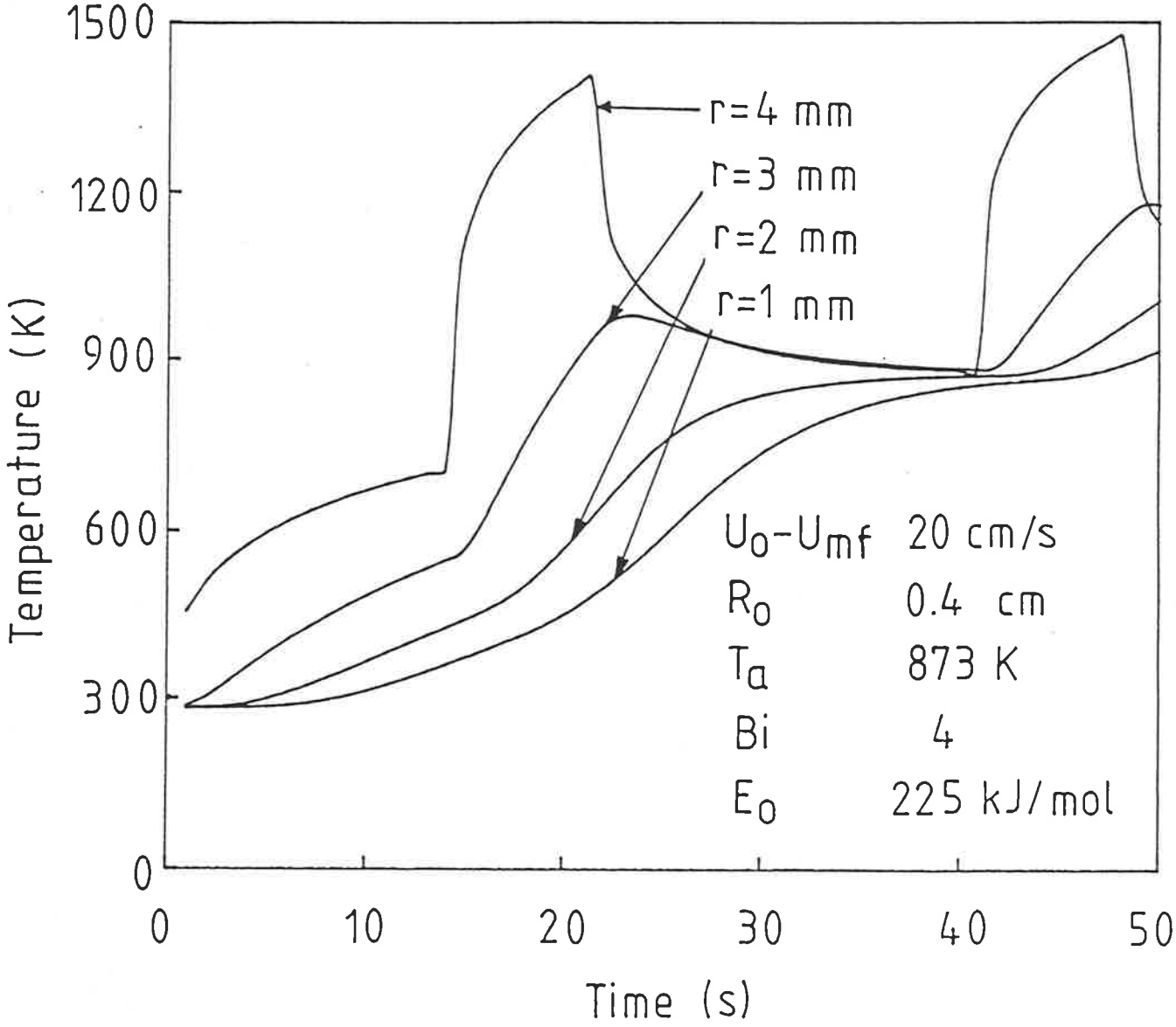

Fig. 4.21 Predicted spatial and temporal temperature profiles

An isothermal particle model would not predict these fluctuations in temperature nor the possibility of high particle temperatures during the volatile combustion stage. As the temperature fluctuations would be localised primarily in the outer regions of the coal particle, the experimental verification of such a phenomenon would be a problem.

Several assumptions of the model require more detailed verification/consideration. Ignition aspects need to be addressed. Though homogeneous ignition may be adequate for large particles, volatiles in smaller particles could combust while still trapped in the solid matrix. Heat transfer aspects in the two phases of the fluidized bed also have to be considered in greater detail. It may be more accurate to obtain heat transfer coefficients from the Froessling correlation while the particle is in the bubble phase and from suitably modified fixed/packed bed correlations while the particle is in the emulsion phase. The increased sophistication in modelling would also have to be matched with experimental data. Unfortunately time resolved coal volatile evolution behaviour in combustion systems does not appear to have been investigated and most experimental investigations have dealt only with the total volatile burn-out time.

The model presented here, however, provides a reasonable first step towards a quantitative link between combustion of coal volatiles around individual particles and fluidized bed parameters. It is expected that volatiles evolved during the time spent by the coal in the emulsion phase could combust within the bed (provided the bed temperature is sufficiently high (Dennis et al., 1982)) or in the freeboard region of the bed. Higher values of excess gas velocity would provide maximum in-bed combustion of coal volatiles. However, due to the limiting values reached by $(t_b/t_e)_{avg}$, certain amount of freeboard combustion of coal volatiles is inescapable. Presence of heat exchange surfaces and/or baffles could break the bubbles and alter the behaviour of the system. As pointed out

earlier, calculations presented here are valid strictly for the cases where either the coal particle is constrained at a specific height within the bed or could be at any location with an equal probability. Optimal design strategies for coal feed port location and distribution would require additional consideration of solids movement patterns inside the bed. As pointed out by Bywater (1980), the general class of one-dimensional models for fluidized bed behaviour can not be expected to yield quantitative information on such aspects. Solid circulation patterns would be controlled by bubble growth; however the effect of the walls as well as the possibility of non-uniform initial bubble formation at the distributor are required to explain the different types of solid circulation patterns observed (Lin et al., 1985). A bubble growth model incorporating these details would be able to predict the experimentally observed (Werther and Molerus, 1973) increased bubble activity in an annular region concentric with the bed axis which may result in plume like behaviour for volatile combustion (Bywater, 1980; Park et al., 1981).

5 EXPERIMENTAL RESULTS AND MODEL COMPARISON

The results of the experimental investigation are presented in this chapter. Experimental data obtained in this study as well as data collected from literature on drying and devolatilization under pyrolysis and combustion conditions are compared with the model predictions. A detailed description of the experimental set-up, experimental procedures, observations during the experiments and analysis methods of the coal samples can be found in Chapter 3.

5.1 OVERALL WEIGHT LOSS DUE TO DEVOLATILIZATION

The experimental data for devolatilization of pre-dried Bowmans coal was collected at 923 K for particle sizes of 10 mm and 1.8 mm. The data are tabulated in Appendix A. The model formulation for devolatilization requires the specification of the mean E_0 and the standard deviation σ of the activation energy distribution. To obtain these values devolatilization experiments on dry coal were performed. The model reported for devolatilization of dry coal (Agarwal et al., 1984b), which assumed heat transfer (both to and through the coal particle) and chemical reaction (presented by DAE kinetics) as rate limiting steps, was used to estimate the values for E_0 and σ. As can be seen in Figures 5.1 and 5.2 the values of E_0 = 210 kJ/mol and σ = 40 kJ/mol are in good agreement with the experimental data obtained for 10 mm and 1.8 mm particles.

The heat transfer Biot numbers for all of the single particle experiments were calculated using the Froessling correlation for single particles in a convective environment (Kunii and Levenspiel, 1969)

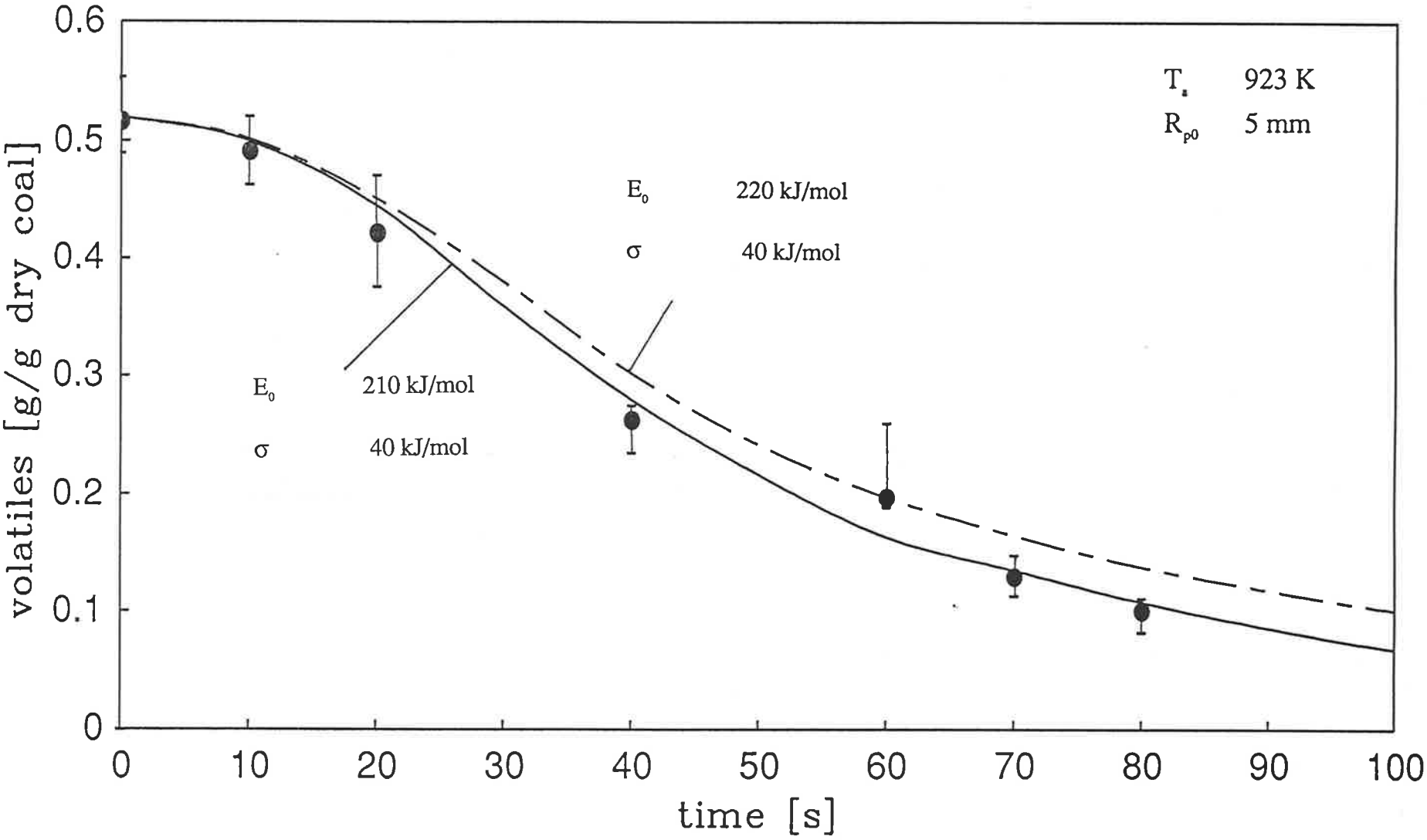

Fig. 5.1 Comparison of model prediction and experimental data for devolatilization of a 10 mm particle

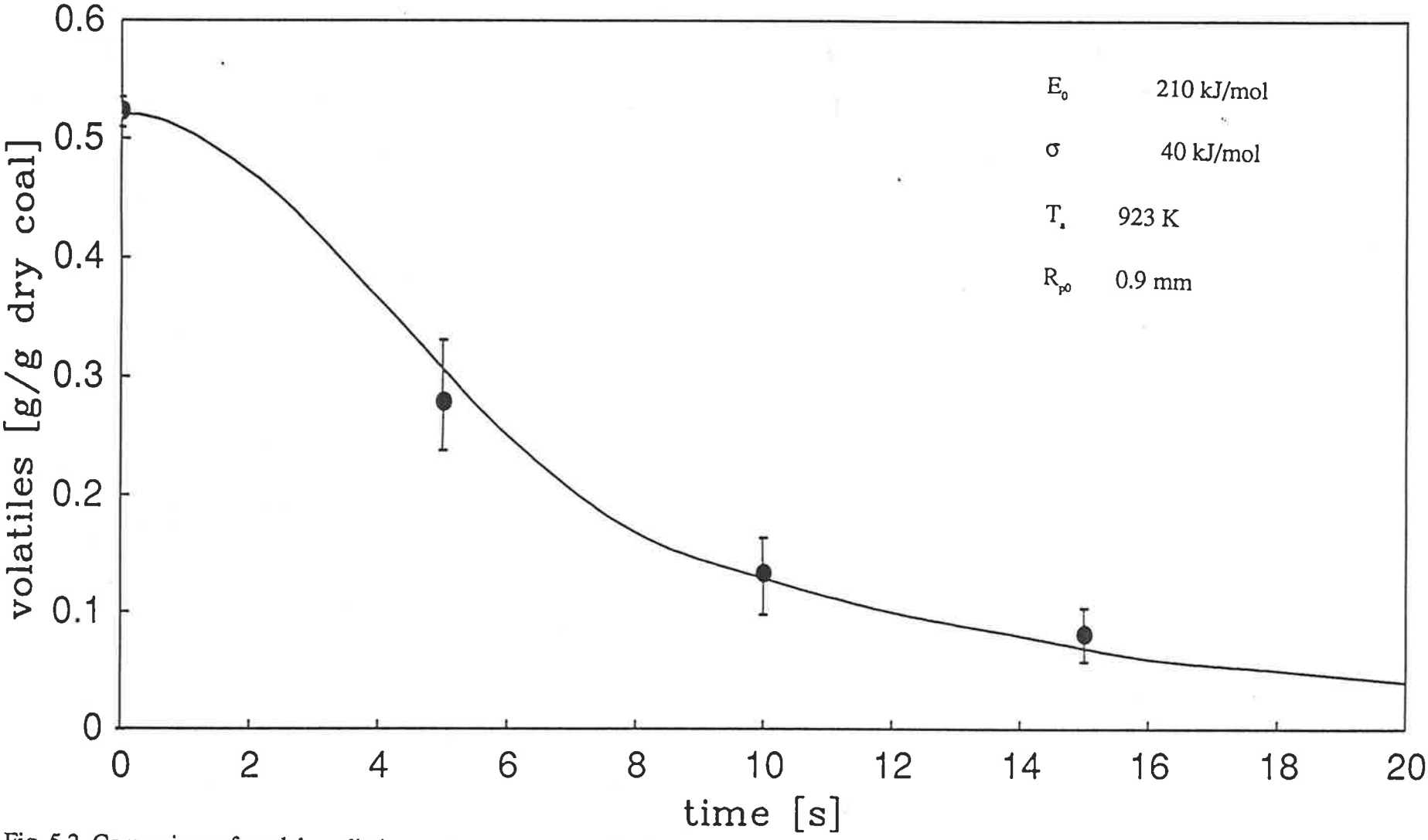

Fig. 5.2 Comparison of model prediction and experimental data for devolatilization of a 1.8 mm particle

$$\mathrm{Nu} = 2 + 0.6 Pr^{1/3} * Re^{1/2} \tag{69}$$

$$Bi = \frac{k_g}{k_s} * \mathrm{Nu} * f_{rad} \tag{70}$$

Where f_{rad} is a radiation factor. Since radiation effects have not been accounted for explicitly in the model, the heat transfer Biot number has been multiplied by $1.0 \leq f_{rad} \leq 1.3$ with the limiting values corresponding to temperatures up to 573 K and 1023 K respectively, to include a rough estimate. The estimated Biot numbers have been included in the data tables in Appendix A.

Only few (Carabogdan, 1965; Waibiao et al., 1987; Masahiro et al., 1987) experimental investigations have been reported on devolatilization of large particles - as used in fluidized beds - in a convective environment.

Weibiao et al. (1987) studied devolatilization of large coal particles 3 - 9 mm in an argon plasma stream at temperatures between 1173 - 1733 K. The coal particles were obtained by pressing pulverized coal in a mould to a spherical shape. This method is however questionable. By pressing the pulverized coal the pore structure and consequently the thermo physical properties of the coal will change. The results of the experiments can not be applied to 'real' coal. The authors also compared their experimental data with a single order kinetics equation and found good agreement for 5 different coal types.

Masahiro et al. (1987) reported experimental data on devolatilization of large single coal particles in nitrogen and air. Two different coal types (Taiheiyo and Datong), temperatures of 1123 K and 1273 K and particle sizes of 2.42 - 3.81 mm were used for the experiments. The authors pointed out the importance of the particle size; however, in the graphs reported no information on particle size was supplied. The large scatter of the data

implies that the whole range of particle sizes has been used. The experimental results have been compared with a first-order rate expression assuming isothermal particles. In the case of combustion the weight loss during the volatile combustion exceeded the value of proximate analysis. Only the weight loss itself (no proximate analysis for residual volatile matter) was determined in the experiments. Therefore, it is impossible to differentiate between weight loss due to volatile or carbon combustion. At least in the final stages of the experiments, simultaneous volatile and char combustion can be expected. In Figures 5.3a,b the experimental data for Taiheiyo coal at 1123 K under pyrolysis and combustion conditions have been compared with the DAE model as outlined by Agarwal et al. (1984b) and Agarwal (1986). The values of E_0 = 260 kJ/mol, σ = 35kJ/mol and $k_0 = 1.67*10^{13}$ s^{-1} have been used for the simulations. In Figure 5.3a the pyrolysis behaviour is shown and compared with model predictions for the particles sizes 2.42 and 3.81 mm. As can be seen most of the data range is inside the two theoretical curves. The combustion behaviour seems to be slightly under predicted in the final stage as seen Figure 5.3b. More information about the experimental technique employed and particle sizes used would be necessary to comment on that. Figures 5.4a,b show the devolatilization behaviour of Datong coal at 1273 K. The values of E_0 = 300 kJ/mol, σ = 60 kJ/mol and $k_0 = 1.67*10^{13}$ s^{-1} have been applied for the model predictions. The predictions for pyrolysis seem to be in reasonable agreement with the experimental data, the model seems to underpredict the volatile combustion behaviour in the final stage.

Ragland and Yang (1985) reported experimental results on combustion of large coal particles in a convective environment. Weight loss versus time data have been collected for volatiles and char combustion of different coal types, temperatures, Reynolds numbers, oxygen concentrations and particle sizes. No analysis on residual moisture, volatile matter and fixed carbon was reported. Loss of volatiles especially in the later stages of

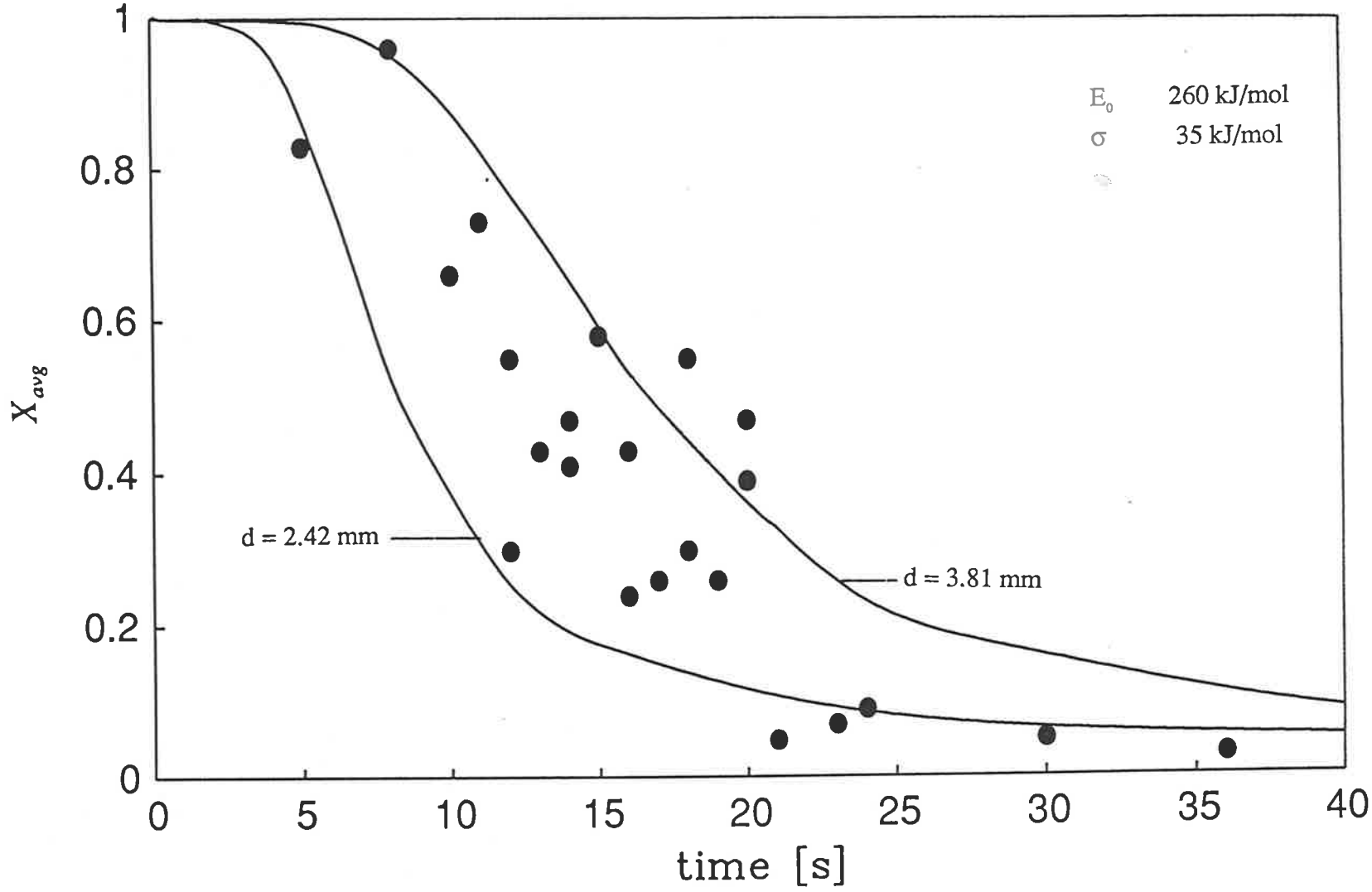

Fig. 5.3a Devolatilization of Taiheiyo coal under pyrolysis conditions at 1123 K (Masahiro et al., 1987)

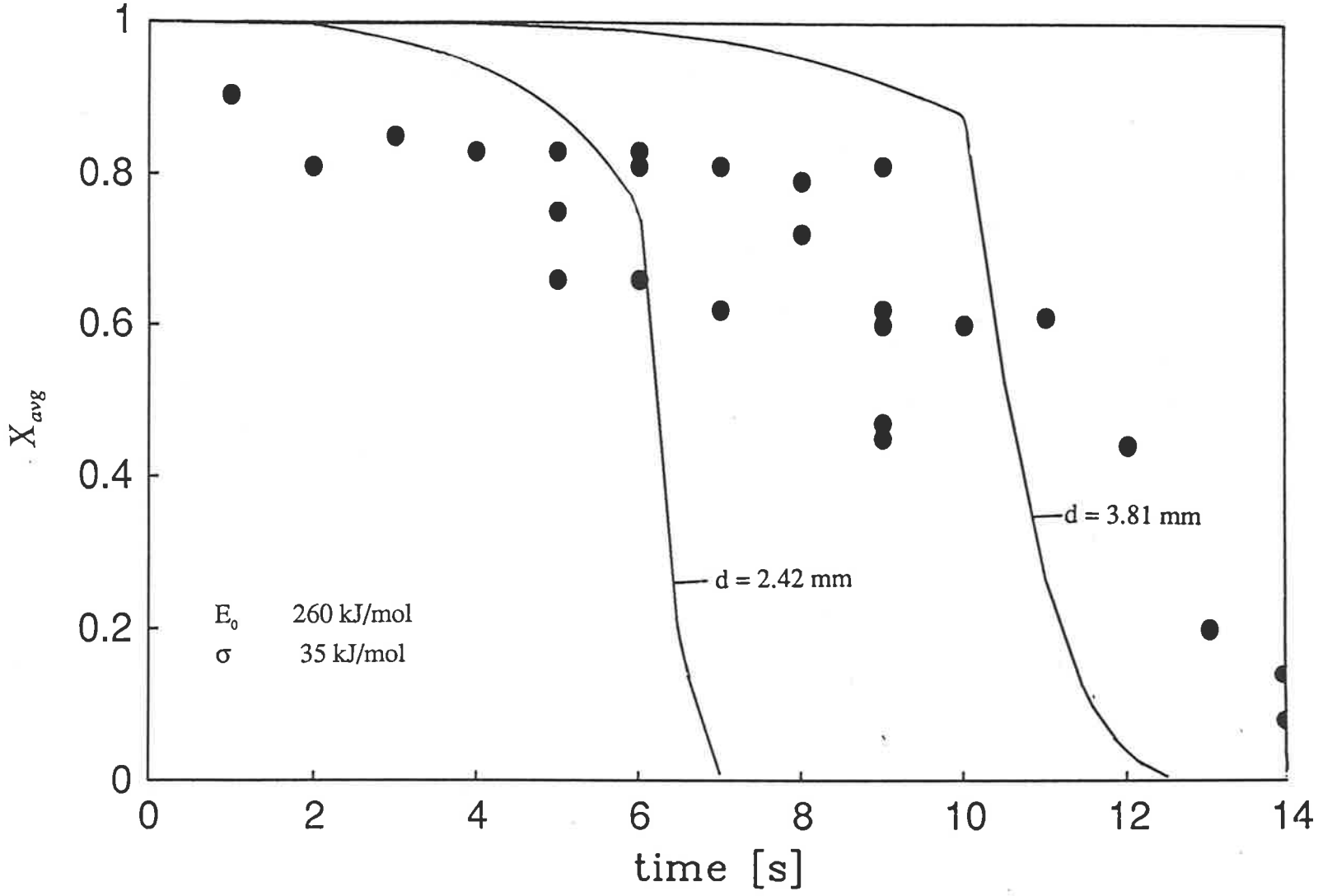

Fig. 5.3b Devolatilization of Taiheiyo coal under combustion conditions at 1123 K (Masahiro et al., 1987)

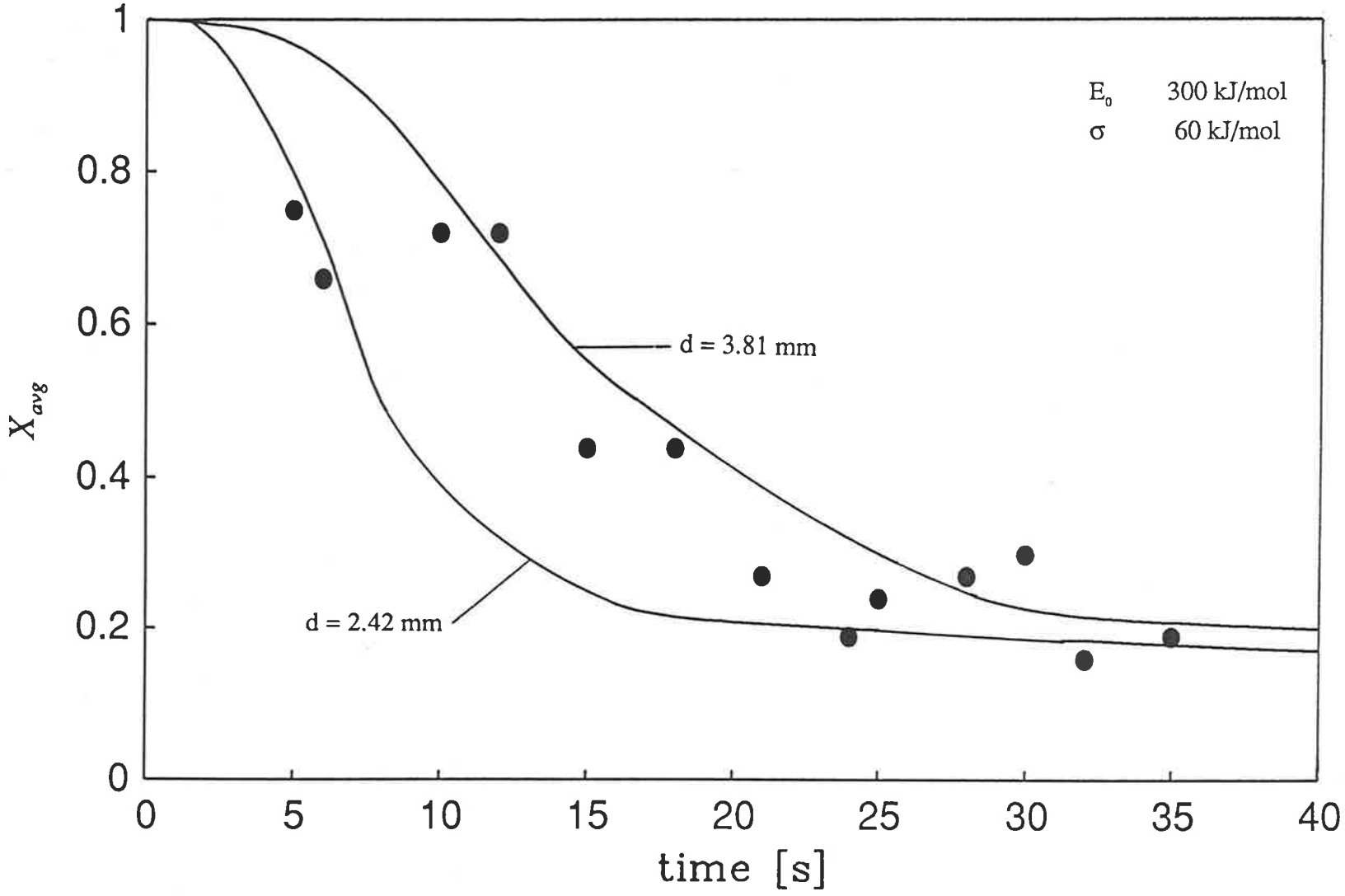

Fig. 5.4a Devolatilization of Datong coal under pyrolysis conditions at 1273 (Masahiro et al., 1987)

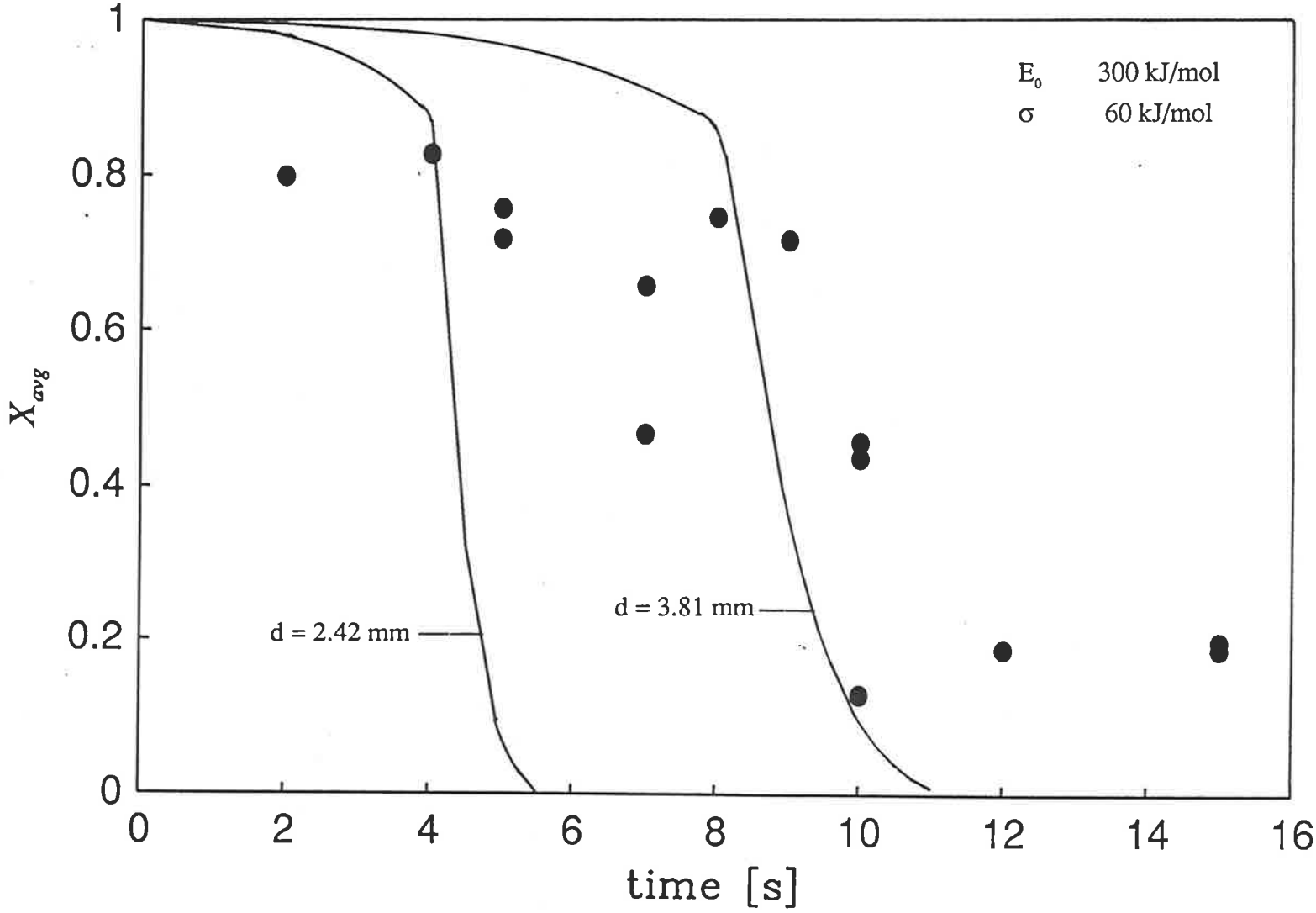

Fig. 5.4b Devolatilization of Datong coal under combustion conditions at 1273 (Masahiro et al., 1987)

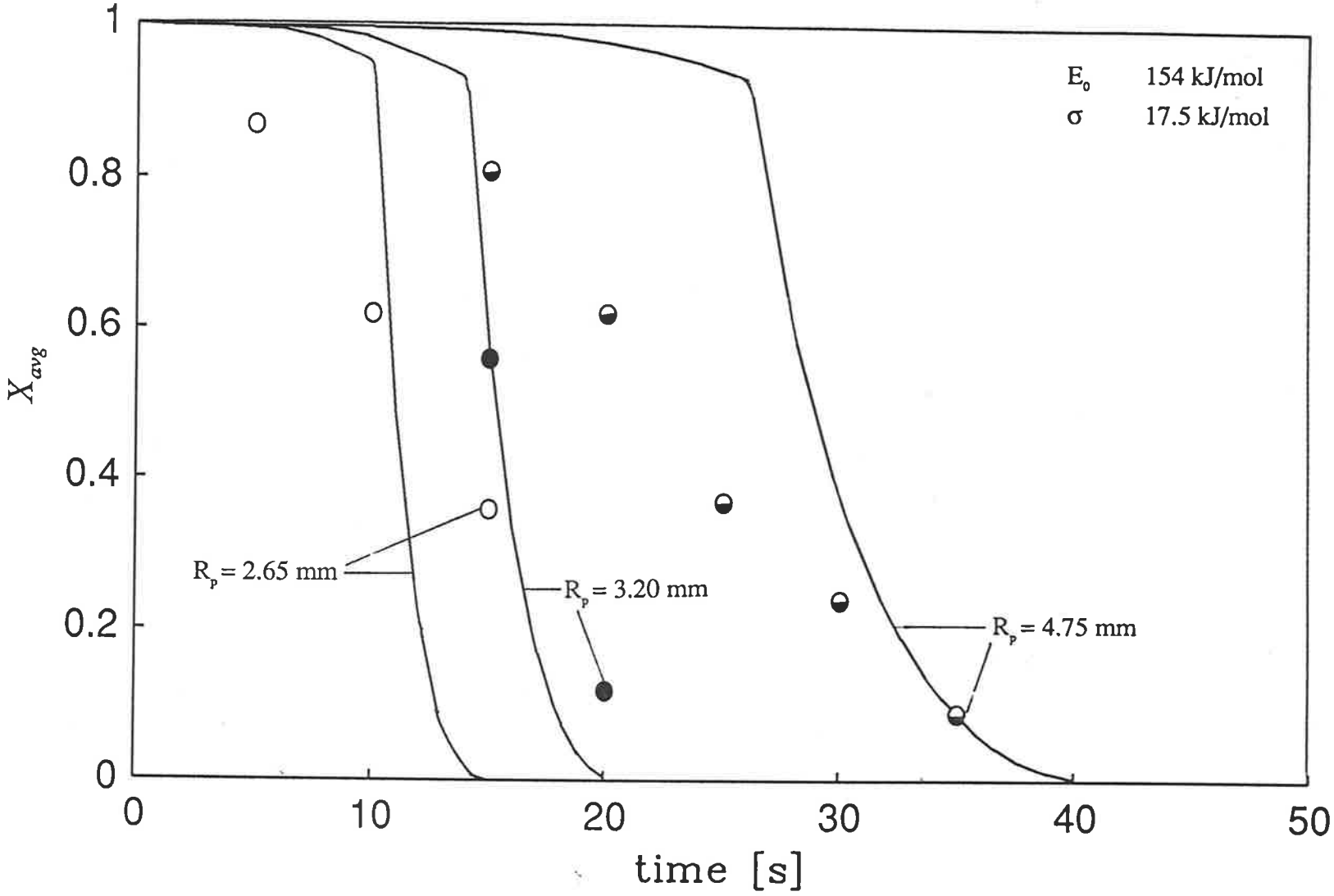

Fig. 5.5 Comparison between model and experimental results (Ragland and Yang, 1985)

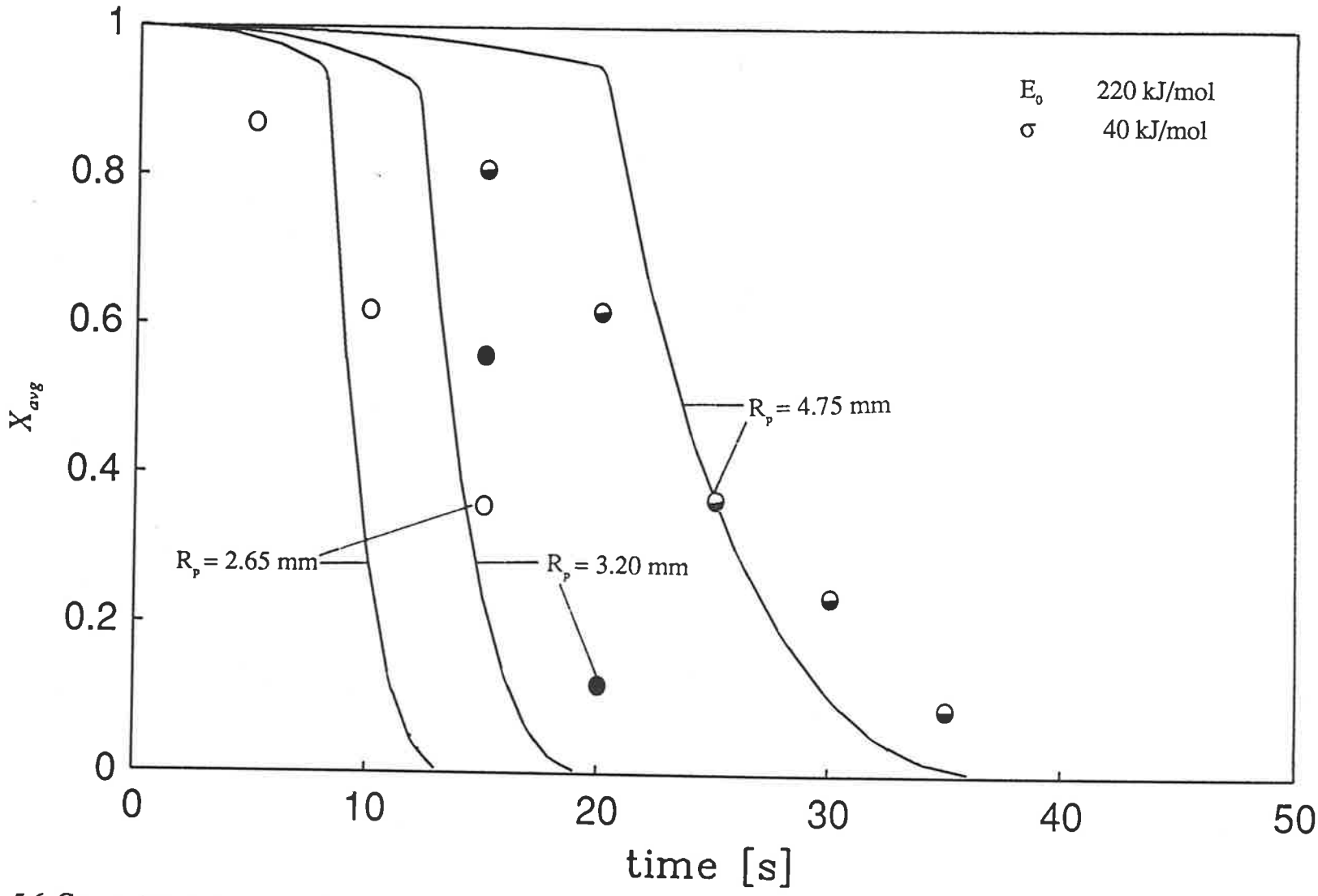

Fig. 5.6 Comparison between model and experimental results (Ragland and Yang, 1985)

combustion could not be separated from fixed carbon loss. That might be the reason for the higher volatile matter yield reported than indicated in the proximate analysis. In most runs only one or two data points have been obtained in the volatile combustion stage which is not sufficient for comparison with the model. Data and model predictions for 5.3, 6.4 and 9.5 mm particles are depicted in Figures 5.5 and 5.6. In Figure 5.5 the values of E_0 = 154 kJ/mol, σ = 17.5 kJ/mol and $k_0 = 2.91*10^8$ s^{-1} as suggest by Ragland and Yang (1985) have been used for the model predictions. A better fit using the values E_0 = 220 kJ/mol, σ = 40 kJ/mol and $k_0 = 1.67*10^{13}$ s^{-1} could be obtained in Figure 5.6.

5.2 EVOLUTION OF VOLATILES SPECIES FOR WET AND DRY COAL

An investigation on the evolution of gaseous volatile species during the pyrolysis of Bowmans coal has been conducted. Concentrations of carbon oxides and lighter hydrocarbons in the off-gas have been measured as a function of time for single wet and dry coal particles (sizes 5mm and 10 mm) exposed to convective heating at different gas temperatures (673 - 873 K). The data are listed in Appendix A.

This investigation was conducted with the following objectives

- to measure the pyrolytic evolution of gaseous species from large particles of coal from Bowmans deposit in South Australia
- to determine the kinetic parameters based on the non-isothermal particle model to ascertain the rank insensitivity hypothesis.

Additionally, low-rank coals contain appreciable amounts of moisture in their 'as-mined' state. Since complete moisture removal prior to utilization is economically impractical, the need to study the effect of coal moisture on the pyrolysis behaviour has

been pointed out (Agarwal et al., 1986). No data appear to have been reported on the influence of moisture on the pyrolytic evolution of volatile species from large wet coal particles. Consequently experiments were conducted with pre-dried as well as wet coal particles. The experimental set-up employed (Chapter 3) enables a more precise estimate of external transport characteristics and residence time of the solid in the hot zone in comparison with a fluidized bed. The effect of fluidized bed reactor operating conditions in modelling efforts is usually incorporated in terms of an appropriate boundary condition (external heat transfer coefficient (Agarwal et al., 1984b)). This study, then, is expected to be of importance in developing methods for predicting the pyrolytic evolution of volatile species from coal in fluidized beds.

In Figure 5.7 the computational flow-sheet for comparison of the experimental results for the evolution of gaseous volatile species of Bowmans coal with the model predictions are depicted.

For the analysis of the volatiles evolution from wet coal, the effect of moisture has to be taken into account. A model for intense convective drying and pyrolysis has been reported by Agarwal et al. (1986). Model calculations revealed that the drying and devolatilization, which have to be treated as coupled processes in general, may be treated as sequential for $Bi \leq 1$ if the presence of the temperature gradient at the end of drying is taken into account for devolatilization. For $Bi \leq 1$, this implies that a uniform temperature initial condition may still be employed in the solution of the transient heat conduction equation for quantifying the volatile evolution characteristics from wet coal. At atmospheric pressure conditions, this uniform temperature is 100°C.

The experimental results described here have been obtained at low nitrogen flow rates and $Bi_d \sim 1$. Hence, for modelling the present experimental data for wet coal, based on

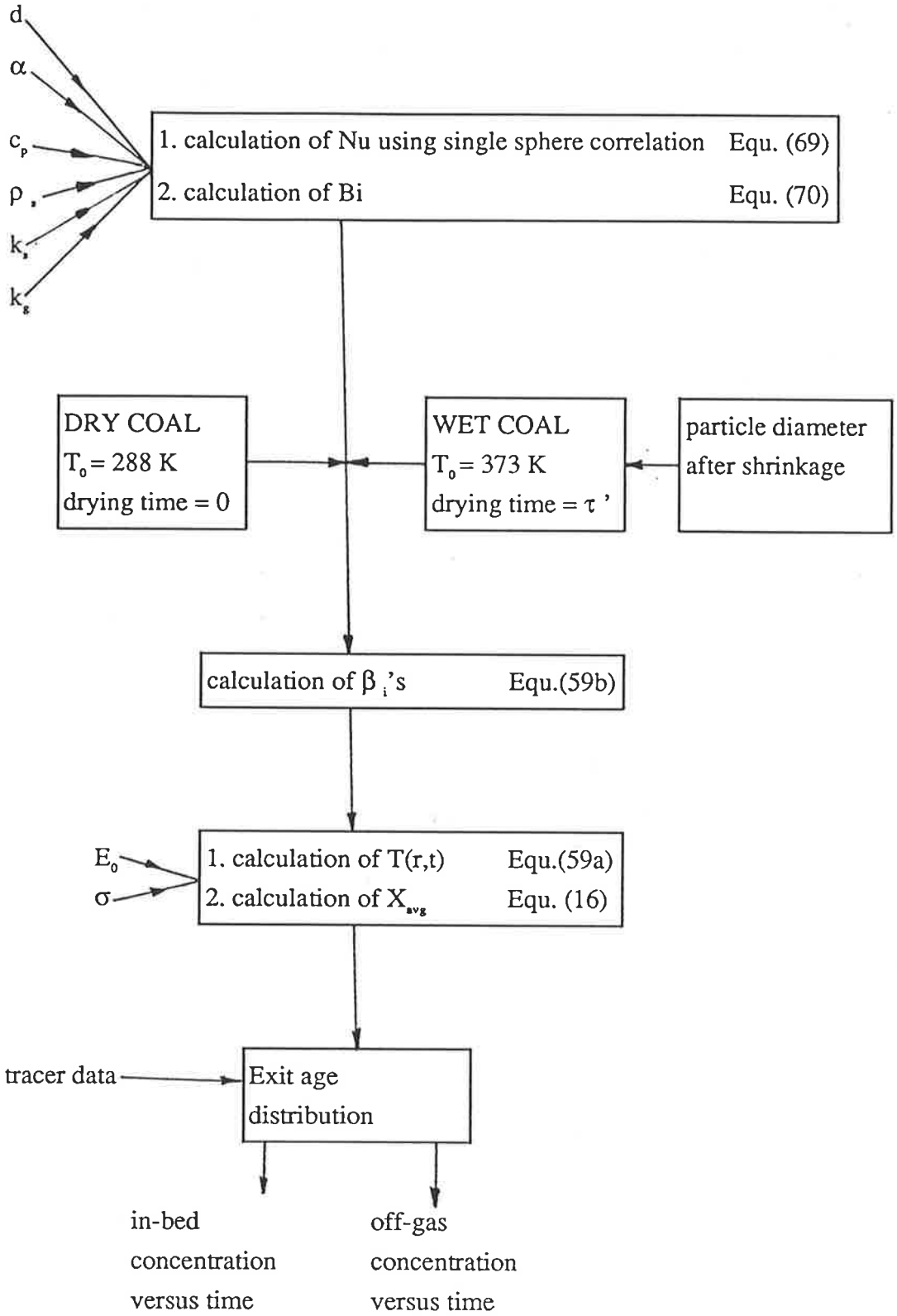

Fig. 5.7 Computational flow-sheet for comparison of volatile species evolution data with model predictions

parametric results (Agarwal et al., 1986) outlined above, the drying was assumed to cause a time lag in the initiation of volatiles release. Further, the pyrolytic evolution of gases from wet coal was determined from the solutions of equations (16a-c). To solve equations (16a-c), the temperature profile, T(r,t), is obtained from the analytical solution (Jacob, 1959) of the unsteady-state heat conduction equation with convective boundary and uniform initial temperature conditions equations (60a-b).

As already pointed out in Chapter 3, the flow through the reactor deviates from plug flow. For the interpretation of the experimental data the results of tracer experiments (Chapter 3) were used to obtain a exit age distribution (Figure 3.3)

Experiments were conducted with 5 mm particles of Bowmans coal at gas temperatures of 673, 773 and 873 K and with 10 mm particles at 873 K. The effect of moisture was considered by performing experiments for pre-dried as well as wet (C_0 = 1.1 g moisture/g dry coal) coal particles

At 673 K, only CO_2 was evolved in measurable quantities. The time-resolved evolution characteristics for dry and wet coal are shown in Figure 5.8. At 773 K, lighter hydrocarbons were evolved in measurable quantities besides CO_2. The results for the evolution characteristics of CO_2, CH_4, C_2H_4 and C_2H_6 are shown both for dry and wet coal in Figures 5.9a-d. Carbon monoxide was not detected at this temperature. At 873 K, measurable amounts of CO were also evolved; the experimental results and the modelling predictions for 5 and 10 mm particles are shown in Figures 5.10a and 5.11a. The evolution characteristics for the other species at 873 K are shown in Figures 5.10b-e and 5.11b-e. The effect of particle size is shown in Figure 5.12 by comparing CO_2 evolution characteristics for 5 and 10 mm dry coal particles at 873 K. The effect of gas temperature is shown by comparing CO_2 concentrations in the off-gas for 5 mm wet particles at 673, 773 and 873 K

in Figure 5.13

The kinetic parameters used in the present simulations are compared with those reported by Solomon and Hamblen (1983) and Agarwal et al. (1987) in Table 5.1. The mean activation energies for the release of CH_4 and C_2H_4 from Bowmans coal appear to be somewhat lower in comparison with other coals; the activation energies for CO, CO_2 and C_2H_6 are in good agreement.

These experimental results and modelling comparisons reveal that the kinetic parameters for the evolution of gaseous volatile species from Bowmans coal are not very different from the coals found elsewhere. Further, the non-isothermal particle model is capable of simulating the trends of volatile release from large pre-dried or wet coal particles. The effect of moisture content can be modelled, for the low Biot number experimental conditions considered here, by incorporating a time lag due to drying in the history of the evolution of the volatile species. The kinetic parameters, it may be noted, have been obtained from different experimental techniques. The trends for volatile species evolution from large wet or dry coal particles in fluidized beds may then predicted using this model with the heat transfer Biot number from an appropriate correlation (Agarwal et al., 1984b).

From the results described above it is concluded that

- the kinetic parameters for the evolution of light hydrocarbon species and carbon oxides from Bowmans coal are similar to coals found elsewhere lending support to the rank insensitive hypothesis;
- the non-isothermal particle model is capable of simulating the trends in the release of volatiles from pre-dried as well as wet coal.

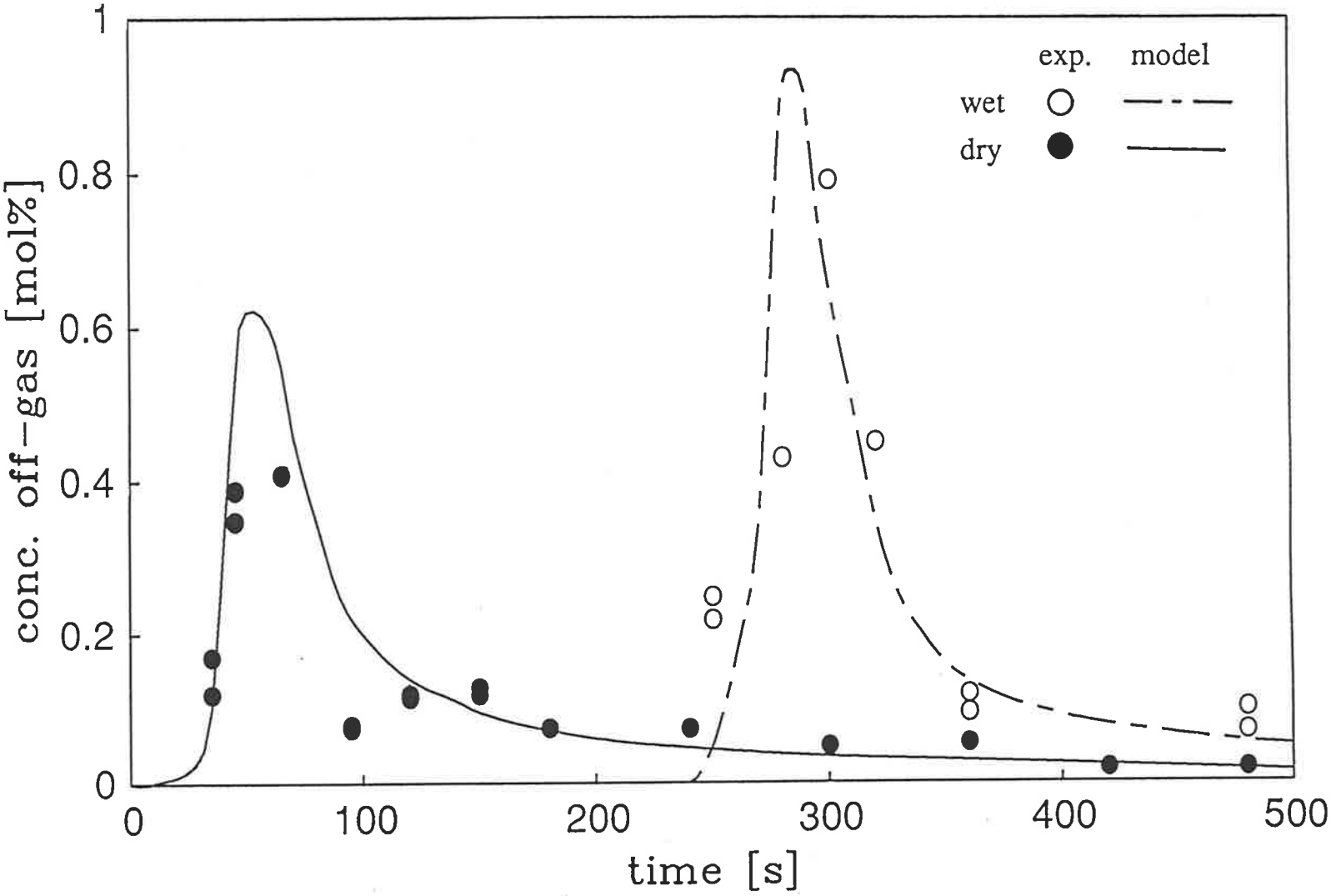

Fig. 5.8 CO_2 evolution from 5 mm Bowmans coal particles at 673 K

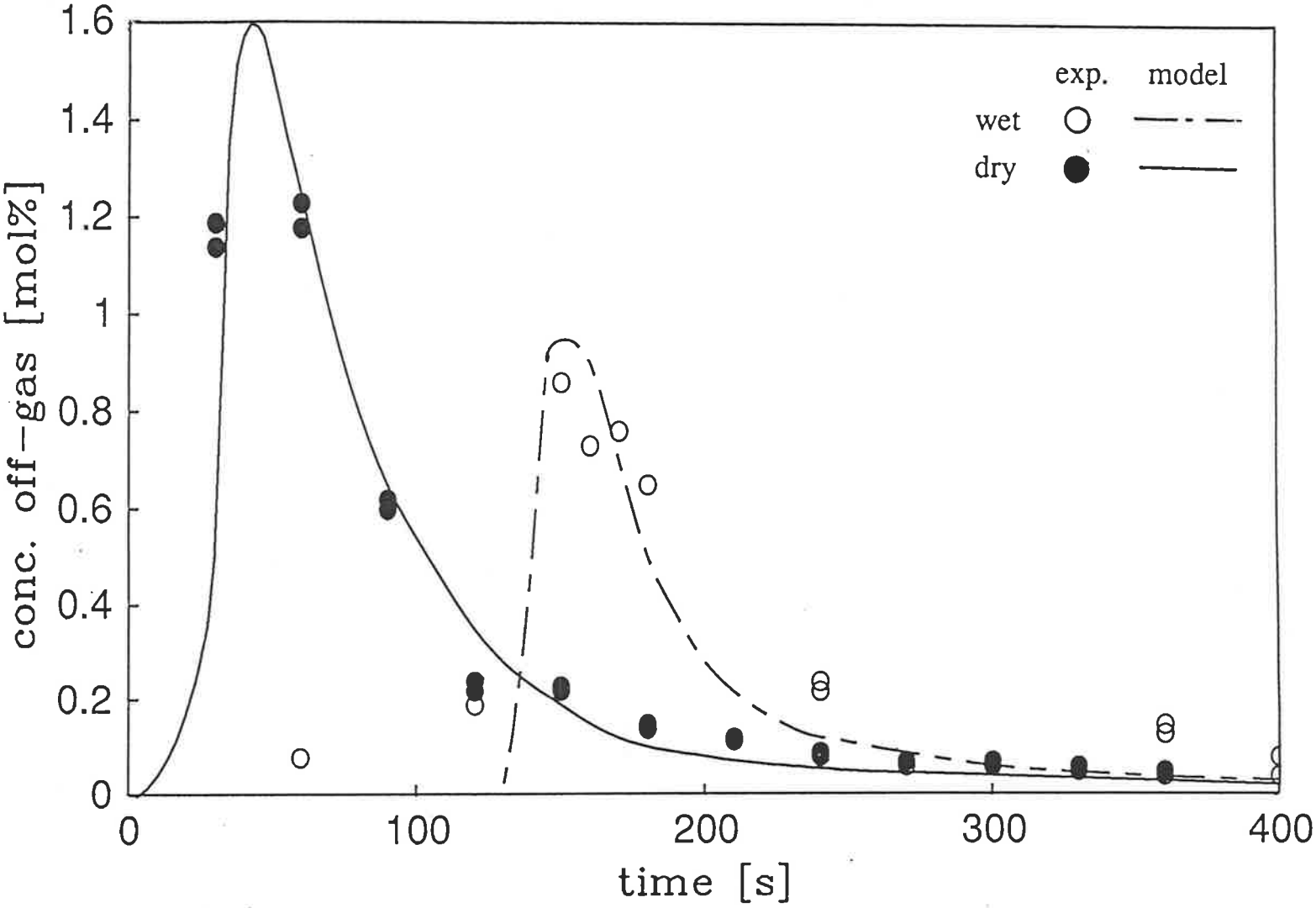

Fig. 5.9a CO_2 evolution from 5 mm Bowmans coal particles at 773 K

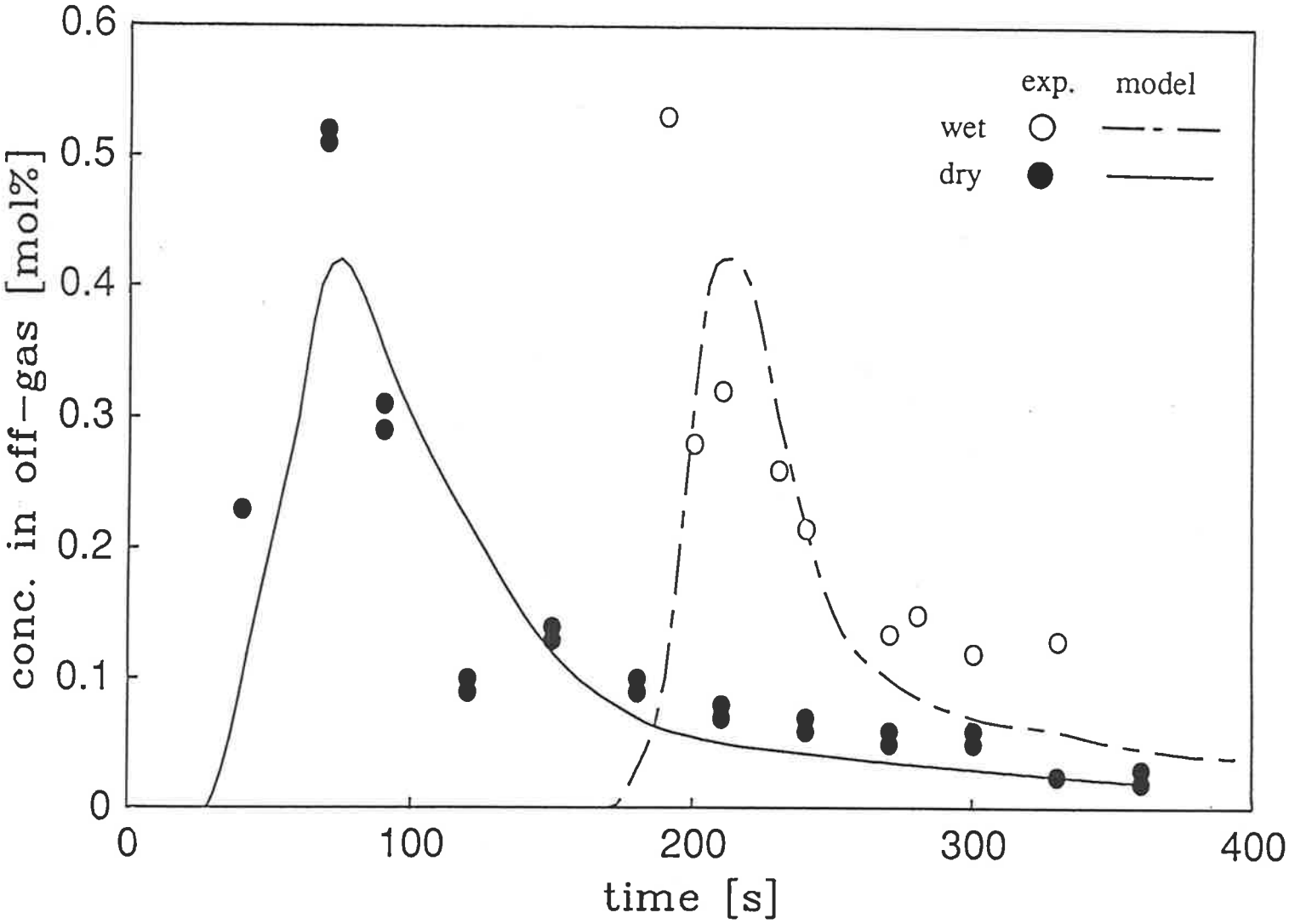

Fig. 5.9b CH_4 evolution from 5 mm Bowmans coal particles at 773 K

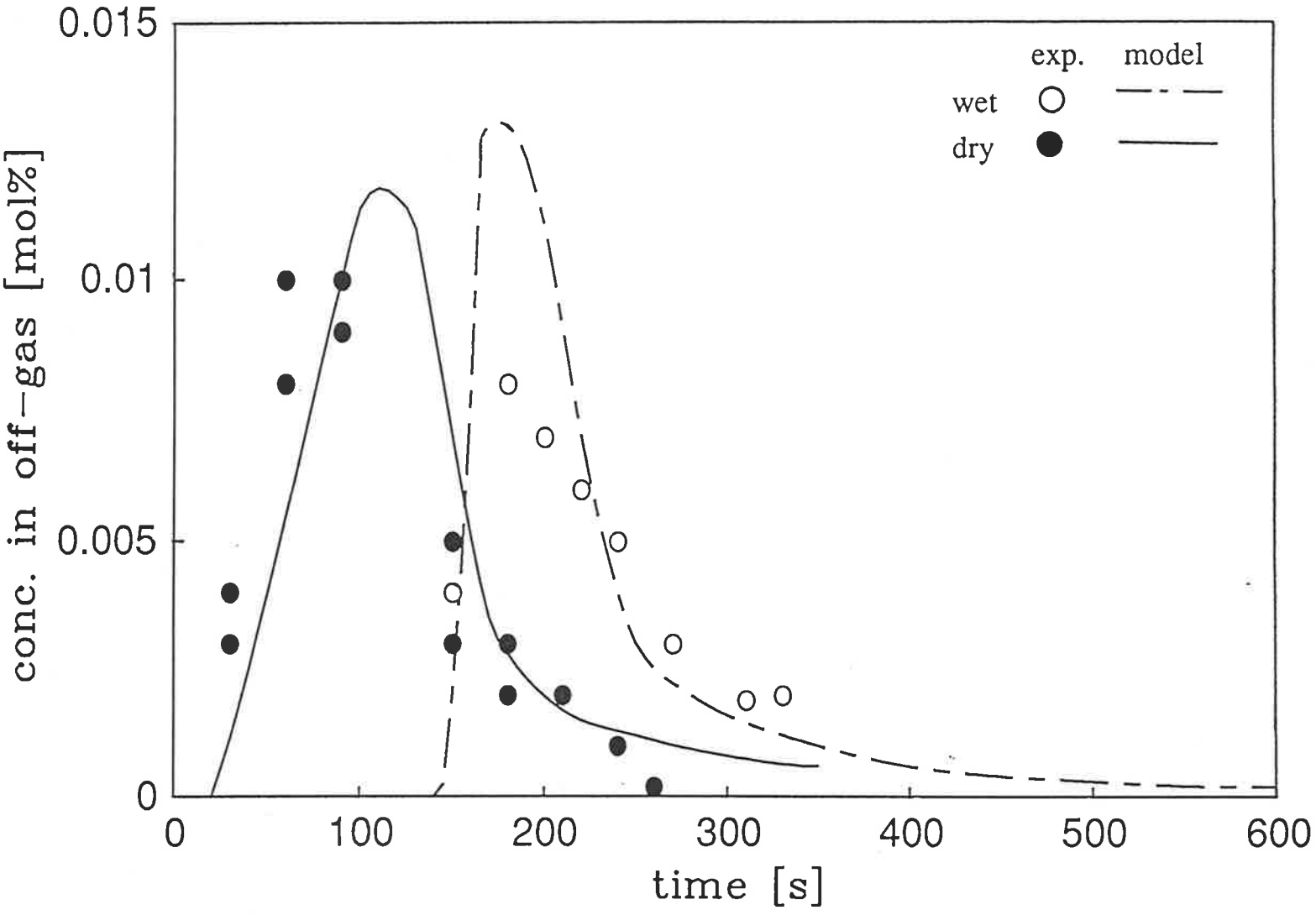

Fig. 5.9c C_2H_4 evolution from 5 mm Bowmans coal particles at 773 K

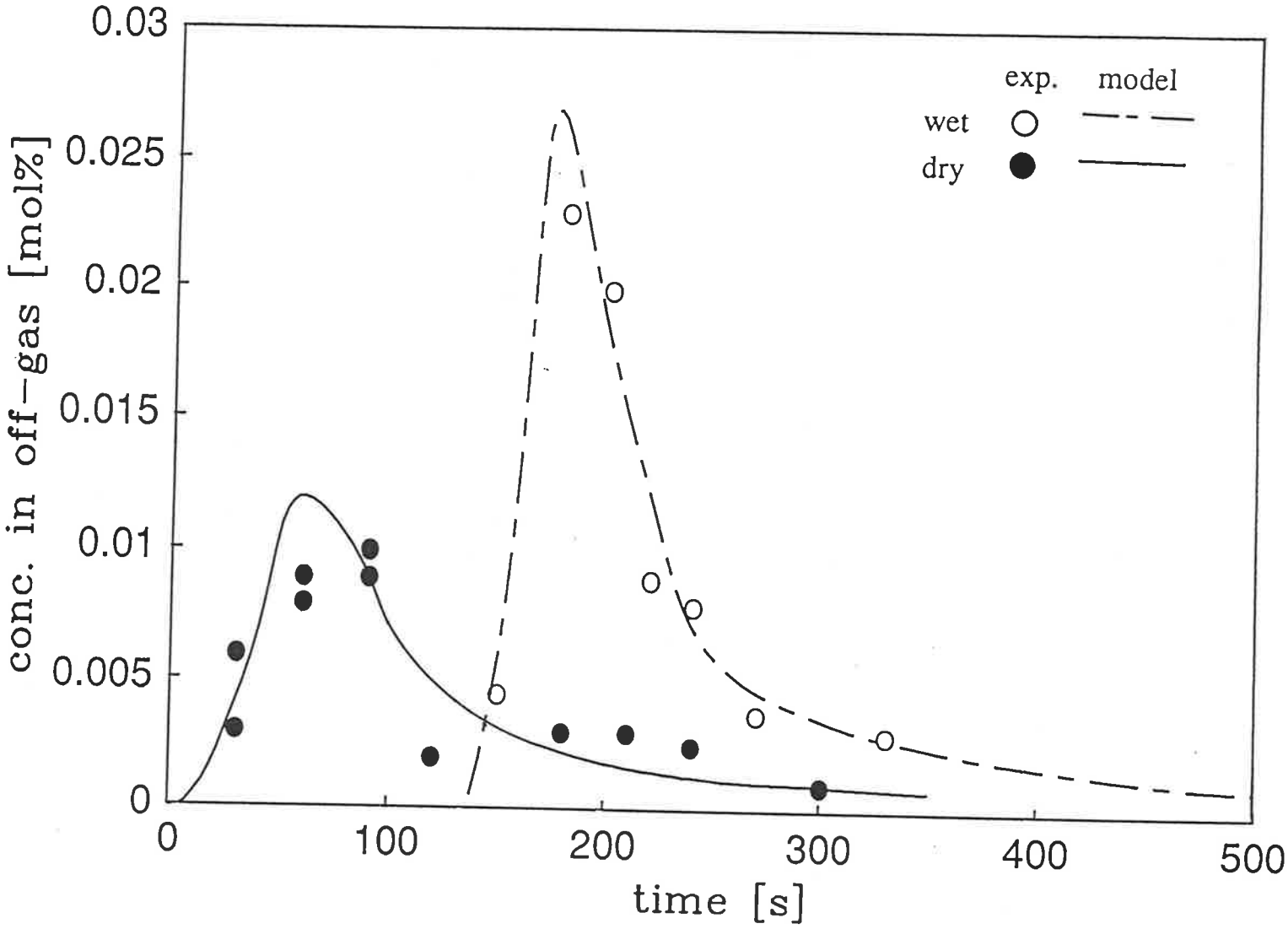

Fig. 5.9d C_2H_6 evolution from 5 mm Bowmans coal particles at 773 K

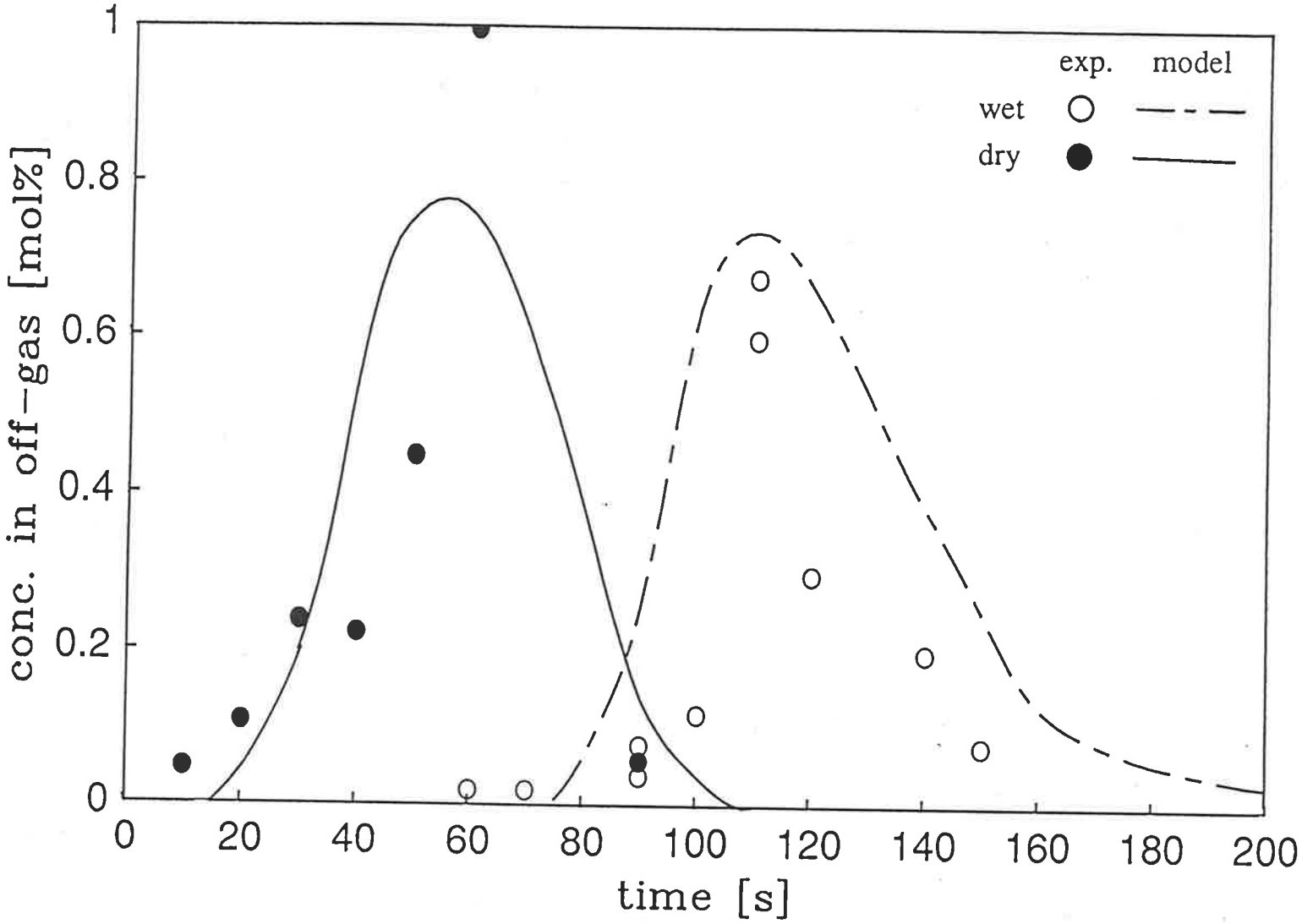

Fig. 5.10a CO evolution from 5 mm Bowmans coal particles at 873 K

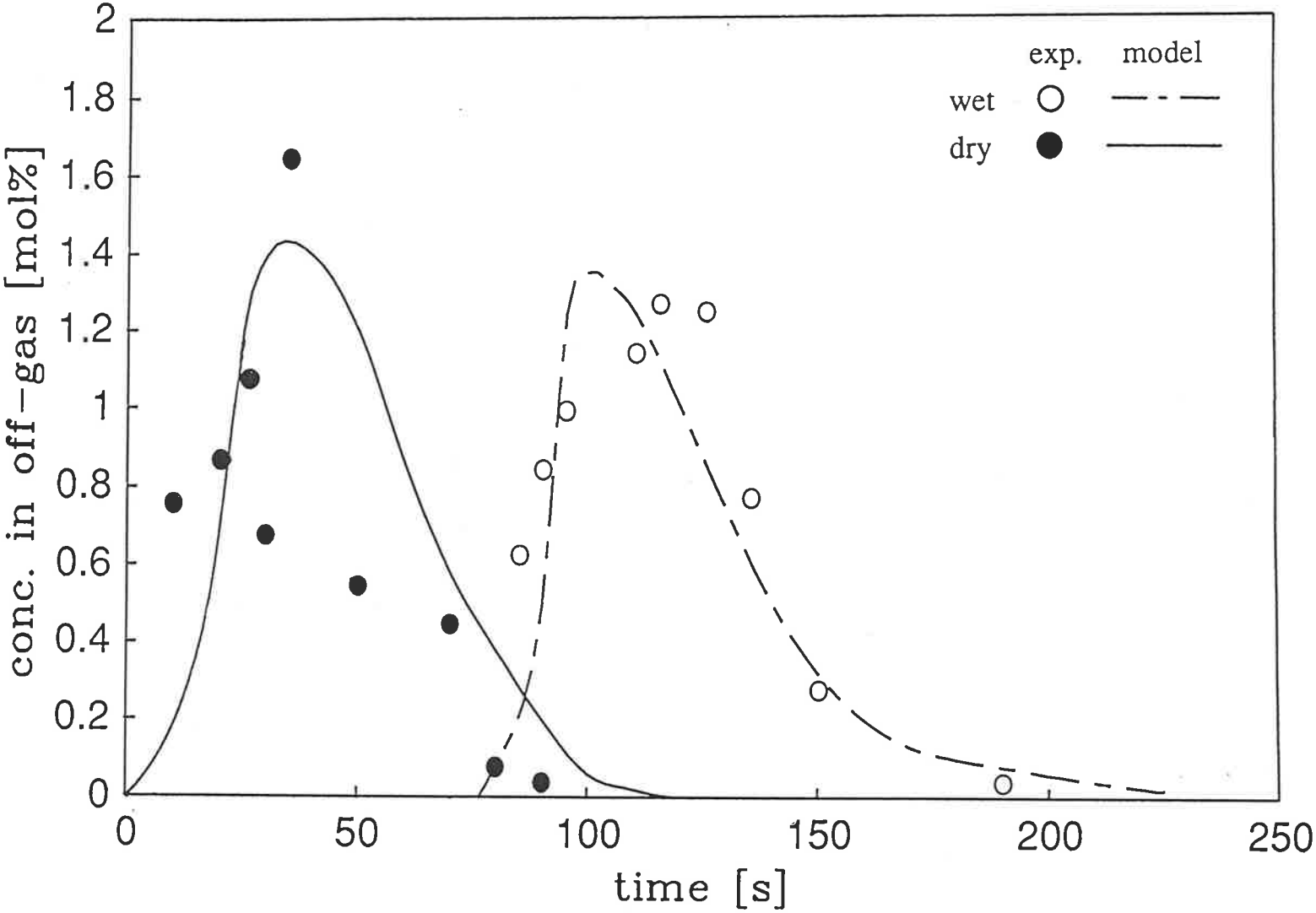

Fig. 5.10b CO_2 evolution from 5 mm Bowmans coal particles at 873 K

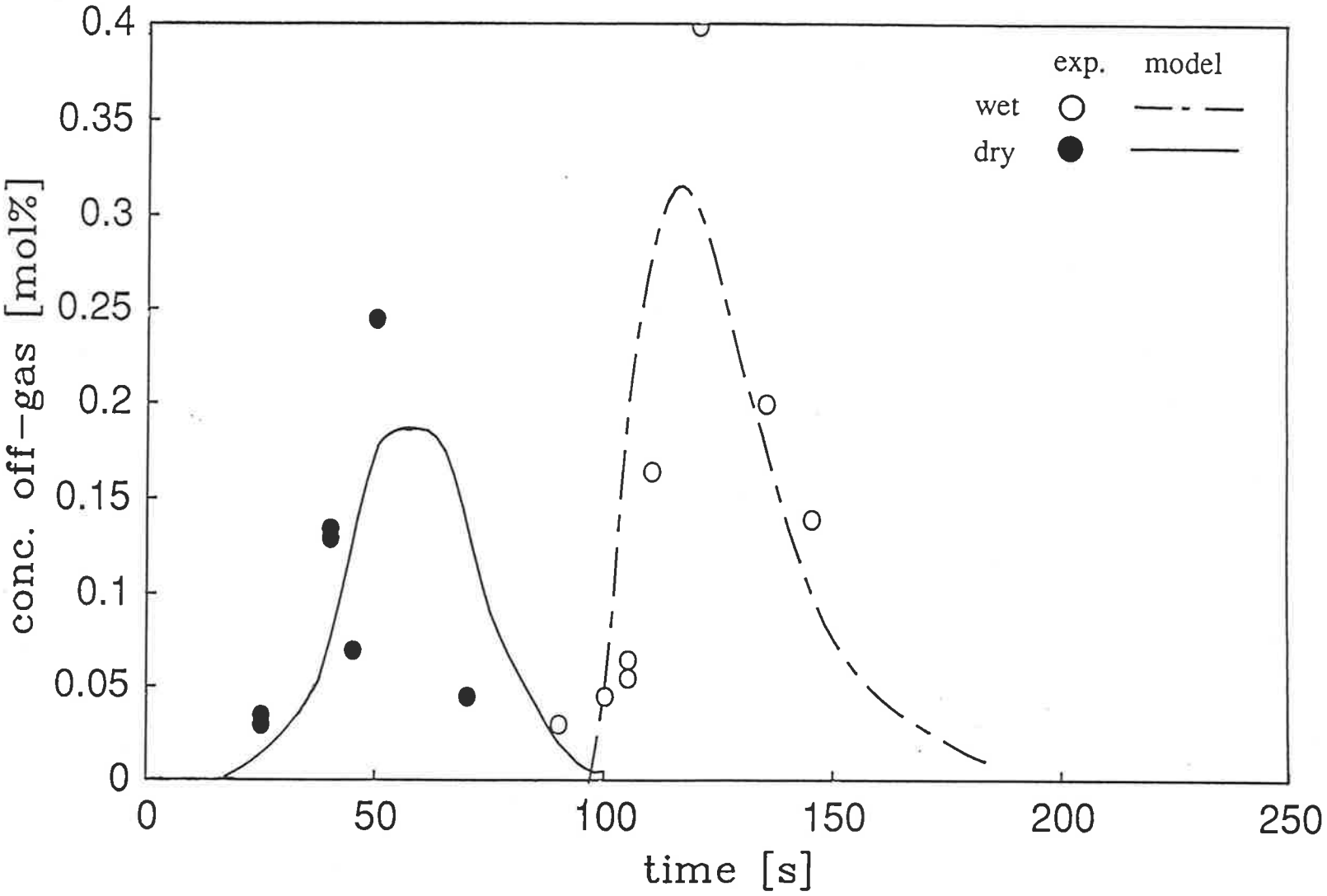

Fig. 5.10c CH_4 evolution from 5 mm Bowmans coal particles at 873 K

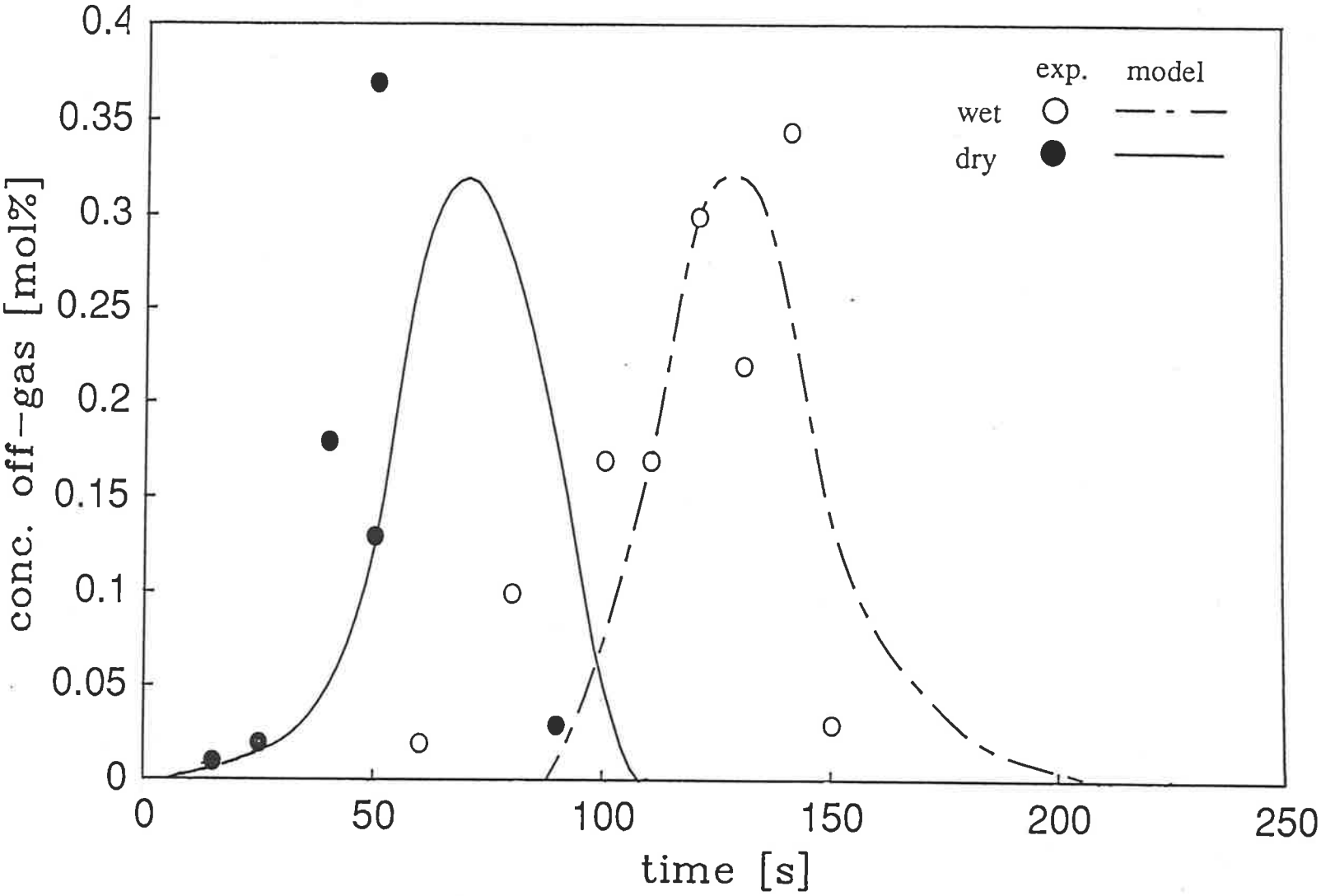

Fig. 5.10d C_2H_4 evolution from 5 mm Bowmans coal particles at 873 K

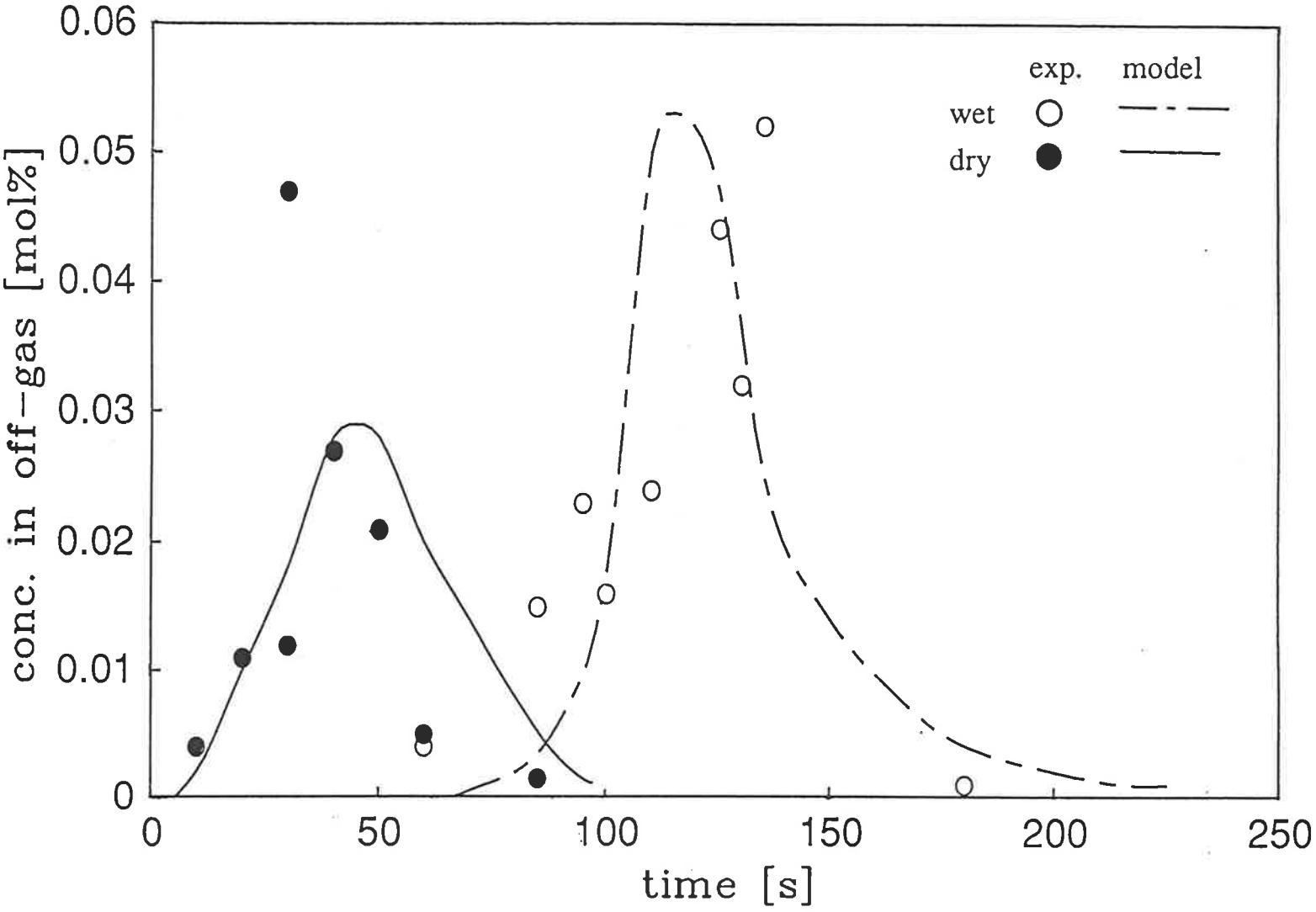

Fig. 5.10e C_2H_6 evolution from 5 mm Bowmans coal particles at 873 K

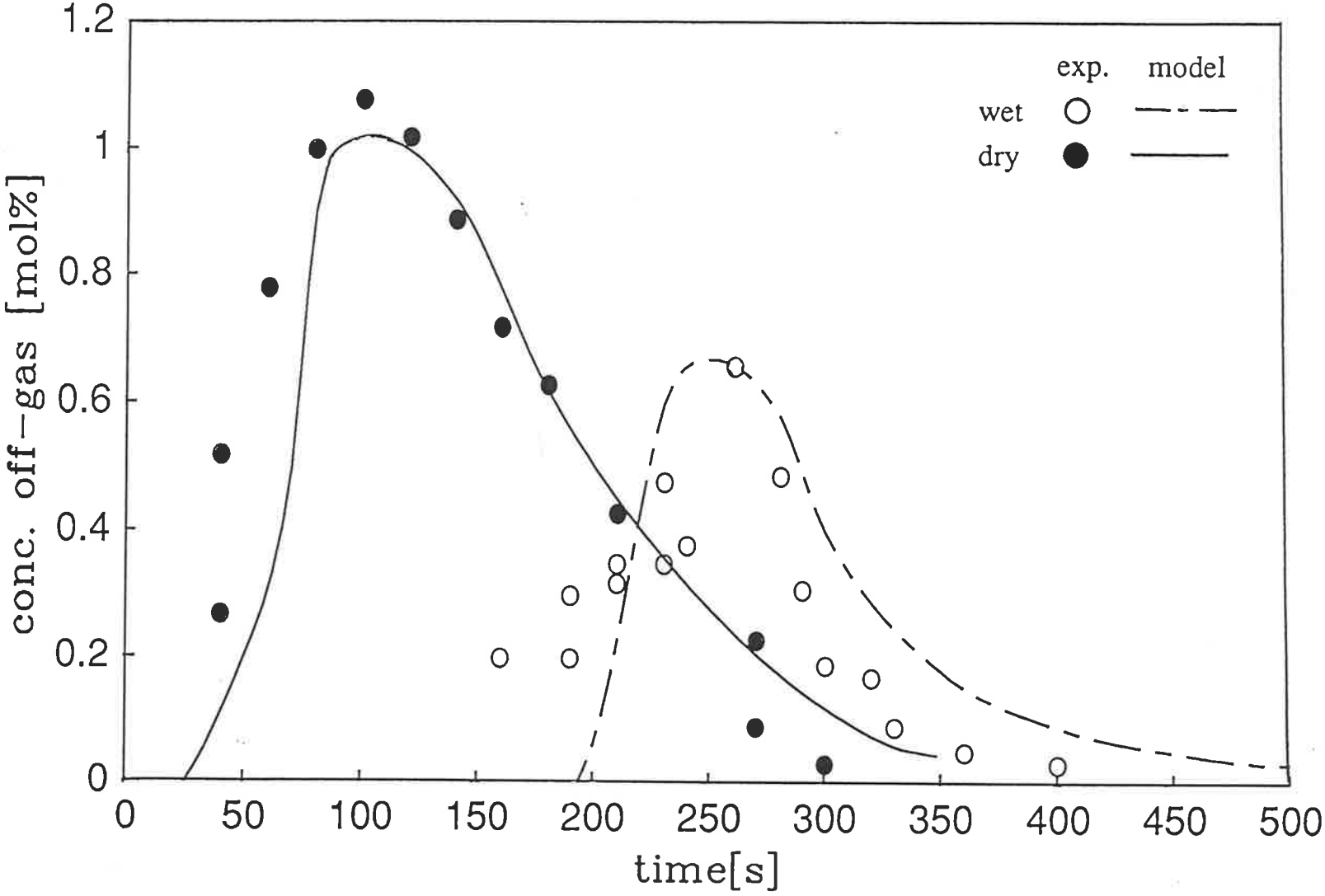

Fig. 5.11a CO evolution from 10 mm Bowmans coal particles at 873 K

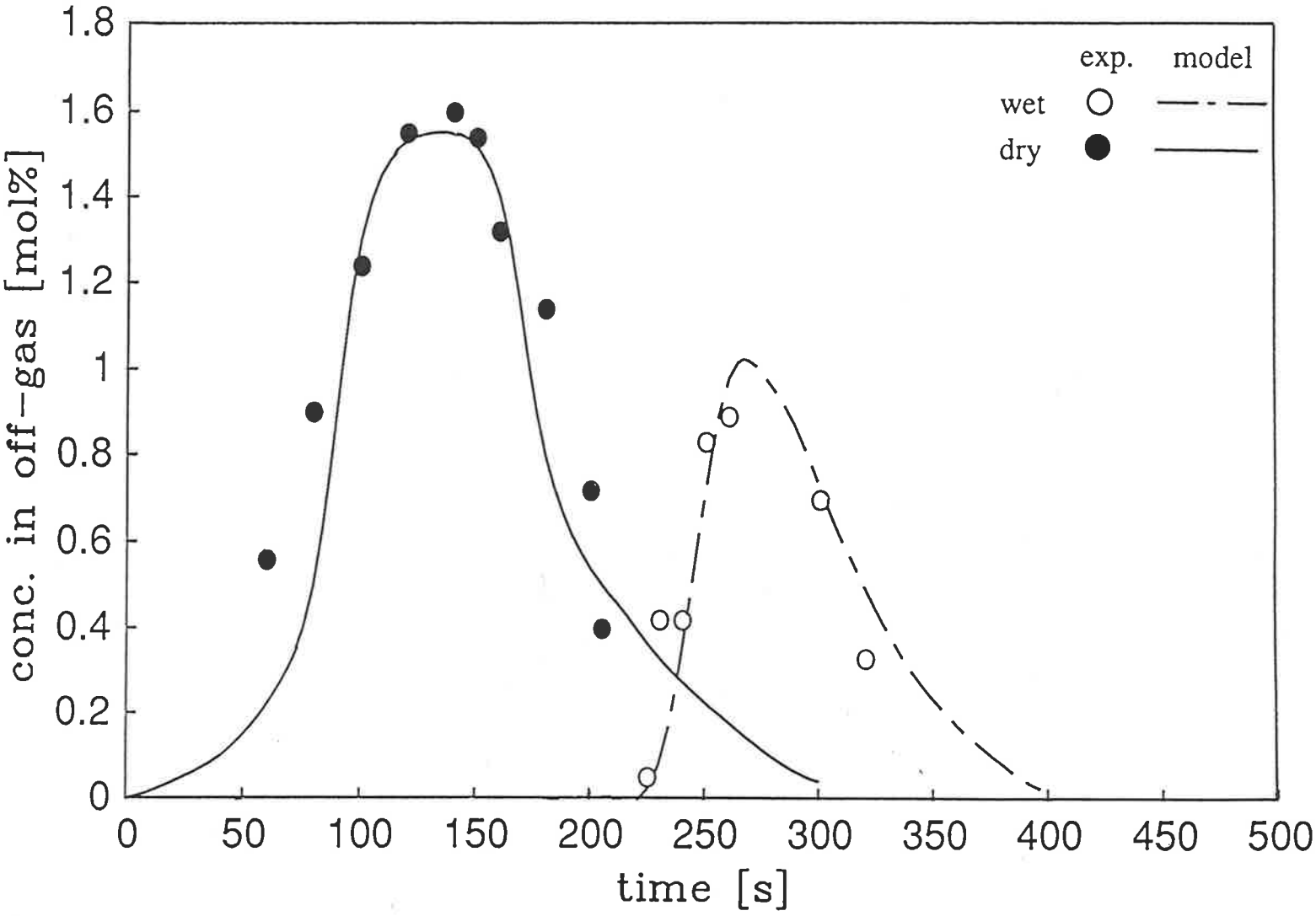

Fig. 5.11b CO_2 evolution from 10 mm Bowmans coal particles at 873 K

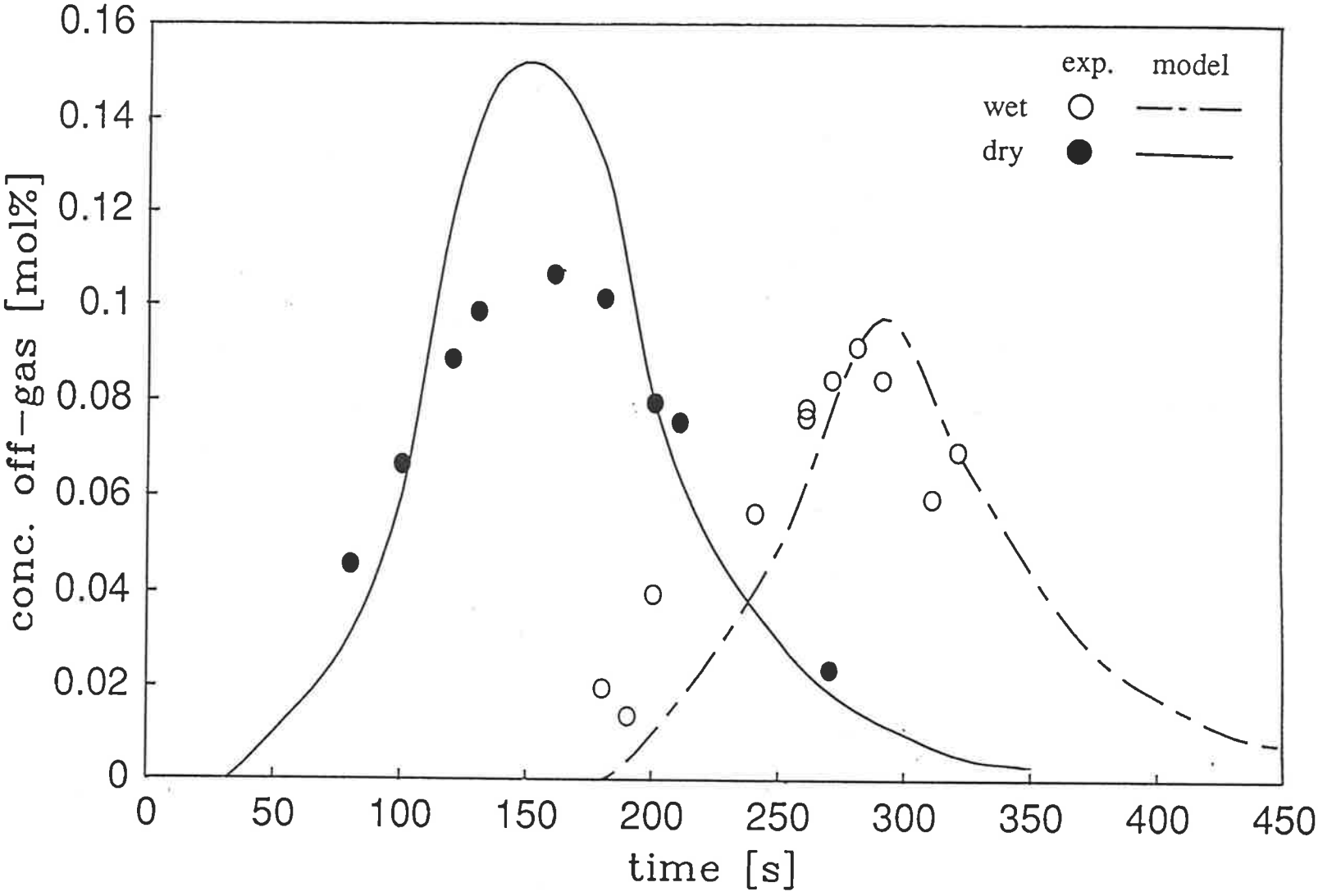

Fig. 5.11c CH_4 evolution from 10 mm Bowmans coal particles at 873 K

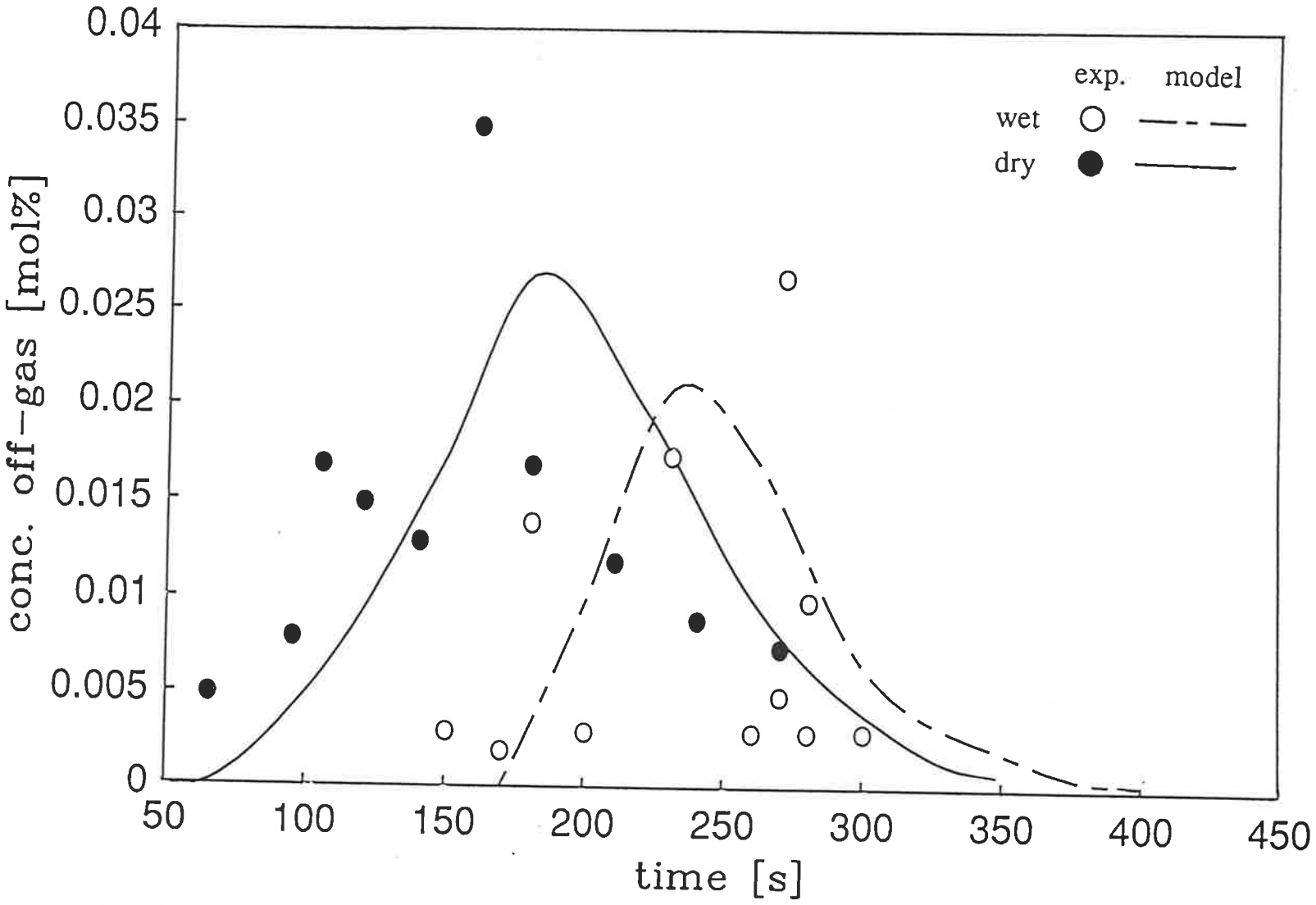

Fig. 5.11d C_2H_4 evolution from 10 mm Bowmans coal particles at 873 K

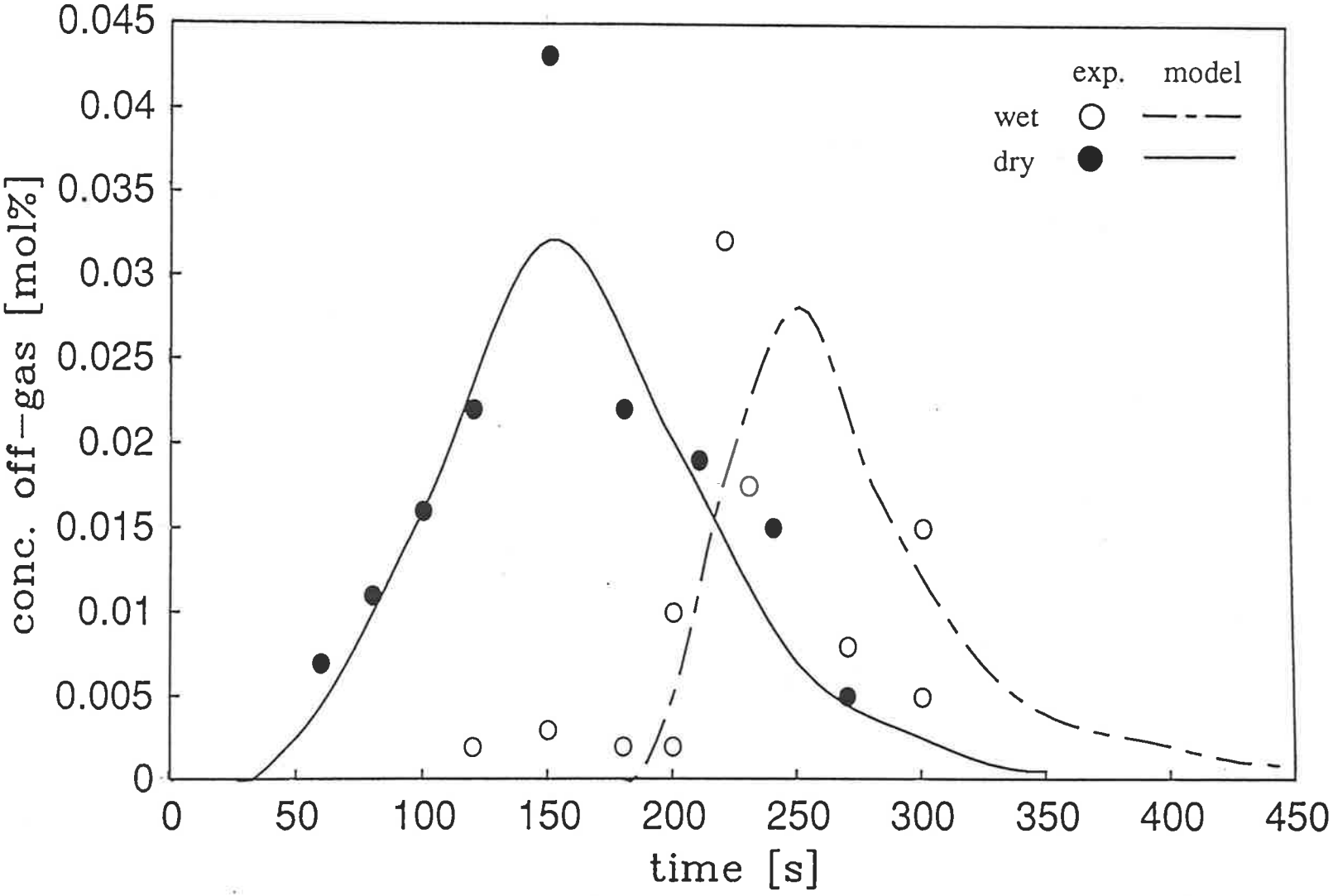

Fig. 5.11e C_2H_6 evolution from 10 mm Bowmans coal particles at 873 K

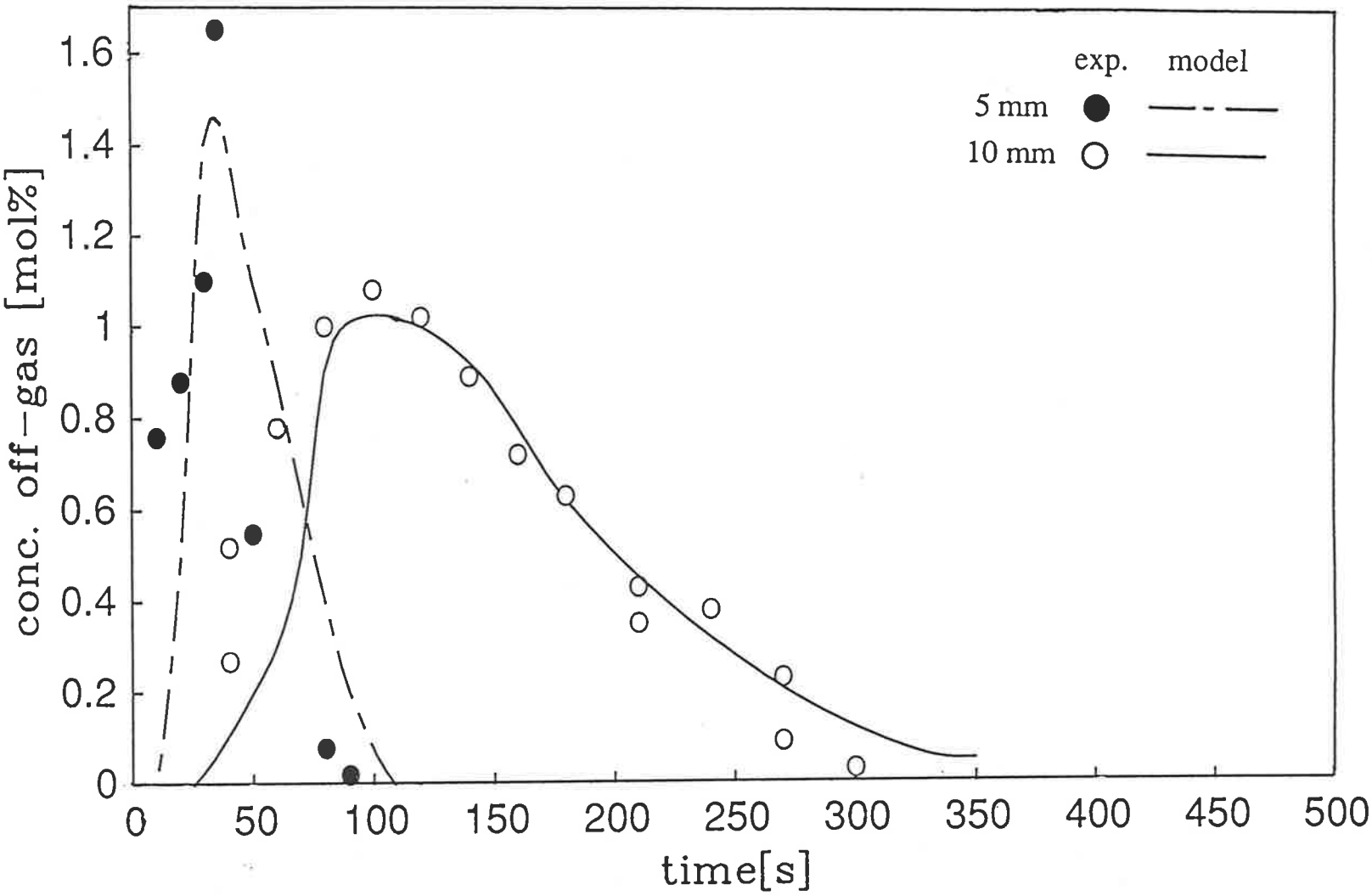

Fig. 5.12 Effect of particle size on CO_2 evolution from dry Bowmans coal particles at 873 K

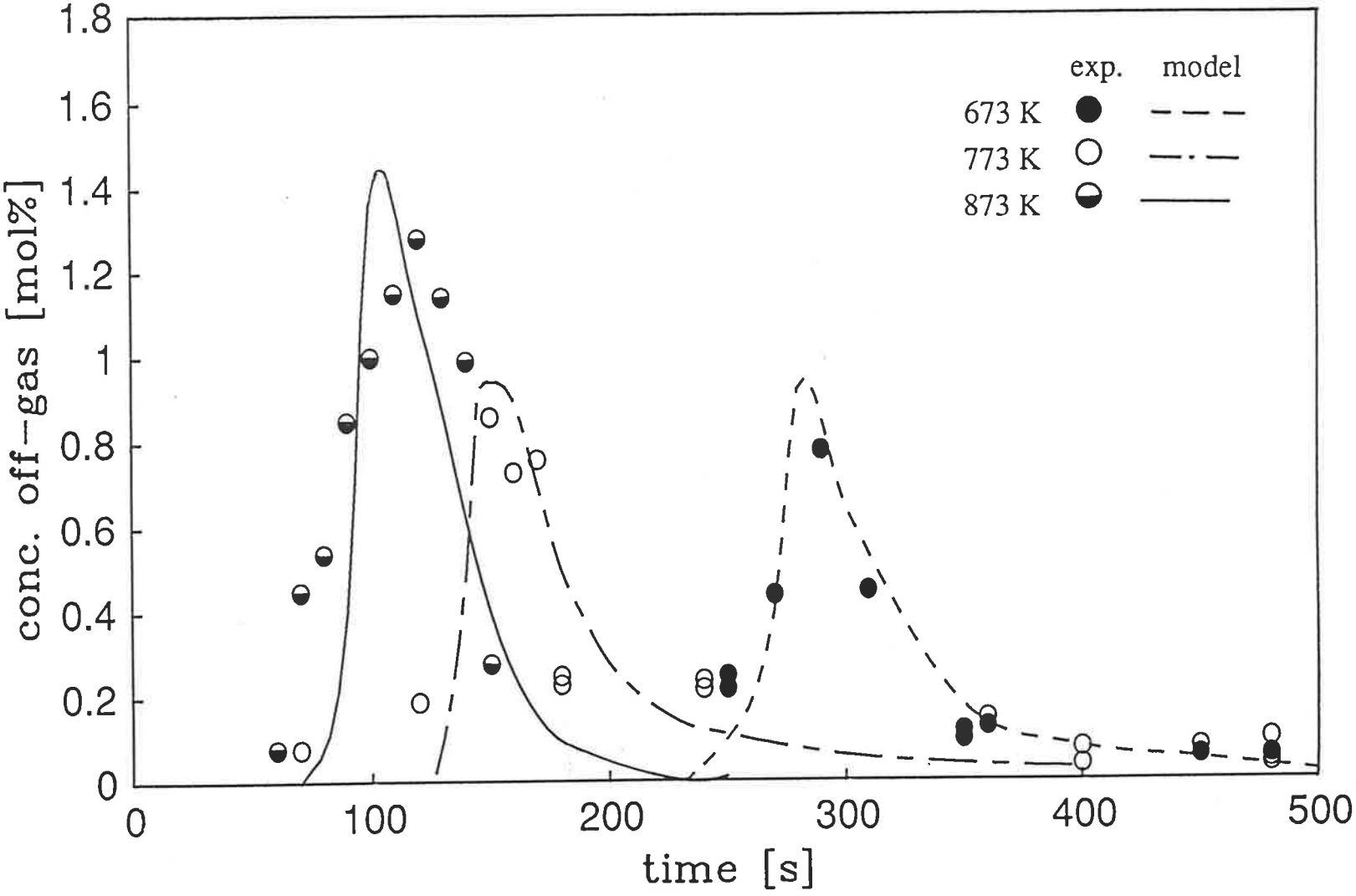

Fig. 5.13 Effect of gas temperature on CO_2 evolution from wet Bowmans coal particles

Table 5.1 KINETIC PARAMETERS FOR THE EVOLUTION OF GASEOUS SPECIES IN THE PYROLYSIS OF BOWMANS COAL

		Solomon and Hamblen (1983)			Agarwal et al. (1987)		Parameters for Bowmans Coal		
CO	Sources	1	2		1	2	1	2	
	V_i^*	0.36	0.64		0.33	0.67	0.33	0.67	
	E_0 (kJ/mol)	208	330		216	300	216	300	
	σ (kJ/mol	20.8	50		28.8	26.7	28.8	26.7	
	$\log_{10}k_{oi}$	11.23	14		13.22	13.22	13.22	13.22	
CO_2	Sources	1	2	3	1		1	2	3
	V_i^*	0.2	0.6	0.2	1.0		0.2	0.6	0.2
	E_0 (kJ/mol)	180	236	300	226		180	236	300
	σ (kJ/mol	16.6	25	27.4	52		16.6	25	27.4
	$\log_{10}k_{oi}$	14	14	14	13.22		14	14	14
CH_4	Sources	1	2		1	2	1	2	
	V_i^*	0.5	0.5		0.5	0.5	0.5	0.5	
	E_0 (kJ/mol)	250	250		250	250	230	230	
	σ (kJ/mol	1205	25		12.5	25	12.5	25	
	$\log_{10}k_{oi}$	14.23	12.23		14.2	12.23	14.23	12.23	
C_2H_4	Sources	1			1		1		
	V_i^*	1.0			1.0		1.0		
	E_0 (kJ/mol)	250			250		230		
	σ (kJ/mol	12.5			12.5		10		
	$\log_{10}k_{oi}$	14.23			13.22		13.22		
C_2H_6	Sources	1			1		1		
	V_i^*	1.0			1.0		1.0		
	E_0 (kJ/mol)	250			220		220		
	σ (kJ/mol	12.5			20		20		
	$\log_{10}k_{oi}$	14.23			13.22		13.22		

5.3 OVERALL WEIGHT LOSS DUE TO DRYING AND DE-VOLATILIZATION UNDER PYROLYSIS CONDITIONS

Experiments for drying (without devolatilization) and coupled drying and de-volatilization were conducted for temperatures of 423 K to 1023 K, particle sizes 1.8 to 10 mm and initial moisture content of 0.64 to 1.1 g moisture/g dry coal under nitrogen atmosphere. The experimental conditions are listed in Table 3.1 and the experimental raw data can be found in Appendix A. The thermo-physical parameters used for the model predictions are listed in Table 5.2 and comparable to data reported in literature (Badzioch et al., 1964).

Table 5.2 THERMO-PHYSICAL PARAMETERS FOR BOWMANS COAL

ρ_s	1250 kg / m³
c_p	1.25 kJ / kg K
α	0.2 mm²/ s
λ	2380 kJ / kg
T_e	373 K
T_0	293 K

This data as well as reported data on drying of coal in literature (Agarwal, 1984; Ziesing et al., 1979; McIntosh, 1976b; Jung and Stanmore, 1980) have been compared with the predictions of pseudo steady-state model without shrinkage as developed by Agarwal et al. (1984a) in Fig. 5.14. As already pointed out earlier the total drying time has to be used as

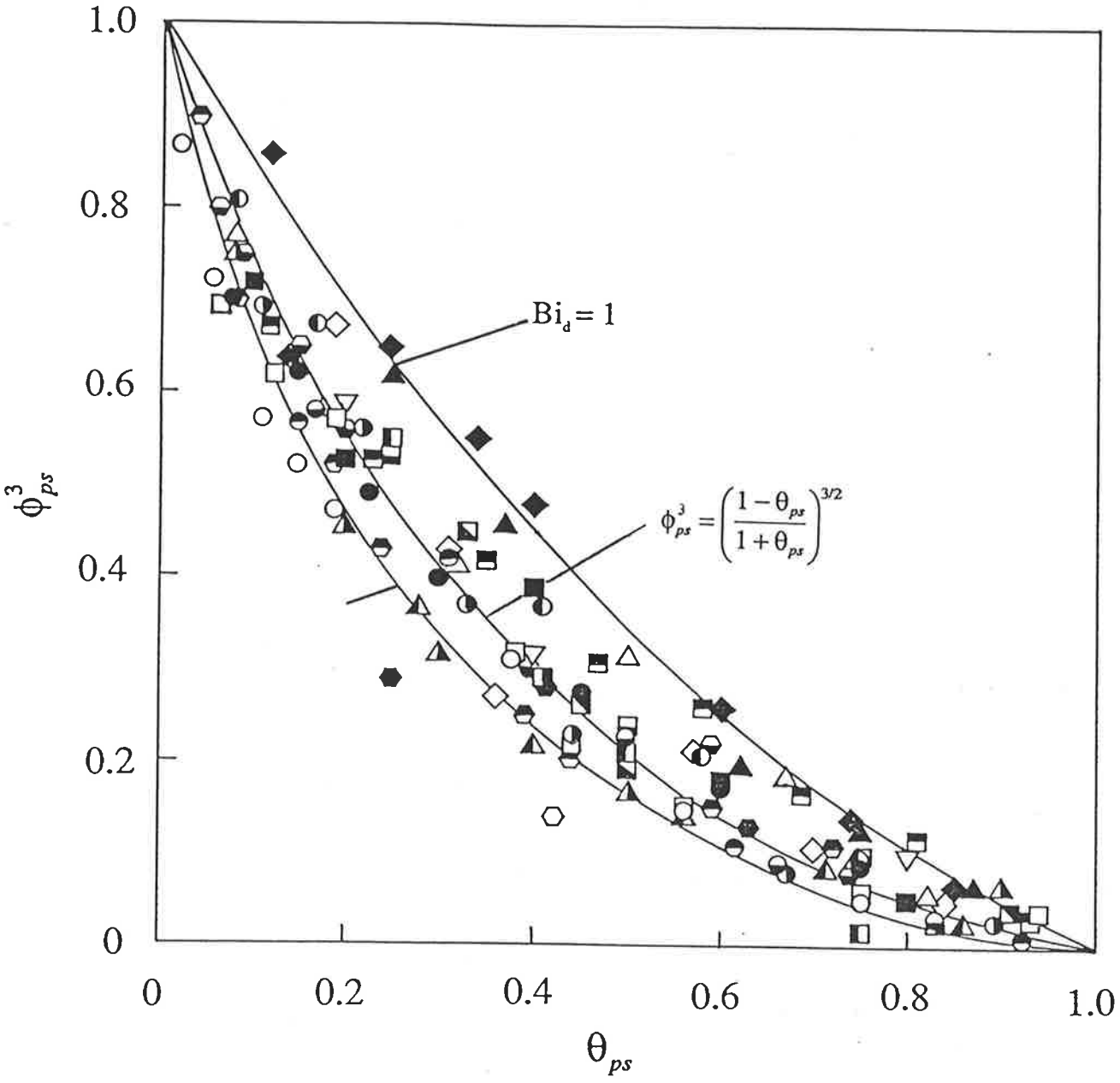

Fig. 5.14 Comparison of pseudo steady-state model with experimental data

Table 5.3 OPERATING CONDITIONS AND ESTIMATED BIOT NUMBERS FOR DATA IN FIG. 5.10

	T_s[K]	R_{p0}[mm]	Bi	C_0[g/g]	τ_{exp}[s]	Symb.
present	423	5	3.1	1.1	667	○
study	573	5	3.2	1.1	400	●
	823	5	4.2	1.1	195	◓
	923	5	4.3	1.1	180	◒
	1023	5	4.4	1.1	120	◐
	923	5	4.3	0.64	90	◑
	423	0.9	0.71	1.1	120	□
	423	0.9	0.71	0.68	80	■
	573	0.9	0.75	1.1	40	◨
	823	0.9	1.1	1.1	15	◨
	923	0.9	1.1	1.1	12	◧
	923	0.9	1.1	0.69	8	◧
	1023	0.9	1.2	1.1	10	◪
	923	2.5	2.1	1.1	60	◪
(1)	423	1.19 - 2.0	5.3	0.66	210	△
	463	1.19 - 2.0	4.5	0.66	180	◭
	538	1.19 - 2.0	4.5	0.69	100	◭
	613	1.19 - 2.0	4.0	0.69	80	▲
	713	1.19 - 2.0	3.0	0.69	50	▽
(2)	993	3.2 - 4.2	5.7	1.36	55	⬢
	1093	2.5 - 2.8	5.0	1.36	35	⬡
(3)	873	3.175	8.0	1.8	74	⬣
	873	6.35	11.0	1.8	180	⬣
(4)	~393	< 1.7	< 2.6			◆
	~473	< 3.175	< 5.8			◇

(1) Agarwal, 1984
(2) Jung and Stanmore, 1980
(3) McIntosh, 1976b
(4) Ziesing et al., 1979

an input parameter for the pseudo steady-state model. The dimensionless time parameter, θ_{ps}, was therefore calculated using the experimental drying time. The relevant operating conditions and estimated Biot numbers for Fig. 5.14 are listed in Table 5.3. As may be seen, the model predictions are in good agreement with data for the different coal types used. It is also possible as Agarwal (1984) suggested to correlate the data with a simple expression

$$\phi_{ps}^3 = C/C_0 = \left(\frac{1-\theta_{ps}}{1+\theta_{ps}}\right)^{3/2} \tag{71}$$

This expression is very close to the pseudo steady-state model predictions with Bi = 4, and could be used as a first estimate on the total drying time.

To estimate the shrinkage proportionality factor, $\overline{F}$, for Bowmans coal, the particle diameters as a function of time and moisture content have been obtained through experiments. In Figure 5.15 the experimental results are plotted as volumetric shrinkage, ε^3, against dimensionless moisture content (C/C_0) and compared with model predictions for different shrinkage proportionality factors. The experimental data are in the range of model predictions for proportionality factor 0.25 to 0.75. No clear distinction between the ambient temperatures and initial particle sizes used, can be made. Therefore shrinkage proportionality factor of 0.5 has been chosen for further model comparison.

To ensure reproducibility of the experimental results, 5 experiments at each condition and time have been carried out. Furthermore one experiment has been completely repeated on a different day. As can be seen in Figure 5.16 there are no differences worth mentioning of between the experimental results of the two series of experiments. To obtain a large enough sample for the analysis roughly the same amount on weight of 1.8 mm

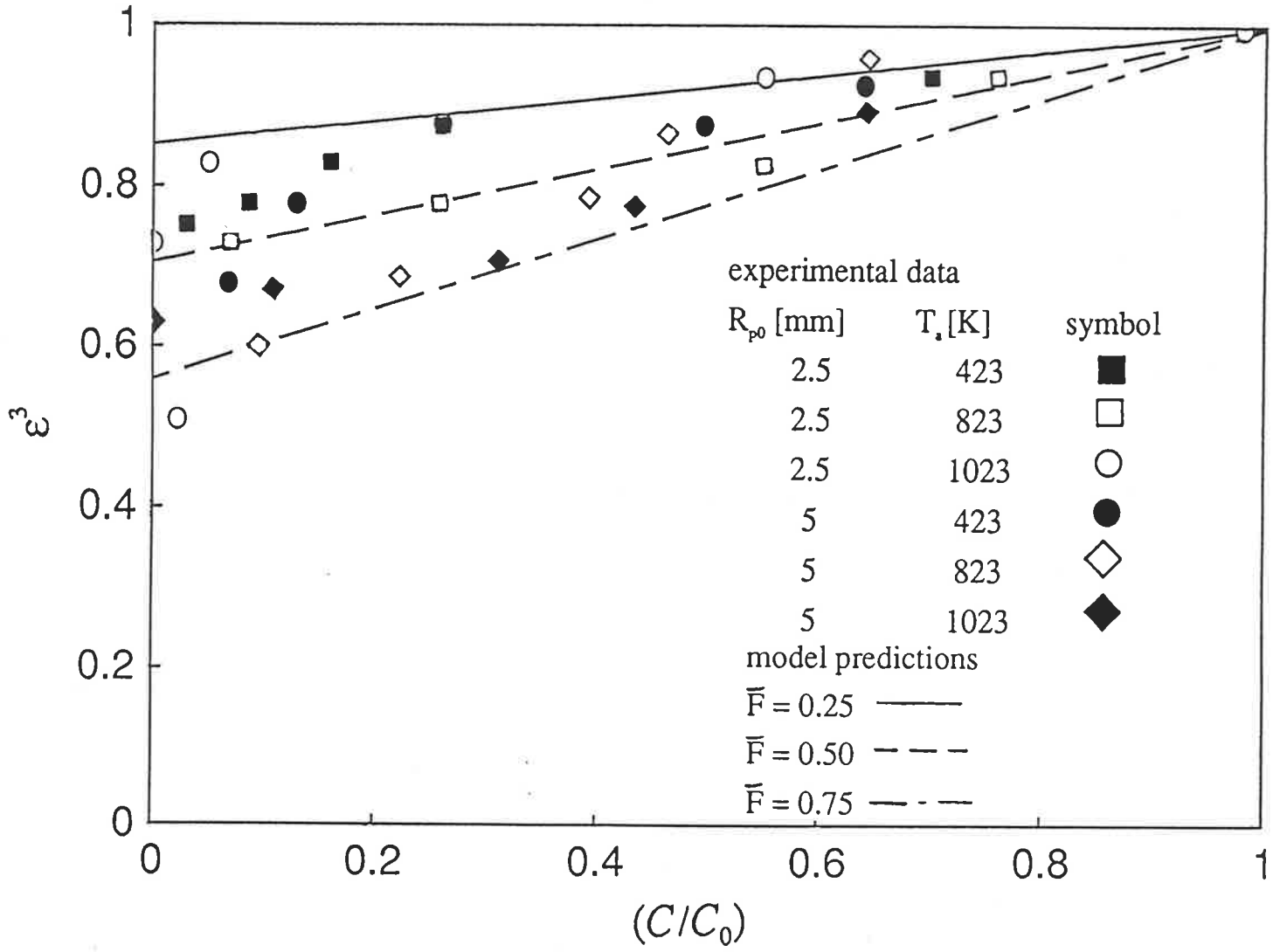

Fig. 5.15 Influence of shrinkage proportionality constant on volumetric shrinkage

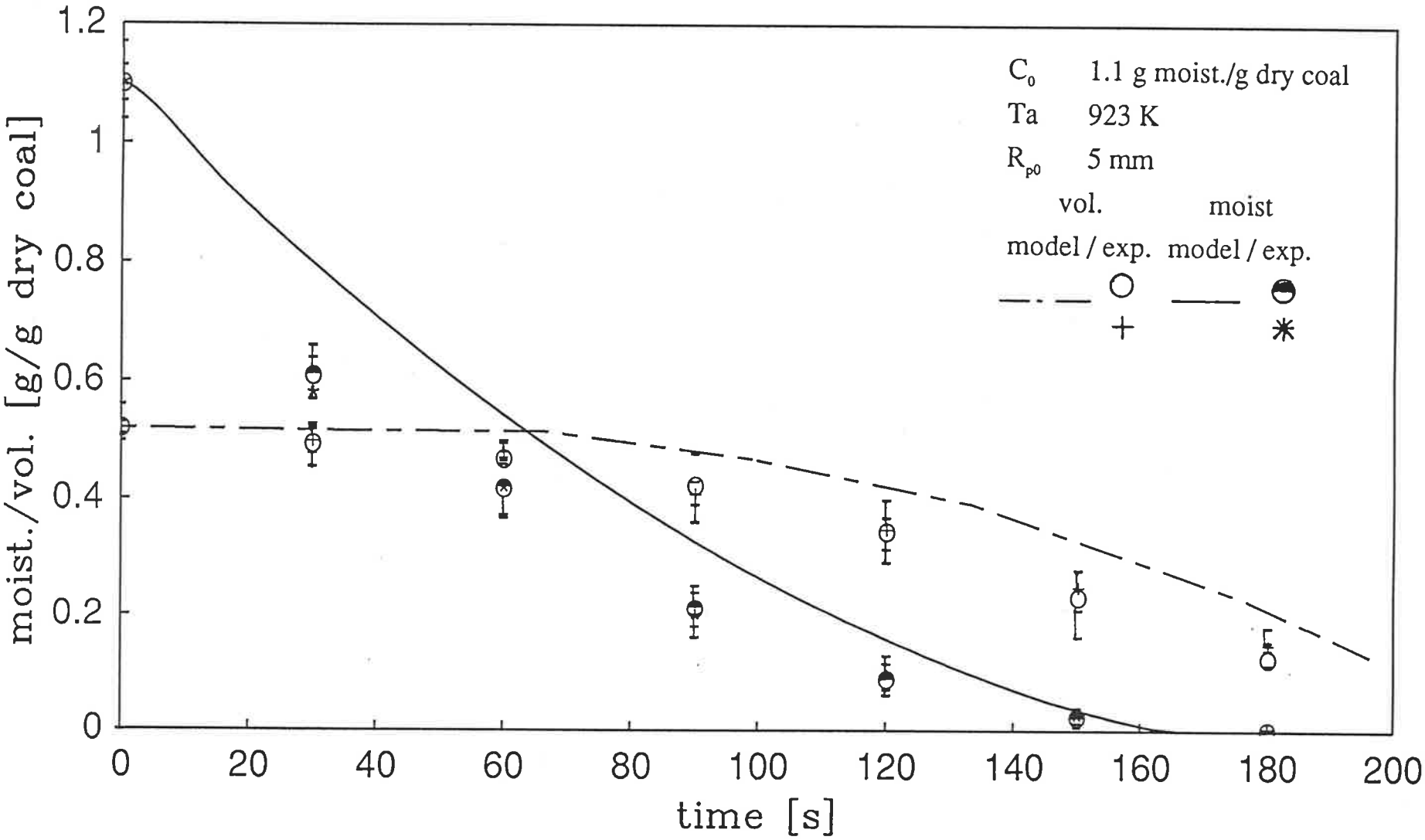

Fig. 5.16 Comparison of model predictions and experimental data for coupled drying and devolatilization under pyrolysis conditions

particles as the large particles has been used for the experiments. The data from detailed experimental investigations are plotted in Figures 5.17 to 5.21 and 5.23 to 5.26; the symbols are the average value of the 5 points and the error bars show the range of data.

The drying history of 1.8 mm particles with initial moisture content of 0.68 g moisture/g dry coal at 423 K is shown in Figure 5.17. In Figure 5.18 the drying behaviour of 10 mm and 1.8 mm particles at 423 K is plotted. Figure 5.19 shows the drying histories for 1.8 and 10 mm particles at 573 K. The drying time for smaller particle size, as one would expect, is much shorter. The model seems to overpredict the drying behaviour. At higher temperatures (823 - 1023 K) this may be due to a time delay in quenching the particles. Further, radiation effects are expected to be important. These effects have not been accounted for explicitly in the model, though the convective heat transfer Biot number has been increased up to 30%, depending on temperature, to include a rough estimate. Since the radiative contribution is proportional to $(T_a^4 - T_s^4)$, the effect of radiation would be stronger in the initial part of drying, which would confirm the experimental data (the discrepancies between model and experiments are higher in the initial stage). However the model also overpredicts the drying behaviour for lower temperatures (423, 573K). At these temperatures the quenching and radiation effects are not important. McIntosh (1976b) observed substantial cracking of the coal particles during drying. The same observation has been made with experiments reported here. It is thought that the cracks allow a more rapid evaporation of the water and a higher drying rate. Furthermore, at low temperatures the particle has more time to build cracks than at higher temperatures (shorter drying times). The model also appears to predict the data for small particles better than for larger ones, Figures 5.18 and 5.19. Experiments on 55 samples also showed that the initial moisture content of the coal particles varied between 1.008 and 1.17 g moisture/g dry coal. This variation is considered in Figure 5.20, the dashed lines show the drying history for the

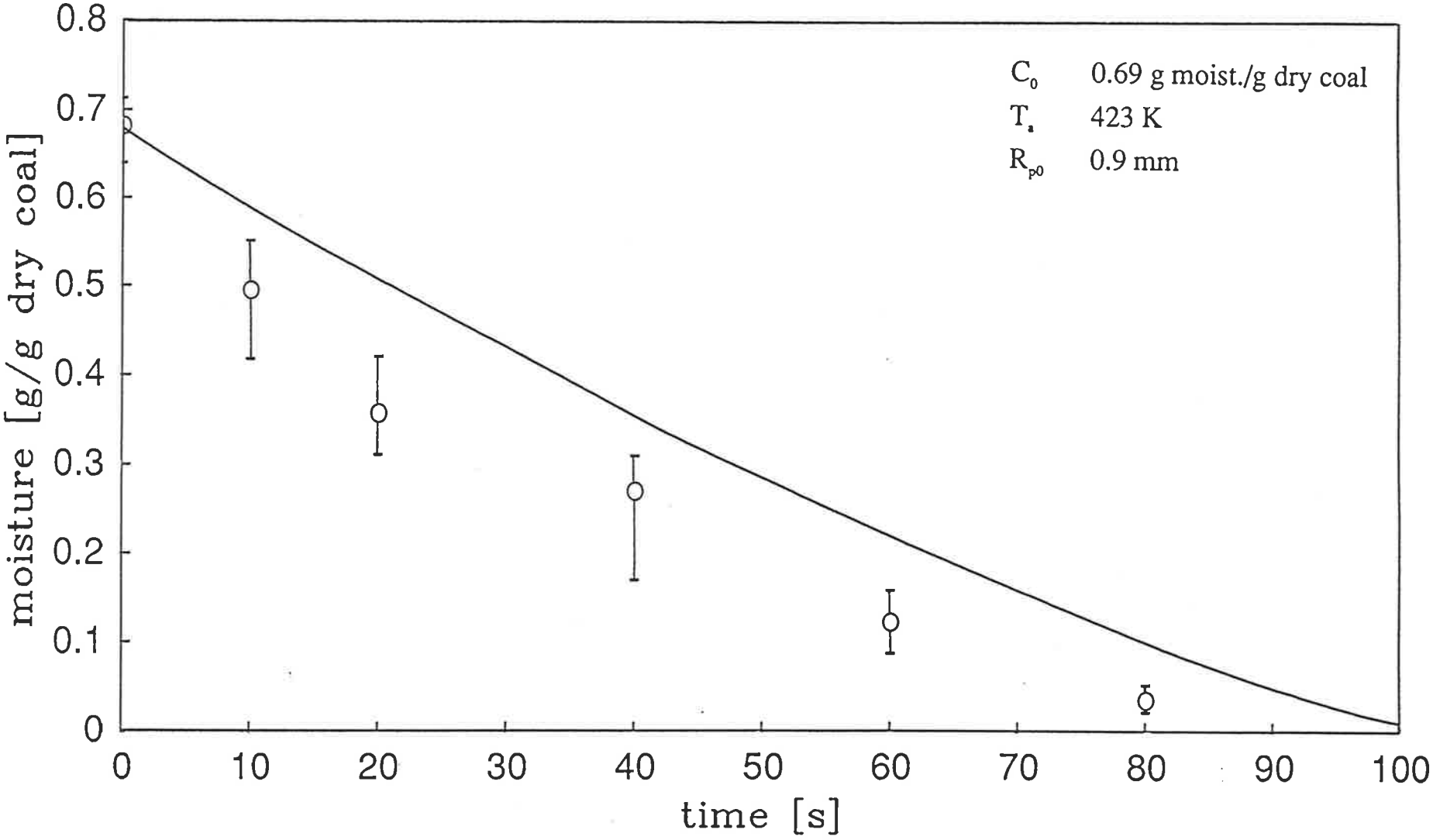

Fig. 5.17 Comparison of model predictions and experimental data for drying with shrinkage

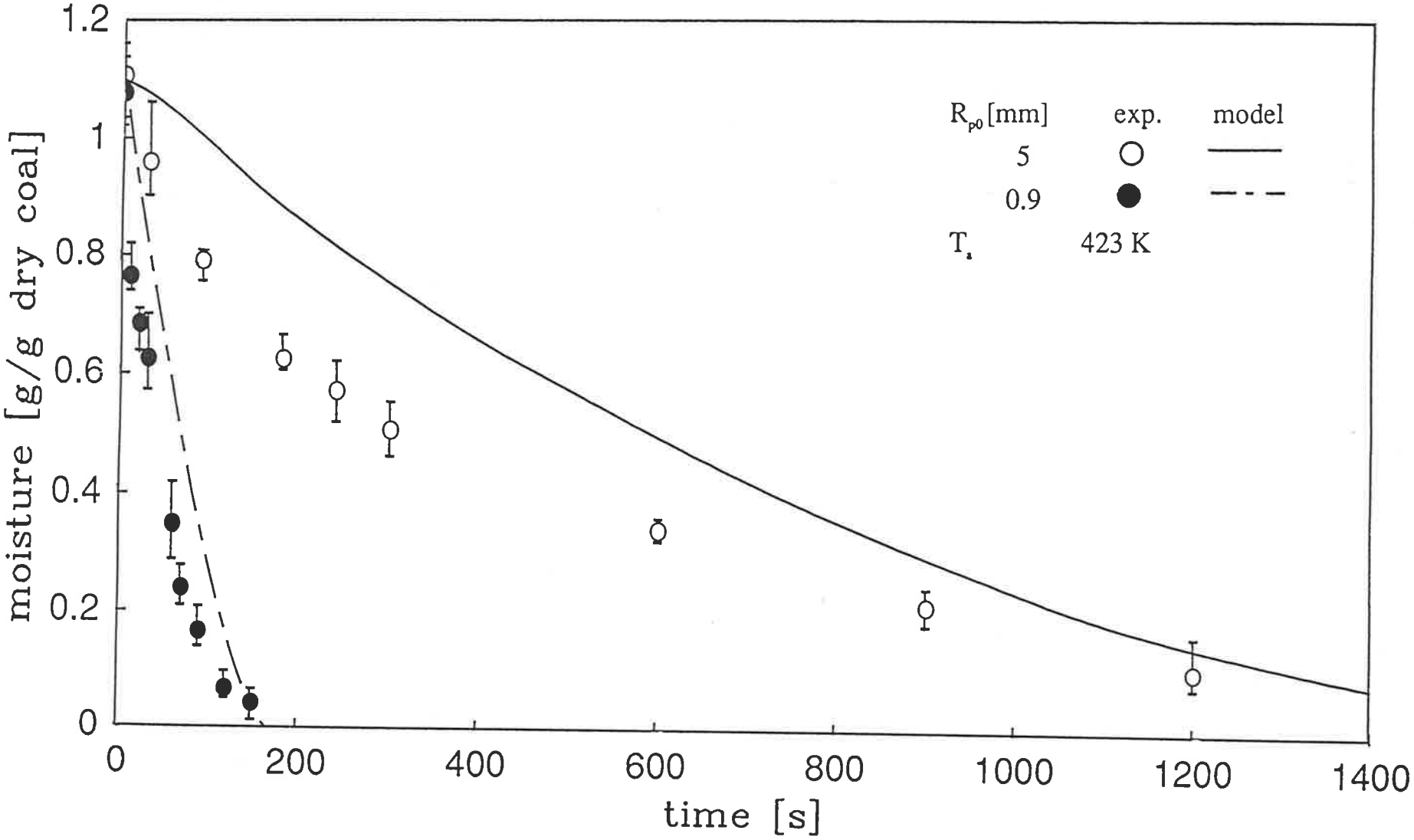

Fig. 5.18 Comparison of model predictions and experimental data for drying with shrinkage

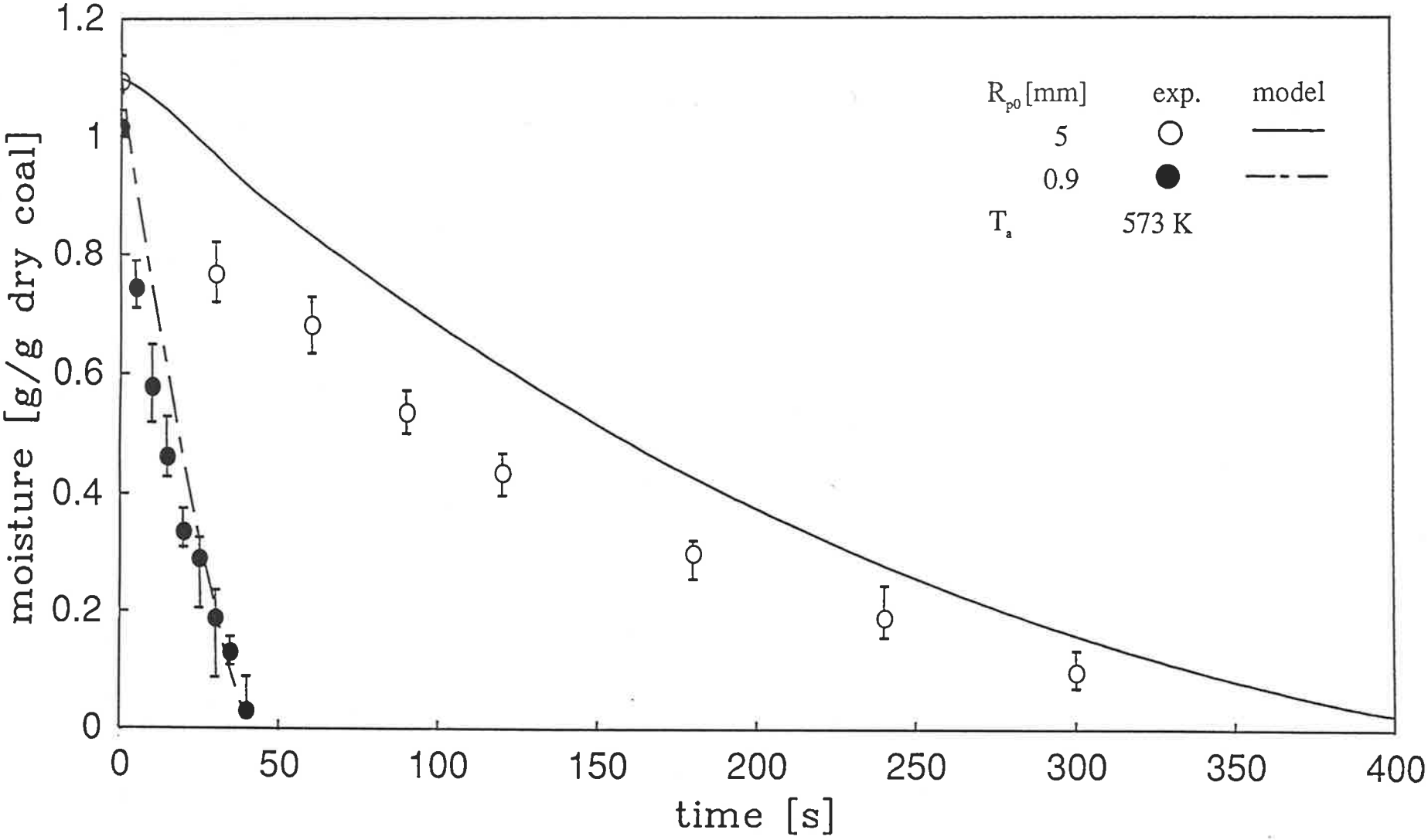

Fig. 5.19 Comparison of model predictions and experimental data for drying with shrinkage

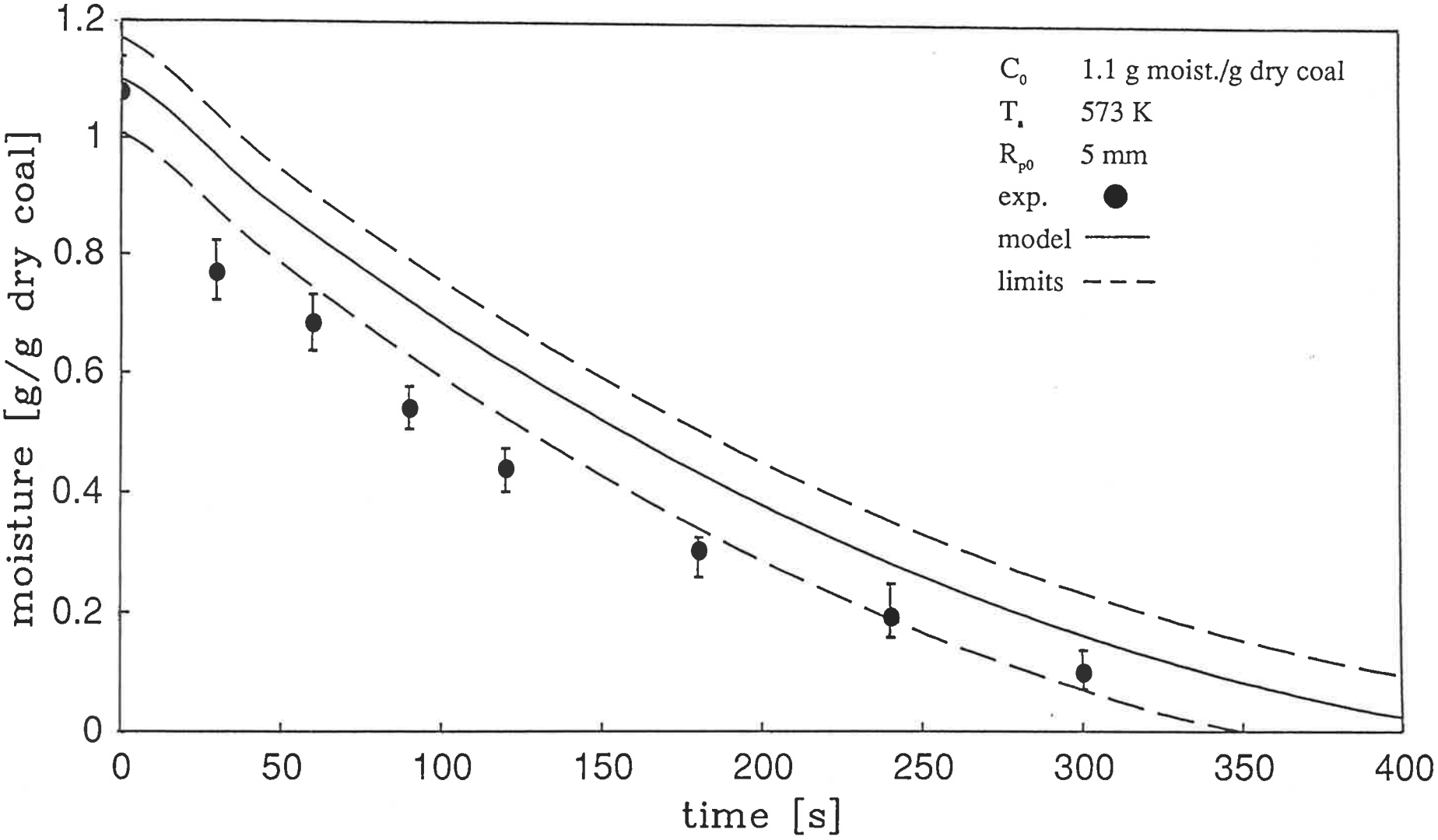

Fig. 5.20 Comparison of model predictions and experimental data for drying with shrinkage

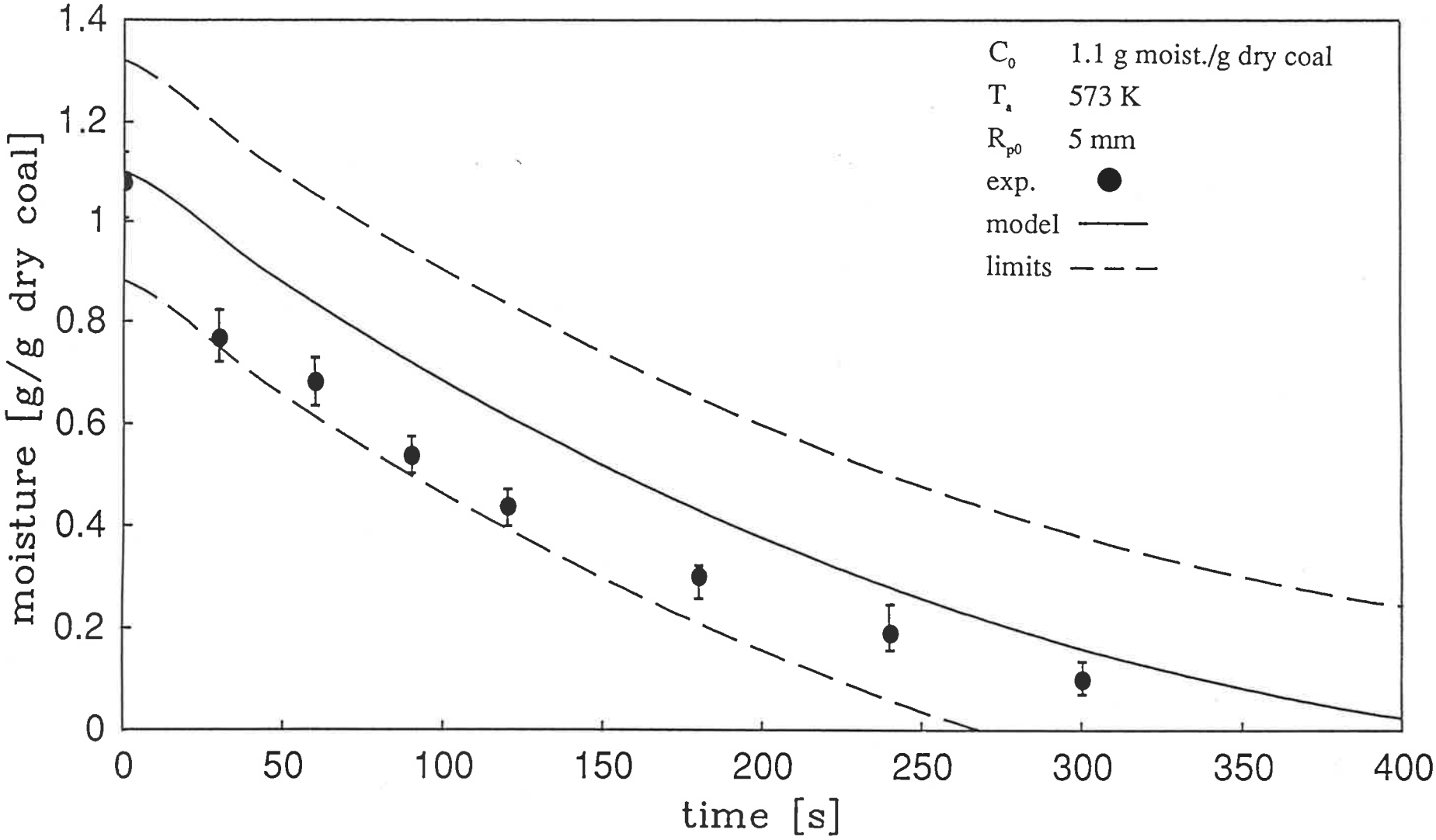

Fig. 5.21 Comparison of model predictions and experimental data for drying with shrinkage

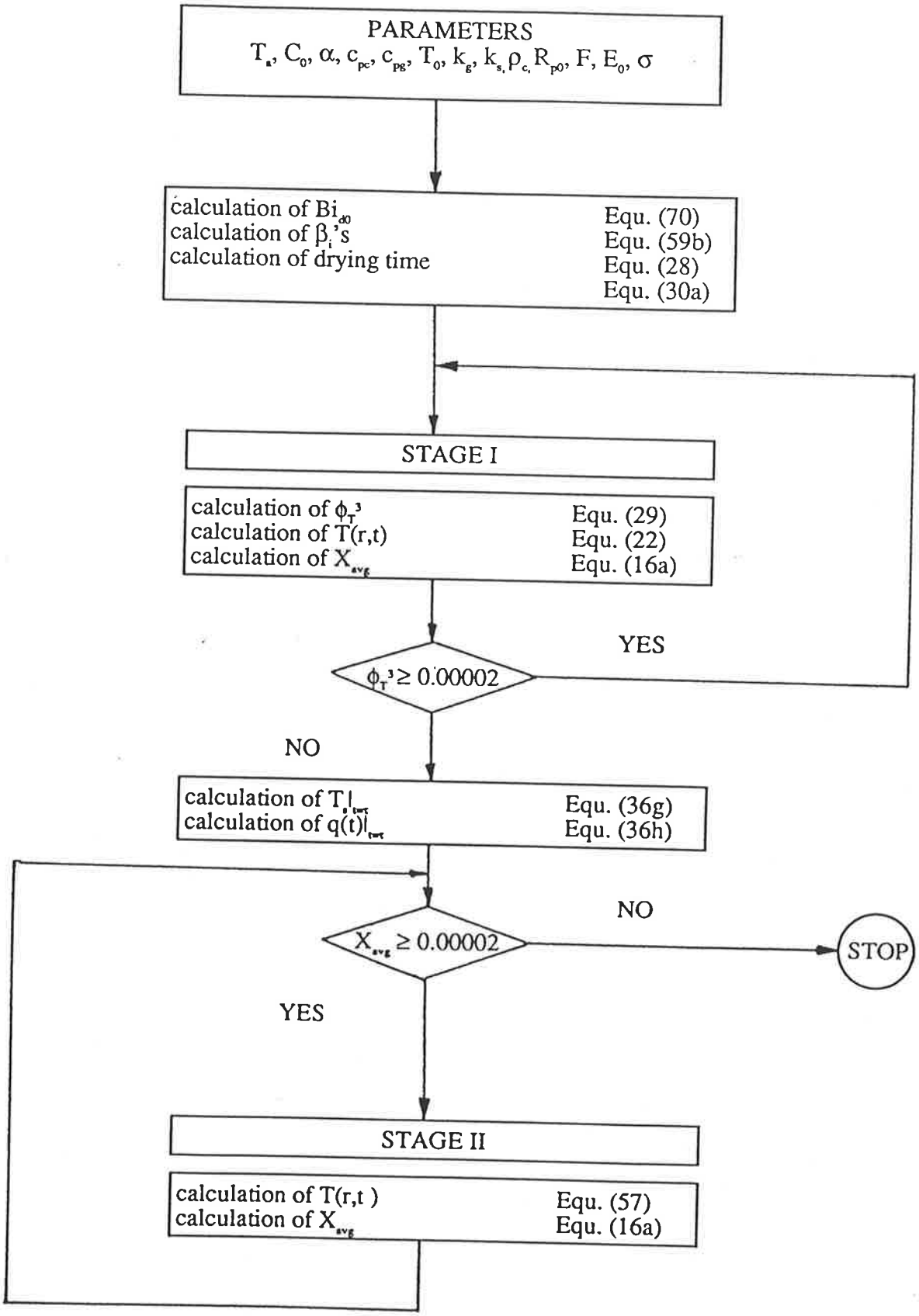

Fig. 5.22 Computational flow-sheet for coupled drying and devolatilization under pyrolysis conditions

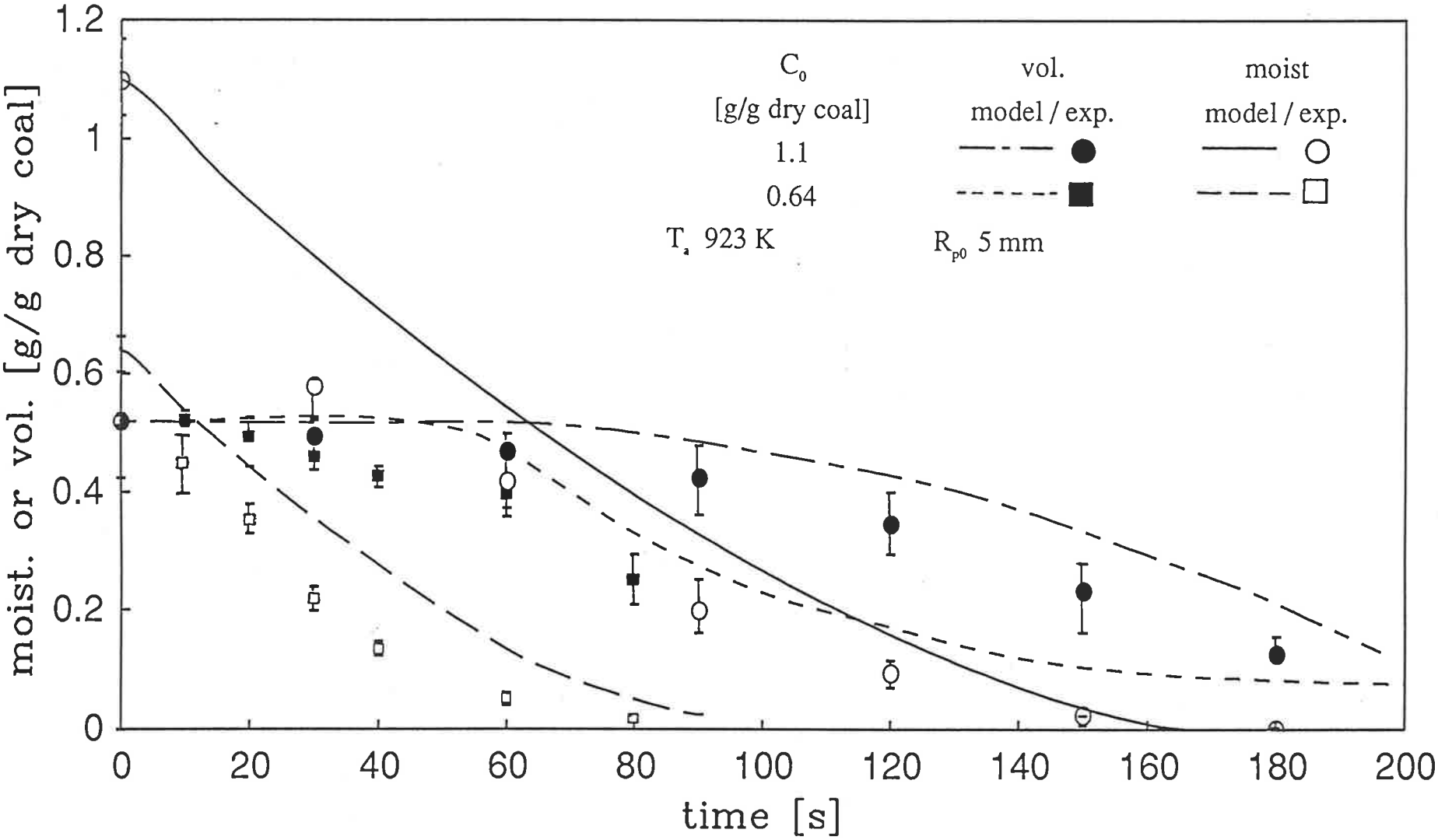

Fig. 5.23 Comparison of model predictions and experimental data for coupled drying and devolatilization under pyrolysis conditions

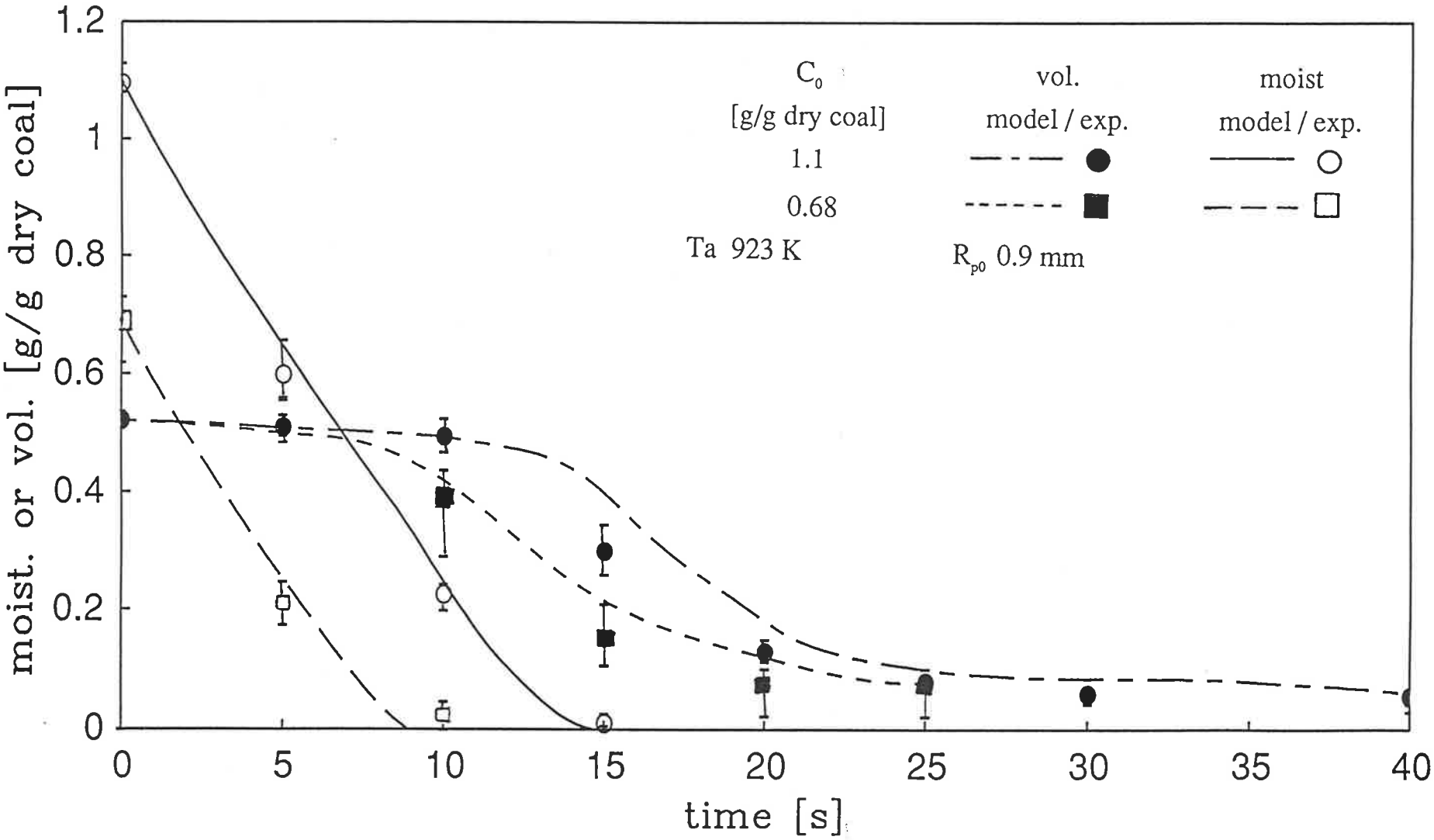

Fig. 5.24 Comparison of model predictions and experimental data for coupled drying and devolatilization under pyrolysis conditions

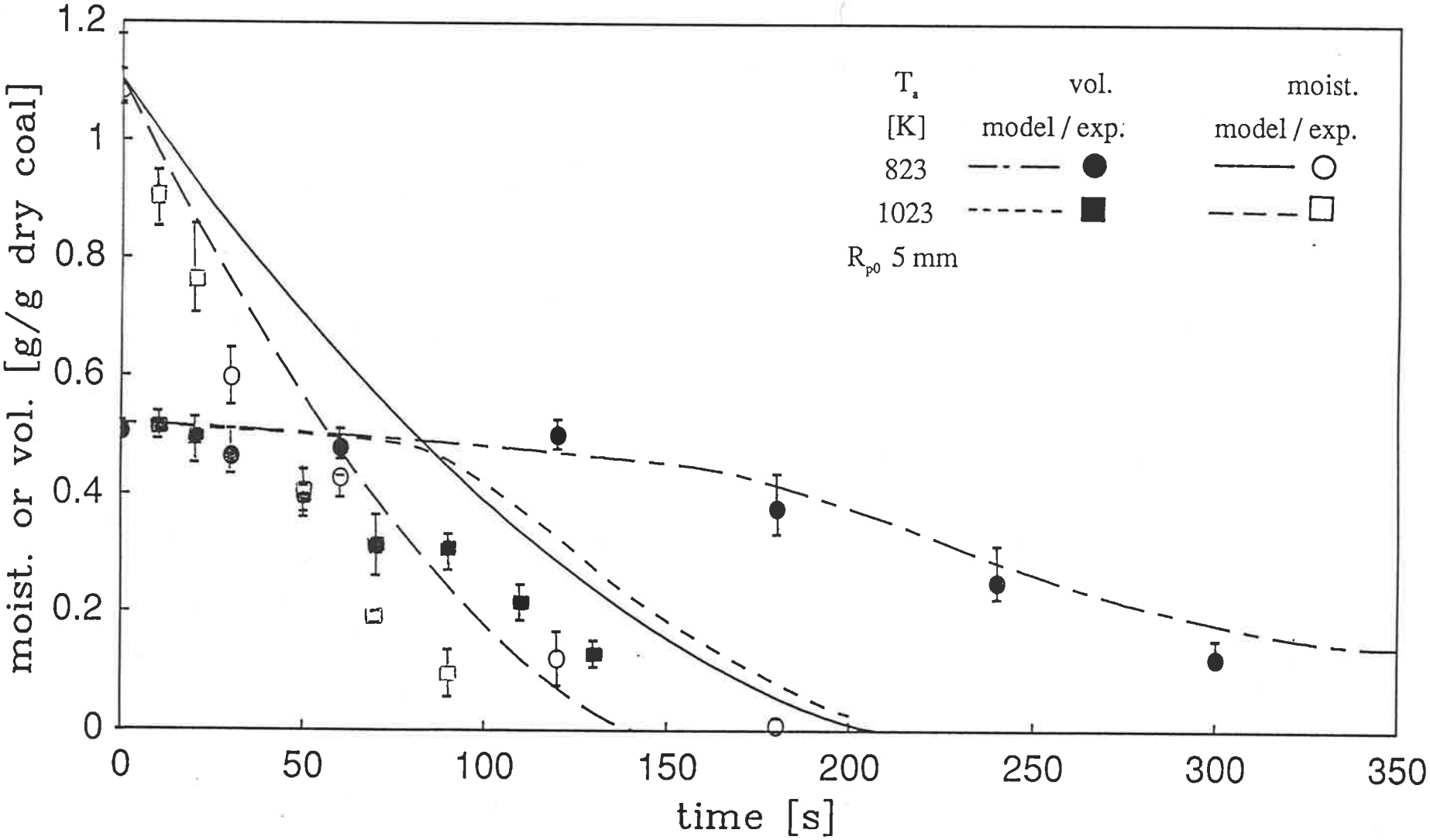

Fig. 5.25 Comparison of model predictions and experimental data for coupled drying and devolatilization under pyrolysis conditions

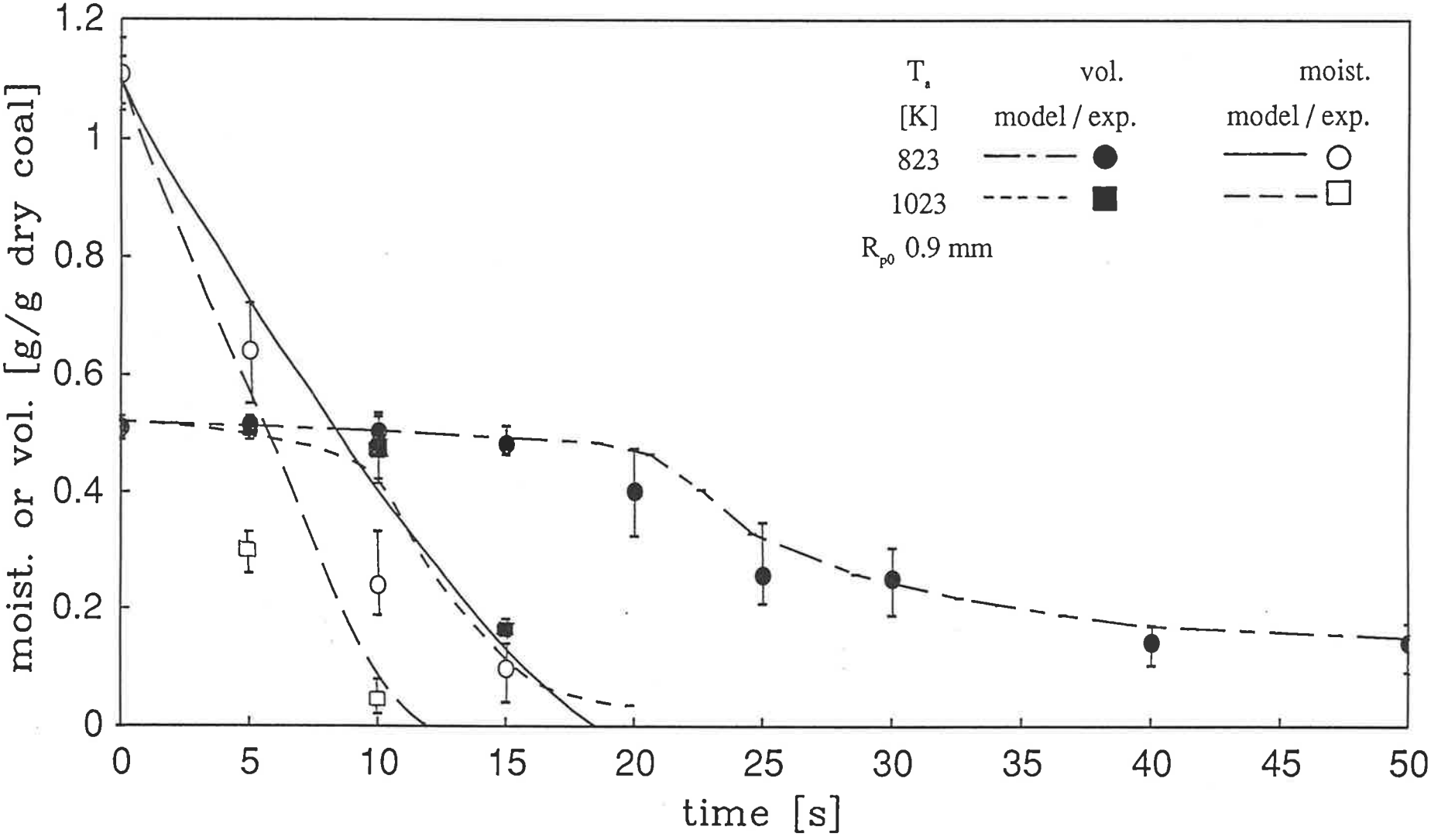

Fig. 5.26 Comparison of model predictions and experimental data for coupled drying and devolatilization under pyrolysis conditions

upper and lower limit in moisture content values. As may be seen the experimental data are in reasonable agreement with the lower limit. By adopting a ± 20% limit for the drying history, Figure 5.21, the data are inside the upper and lower limit of the model predictions. As already pointed out earlier coal is an inhomgeneous substance with wide variations in chemical and physical properties and a 20% variation is common.

In Figure 5.22 the computational flow-sheet for comparison of the data with model predictions for coupled drying and devolatilization (shrinkage included) under pyrolysis condition is depicted. In Figures 5.23 to 5.26 the coupled drying and devolatilization behaviour of coal particles are plotted. For devolatilization the values obtained for the mean E_0 = 210 kJ/mol and standard deviation σ = 40 kJ/mol of the activation energy for the dry coal experiments have been used. In Figures 5.23 and 5.24 two different initial moisture contents (0.64 and 1.1 g moisture / g dry coal) have been chosen. Initial moisture content of 1.1 g moisture / g dry coal results in about twice as long drying and devolatilization time. In Figures 5.25 and 5.26 the influence of different ambient temperatures has been investigated. The drying and devolatilization times at 823 K are longer than at 1023 K as expected. It also can be seen that for small particle size (1.8 mm) and low Biot number the drying and devolatilization process can be decoupled (Agarwal et al., 1986); drying is nearly completed when devolatilization starts. It may be seen that though the model overpredicts drying history, the agreement with devolatilization characteristics is very good for all the experimental conditions. Devolatilization depends on the temperature profile in the dry shell; this agreement supports the basic applicability of the drying model and the possibility of the fissures increasing the moisture removal rate in the earlier stages of drying. In this model drying has been considered as a physical process -

no chemical impact of drying on devolatilization has been considered. The fact that kinetic parameters obtained from the devolatilization of dry coal are capable of simulation devolatilization of wet coal (Figures 5.23 to 5.26) appears to substantiate this assumption.

5.3 OVERALL WEIGHT LOSS DUE TO DRYING AND DEVOLATILIZATION UNDER COMBUSTION CONDITIONS

Experiments for coupled drying and devolatilization under combustion conditions were conducted for temperatures 823 to 1023 K, particle sizes 1.8 to 10 mm and initial moisture contents 0.49 to 1.1 g moisture/g dry coal. The experimental conditions are listed in Table 3.1 and the experimental raw data can be found in Appendix A. The thermo-physical parameters used for the model predictions are the same as for coupled drying and devolatilization under combustion conditions listed in Table 5.2

In Figure 5.27 the computational flow-chart for comparison of the experimental results for coupled drying and devolatilization under combustion conditions are depicted. The data for drying and devolatilization under combustion condition are compared with the model in Figures 5.28 to 5.32. In Figure 5.28 the drying and devolatilization histories for 1.8 mm particles are shown. As expected the drying and devolatilization times for lower initial moisture contents are smaller. It may be seen, that drying is already completed for the lower moisture content experiment when ignition takes place. The model seems to overpredict the drying history in the initial stage of drying when the low moisture content coal was used. However it may be noted, that the first data point was obtained after 2.5 seconds so that only a small time delay in quenching the particles could produce a much lower moisture content result. The time-lag for blowing out the particle into the dry-ice container is about 1 second. In Figure 5.29 the drying and devolatilization histories for a

10 mm particle for initial moisture contents of 0.47 and 1.1 g moisture/g dry coal at 923 K are depicted. As can be seen the experimental results and model predictions compare well especially for the lower moisture content, where less shrinkage of the particle can be expected. The initial moisture contents for both conditions seems to be proportional to the drying time. Figure 5.30 shows the drying and devolatilization histories of 5 mm particles at 923 K. The model predictions and experimental data are in good agreement. Comparing Figures 5.28, 5.29 and 5.30, it may be seen that smaller particles result in more rapid drying and devolatilization. Figures 5.31 and 5.32 depict the drying and devolatilization behaviour for different ambient temperatures. As can be seen for both particle sizes the drying and devolatilization times increase by about 40% for a temperature change from 823 to 1023 K. Discrepancies between model predictions and experimental data for the drying behaviour may be due to not fast enough quenching, radiation effects in the initial stages of drying and fracturing of particles. The agreement with devolatilization is good for all experimental conditions. In Table 5.4 experimental ignition times and ignition times predicted by the model are listed. It seems that the model slightly overpredicts the ignition time. It may be noted, however, that due to the lack of a satisfactory ignition criterion it is assumed that homogeneous ignition takes place when approximately 5% of the initial volatiles content has been released. In reality a lower percentage could be possible. The ratio between experimental ignition time and model prediction is also listed in Table 5.4. The ratios are between 0.87 and 0.95 for wet coal. For dry coal a ratio of 1.33 was obtained for 1.8 mm particles with 0.0 moisture content. Since the ignition time is very short 4 s experimental and 3 s model the value of the ratio can only be seen as qualitatively.

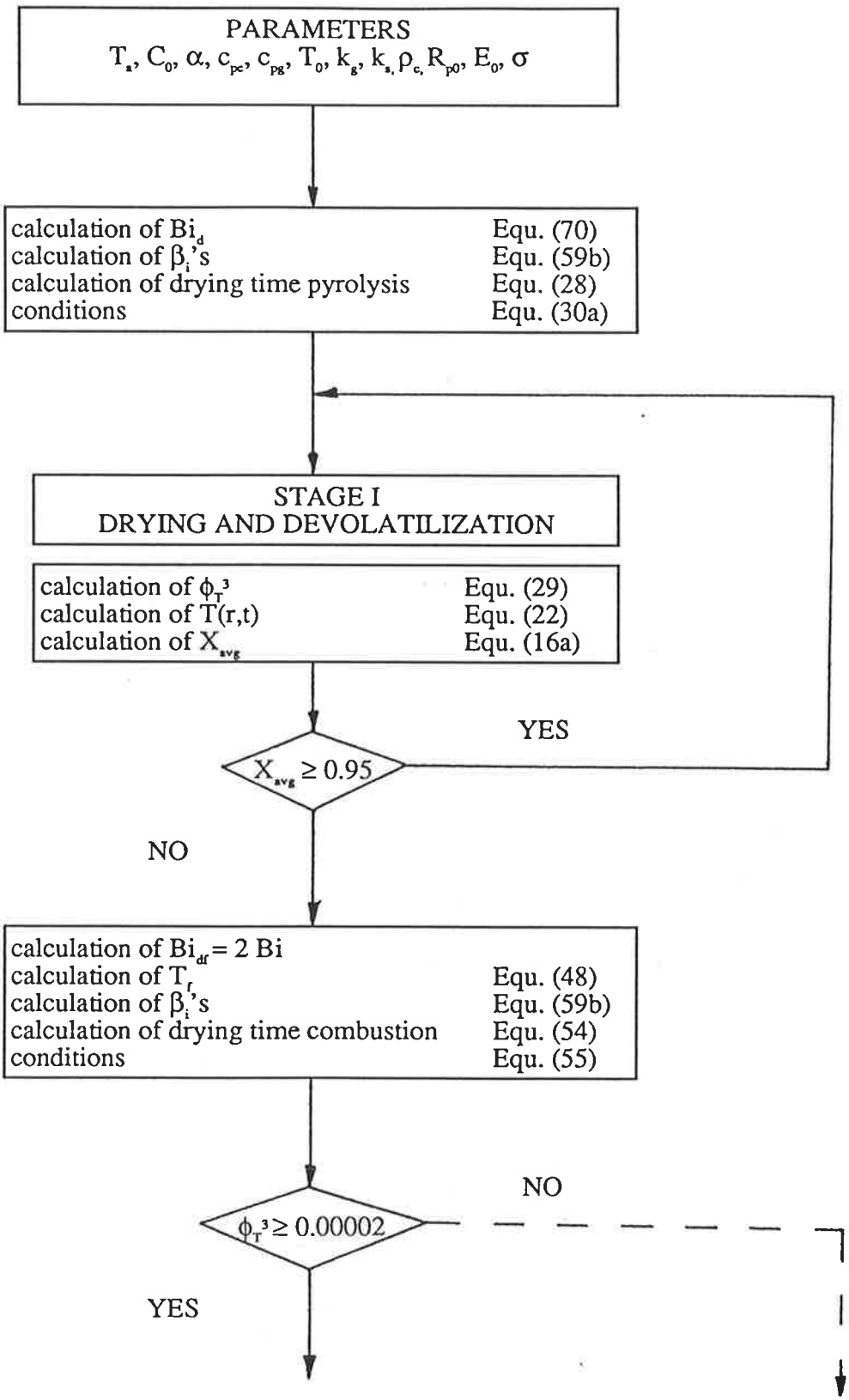

Fig. 5.27 Computational flow-sheet for coupled drying and devolatilization under combustion conditions

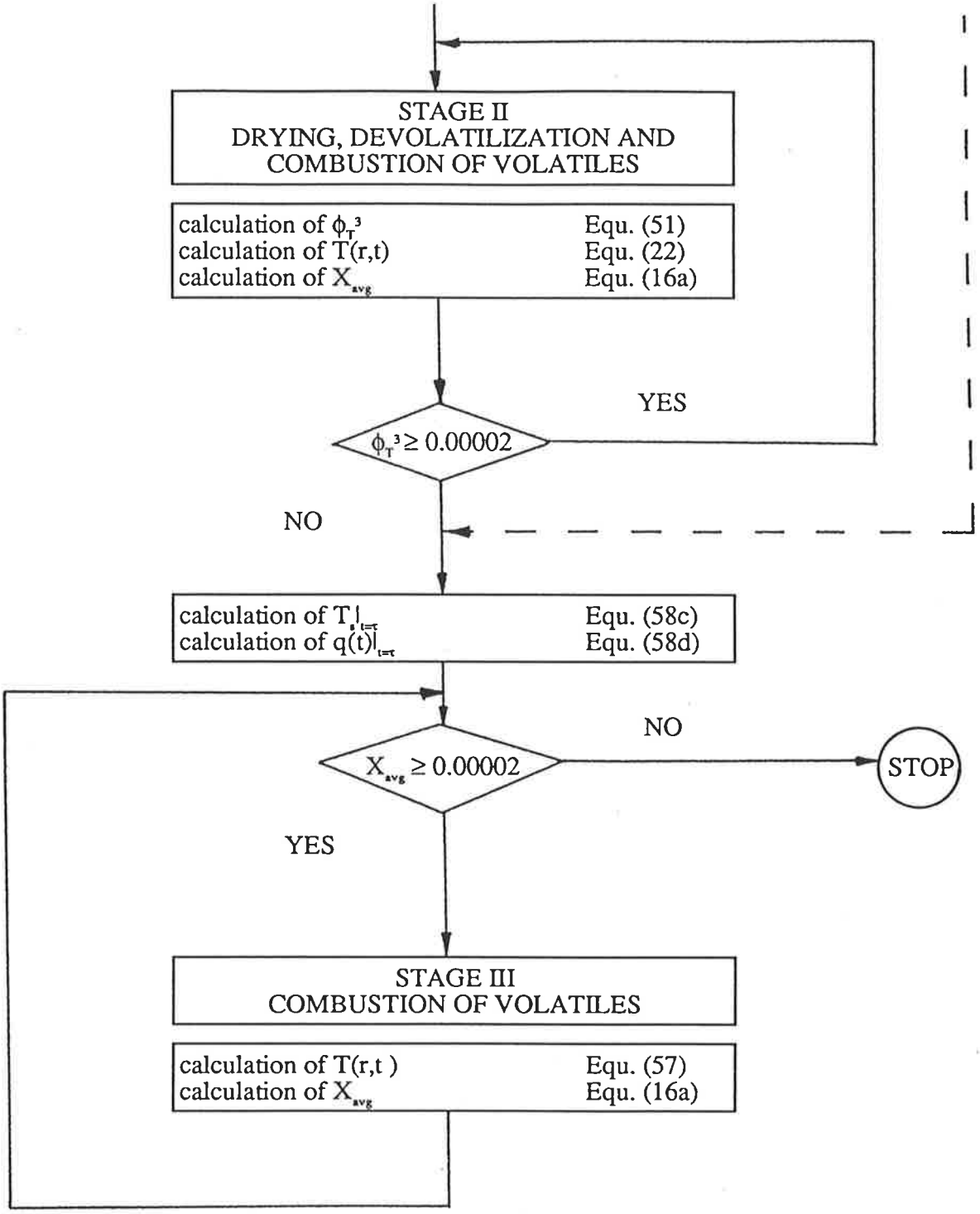

Fig. 5.27 (contd.) Computational flow-sheet for coupled drying and devolatilization under combustion conditions

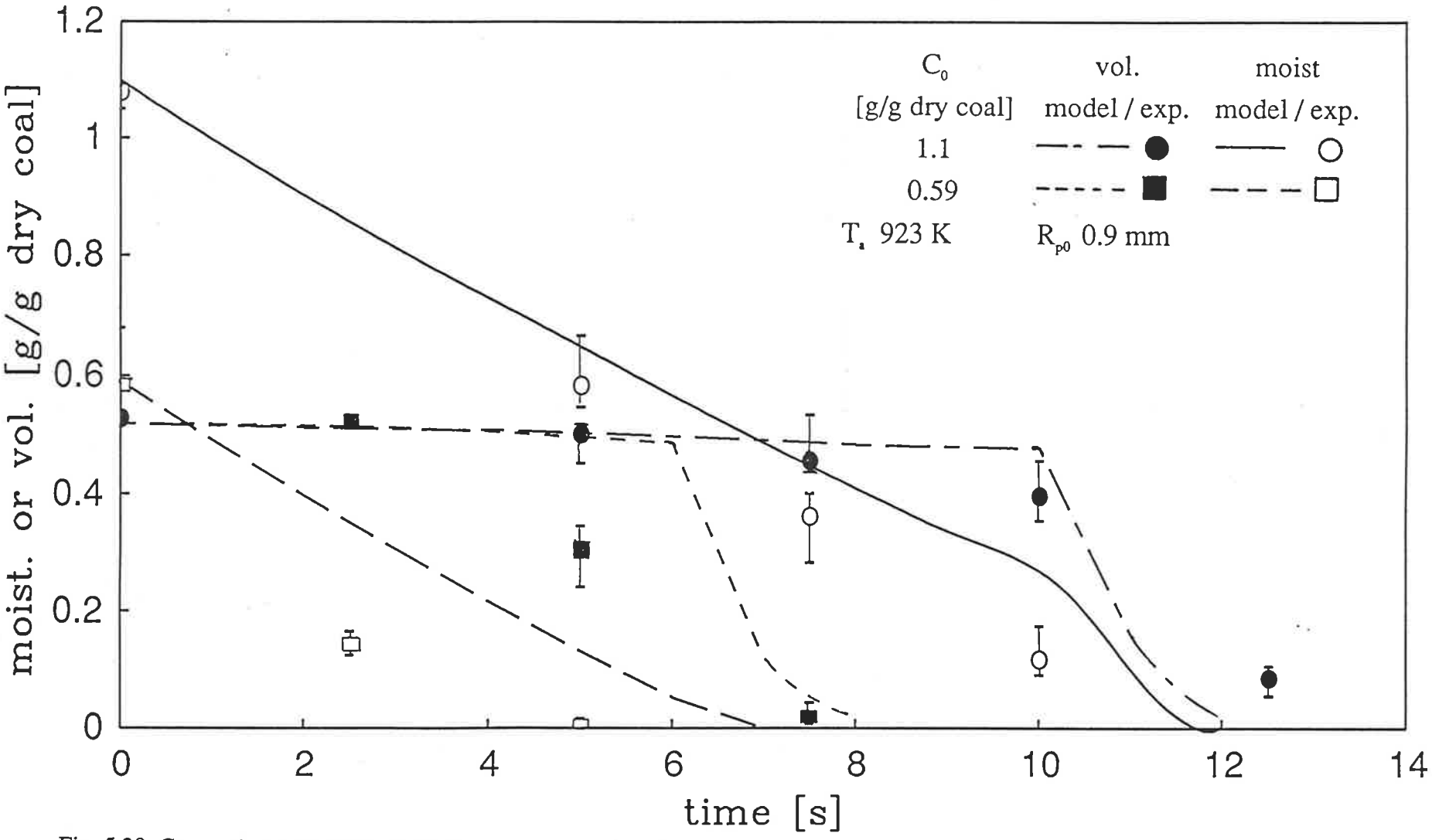

Fig. 5.28 Comparison of model predictions and experimental data for coupled drying and devolatilization under combustion conditions

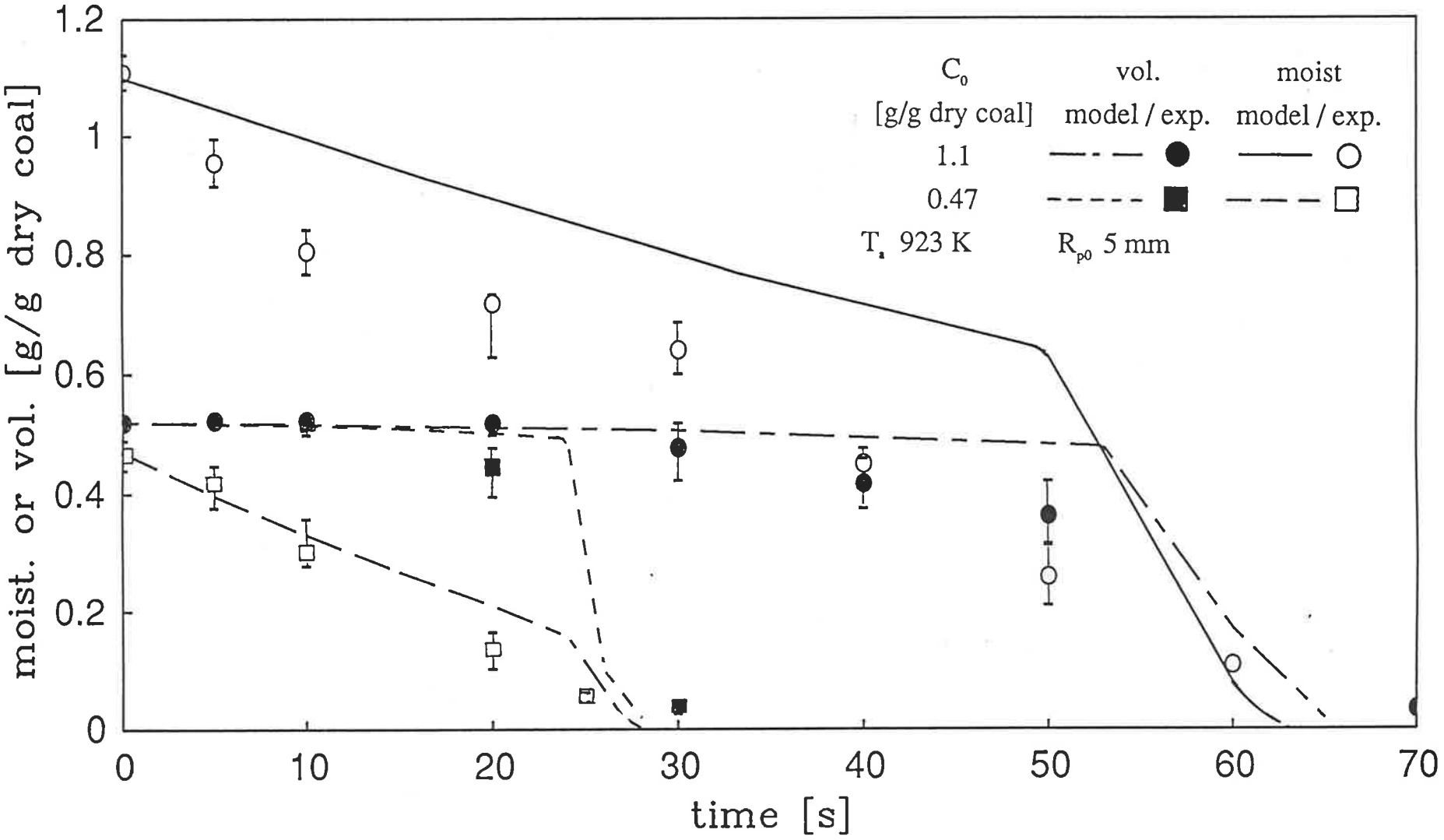

Fig. 5.29 Comparison of model predictions and experimental data for coupled drying and devolatilization under combustion conditions

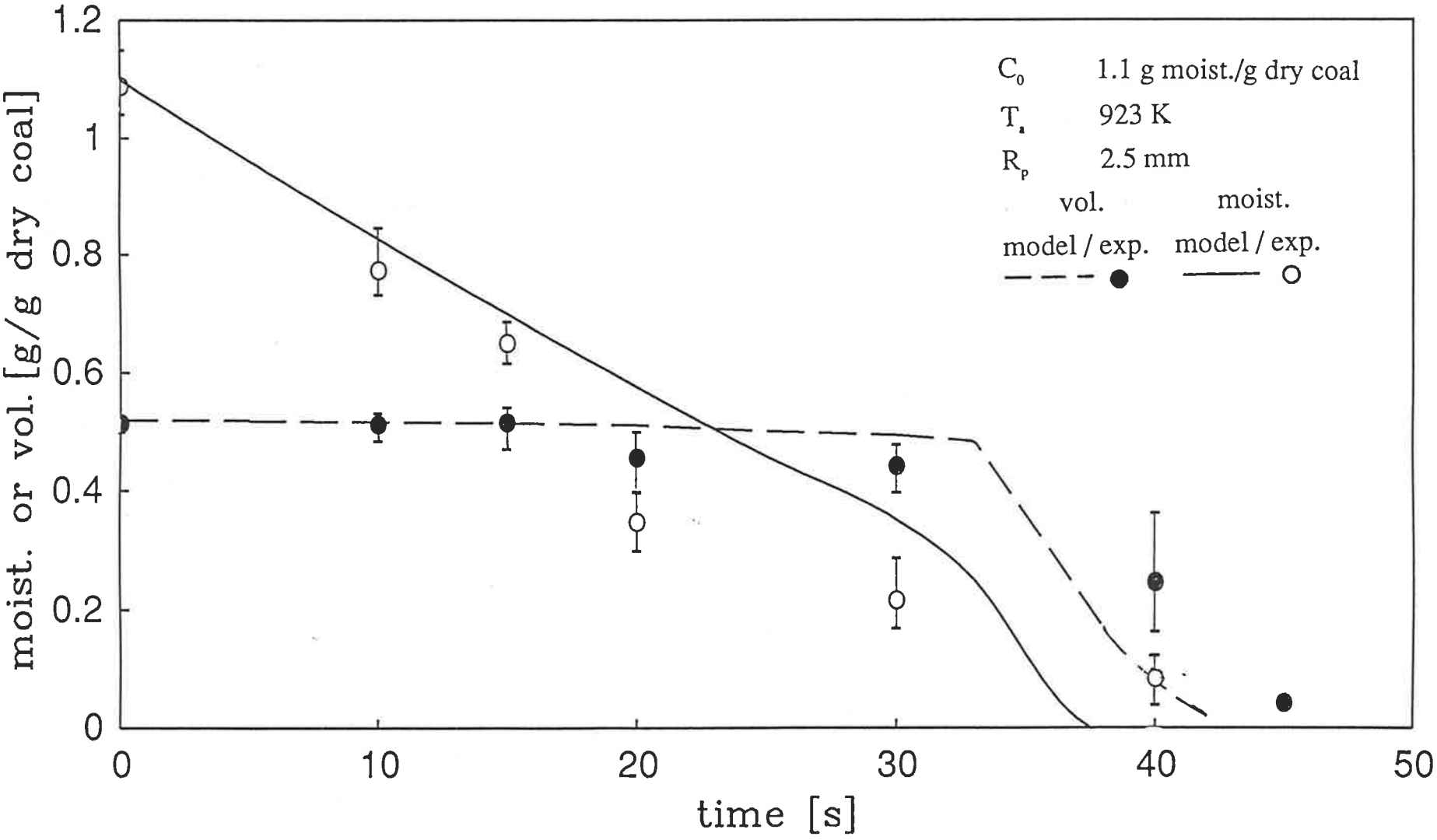

Fig. 5.30 Comparison of model predictions and experimental data for coupled drying and devolatilization under combustion conditions

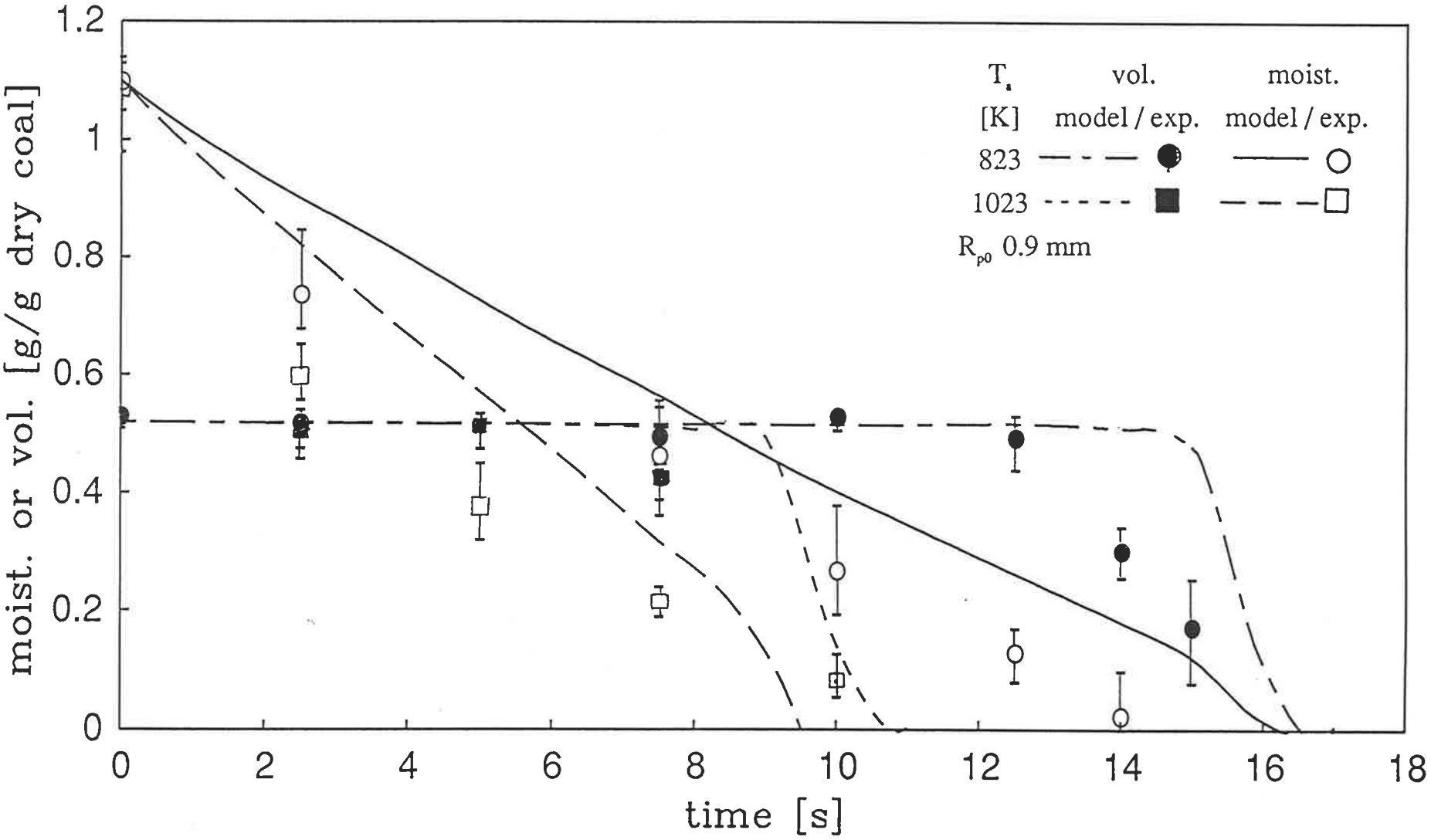

Fig. 5.31 Comparison of model predictions and experimental data for coupled drying and devolatilization under combustion conditions

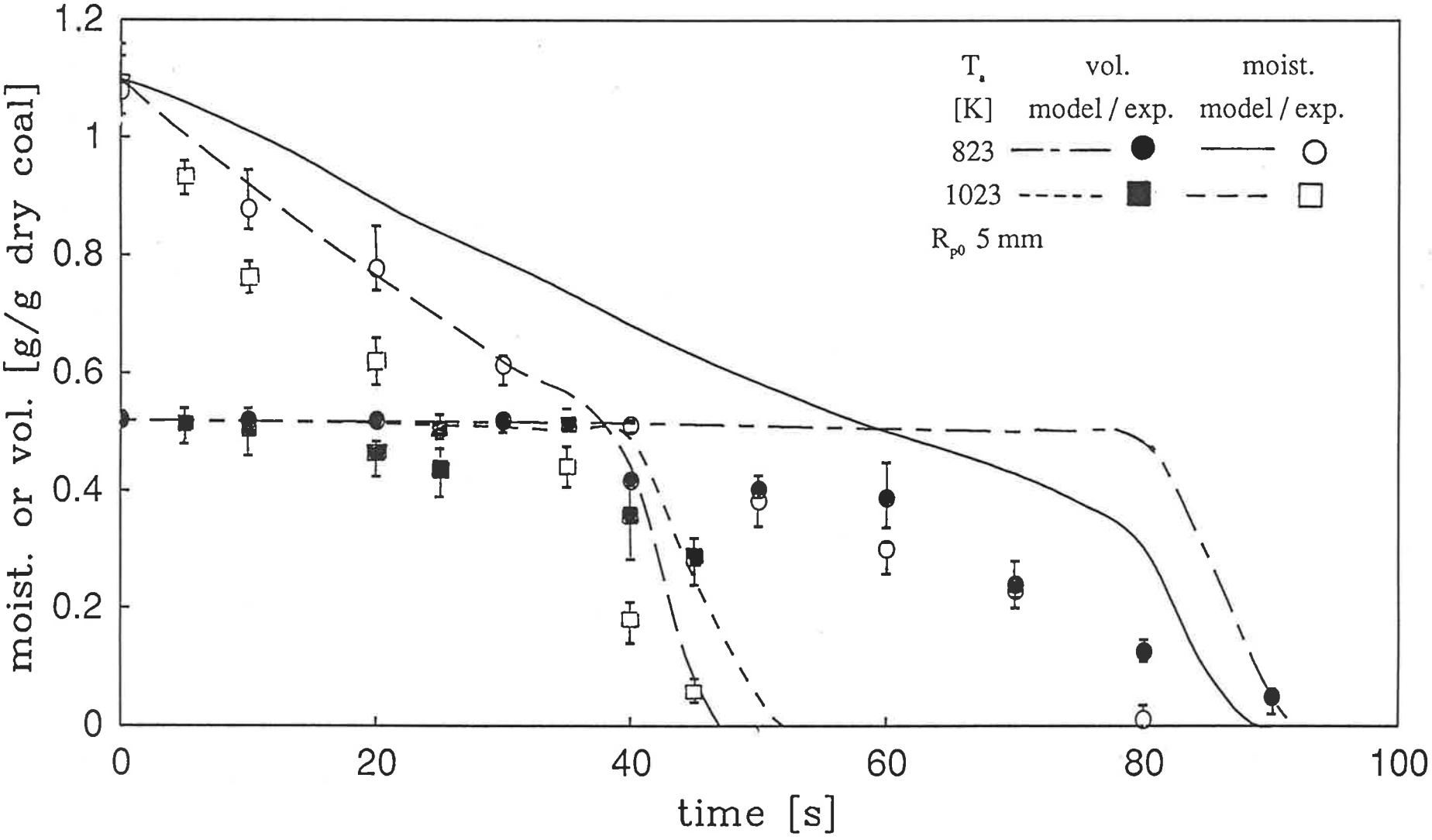

Fig. 5.32 Comparison of model predictions and experimental data for coupled drying and devolatilization under combustion conditions

Table 5.4 COMPARISON OF PREDICTED IGNITION TIMES WITH EXPERIMENTAL IGNITION TIMES

R_{p0} [mm]	C_0 [g/g dry coal]	T_a [K]	t_i [s] exp.	t_i [s] model	t_{iex}/t_{imod}
5.0	1.1	823	72 - 79	85	0.89
5.0	0.47	923	19 - 22	26	0.79
5.0	1.1	923	47 -52	60	0.83
5.0	1.1	1023	35-37	45	0.80
2.5	1.1	923	28-33	36	0.86
0.9	1.1	823	13 - 14	14	0.94
0.9	0.0	923	4	3	0.75
0.9	0.59	923	6	7	0.86
0.9	1.1	923	8 - 9	11	0.78
0.9	1.1	1023	7 - 8	9	0.82

5.4 FLUIDIZED BED APPLICATIONS

The comparison of fluidized bed experimental data obtained by CSIRO (Wildegger-Gaissmaier et al., 1988) for a Victorian brown coal in a bench-scale fluidized bed are shown in Figures 5.33 to 5.36.

For a single particle in convective flow, the heat transfer Biot number can be estimated using available correlations (Agarwal, 1988). For a fluidized bed, however the heat transfer is affected by gas convection as well as particle-particle interaction and radiation. Correlations are available for gas-particle heat transfer in beds of monosize particles. Heat transfer to and from cylinders or spherical objects, large in comparison with bed particle size and immersed at a fixed in-bed location, has also been studied extensively (Kunii and Levenspiel, 1969). However, transfer from a freely moving large particle in a bed of smaller and more dense particles has received scant attention and the estimation of Biot number is difficult. Available results (Prins, 1987; Pillai, 1976) indicate that for the present conditions the heat transfer Biot number could range from about 1.2 to 5. Due to the current lack of information, the Biot number has been treated as an adjustable parameter. The model also requires specification of the mean E_0 and the standard deviation σ of the activation energy distribution; the values used - E_0 = 210 kJ/mol and σ = 40 kJ/mol - are in good agreement with coals found elsewhere (Anthony and Howard, 1976). The value for the thermal diffusivity of coal α has been chosen as α = 0.2 mm²/s, comparable in magnitude with other coals (Badzioch et al., 1964).

Figure 5.33 shows an example of raw data obtained and the model predictions plotted as g moisture/g dry coal. As there are not many data points in the first part of drying available no distinctive statement can be made. Generally speaking the model seems to slightly over-predict the drying behaviour. The differences may be due to a time delay in

quenching the particles. The moisture content drops rapidly during drying and even a small delay in quenching might prove important. As expected the feed to the hotter bed dries more rapidly. The same can be said for the smaller particle size feed.

Figure 5.34 provides an example of typical devolatilization curves obtained by the model predictions and compared with the experimental data. As can be seen the agreement between the model and experimental data is good.

Figures 5.35 and 5.36 show the coupled drying and devolatilization behaviour for 4.075 mm particles, initial moisture content 62.3 % w.b. and 6.05 mm particles, initial moisture content 53.2 % w.b. for 650°C and 850°C. At lower temperatures a longer time-lag is observed for the initiation of devolatilization.

Jung and Stanmore (1980) reported drying and devolatilization histories under pyrolysis and combustion conditions for Victorian brown coal. The shrinkage of the coal particles has been investigated. In Figure 5.37 the experimental results are plotted as volumetric shrinkage, ε^3, against dimensionless moisture content (C/C_0) and compared with model predictions for different shrinkage proportionality factors. The experimental data are in the range of model predictions for proportionality factor 0.25 and 0.75. The shrinkage seems to be independent of temperatures and conditions of the experiments. A shrinkage factor of 0.5 has been chosen for further comparisons. Figures 5.38 and 5.39 show coupled drying and devolatilization behaviour under pyrolysis and combustion conditions for 993 K (Figure 5.38) and 1043 K (Figure 5.39). A slight overprediction of the model for the pyrolysis stage can be seen. However as soon as ignition takes place the model underpredicts the drying and devolatilization behaviour. The single particle model assumes the flame sheet will be positioned around the coal particle during the whole time of volatile combustion, in a fluidized bed however the coal particle would be alternatively

in the bubble and emulsion phase and depending on the position of the particle the flame temperature or the bed temperature would be the actual environment. Therefore one would expect an underprediction of the model. The single particle model is not able to predict coupled drying and devolatilization under combustion conditions in fluidized beds accurately.

No time resolved histories on volatile combustion of dry coal in fluidized beds could be found in literature. Salam et al. (1988) investigated devolatilization times as a function of fluidizing gas oxygen concentration. It was found, that decreasing oxygen concentration resulted in longer devolatilization time. The same observation has been made in the parametric studies reported in Chapter 4 (Figure 4.19c) using the fluidized bed model.

In Table 5.5 ignition times for single particle (Ragland and Yang, 1985; present study) and fluidized bed experiments (Prins, 1987) have been listed. As can be seen ignition times are dependent on ambient temperature, initial moisture content and particle size. Higher ambient temperatures, lower initial moisture contents and smaller particle sizes result in smaller ignition times. The ignition time seems to be independent (Ragland and Yang, 1985) of oxygen concentration.

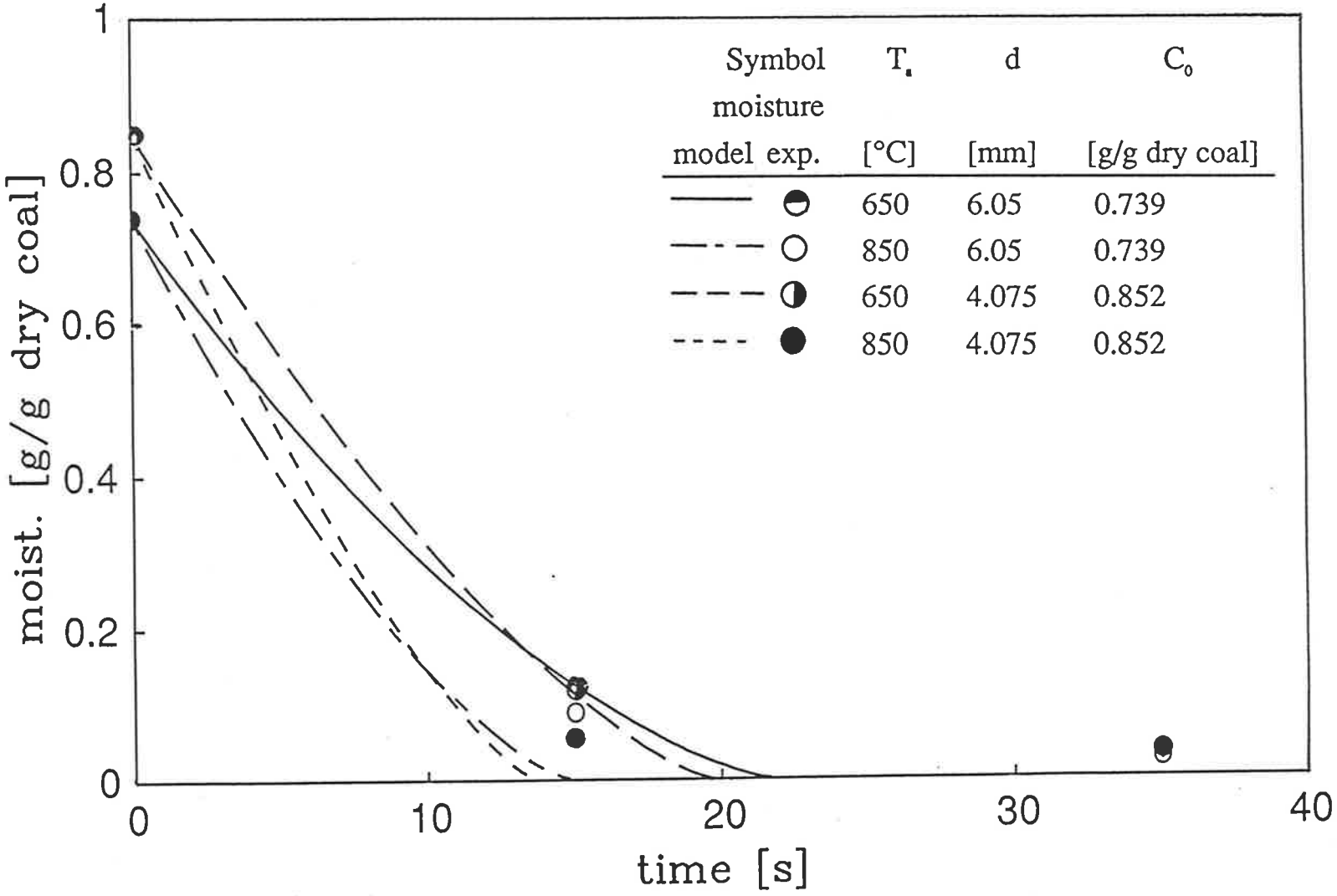

Fig. 5.33 Comparison of experimental data obtained by CSIRO with model predictions

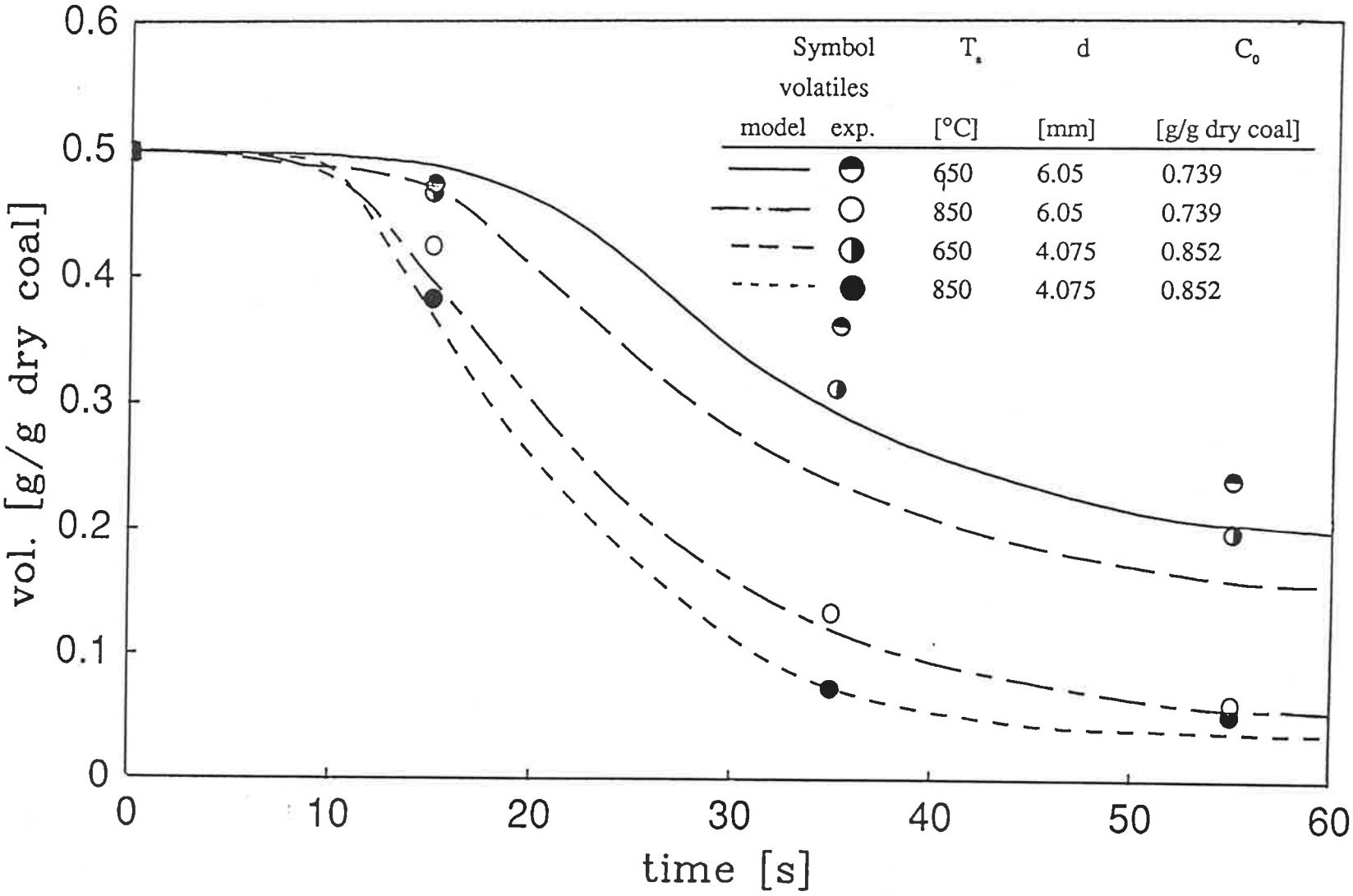

Fig. 5.34 Comparison of experimental data obtained by CSIRO with model predictions

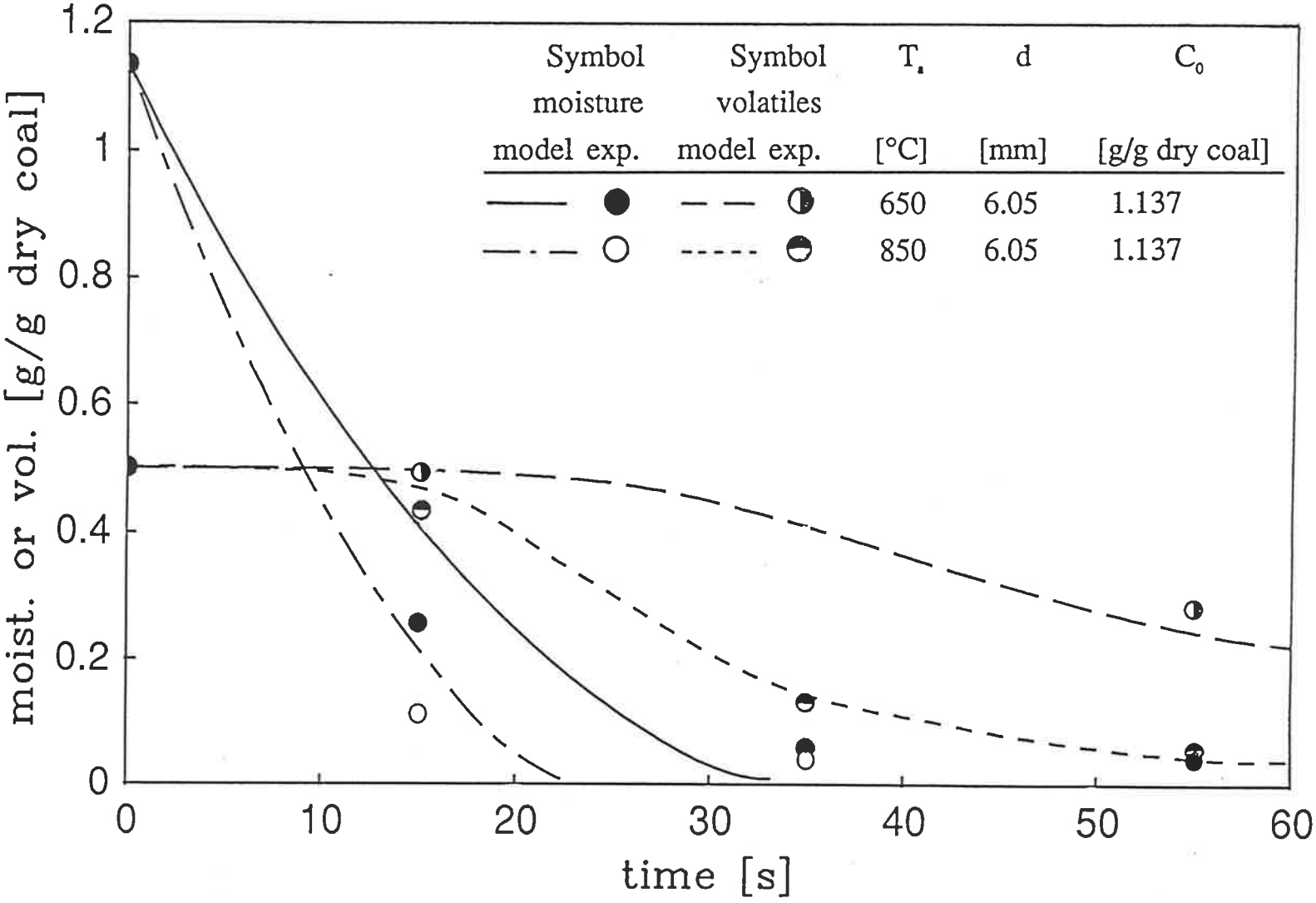

Fig. 5.35 Comparison of experimental data obtained by CSIRO with model predictions

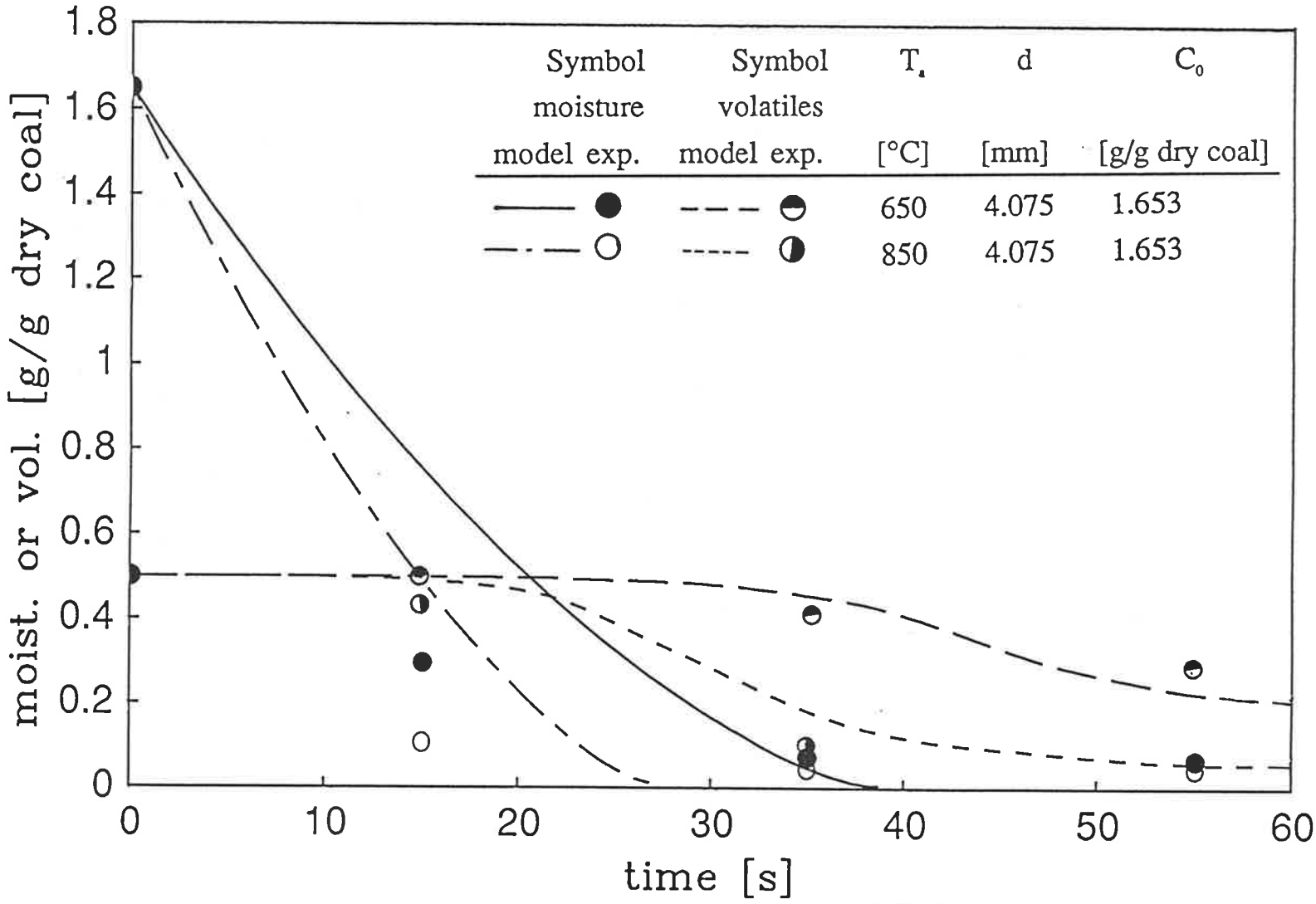

Fig. 5.36 Comparison of experimental data obtained by CSIRO with model predictions

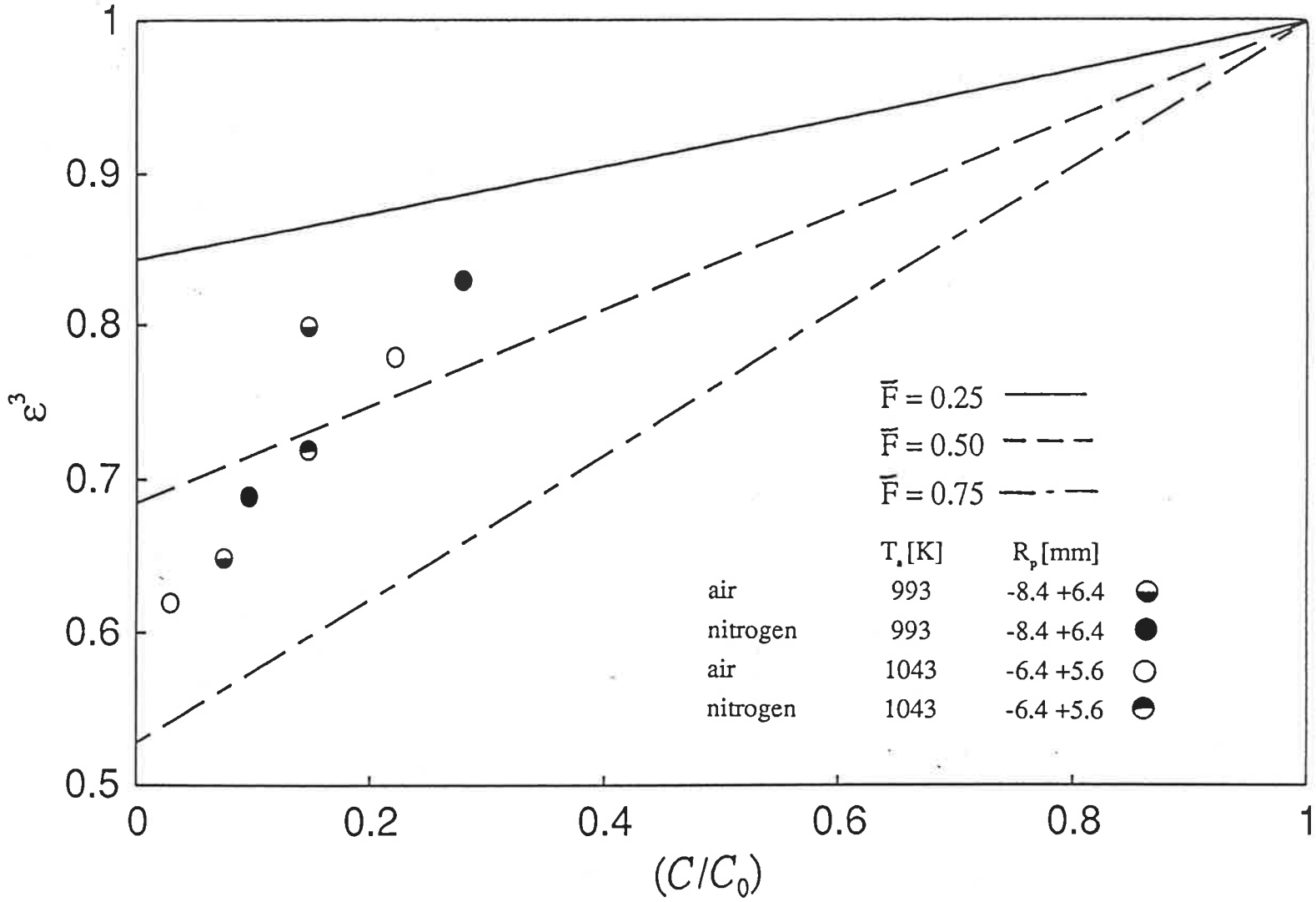

Fig. 5.37 Comparison of experimental data obtained by Jung and Stanmore (1980) with model predictions

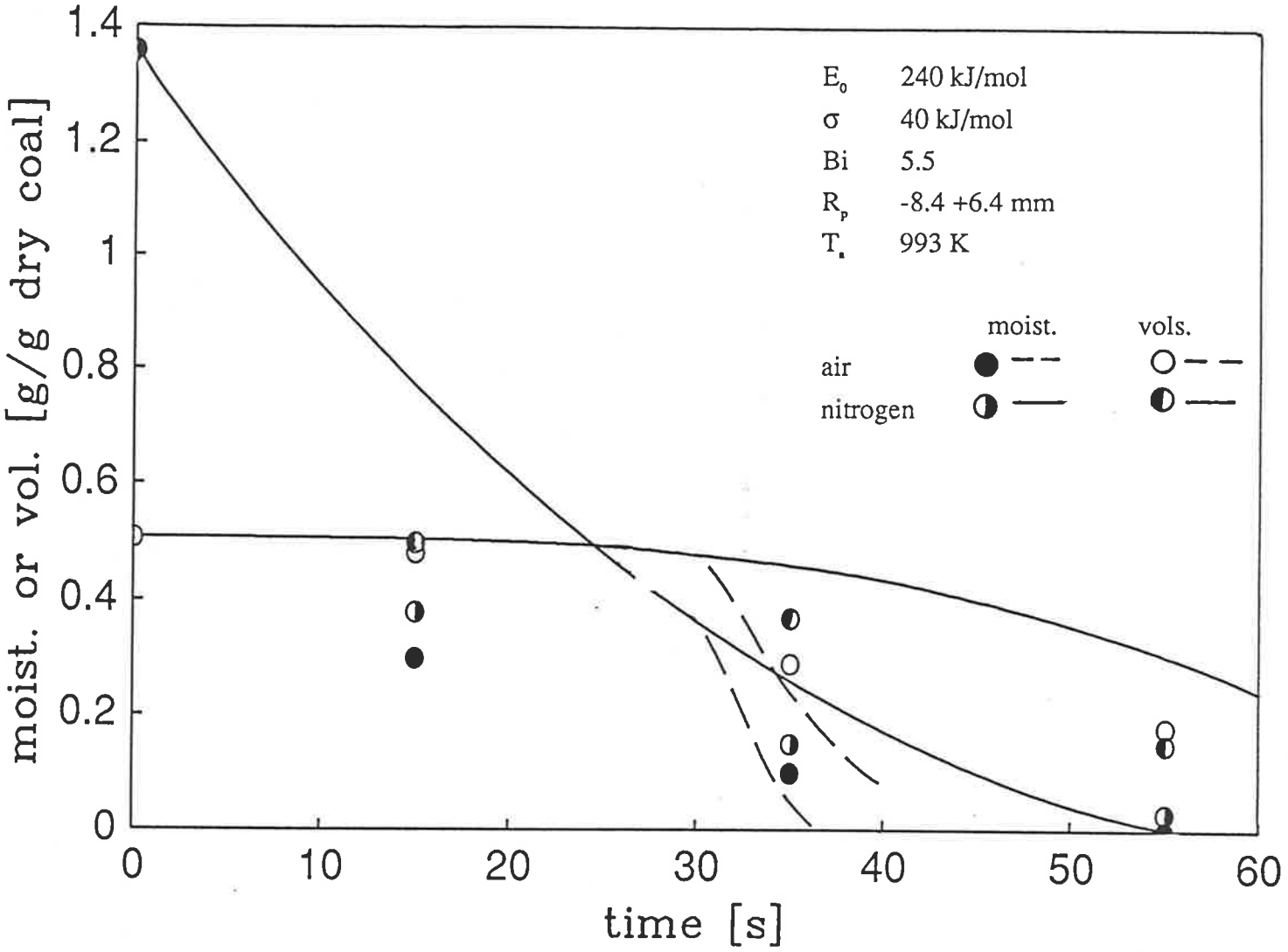

Fig. 5.38 Comparison of experimental data obtained by Jung and Stanmore (1980) with model predictions

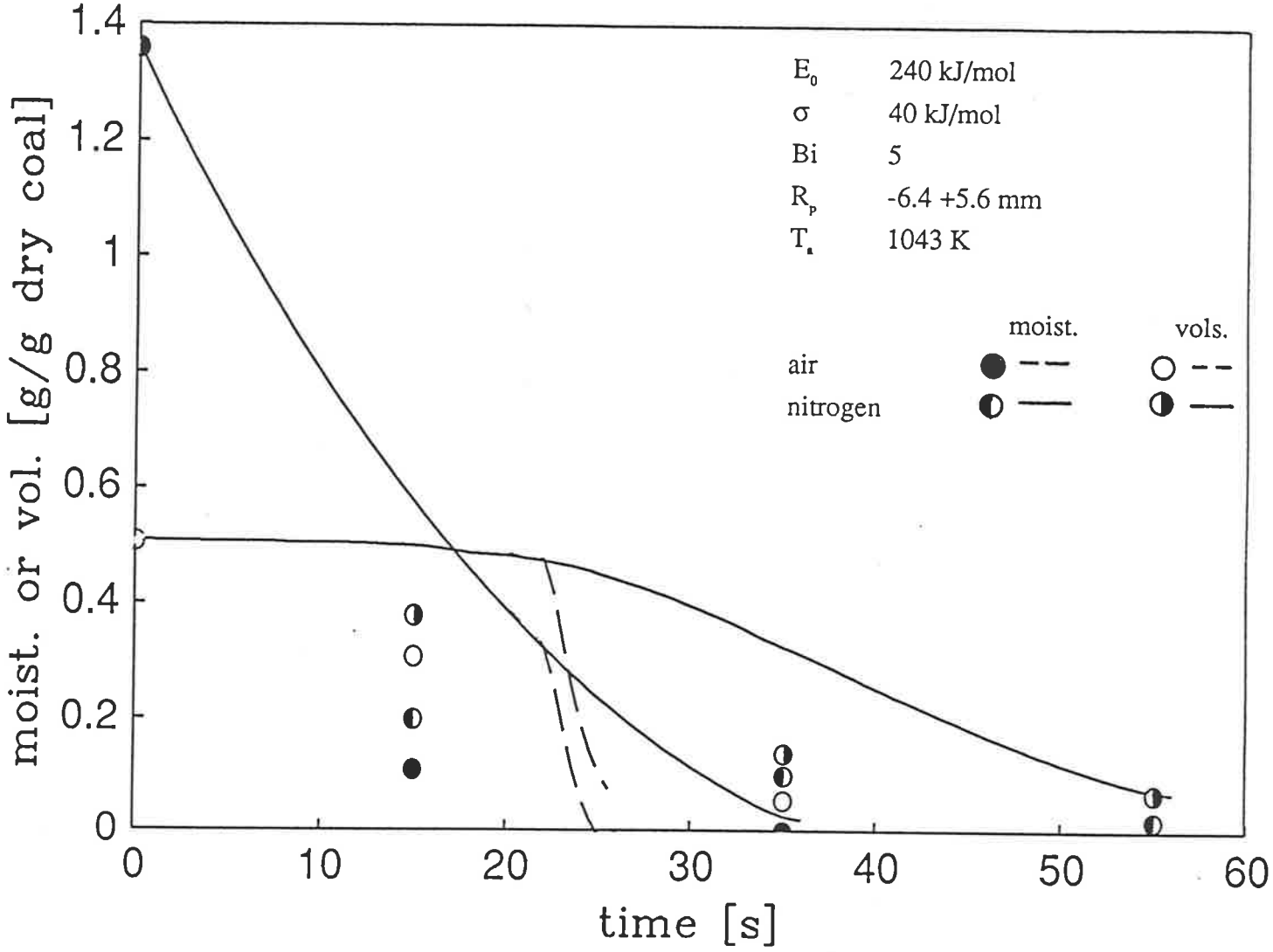

Fig. 5.39 Comparison of experimental data obtained by Jung and Stanmore (1980) with model predictions

TABLE 5.5 REPORTED IGNITION TIMES FOR SINGLE PARTICLE (SP) AND FLUIDIZED BED (FB) EXPERIMENTS

Ref.	T_a [K]	C_0 [g/g dry coal]	d [mm]	O_2-conc. [%]	Bi	t_{ig} [s]	
Ragland and Yang (1985)	900	0.065	5.3	21	3.17	39	SP
	1100	0.065	5.3	21	3.17	7	
	1200	0.065	5.3	21	3.17	5	
	1100	0.065	5.3	21	3.13	7	
	1100	0.065	5.3	21	3.6	7	
	1100	0.065	5.3	21	4.0	7	
	1200	0.065	5.3	4.5	3.17	6	
	1200	0.065	5.3	10.5	3.17	5	
	1200	0.065	5.3	14.0	3.17	5	
	1200	0.065	5.3	21	3.17	5	
	1200	0.065	6.4	21	3.83	5	
	1200	0.065	7.5	21	4.49	5	
	1200	0.065	9.9	21	5.92	5	
Prins (1987)	953	0	4.7	21		9	FB
	953	0	8.6	21		17.6	
	953	0.941	9.3	21		45.9	
	1023	0	4.7	21		2.8	
	1023	0	8.6	21		3.3	
	1023	0.941	9.3	21		19.2	
	1123	0	4.7	21		12.4	
	1123	0	8.6	21		32.3	
	1123	0.941	9.3	21		53.9	
present study	823	1.1	10	21	4.2	75.6	SP
	923	1.1	10	21	4.2	49.6	
	923	0.47	10	21	4.3	20.5	
	1023	1.1	10	21	4.4	36.1	
	923	1.1	5	21	2.1	30.8	
	823	1.1	1.8	21	1.1	13.2	
	923	1.1	1.8	21	1.1	8.6	
	923	0.59	1.8	21	1.1	6.0	
	923	0.0	1.8	21	1.1	4.0	
	1023	1.1	1.8	21	1.2	7.4	

6 CONCLUSIONS AND RECOMMENDATIONS

SINGLE PARTICLE ANALYSIS

Drying, devolatilization and coupled drying and devolatilization under pyrolysis and combustion conditions of single wet low-rank coal particles have been studied experimentally as well as theoretically. The aspects of volatiles combustion of dry coal particles in fluidized beds have been investigated theoretically.

A transient model incorporating shrinkage of particles was developed. Heat transfer to and through the coal particle was assumed to be the rate limiting step and was modelled on a moving wet-core formulation.

It has been assumed, that shrinkage to be directly proportional to the volume of the water being removed. Evans (1973) however investigating shrinkage on Victorian brown coal found out that the extent of shrinkage varies with the type of water being removed. Clearly a model which could distinguish between the type of water removed would be preferable. However, additional parameters and added computational difficulties could be expected.

The model seems to overpredict the drying behaviour. Possible causes could be:

- radiation effects in the model have not been accounted for explicitly;
- time-lag in quenching;
- formation of cracks which may lead to faster removal of moisture.

The model could be improved by the inclusion of the effects of radiation and cracking. Further the temperature and the heat flux at the surface of the particle was estimated using the predictions of the pseudo steady-state model as developed by Agarwal (1984a); improvement is clearly desirable.

The model for devolatilization for pre-dried and wet coal assumes that heat transfer to and through the coal particle and chemical reaction are the rate limiting steps. The model used the distributed activation energy model for modelling the kinetics of coal decomposition. Devolatilization depends on temperature profile in the dry shell of a wet particle or the temperature profile of a dry particle. The unsteady state heat conduction equation with appropriate boundary conditions was applied to obtain the temperature profiles. The model predictions were compared with data for wet and dry Bowmans coal for overall decomposition and the evolution of single volatiles species. The model predicts the overall coal decomposition well for wet and dry coal particles. The kinetic parameters obtained from the devolatilization of dry particles are capable to simulate the devolatilization of wet coal well. The assumption that drying is a physical process - no chemical interaction of drying on devolatilization has been considered - seems to be valid. For the evolution of volatiles species it was assumed that drying and devolatilzation are sequential processes for the low Biot number experimental conditions considered here. The experimental results of the evolution of gaseous volatile species from Bowmans coal reveal that the kinetic parameters for the evolution of light hydrocarbons and carbon oxides are similar to coals found elsewhere lending support to the rank insensitive kinetics hypothesis. The non-isothermal particle model is capable of simulating the trends in the release of volatiles from pre-dried as well as wet coal. The simple modification of decoupling drying and devolatilization however is only applicable for experimental conditions corresponding to Bi ≤ 1.

Experimental data for Bowmans coal are seen to be in good agreement with the model proposed for predicting the influence of drying on devolatilization and volatiles combustion for single particles. General the same restrictions as already pointed out above apply for it. Slight discrepancies have been observed between predicted and experimental

ignition times. Homogeneous ignition was assumed to take place when ~ 5% of the volatiles are released. A more detailed analysis of the ignition aspect is desirable. Also though homogeneous ignition may be adequate for large particles, volatiles in smaller particles could combust while still trapped in the solid matrix.

The flame temperature was estimated using a modified Shwab-Zeldovich approach to the fuel droplet combustion problem. The method described requires some further refinement. As Kanury (1975) pointed out the major restriction in the analysis involves unity Lewis number assumption. Also a more detailed analysis should consider the time-dependent movement of the flame front which would require the consideration of the transient conservation equations in the gas phase. Moreover, the presence of non-combustibles in the volatiles released like CO_2, must be taken into account. Experimental verification of the predicted flame temperatures are necessary.

APPLICATION OF SINGLE PARTICLE ANALYSIS TO FLUIDIZED BEDS

In principle, if the heat transfer Biot number was known the model for coupled drying and devolatilization under pyrolysis conditions could be applied to predict the drying and devolatilization characteristics in a fluidized bed. An attempt was made to use this model to predict the drying and devolatilization behaviour data obtained by CSIRO for a Victorian brown coal in a fluidized bed. For a single particle in convective flow, the heat transfer Biot number can be estimated using available correlations (Agarwal, 1988). For a fluidized bed, however, the heat transfer is affected by gas convection as well as particle-particle interaction and radiation. Correlations are available for gas-particle heat transfer in beds of monosize particles. Heat transfer to and from cylinders or spherical

objects, large in comparison with bed particle size and immersed at a fixed in-bed location, has also been studied extensively (Kanury, 1975). However, transfer from a freely moving large particle in a bed of smaller and more dense particles - as applicable in a fluidized bed combustor - has received scant attention (Prins, 1987) and the estimation of Biot number is difficult. In our simulation of fluidized bed drying and devolatilization, the Biot number had to be treated as an adjustable parameter, these values were, however, in agreement with the approximation (Ross and Davidson, 1979) $Nu \sim Sh/\varepsilon'$. More detailed analysis of heat transfer to freely moving objects in fluidized beds is thought necessary.

FLUIDIZED BED ANALYSIS

A single particle model was proposed for the combustion of coal volatiles around coal particles in fluidised beds. The coal particle phenomena were modelled using the coupled heat transfer (to and through the coal particle) and chemical reaction (represented by the distributed activation energy model) approach. The analysis was divided in pre- and postignition stages. The effect of the heat conduction from the volatiles flame was taken into account. The coal particle was assumed to be in contact with the bubble and the emulsion phase for specific time periods. The frequency of the bubble-emulsion contact cycle as well as the residence time of the coal particle within each phase during the cycle are calculated from a bubble coalescence model proposed by Agarwal (1985). It was possible to relate volatile combustion behaviour with fluidized bed design parameters like bed height, excess gas velocity and distributor design. Several assumption of the model require more detailed verification/consideration. The ignition problem has already been addressed above. Heat transfer aspects in the two phases have to be considered in greater detail. It may be more accurate to obtain heat transfer coefficients from the Froessling

correlation while the particle is in the bubble phase and from suitable modified fixed/packed bed correlations while the particle is in the emulsion phase. The model also assumes that the coal particle is constrained at a specified height within the bed or could be at any bed location with an equal probability. It is obvious that solid circulation patterns should be included in the model. The increased sophistication in modelling would also have to be matched with experimental data. Unfortunately time resolved coal volatile evolution behaviour in combustion systems does not appear to have been investigated, most experimental investigations have dealt only with the total volatile burn-out time.

NOMENCLATURE

A	coefficients defined in equ. (28), (30), (52) and (55)
A_i (i=1 to 4)	coefficients defined in Table 4.4
A'	coefficient defined in equ. (43b)
A_t	cross sectional area of the distributor plate [cm^2]
B	mass transfer number
b	conserved variable in the solution to the fuel droplet combustion problem
Bi	Biot number
Bi_d	Biot number based on particle diameter
Bi_{d0}	initial Biot number based on particle diameter
Bi_{fd}	Biot number under combustion conditions based on particle diameter
Bi_r	Biot number based on particle radius
C	moisture content [g/g dry coal]
C_0	initial moisture content [g/g dry coal]
C_i (i=1 to 3)	coefficients defined in Table 4.4
c	mean concentration of volatiles in coal particle
c_{pc}	specific heat of coal [kJ K/kg]
c_{pg}	specific heat of gas [kJ K/mol]

c_{pw}	specific heat of water [kJ K/kg]
D	effective diffusivity of volatiles through char [mm²/s]
D_i (i=1 to 3)	coefficients defined in Table 4.6
d	diameter [mm]
d_0	initial particle radius [mm]
d_{bo}	initial bubble diameter [cm]
$\overline{d}_b'$	average of the bubble diameter distribution [cm]
E	activation energy [kJ/mol]
E_0	mean of the activation energy distribution [kJ/mol]
F	coefficients defined in Tables 4.3 and 4.5
F_i (i=1 to 4)	coefficients defined in Table 4.6
$\overline{F}$	shrinkage proportionality constant
f	stochiometric coefficient [kg fuel/kg oxygen]
f_c	bubble emulsion cycle frequency at any specific bed location[s^{-1}]
$\bar{f}_c$	the average bubble emulsion cycle frequency over the total bed height [s^{-1}]
f_l	level frequency of bubbles [cm²/s]
f_{rad}	radiation factor
H	total bed height [cm]
ΔH	heat of combustion of volatiles [kJ/kg]

h	heat transfer coefficient [kW K/m²]
i	variable
K	coefficient defined in equ. (6)
k	thermal conductivity [W/m K]
k_g	thermal conductivity of gas [W/m K]
k_s	thermal conductivity of coal [W/m K]
k_0	preexponential factor [s^{-1}]
k'	constant
k_v	constant [s/mm^n]
L	$\lambda' C_0/c_p$ [K]
$N_{i,j,k}$(i,j,k=1 to ∞)	coefficients
Nu	Nusselt number
n	constant equ. (3)
n_d	number of perforations in the distributor plate
Pr	Prandtl number
p	probability of the coal particle being in the bubble phase
p'	permeability of char
Q	sensible heat required / kg volatiles released
Q'	average sensible heat required / kg volatiles released
q	probability of the coal particle being in the emulsion phase

$q(t)$	heat flux at the surface [kW/m²]
$q(t)_c$	heat flux at the surface under combustion conditions [kW/m²]
$q(t)_i$	heat flux at the surface at ignition time [kW/m²]
R	universal gas constant [kJ/mol]
Re	Reynolds number
R_p	particle radius [mm]
R_{p0}	initial particle radius [mm]
r	radius [mm]
r_e	radius wet-dry interface [mm]
r_{e_i}	radius wet-dry interface at ignition time [mm]
r_f	flame radius [mm]
T	temperature [K]
T_0	initial temperature [K]
T_a	ambient temperature [K]
T_e	temperature wet-dry interface [K]
T_{eff}	effective temperature [K]
T_f	flame temperature [K]
T_s	surface temperature [K]
T_{s_c}	surface temperature at ignition time [K]
T_{s_i}	surface temperature at ignition time [K]

T_s'	average surface temperature [K]
T_{wb}	wet bulb temperature [K]
T_2	temperature at which devolatilization is complete [K]
t	time
t'	$t' = t - \tau$ [s]
t_b	time spent in bubble phase [s]
t_e	time spent in emulsion phase [s]
t_{ig}	ignition time [s]
t_{iexp}	experimental ignition time [s]
t_{imod}	ignition time predicted by model [s]
U_0	superficial gas velocity [cm/s]
U_{mf}	minimum fluidizing velocity [cm/s]
V	volatile content of coal [g/g dry coal]
V^0	initial volatile content of coal [g/g dry coal]
V_i^*	fractional maximum volatile yield from the i^{th} cluster of sources
v	Tr, transformation variable
v_e	Tr_e, transformation variable
v_p	TR_p, transformation variable
$\bar{v}'$	average of the bubble velocity density function [cm/s]
$\dot{w}$	mass flux of volatiles

X	DAE kinetics expression for volatile species
X_{avg}	volumetric average fraction of volatiles retained
x_v	initial volume fraction of water
Y_{oa}	oxygen mass fraction in the oxydizing environment
Y_{FR}	initial volatile fraction released
Z	height above the distributor within the fluidized bed [cm]

Greek Symbols

α	thermal diffusivity of coal [mm²/s]
α_g	thermal diffusivity of gas [mm²/s]
$\beta_{i,j,k}$	roots
δ	momentum boundary layer thickness [mm]
δ_b	conduction thickness [mm]
δ_{hf}	conduction thickness in the presence of the flame [mm]
ε	volumetric shrinkage equ. (5)
ε_b	volume fraction of the bubble phase
$\bar{\varepsilon}_T$	coefficient defined in equ. (30b)
η	vbiscosity of flowing volatiles [kg/m s]
θ	dimensionless time

θ_{dry}	dimensionless time when particle is dry
λ	latent heat of vaporization [kJ/kg]
λ'	sum of sensible heat and latent heat of vaporization [kJ/kg]
ρ_c	density of wet coal [kg/m^3]
ρ_d	'drop' density, equ. (10)
ρ_v	molar density of volatiles [mol/m^3]
σ	standard deviation of the activation energy distribution [kJ/mol]
τ	drying time [s]
τ_c	drying time under combustion conditions [s]
τ_i	ignition time [s]
τ_v	devolatilization time measured as the time between flame ignition and extinction [s]
τ_{vfb}	devolatilization time in a fluidized bed [s]
τ_{ve}	devolatilization time if the coal particle was in the emulsion phase [s]
τ_{vg}	devolatilization time if the coal particle was in the bubble phase [s]
Φ	parameter defined in equ. (65c)
ϕ_{ps}	r_c/R_p pseudo steady-state model
ϕ_T	r_c/R_p transient model
ϕ_{T_i}	r_c/R_p transient model at ignition time

ϕ'	space variable

BIBLIOGRAPHY

A.I.E., *Energy 83*, Canberra, National Conference Publication, 1983, 83(2), 145

Agarwal, P.K. and Pedler, I., *Fuel*, 1986, 65, 640

Agarwal, P.K., Agnew, J.B., Ravindran, N., Weimann, R., *Fuel*, 1987, 66, 1097

Agarwal, P.K., accepted in *Chem. Eng. Sci*, 1988

Agarwal, P.K., *Chem. Eng. Res. Des.*, 1985, 63, 323

Agarwal, P.K., *Fluidized Bed Combustion*, Ph.D. Thesis, University of Mississippi, 1984

Agarwal, P.K., *Fuel*, 1985, 64, 870

Agarwal, P.K., *Fuel*, 1986, 65, 803

Agarwal, P.K., Genetti, W.E. and Lee, Y.Y, *Chem. Eng. Sci.*, 1986, 41(9), 2373

Agarwal, P.K., Genetti, W.E. and Lee, Y.Y., *Chem. Engng. Commun.*, 1984a, 27, 9

Agarwal, P.K., Genetti, W.E. and Lee, Y.Y., *Fuel*, 1984b, 63, 1157

Agarwal, P.K., Genetti, W.E. and Lee, Y.Y., *Fuel*, 1984c, 63, 1748

Agarwal, P.K., Genetti, W.E. and Lee, Y.Y., *Proc. 4th Intl. Drying Symp. (IDS '84)*, Kyota, Japan, 1984d

Agarwal, P.K., Genetti, W.E., Lee, Y.Y. and Prasad, S.N., *Fuel*, 1984e, 63, 1020

Ahluwalia, R.K. and Chung, P.M., *Combust. Sci. Tech.*, 1978, 17, 169

Androutsopoulos, G.P. and Linardos, Th. J., *Powder Technology*, 1986, 47, 9

Annamalai, K. and Durbetaki, P., *Combust. Flame*, 1977, 29, 193

Anthony, D.B. and Howard, J.B., *AIChE J.*, 1976, 22(4), 625

Aoyagi, M. and Kunii, D., *Chem. Eng. Comm.*, 1974, 1, 191

Asay, B.W., Smoot, L.D. and Hedman, P.O., *Comb. Sci. Tech.*, 1983, 35, 15

Ashworth, J.C., *Ph.D. Thesis*, University of Canterbury, 1977

Atimay, A., in *'Fluidization'*, (Eds. Grace, J.R. and Matsen, J.M.), 1980, 159

Avedesian, M.M. and Davidson, J.F., *Trans. I. Chem. E.*, 1973, 51, 121

Badzioch, S., Gregory, D.R. and Field, M.A., *Fuel*, 1964, 43, 267

Bale, H.D., Carlson, M.L. and Schobert, H.H., *Fuel*, 1986, 65, 1185

Bandyopadhyay, S. and Bhaduri, D., *Combust. Flame*, 1972, 18, 411

Berger, D. and Pei, D.C.T., *Int. J. Heat Mass Transfer*, 1973, 16, 293

Berkowitz, N., *Fuel*, 1960, 39, 47

Bliek, A., van Poelje, W.M., van Swaaij, W.P.M. and van Beckum, F.P.H., *AIChE J.*, 1985, 31(10), 1666

Bliek, A., *'Mathematical Modelling of a Cocurrent Fixed Bed Coal Gasifier*, Ph.D. Thesis, Twente University, (The Netherlands), 1984

Boiarski, A.A., Nagarajan, V., Wright, I.G. and Carlton, H.E., *J. Inst. Energy*, 1984, 252

Borghi, G., Sarofim, A.F. and Beer, J.M., *A.I.Ch.E. 70th Annual Meeting*, New York, November, 1977

Borghi, G., Sarofim, A.F. and Beer, J.M., *Combust. Flame*, 1985, 61, 1

Brzustowski, T.A., *Combust. Sci. Tech.*, 1983, 35, 59

Bywater, R.J., *6th Int. Conf. Fluidized Bed Combustion*, Atlanta, Georgia, 1980, Vol III, 1092

Carabogdan, I., *St. cerc. energ. electr.*, Bucaresti, 1965, 15(2)

Carabogdan, I., *St. cerc. energ. electr.*, Bucaresti, 1967, 1

Chakraborty, R.K. and Howard, J.R., *J. Inst. Energy*, 1981, 48, 48

Chakraborty, R.K. and Howard, J.R., *J. Inst. Fuel*, 1978, 51, 220

Perry, R.H., Green, D.W. and Maloney, J.O. (Eds.), *Chemical Engineer's Handbook*, McGraw-Hill, New York, 1984

Chen, T. and Saxena, S., *Fuel*, 1977, 56, 401

Choi, S. and Kruger, C.H., *Combust. Flame*, 1985, 61, 131

Corey, R.C., *Chemical Engg.*, Jan. 16, 1978, 111

Cowley, L.T. and Roberts, P.T., *Fluidized Combustion Conference*, Cape, Town, 1981, 443

Damberger, H.H., Harvey, R.D., Rodney, R.R. and Thomas,J., in *'The Science and Technology of Coal and Coal Utilization'*, (Ed. Cooper, B.R. and Ellingham, W.A.), Plenum Press, New York, 1984, 8

Das, A.K., *Fluidized Bed Combustion of Moist Brown Coal Particles*, Ph.D. Thesis, University of Melbourne, 1983

Deevi, S.C. and Suuberg, E.M., *Fuel*, 1987, 66, 454

Dennis, J.S., Hayhurst, A.N. and Mackley, I.G., *Nineteenth Symp. (Intl) Combustion*, Combustion Institute, Pittsburgh, 1982, 1205

Department of Mines and Energy, Coal Deposits in South Australia, *Mineral Information Series*, 1984

Department of Mines and Energy, Outlook on Energy, *Energy Information*, No.5, 1982

Devanathan, N. and Saxena, S.C., *Ind. Eng. Chem. Res.*, 1987, 26, 539

Ergun, S., in *'Coal Conversion Technology'*, (Ed. Wen, C.Y. and Lee, E.S.), Addison-Wesley, Massachussets, 1979, 1

Essenhigh, R. in *'Coal Conversion Technology'*, (Ed. Wen, C.Y. and Lee, E.S.), Addison-Wesley, Massachussets, 1979, 171

Essenhigh, R.H., *J. Eng. Power*, 1963, 85, 183

Evans, D.G., *Fuel*, 1973, 52, 186

Felder, R.M., Kau, C.C., Ferrell, J.K. and Ganesan, S., US Environmental Protection Agency, Report EPA-600/57-82-027, 1982

Fortes, A. and Okos, M.R., in *'Advances in Drying'*, (Ed. Mujumdar, A.S.), Hemisphere Publishing Co., Washington, 1980, Vol I, 119

Fasano, A. and Primicerio, M. (Eds.), *Free Boundary Problems: Theory and Applications*, Pitman, Vol. I & II, 1983

Gavalas, G.R., *Coal Pyrolysis*, Elsevier Scientific Publishing Co., New York, 1982

Gokhale, A.J. and Mahalingam, R., *Fuel*, 1985, 64, 419

Gomez, C.O. and Vastola, F.J., *Fuel*, 1985, 64, 558

Gomez, C.O. and Vastola, F.J., General Papers - Poster Session, The Division of Petroleum Chemistry, Inc. American Chemical Society, Washington, D.C. Meeting, August 28 - September 2, 1983

Hallett, W.L.H., *Combust. Flame*, 1986, 65, 117

Howard, J.B. and Essenhigh, R.H., *Eleventh Symp. (Intl) Combustion*, Combustion Institute, Pittsburgh, 1967, 399

Ivanova, I.P. and Babii, V.L., *Teploenergetika*, 1966, 13(4), 54

Jacob, M., *'Heat Transfer'*, John Wiley and Sons, New York, 1959

Jones, J.F., Schmid, J.R. and Eddinger, R.T., *Chem. Eng. Progr.*, 1964, 60(6), 69

Jung, K. and Stanmore, B.R., *Fuel*, 1980, 59, 74

Jung, K., *M.Eng.Sc. Thesis*, University of Melbourne, 1979

Juntgen, H. and van Heek, K.H., *Fuel Processing Tech.*, 1979, 2, 261

Kansa, E.J. in *'Drying '82'*, (Ed. Mujumdar, A.S.), Hemisphere Publishing Co., New York, 1982, 25

Kanury, A.M., *Introduction to Combustion Phenomena*, Gordon and Breach Publishers, New York, 1975

Karzc, H., Kordylewski, W., Rybak, W. and Zembruski, M., *Archivum Combustionis*, 1983, 3(4), 247

Keey, R.B. in *'Advances in Drying'*, (Ed. Mujumdar, A.S.), Hemisphere Publishing Co., Washington, Vol. I, 1980

Keey, R.B., *AIChE Symp. Ser.*, 1977, 163(73), 1

Krischer, O., *Die wissenschaftlichen Grundlagen der Trocknungstechnik*, 2nd Edition, Springer-Verlag, Berlin, 1963

Kumar, I.J. and Narang, H.N., *Int. J. Heat Mass Transfer*, 1965, 8, 567

Kunii, D. and Levenspiel, O., *Fluidization Engineering*, John Wiley & Sons, 1969

LaNauze, R.D., *Chem. Eng. Res. Des.*, 1985, 63, 3

LaNauze, R.D., *Fuel*, 1982, 61, 771

Lee, C.K. and Diehl, J.R., *Combust. Flame*, 1981, 42, 123

Lin, J.S., Chen, M.M. and Chas, B.T., *AIChE J.*, 1985, 31 (30), 465

Luikov, A.V. and Mikhailov, A., *Theory of Energy and Mass Transfer*, Prentice-Hall, Englewood Cliffs, N.J., 1961

Masahiro, S., Masayoshi, S., Masayuiki, S. and Takeshi, S., *Fuel*, 1987, 66, 717

Massaquoi, J.G.M. and Riggs, J.B., *AIChE J.*, 1983a, 29(6), 976

Massaquoi, J.G.M. and Riggs, J.B., *Chem. Eng. Sci.*, 1983b, 38(10), 1747

Massaquoi, J.G.M. and Riggs, J.B., *Chem. Eng. Sci.*, 1983c, 38(10), 1757

McIntosh, M.J., *Fuel*, 1976a, 55, 47

McIntosh, M.J., *Fuel*, 1976b, 55, 53

Merrick, D., *Fuel*, 1983, 62, 547

Mikhailov, M.D., *Int. J. Heat Mass Transfer*, 1975, 18, 797

Minchener, A.J. and Stringer, J., *J. Inst. Energy*, 1984, 240

Miwa, K., Mori, S., Kato, T. and Muchi, I., *Intl. Chem. Eng.*, 1972, 12(1), 187

Ockendon, J.R. and Hodgkins, W.R. (Eds.), *Moving Boundary Problems in Heat Flow and Diffusion*, Clarendon Press, Oxford, 1975

Park, D., Levenspiel, O. and Fitzgerald, T.J., *AIChE Symp Ser*, 1981, 77, 116

Park, D., Levenspiel, O. and Fitzgerald, T.J., *AIChE Symp. Ser.*,1981, 77, 142

Park, D., Levenspiel, O. and Fitzgerald, T.J., *Chem. Eng. Sci.*, 1980, 35, 295

Park, D., Levenspiel, O. and Fitzgerald, T.J., *Fuel*, 1981, 60, 295

Peck, R.E. and Wasan, D.T., *Advances in Chem. Eng.*, 1974, 9, 247

Peck, R.E., Vyas, K.C. and Toei, R., *AIChE Symp. Ser.*, 1977, 163(73), 63

Peters, W. and Bertling, H., *Fuel*, 1965, 44, 317

Pillai, K.K., *J. Inst. Energy*, 1981, 142

Pillai, K.K., *J. Inst. Energy*, 1982, 132

Pillai, K.K., *Letters in Heat and Mass Transfer*, 1976, 3, 131

Pitt, G.J., *Fuel*, 1962, 41, 267

Potter, O.E. and Keogh, A.J., *Fuel Processing Technology*, 1981, 4, 217

Prins, W., *'Fluidized Bed Combustion of a Single Coal Particle'*, Ph.D. Thesis, Universiteit Twente, The Netherlands, 1987

Pyle, D.L., Fluidized Combustion Models (Rapporteur's Report), *Inst. Fuel Symp. Ser.*, 1975, 2(1), 6

Ragland, K.W. and Weiss, C.A., *Energy*, 1979, 4, 341

Ragland, W.K. and Yang, J.-T., *Combust. Flame*, 1985, 60, 285

Rah, S.C., Sarofim, A.F. and Beer, J.M., *Combust. Sci. Tech.*, 1986a, 48, 237

Rah, S.C., Sarofim, A.F. and Beer, J.M., *Combust. Sci. Tech.*, 1986b, 49, 169

Rehmat, A., Saxena, S.C. and Land, R.H., ANL/CEN/FE-80-13, Sept. 1980

Ross, I.B. and Davidson, J.F., *Trans. I. Chem. E.*, 1979, 57, 215

Rubinstein, L.I., *The Stefan Problem*, Translations of Mathematical Monographs, American Math. Soc., Providence, R.I., Vol. 27, 1967

Saito, M., Sadakata, M., Sato, M. and Sakai, T., *Fuel*, 1987, 66, 717

Salam, T.F., Shen, X.L. and Gibbs, B.M., *Fuel*, 1988, 67, 414

Saxena, S.C. and Rhemat, A., *Fluidized Bed Combustion - 6th Intl Conf.*, Proceedings, 1980, III, 1138

Schoeber, W.J.A.H. and Thijssen, H.A.C., *AIChE Symp, Ser.*, 1977, 163(73), 12

Solomon, P.R. and Hamblen, D.G., *Prog Energy Combust. Sci.*, 1983, 9, 323

Stambuleanu, A., *Flame Combustion Processes in Industry*, Abacus Press, Kent 1976

Stewart, R. and Evans, D.G., *Fuel*,1967, 46, 263

Stubington, J.F. and Sumaryono, *Fuel*, 1984, 63, 1013

Sugiyama, S., Hasatani, M. and Nakamura, M., *Int. J. Heat Mass Transfer*, 1974, 17, 899

Suuberg, E.M., Peters, W.A. and Howard, J.B., *Ind. Eng. Chem. Process Des. Dev.*, 1978, 17, 37

Thomas, G.R., Harris, J.J. and Evans, D.G., *Combust. Flame*, 1968, 12, 391

Tsang, T.H. and Edgar, T.F., *In Situ*, 1983, 7(3), 237

Tsang, T.H. and Edgar, T.F., *In Situ*, 1983, 7(3), 265

Turnbull, E. and Davidson, J.F., *AIChE J.*, 1984, 30(6), 881

Vanecek, V., Markvart, M., Drbohlav, R. and Hummel, R.L., *Chem. Engg. Prog. Symp. Ser.*, 66(105), 243

van Brakel, J., in *'Advances in Drying'*, (Ed. Mujumdar, A.S.), Hemisphere Publishing Co., Washington, Vol. I, 1980, 217

van Krevelen, D.W., *Fuel*, 1982, 61, 786

Waibiao, F., Yangping, Z., Hongqiao, H. and Yuning, D., *Combustion and Flame*, 1987, 70, 253

Weimer, R.F. and Ngan, D.Y., Am. Chem. Soc. Div. Fuel Chem. Preprints, 1979, 24(3), 129

Wen, C.Y. and Dutta, S., in *'Coal Conversion Technology'*, (Ed. Wen, C.Y. and Lee, E.S.), Addison-Wesley, 1979, 57

Wen, C.Y. and Dutta, S., in *'Coal Conversion Technology'*, Ed. C.Y. Wen and E. S. Lee, (Addison - Wesley), 1979, 57

Werther, J. and Molerus, O., *Intl J Multiphase Flow*, 1973, 1, 123

Westmoreland, P.R. and Forrester, III, R.C., *ACS Div. of Fuel Chem.*, 1977, 22(1), 93

Whitaker, S. in *'Advances in Drying'*, (Ed. Mujumdar, A.S.), Hemisphere Publishing Co., Washington, 1980, Vol. I, 101

Whitaker, S., *Ind. Eng. Chem. Fundam.*,1977, 16, 408

Wildegger-Gaissmaier, A.E., Agarwal, P.K., La Nauze, R.D. and Jung, K., *3rd Australian Coal Science Conference*, Adelaide, 1988

Wilson, D.G., Solomon, A.D. and Boggs, P.T (Eds.), *Moving Boundary Problems*, Academic Press, New York, 1978

Yates, J.G., Macgillivray, M. and Cheesman, D.J., *Chem. Eng. Sci.*, 1980, 35, 2361

Young, B.C., Mullins, P.J. and Smith, I.W., *CHEMECA 87*, Melbourne, 1987, 2, 84.1

Ziesing, G.F., Forgarrd, K., Lefever, J., Rhodes, B. and Griffiths, V., *Tenth Lignite Symp.*, GFETC/IC - 79/1, CONF - 790579, 1979, 459

APENDIX A

A = crucible weight [mg]

B = crucible + sample weight [mg]

C = crucible + dry sample weight [mg]

D = **crucible + devolatilized sample weight** [mg]

M = moisture content [g/g dry coal]

V = volatiles content [g/g dry coal]

$V_{avg.}$ = average volatiles content of original sample [g/g dry coal]

Calculation of volatile content [g/g dry coal]

$$V = (C - D) / ((1. + V_{avg.} / (1. - V_{avg.})) (D - A))$$

Calculation of moisture content [g/g dry coal]

$$M = (B - C) / ((1. + V_{avg.} / (1. - V_{avg.})) (D - A))$$

WEIGHT LOSS EXPERIMENTS

Temperature: 423 K

Particle size: 10 mm

Initial moisture content: 1.1 g/g dry coal

Fluidizing velocity: 4.2 m/s

Estimated Biot number: 3.1

Condition: Pyrolysis

Time (sec)	Cruc. wt (mg)	Cruc. + smpl. wt. (mg)	Cruc. + dry smpl. wt. (mg)	Moist. g/g dry coal
30	10483	11169	10841	0.916
30	12343	12991	12657	1.063
30	10919	11568	11260	0.903
30	10930	11623	11275	1.008
30	14971	15654	15328	0.913
90	9747	10225	10019	0.757
90	10010	10477	10270	0.790
90	9979	10686	10373	0.798
90	10243	10837	10567	0.830
90	10482	11054	10802	0.788
180	12343	12793	12619	0.630
180	10920	11379	11195	0.669
180	10930	11417	11230	0.623
180	14971	15467	15278	0.615
180	9747	10188	10021	0.609
240	10008	10599	10387	0.559
240	9978	10568	10341	0.625
240	10243	10691	10537	0.524
240	10482	11039	10827	0.614
240	12344	12815	12646	0.559
300	10919	11410	11234	0.558
300	10930	11353	11209	0.516

300	14971	15426	15281	0.468
300	9747	10230	10075	0.473
300	10009	10439	10287	0.546
600	9978	10322	10231	0.359
600	10243	10641	10538	0.349
600	10483	10999	10861	0.365
600	12344	12698	12609	0.336
600	10920	11386	11271	0.327
900	10930	11316	11239	0.249
900	14972	15394	15328	0.185
900	9748	10132	10055	0.250
900	10243	10631	10568	0.190
900	10483	10849	10782	0.224
1200	12343	12757	12715	0.113
1200	10920	11285	11232	0.169
1200	10929	11186	11167	0.080
1200	14970	15273	15249	0.086
1200	9746	10033	10015	0.104
0	10244	10891	10551	1.107
0	10483	11195	10835	1.023
0	12343	13105	12696	1.158
0	10920	11670	11278	1.095
0	10930	11718	11274	1.163

Temperature: 573 K

Particle size: 10 mm

Intial moisture content: 1.1 g/g dry coal

Fluidizing velocity: 4.2 m/s

Estimated Biot number: 3.2

Condition: Pyrolysis

Time (sec)	Cruc. wt (mg)	Cruc. + smpl. wt (mg)	Cruc. + dry smpl. wt (mg)	Moist. g/g dry coal
30	13704	14300	14031	0.823
30	15032	15622	15366	0.766
30	15262	15773	15559	0.721
30	9498	10044	9810	0.750
30	11896	12503	12237	0.780
60	14206	14762	14538	0.675
60	13717	14140	13969	0.679
60	9489	10032	9830	0.636
60	11896	12478	12233	0.730
60	14630	15274	15010	0.695
90	12721	13067	12951	0.504
90	14683	15154	14983	0.570
90	9837	10322	10145	0.575
90	11896	12332	12183	0.519
90	14639	14962	14856	0.529
120	13468	13904	13773	0.429
120	10287	10786	10626	0.472
120	10424	10875	10733	0.459
120	13480	13906	13776	0.439
120	14204	14410	14351	0.400
180	5419	5864	5756	0.320
180	5419	5872	5766	0.305
180	5710	6151	6043	0.324

180	5037	5430	5349	0.259
180	5456	5841	5750	0.309
240	13722	13991	13936	0.204
240	14097	14373	14330	0.185
240	5460	5792	5726	0.248
240	5381	5692	5647	0.169
240	5442	5656	5690	0.159
300	13476	13787	13762	0.087
300	13474	13815	13774	0.137
300	4134	4506	4471	0.104
300	5499	5776	5750	0.104
300	5411	5648	5632	0.072
0	13602	14281	13940	1.008
0	14850	15599	15200	1.140
0	14424	15011	14702	1.110
0	15261	15941	15587	1.086
0	15031	15739	15376	1.052

Temperature: 823 K
Particle size: 10 mm
Initial moisture content: 1.1 g/g dry coal
Fluidizing velocity: 4.2 m/s
Estimated Biot number: 4.2
Condition: Pyrolysis

Time	Cruc. wt	Cruc. + smpl. wt	Cruc. + dry smpl. wt	Cruc. + dev. smpl. wt.	Moist.	Vols.
(sec)	(mg)	(mg)	(mg)	(mg)	g/g dry coal	g/g dry coal
30	10483	11063	10844	10674	0.564	0.438
30	12343	12823	12637	12487	0.636	0.513
30	10930	11461	11264	11106	0.551	0.442
30	14958	15479	15277	15127	0.588	0.437
30	9758	10328	10103	9929	0.647	0.500
60	13602	14052	13915	13762	0.421	0.470
60	10220	10652	10518	10363	0.461	0.533
60	9989	10428	10290	10149	0.424	0.433
60	9990	10418	10286	10135	0.447	0.512
60	12351	12798	12666	12515	0.396	0.453
120	10505	10823	10778	10638	0.166	0.518
120	10932	11255	11230	11073	0.087	0.527
120	12356	12707	12669	12513	0.119	0.488
120	10944	11306	11257	11092	0.163	0.479
120	14973	15290	15268	15118	0.074	0.509
180	14973	15217	15211	15108	0.022	0.375
180	9770	10048	10044	9933	0.012	0.335
180	13616	13849	13849	13753	0.000	0.344
180	10243	10524	10521	10390	0.010	0.438
180	10010	10288	10288	10163	0.000	0.402
240	9979	10186	10186	10119	0.000	0.235
240	12356	12543	12543	12482	0.000	0.238
240	9747	9970	9970	9883	0.000	0.315

240	14971	15163	15163	15098	0.000	0.252
240	10919	11114	11114	11053	0.000	0.224
300	9748	9981	9981	9851	0.000	0.121
300	13606	13785	13785	13752	0.000	0.111
300	10196	10365	10365	10333	0.000	0.115
300	10483	10630	10630	10595	0.000	0.154
300	12343	12496	12496	12467	0.000	0.115
0	13610	14372	13973	13784	1.100	0.520
0	10208	10876	10528	10361	1.088	0.522
0	10496	11207	10841	10668	1.061	0.501
0	10483	11205	10833	10659	1.063	0.497
0	10189	10889	10519	10354	1.120	0.500

Temperature: 923 K
Particle size: 10 mm
Initial moisture content: 1.1 g/g dry coal
Fluidizing velocity: 4.2 m/s
Estimated Biot number: 4.3
Condition: pyrolysis

Time (sec)	Cruc. wt (mg)	Cruc. + smpl. wt (mg)	Cruc. + dry smpl. wt (mg)	Cruc. + dev. smpl.wt (mg)	Moist. (g/g dry coal)	Vols. (g/g dry coal)
30	10188	10700	10509	10344	0.590	0.510
30	13313	13822	13640	13481	0.522	0.456
30	10904	11175	11234	11067	0.574	0.504
30	12628	12958	12829	12724	0.647	0.527
30	10217	10492	10391	10304	0.560	0.482
60	12626	13017	12913	12767	0.475	0.499
60	9449	9868	9742	9539	0.419	0.497
60	13313	13763	13623	13474	0.374	0.446
60	10893	11304	11189	11041	0.379	0.482
60	9448	9760	9668	9565	0.252	0.424
90	14962	15332	15255	15109	0.185	0.478
90	9465	9801	9730	9650	0.219	0.408
90	10978	11333	11267	11123	0.186	0.479
90	13314	13607	13554	13451	0.161	0.362
90	10213	10554	10501	10371	0.101	0.397
120	14968	15329	15292	15145	0.092	0.400
120	10963	11284	11250	11141	0.099	0.295
120	12621	12875	12846	12761	0.116	0.293
120	10203	10521	10203	10500	0.071	0.388
120	10199	10546	10519	10382	0.023	0.361
150	14966	15165	15159	15091	0.007	0.262
150	10956	11152	11150	11092	0.039	0.206
150	10206	10362	10353	10316	0.030	0.162

150	13318	13602	13591	13496	0.023	0.257
150	10920	11122	11116	11044	0.030	0.279
180	12631	12795	12795	12755	0.000	0.155
180	10221	10421	10420	10380	0.003	0.121
180	14962	15159	15159	15121	0.000	0.115
180	9481	9677	9677	9638	0.000	0.119
180	10984	11179	11179	11140	0.000	0.121
0	12277	13009	12628	12442	1.085	0.530
0	9774	10459	10096	9932	1.128	0.509
0	14962	15625	15287	15118	1.040	0.520
0	10221	10925	10545	10379	1.170	0.512
0	10984	11665	11311	11114	1.080	0.520

Temperature: 923 K
Particle size: 10 mm
Initial moisture content: 0.64 g/g dry coal
Fluidizing velocity: 4.2 m/s
Estimated Biot number: 4.3
Condition: Pyrolysis

Time (s)	Cruc. wt. (mg)	Cruc. + smpl. wt. (mg)	Cruc. + sry smpl. wt. (mg)	Cruc. + dev. smpl. wt. (mg)	Moist. (g/g dry coal)	Vols. (g/g dry coal)
10	12760	13397	13200	12966	0.458	0.533
10	11266	11861	11671	11468	0.451	0.516
10	13503	13953	13811	13653	0.453	0.513
10	14237	14814	14647	14437	0.400	0.512
10	14049	14747	14521	14267	0.496	0.538
20	13782	14249	14125	13960	0.334	0.444
20	14789	15178	15079	14927	0.344	0.527
20	9947	10382	10265	10107	0.350	0.473
20	14828	15244	15136	14978	0.345	0.504
20	9831	10355	10211	10012	0.381	0.526
30	13571	13999	13919	13748	0.216	0.463
30	14088	14384	14331	14215	0.200	0.437
30	14875	15216	15146	15016	0.238	0.441
30	9956	10503	10401	10177	0.221	0.485
30	10058	10541	10443	10253	0.241	0.467
40	13575	13862	13827	13711	0.123	0.409
40	15161	15524	15474	15324	0.147	0.441
40	10056	10388	10349	10208	0.123	0.444
40	9401	9758	9712	9566	0.134	0.424
40	14568	14926	14878	14735	0.138	0.410
60	12752	13146	13124	12939	0.056	0.474
60	14047	14351	14337	14209	0.041	0.378
60	9935	10222	10208	10091	0.043	0.359

60	14241	14535	15522	14391	0.061	0.361
60	14797	15147	15130	14980	0.044	0.393
80	14953	15227	15222	15123	0.014	0.279
80	15161	15456	15447	15347	0.023	0.258
80	9845	10144	10137	10048	0.017	0.210
80	15163	15419	15412	15335	0.019	0.214
80	14343	14545	14542	14466	0.012	0.296
0	13780	14393	14150	13960	0.656	0.514
0	10055	10691	10441	10242	0.648	0.515
0	14831	15326	15133	14972	0.639	0.533
0	9399	9949	9742	9564	0.603	0.518
0	13508	14024	13814	13655	0.664	0.526

Temperature: 923 K

Particle size: 10 mm

Initial moisture content: 0.0 g/g dry coal

Fluidizing velocity: 4.2 m/s

Estimated Biot number: 4.3

Condition: Pyrolysis

Time (s)	Cruc. wt. (mg)	Cruc. + smpl. wt. (mg)	Cruc. + dev. smpl.wt. (mg)	Vols. (g/g dry coal)
10	12737	12937	12835	0.503
10	9420	9913	9657	0.522
10	15701	16100	15904	0.466
10	11086	11446	11261	0.511
10	13375	13665	13523	0.463
20	14670	14993	14835	0.463
20	13883	14215	14062	0.413
20	13860	14230	14068	0.376
20	14142	14296	14220	0.471
20	15320	15654	15505	0.389
40	10484	10776	10674	0.259
40	13299	13630	13510	0.274
40	10085	10391	10281	0.271
40	15334	15645	15543	0.236
40	11077	11409	11289	0.273
60	13604	13896	13806	0.215
60	9492	9806	9711	0.209
60	12733	11955	12910	0.261
60	9411	9560	9518	0.190
60	15699	16003	15944	0.116
70	14674	14963	14895	0.149
70	13740	14004	13954	0.113
70	10473	10741	10681	0.139

70	13517	13782	13731	0.115
70	13869	14140	14081	0.134*
80	14139	14375	14331	0.110*
80	13614	13855	13810	0.111*
80	9411	9646	9606	0.099*
80	15699	15966	15927	0.083*
0	10492	10867	10659	0.554
0	13306	13704	13499	0.515
0	10094	10457	10279	0.490
0	15346	15734	15534	0.515
0	9528	9916	9717	0.512

*fractured

Temperature: 1023 K
Particle size: 10 mm
Initial moisture content: 1.1 g/g dry coal
Fluidizing velocity: 4.2 m/s
Estimated Biot number: 4.4
Condition: Pyrolysis

Time (s)	Cruc. wt. (mg)	Cruc. + smpl. wt. (mg)	Cruc. + dry smpl. wt. (mg	Cruc. + dev. smpl. wt. (mg)	Moist. (g/g dry coal)	Vols. (g/g dry coal)
10	10588	11050	10835	10710	0.853	0.4959
10	13600	14295	13966	13768	0.948	0.540
10	10983	11620	11315	11143	0.923	0.520
10	14965	15576	15283	15119	0.921	0.515
10	9786	10500	10166	9974	0.860	0.494
20	12344	12970	12681	12507	0.858	0.517
20	9892	10521	10254	10075	0.706	0.473
20	10778	11268	11055	10913	0.764	0.509
20	10586	11149	10909	10740	0.754	0.531
20	13602	14204	13945	13779	0.708	0.454
50	10974	11451	11310	11155	0.377	0.414
50	14963	15315	15206	15102	0.379	0.362
50	9781	10295	10136	9966	0.416	0.445
50	12347	12880	12722	12553	0.371	0.397
50	10771	11234	11086	10946	0.409	0.387
70	12347	12735	12660	12544	0.184	0.285
70	10590	10898	10843	10734	0.185	0.366
70	13609	14006	13922	13812	0.200	0.262
70	10972	11361	11288	11165	0.183	0.308
70	14972	15397	15315	15178	0.193	0.322
90	9773	10001	9986	9899	0.057	0.334
90	12351	12740	12698	12573	0.091	0.272
90	10766	11021	10983	10900	0.137	0.299

90	9883	10087	10068	9992	0.084	0.337
90	10575	10871	10849	10743	0.063	0.305
110	12339	12560	12560	12494	0.000	0.206
110	9858	10072	10072	10004	0.000	0.225
110	10576	10821	10821	10750	0.000	0.197
110	13590	13766	13766	13717	0.000	0.187
110	10933	11119	11119	11056	0.000	0.248
130	10751	10931	10931	10888	0.000	0.152
130	13600	13777	13777	13740	0.000	0.128
130	10944	11184	11184	11138	0.000	0.115
130	14959	15190	15190	15137	0.000	0.144
130	9750	9909	9909	9880	0.000	0.107
0	12338	13052	12338	12681	1.082	0.525
0	9743	10481	10092	9919	1.114	0.524
0	14960	15789	15343	15148	1.164	0.509
0	10744	11341	11033	10885	1.065	0.512
0	9855	10586	10189	10018	1.180	0.512

Temperature: 923 K

Particle size: 5 mm

Initial moisture content: 1.1 g/g dry coal

Fluidizing velocity: 1.2 m/s

Estimated Biot number: 2.1

Condition: Pyrolysis

Time (s)	Cruc. wt. (mg)	Cruc. + smpl. wt. (mg)	Cruc. + dry smpl. wt. (mg)	Cruc. + dev. smpl. wet (mg)	Moist. (g/g dry coal)	Vols. (g/g dry coal)
20	9832	10280	10128	9965	0.555	0.550
20	14089	14660	14480	14286	0.444	0.478
20	14870	15770	15223	15047	0.502	0.483
20	14456	14860	14732	14602	0.426	0.432
20	14781	15341	15156	14965	0.489	0.504
30	11242	11661	11585	11420	0.208	0.450
30	13829	14203	13980	14141	0.191	0.516
30	9933	10273	10220	10084	0.171	0.438
30	12749	13152	13077	12910	0.226	0.504
30	13785	14081	14030	13914	0.192	0.437
40	15163	15446	15435	15308	0.037	0.426
40	13577	13858	13847	13717	0.038	0.451
40	14837	15183	15162	15010	0.059	0.427
40	13112	13419	13405	13254	0.048	0.516
40	10050	10291	10282	10165	0.038	0.494
60	14940	15163	15163	15069	0.000	0.354
60	9395	9668	9668	9562	0.000	0.308
60	14798	15058	15057	14941	0.003	0.394
60	9826	10067	10067	9963	0.000	0.368
60	14419	14686	14686	14576	0.000	0.341
80	14467	14684	14684	14632	0.000	0.153
80	13772	13942	13942	13893	0.000	0.197
80	13101	13307	13307	13257	0.000	0.156

80	13560	13770	13770	13715	0.000	0.172
80	12741	12921	12921	12871	0.000	0.187
0	15155	15776	15456	15313	1.063	0.475
0	13821	14775	14131	13970	1.077	0.519
0	9395	10082	9781	9550	1.130	0.520
0	14789	15423	15087	14926	1.130	0.540
0	9826	10538	10164	9988	1.110	0.520

Temperature: 423 K
Particle size: 1.8 mm
Initial moisture content: 0.69 g/g dry coal
Fluidizing velocity: 0.5 m/s
Estimated Biot number: 0.71
Condition: Pyrolysis

Time (s)	Cruc. wt. (mg)	Cruc. + smpl. wt. (mg)	Cruc. + dry smpl. wt. (mg)	Moist. (g/g dry coal)
10	5358	5716	5591	0.536
10	5414	5788	5655	0.552
10	5577	5971	5848	0.454
10	5461	5739	5644	0.520
10	4084	4420	4321	0.418
20	5503	5921	5815	0.339
20	5433	5744	5662	0.358
20	5420	5733	5650	0.361
20	5420	5734	5731	0.421
20	5461	5751	5682	0.312
40	5539	5933	5863	0.216
40	5335	5720	5662	0.177
40	5298	5704	5623	0.249
40	5413	5838	5771	0.187
40	5444	5706	5660	0.213
60	5418	5668	5641	0.121
60	5501	5843	5796	0.159
60	4838	5145	5120	0.088
60	5500	5787	5754	0.130
60	5599	5827	5802	0.123
80	5534	5687	5683	0.030
80	4136	4460	4452	0.025
80	5501	5799	5798	0.053

80	5614	5892	5886	0.022
80	5439	5598	5590	0.052
0	5474	6101	5870	0.680
0	5582	6151	5922	0.673
0	5384	5971	5728	0.706
0	5371	5983	5728	0.714
0	5384	5988	5769	0.640

Temperature: 423 K
Particle size: 1.8 mm
Initial moisture content: 1.1 g/g dry coal
Fluidizing velocity: 0.5 m/s
Estimated Biot number: 0.71
Condition: Pyrolysis

Time (s)	Cruc. wt. (mg)	Cruc. + smpl. wt. (mg)	Cruc. + dry smpl. wt. (mg)	Moist. (g/g dry coal)
10	5275	5748	5537	0.778
10	5392	5947	5693	0.820
10	5508	6002	5785	0.739
10	5465	6051	5795	0.749
10	5406	5935	5705	0.740
20	5521	5967	5775	0.709
20	4362	4804	4617	0.668
20	5438	5923	5715	0.702
20	4201	4591	4432	0.639
20	5339	5865	5637	0.708
30	5352	5736	5584	0.620
30	5502	6025	5821	0.700
30	5442	5981	5775	0.590
30	4086	4643	4433	0.573
60	5556	6045	5895	0.421
60	5647	6089	5954	0.407
60	5458	5638	5593	0.333
60	5416	5763	5685	0.290
60	5445	5768	5689	0.302
70	5626	5953	5888	0.220
70	5283	5573	5533	0.280
70	5418	5673	5613	0.260
70	5608	5866	5815	0.211

90	5369	5596	5647	0.159
90	5419	5760	5699	0.209
90	5506	5958	5716	0.141
90	5318	5651	5596	0.181
90	5553	5854	5811	0.149
120	5603	5875	5875	0.071
120	5336	5637	5622	0.052
120	5409	5690	5675	0.056
120	5596	5596	5835	0.092
120	4131	4381	4364	0.073
150	5450	5774	5750	0.013
150	5389	5669	5651	0.068
150	4430	4721	4708	0.046
150	5460	5735	5736	0.045
150	5473	5773	5758	0.050
0	5446	6153	5793	1.037
0	4149	4988	4541	1.140
0	5293	5992	5630	1.070
0	5399	6125	5742	1.116
0	5391	6094	5735	1.044

Temperature: 573 K

Particle size: 1.8 mm

Initial moisture content: 1.1 g/g dry coal

Fluidizing velocity: 0.5 m/s

Estimated Biot number: 0.75

Condition: Pyrolysis

Time (s)	Cruc. wt. (mg)	Cruc. + smpl. wt. (mg)	Cruc. + dry smpl. wt. (mg)	Moist. (g/g dry coal)
5	5377	5360	5658	0.719
5	5502	6048	5807	0.790
5	5329	5846	5626	0.741
5	5564	6036	5837	0.729
5	5280	5826	5594	0.739
10	5289	5393	5355	0.576
10	5386	5776	5632	0.585
10	5553	5962	5822	0.520
10	5471	5946	5774	0.568
10	5412	5732	5606	0.649
15	5420	5798	5667	0.530
15	4058	4439	4321	0.448
15	4160	4507	4396	0.470
15	5337	5762	5634	0.431
15	5520	5929	5804	0.440
20	5384	5763	5673	0.311
20	4117	4436	4358	0.323
20	5390	5786	5685	0.342
20	5591	5990	5890	0.334
20	5429	5828	5719	0.376
25	4132	4396	4336	0.294
25	5422	5691	5645	0.206
25	5571	5926	5840	0.319

25	5564	5937	5845	0.327
25	5390	5643	5583	0.311
30	5501	5781	5731	0.217
30	5386	5697	5638	0.234
30	5417	5672	5623	0.237
30	5420	5689	5650	0.169
30	5463	5709	5689	0.088
35	5441	5737	5703	0.129
35	4138	4423	4384	0.158
35	5417	5614	5591	0.110
35	5386	5675	5638	0.147
35	5512	5813	5781	0.118
40	5474	5759	5735	0.090
40	7138	73575	7370	0.020
40	10475	10722	10718	0.016
40	6450	6622	6618	0.023
40	10648	10860	10858	0.009
0	6657	7346	6980	1.130
0	11440	12186	11793	1.110
0	12348	13084	12702	1.080
0	11379	12079	11706	1.140

Temperature: 823 K
Particle size: 1.8 mm
Initial moisture content: 1.1 g/g dry coal
Fluidizing velocity: 0.5 m/s
Estimated Biot number: 1.1
Condition: Pyrolysis

Time (s)	Cruc. wt. (mg)	Cruc. + smpl. wt. (mg)	Cruc. + dry smpl. wt. (mg)	Cruc. + dev. smpl. wet (mg)	Moist. (g/g dry coal)	Vols. (g/g dry coal)
5	12346	12850	12675	12501	0.552	0.530
5	9971	10516	10299	10131	0.663	0.512
5	14966	15506	15291	15129	0.645	0.498
5	9738	10299	10067	9895	0.722	0.523
5	13608	14144	13939	13767	0.630	0.519
10	10920	11290	11224	11068	0.218	0.515
10	10841	10889	10811	10640	0.190	0.416
10	10185	10585	10508	10340	0.243	0.530
10	12345	12764	12689	12509	0.224	0.536
10	9972	10471	10350	10149	0.334	0.535
15	13610	13938	13911	13762	0.087	0.479
15	9735	10086	10051	9889	0.111	0.514
15	11181	11204	11181	11047	0.084	0.489
15	14968	15366	15305	15139	0.174	0.475
15	10466	10759	10747	10610	0.041	0.465
20	10163	10418	10418	10316	0.000	0.326
20	12346	12599	12599	12485	0.000	0.401
20	9965	10263	10263	10126	0.000	0.416
20	13608	13839	13839	13735	0.000	0.400
20	10457	10666	10666	10563	0.000	0.475
25	14965	15209	15209	15131	0.000	0.229
25	9730	9958	9958	9863	0.000	0.349
25	10909	11079	11079	11028	0.000	0.210

25	10160	10347	10347	10279	0.000	0.279
25	12351	12508	12508	12458	0.000	0.228
30	9963	10071	10071	10037	0.000	0.225
30	13607	13779	13799	13725	0.000	0.307
30	10458	10626	10626	10563	0.000	0.293
30	14971	15211	15211	15144	0.000	0.189
30	10899	11060	11060	11005	0.000	0.254
40	9723	9828	9828	9802	0.000	0.161
40	9715	9926	9926	9871	0.000	0.172
40	13612	13765	13765	13738	0.000	0.105
40	10879	10998	10998	10972	0.000	0.137
50	14968	15082	15082	15064	0.000	0.092
50	10451	10593	10593	10559	0.000	0.154
50	12349	12459	12459	12433	0.000	0.151
50	9962	10099	10099	10063	0.000	0.174
50	10157	10290	10290	10260	0.000	0.142
0	9719	10469	10070	9885	1.139	0.527
0	13606	14359	13968	13776	1.080	0.530
0	10883	11610	11230	11056	1.095	0.501
0	14964	15726	15314	15141	1.170	0.495
0	10438	11190	10805	10621	1.049	0.502

Temperature: 923 K
Particle size: 1.8 mm
Initial moisture content: 0.0 g/g dry coal
Fluidizing velocity: 0.5 m/s
Estimated Biot number: 1.1
Condition: Pyrolysis

Time (s)	Cruc. wt. (mg)	Cruc. + dry smpl. wt. (mg)	Cruc. + dev. smpl. wet (mg)	Vols. (g/g dry coal)
5	13600	13873	13782	0.238
5	13594	14241	13809	0.286
5	9665	9938	9826	0.331
5	14953	15189	15104	0.267
5	10060	10307	10216	0.278
10	12341	12586	12544	0.098
10	14964	15237	15169	0.158
10	10369	10601	10555	0.118
10	9909	10154	10102	0.128
10	13600	13826	13768	0.164
15	9664	9925	9878	0.105
15	14964	15237	15204	0.065
15	10068	10251	10231	0.058
15	10838	11053	11016	0.099
15	10333	10567	10532	0.084
0	10061	10641	10334	0.529
0	10317	10905	10592	0.532
0	10813	11370	11072	0.535
0	13596	14165	14441	0.515
0	14953	15531	15263	0.510

Temperature: 923 K
Particle size: 1.8 mm
Initial moisture content: 0.69 g/g dry coal
Fluidizing velocity: 0.5 m/s
Estimated Biot number: 1.1
Condition: Pyrolysis

Time (s)	Cruc. wt. (mg)	Cruc. + smpl. wt. (mg)	Cruc. + dry smpl. wt. (mg)	Cruc. + dev. smpl. wet (mg)	Moist. (g/g dry coal)	Vols. (g/g dry coal)
5	12349	12692	12633	12490	0.200	0.485
5	9950	10246	10189	10060	0.248	0.561
5	10137	10458	10409	10271	0.175	0.492
5	10131	10628	10391	10258	0.192	0.501
5	13603	13901	13851	13725	0.196	0.493
10	9701	9901	9906	9808	0.022	0.438
10	14949	15144	15140	15051	0.019	0.417
10	10870	11029	11027	10954	0.011	0.415
10	12348	12386	12386	12370	0.000	0.347
10	10425	10602	10592	10529	0.046	0.290
15	9938	10226	10226	10151	0.000	0.168
15	10088	10229	10229	10186	0.000	0.210
15	13602	13819	13819	132767	0.000	0.148
15	9693	9853	9853	9824	0.000	0.106
15	14962	15163	15163	15115	0.000	0.150
20	10842	11029	11029	10999	0.000	0.091
20	12346	12485	12485	12613	0.000	0.023
20	10414	10660	10660	10613	0.000	0.113
20	9927	10062	10062	10043	0.000	0.078
20	10094	10198	10198	10185	0.000	0.068
25	13608	13716	13716	13703	0.000	0.065
25	9680	9813	9813	9794	0.000	0.080
25	14964	15016	15016	15008	0.000	0.087

0	10844	11496	11230	11026	0.689	0.528
0	12354	12897	12751	12538	0.619	0.536
0	10390	11011	10755	10563	0.726	0.526
0	9925	10634	10347	10133	0.680	0.507
0	9904	10586	10298	10095	0.730	0.515

Temperature: 923 K

Particle size: 1.8 mm

Initial moisture content: 1.1 g/g dry coal

Fluidizing velocity: 0.5 m/s

Estimated Biot number: 1.1

Condition: Pyrolysis

Time (s)	Cruc. wt. (mg)	Cruc. + smpl. wt. (mg)	Cruc. + dry smpl. wt. (mg)	Cruc. + dev. smpl. wet (mg)	Moist. (g/g dry coal)	Vols. (g/g dry coal)
5	9899	10374	10187	10035	0.657	0.534
5	14564	15159	14943	14750	0.555	0.496
5	10719	11290	10936	10823	0.627	0.519
5	13528	14086	13881	13701	0.566	0.497
5	9844	10343	10156	9994	0.595	0.516
10	14475	14856	14785	14623	0.229	0.523
10	14480	14689	14649	14563	0.230	0.495
10	15648	15988	15929	15790	0.199	0.468
10	10412	10598	10561	10485	0.242	0.498
10	9899	10118	10076	9986	0.230	0.494
15	13540	13703	13702	13645	0.004	0.259
15	9459	9560	9557	9516	0.025	0.344
15	13610	13743	13742	13689	0.006	0.321
15	9844	9987	9985	9933	0.011	0.279
15	14475	14634	14632	14572	0.010	0.296
20	15583	15760	15760	15725	0.000	0.117
20	14056	14267	14265	14228	0.009	0.103
20	13095	13214	13250	13213	0.019	0.150
20	9881	10137	10136	10075	0.004	0.150
25	13544	13599	13599	13590	0.000	0.093
25	10717	10834	10834	10813	0.000	0.105
25	13531	13651	13651	13646	0.000	0.021
25	14566	14704	14704	14688	0.000	0.063

25	9838	9972	9972	9953	0.000	0.079
30	11404	11449	11449	11445	0.000	0.046
30	14734	14819	14819	14812	0.000	0.043
30	14480	14546	14546	14536	0.000	0.085
30	13544	13623	13623	13614	0.000	0.061
30	11404	11515	11515	11502	0.000	0.063
40	13506	13608	13608	13599	0.000	0.046
40	14571	14630	14630	14623	0.000	0.064
40	9462	9544	9544	9534	0.000	0.066
40	15587	15673	15673	15668	0.000	0.029
40	13460	13506	13506	13500	0.000	0.071
0	13528	14271	13885	13728	1.080	0.521
0	9844	10583	10191	10011	1.130	0.519
0	14475	15241	14843	14652	1.080	0.519
0	14480	15225	14834	14646	1.105	0.531
0	13540	14321	13915	13720	1.083	0.520

Temperature: 1023 K
Particle size: 1.8 mm
Initial moisture content: 1.1 g/g dry coal
Fluidizing velocity: 0.5 m/s
Estimated Biot number: 1.2
Condition: Pyrolysis

Time (s)	Cruc. wt. (mg)	Cruc. + smpl. wt. (mg)	Cruc. + dry smpl. wt. (mg)	Cruc. + dev. smpl. wet (mg)	Moist. (g/g dry coal)	Vols. (g/g dry coal)
5	9843	10140	10068	9949	0.334	0.529
5	15618	15893	15836	15725	0.262	0.509
5	9988	10288	10121	10102	0.329	0.491
5	13943	14245	13187	13118	0.282	0.521
5	15266	15652	15572	15416	0.262	0.510
10	14260	14429	14418	14342	0.066	0.455
10	14054	14253	14239	14140	0.080	0.535
10	13255	13344	13342	13300	0.022	0.458
10	13975	14031	14029	14004	0.034	0.423
10	10284	10333	10332	10308	0.020	0.491
15	14381	14486	14486	14446	0.000	0.182
15	13536	13635	13635	13613	0.000	0.140
15	12965	13059	13059	13035	0.000	0.168
15	14262	14704	14704	14690	0.000	0.181
15	10409	10581	10581	10541	0.000	0.149
0	14053	14808	14416	14227	1.080	0.521
0	15265	16005	15611	15435	1.138	0.508
0	13248	14076	13650	13453	1.059	0.490
0	11220	11993	11582	11398	1.138	0.508
0	12961	13691	13312	13130	1.080	0.518

Temperature: 823 K
Particle size: 10 mm
Initial moisture content: 1.1 g moist./g dry coal
Fluidizing velocity: 4.2 m/s
Estimated Biot number: 4.2
Condition: combustion
1) yellow flame
2) white flame

Time	Cruc. wt	Cruc. + smpl. wt	Cruc. + dry smpl. wt	Cruc. + dev. smpl.wt	Moist.	Vols.	t_i
(sec)	(mg)	(mg)	(mg)	(mg)	(g/g dry coal)	(g/g dry coal)	(s)
10	10473	11038	10775	10620	0.855	0.513	-
10	9836	10306	10090	9957	0.853	0.524	-
10	10563	11279	10952	10748	0.845	0.524	-
10	10478	10860	10851	10574	0.945	0.522	-
10	10935	11649	11313	11113	0.902	0.530	-
20	10560	10974	10794	10672	0.768	0.521	-
20	10563	11166	10902	10729	0.760	0.510	-
20	10932	11466	11229	11386	0.849	0.528	-
20	11203	11771	11526	11361	0.741	0.510	-
20	10927	11538	11278	11140	0.783	0.530	-
30	9834	10186	10051	9936	0.632	0.530	-
30	10474	10934	10760	10617	0.582	0.500	-
30	9835	10436	10207	10009	0.629	0.532	-
30	11200	11603	11449	11318	0.623	0.525	-
30	9836	10197	10059	9944	0.611	0.515	-
40	10560	10894	10844	10710	0.519	0.427	-
40	11201	11646	11486	11353	0.503	0.418	-
40	10928	11178	11086	11013	0.517	0.411	-
40	10473	10891	10739	10616	0.508	0.411	-
40	10556	10886	10766	10667	0.516	0.426	-
50	10465	10640	10584	10530	0.412	0.397	-

50	10568	10727	10676	10627	0.413	0.397	-
50	9836	10122	10042	9947	0.344	0.409	-
50	11200	11405	11376	11297	0.343	0.389	-
50	10560	10972	10844	10710	0.407	0.427	-
60	10926	11062	11026	10986	0.287	0.319	-
60	10473	10627	10582	10556	0.259	0.449	-
60	10567	10773	10716	10657	0.302	0.313	-
60	9840	9996	9955	9901	0.321	0.423	-
60	11195	11448	11380	11291	0.338	0.443	-
70	9960	10067	10037	10011	0.281	0.243	-
70	10481	10557	10536	10518	0.272	0.232	-
70	11811	11913	11890	11838	0.207	0.241	-
70	10932	11074	11039	11005	0.229	0.222	-
70	9840	9957	9929	9901	0.219	0.219	-
80	11199	11280	11280	11261	0.000	0.146	72
80	10563	10659	10659	10639	0.000	0.126	75
80	10431	10490	10490	10479	0.000	0.110	74
80	10934	11275	11256	11192	0.035	0.118	77
80	10570	10645	10642	10626	0.025	0.137	75
90	11199	11279	11279	11272	0.000	0.045	77
90	10954	10978	10978	10977	0.000	0.021	74
90	10572	10616	10616	10611	0.000	0.061	76
90	10468	10495	10495	10492	0.000	0.059	79
90	9839	9899	9899	9892	0.000	0.063	77
0	11194	11902	11561	11367	0.930	0.528	-
0	10462	11150	10806	10627	1.000	0.520	-
0	10559	11294	10909	10724	1.100	0.528	-
0	9836	10565	10183	10005	1.100	0.512	-
0	10927	11706	11315	11113	1.010	0.524	-

Temperature: 923 K
Particle size: 10 mm
Initial moisture content: 1.1 g moist./g dry coal
Fluidizing velocity: 4.2 m/s
Estimated Biot number: 4.3
Condition: combustion
1) yellow flame
2) white flame

Time (sec)	Cruc. wt (mg)	Cruc. + smpl. wt (mg)	Cruc. + dry smpl. wt (mg)	Cruc. + dev. smpl.wt (mg)	Moist. (g/g dry coal)	Vols. (g/g dry coal)	t_i (s)
5	11046	11645	11363	11193	0.92	0.54	-
5	11039	11728	11389	11210	0.95	0.51	-
5	10078	10529	10314	10425	0.99	0.33	-
5	11183	11783	11489	11324	0.99	0.54	-
5	10616	11232	10938	10767	0.93	0.53	-
10	11840	12220	12056	11942	0.77	0.53	-
10	11186	11600	11412	11297	0.81	0.51	-
10	11122	11547	11361	11237	0.77	0.52	-
10	10079	10716	10427	10243	0.84	0.53	
10	10070	10709	10519	10234	0.84	0.53	-
20	10082	10559	10344	10205	0.84	0.53	-
20	11838	12132	12024	11920	0.63	0.51	-
20	10623	11030	10865	10384	0.70	0.50	-
20	11123	11537	11368	11238	0.70	0.53	-
20	11121	11627	11415	11259	0.73	0.53	-
30	11121	11574	11402	11258	0.60	0.50	-
30	11122	11346	11256	11192	0.61	0.44	-
30	11041	11528	11320	11189	0.67	0.42	-
30	11838	12201	12053	11941	0.69	0.52	-
30	11180	11531	11394	11283	0.64	0.52	-
40	11196	11596	11459	11343	0.45	0.38	-

40	10623	10883	10801	10719	0.41	0.41	-
40	11838	11240	12106	11978	0.46	0.44	-
40	11037	11289	11204	11122	0.48	0.46	-
40	11037	11270	11189	11118	0.48	0.42	-
50	10625	11002	10909	10780	0.29	0.40	-
50	10075	10686	10527	10315	0.32	0.42	47
50	11188	11354	11319	11267	0.21	0.31	49
50	10616	10805	10764	10702	0.23	0.34	48
50	11829	11986	11948	11898	0.26	0.35	47
60							52
60							50
60							52
60							52
60							50
70							48
70							51
70							50
70							47
70							51
60	9859	10015	10015	9986	0.00	0.11	
70	10939	11143	11143	11129	0.00	0.04	
0	10074	10784	10406	10230	1.14	0.53	-
0	11832	12541	12173	11999	1.08	0.51	-
0	10624	11401	10994	10802	1.10	0.52	-
0	10079	10829	10438	10248	1.09	0.53	-
0	11014	11748	11360	11180	1.12	0.52	-

Temperature: 923 K

Particle size: 10 mm

Initial moisture content: 0.47 g moist./g dry coal

Fluidizing velocity: 4.2 m/s

Estimated Biot number: 4.3

Condition: combustion

1) white flame

2) yellow flame

Time	Cruc. wt	Cruc. + smpl. wt	Cruc. + dry smpl. wt	Cruc. + dev. smpl.wt	Moist.	Vols.	t_i
(sec)	(mg)	(mg)	(mg)	(mg)	(g/g dry coal)	(g/g dry coal)	(s)
5	10979	11507	11356	11157	0.42	0.528	-
5	10559	11025	10900	10722	0.38	0.5226	-
5	10961	11486	11327	11137	0.44	0.519	-
5	10547	11026	10882	10621	0.44	0.510	-
5	10955	11387	11259	11101	0.43	0.520	-
10	10563	11003	10904	10727	0.29	0.519	-
10	10414	10764	10688	10541	0.29	0.536	-
10	10406	10872	10751	10572	0.36	0.519	-
10	10396	10832	10737	10563	0.28	0.510	-
10	10449	10877	10778	10610	0.30	0.510	-
20	10552	10705	10689	10628	0.10	0.396	-
20	10970	11319	11274	11131	0.14	0.437	19
20	10554	10893	10844	10700	0.17	0.486	-
20	10532	10828	10794	10665	0.13	0.478	-
20	10528	10869	10817	10684	0.16	0.420	-
25	10503	10665	10665	10647	0.00	0.062	22
25	10552	10689	10689	10676	0.00	0.052	22
25	10458	10672	10672	10646	0.00	0.068	21
25	10421	10650	10650	10630	0.00	0.047	19
25	10543	10763	10763	10741	0.00	0.055	22
30	10465	10700	10700	10686	0.00	0.031	19

30	10539	10751	10751	10740	0.00	0.027	20
30	10449	10625	10625	10613	0.00	0.036	22
30	10961	11138	11138	11129	0.00	0.026	20
30	10002	10127	10127	10120	0.00	0.029	20
0	10543	11046	10889	10709	0.45	0.520	-
0	10386	10931	10764	10571	0.44	0.510	-
0	10527	11009	10854	10654	10681	0.47	-
0	10451	10973	10807	10620	0.49	0.525	-
0	10955	11435	11314	11131	0.48	0.510	-

Temperature: 1023 K
Particle size: 10 mm
Initial moisture content: 1.1 g moist./g dry coal
Fluidizing velocity: 4.2 m/s
Estimated Biot number: 4.4
Condition: combustion
1) white flame
2) yellow flame

Time	Cruc. wt	Cruc. + smpl. wt	Cruc. + dry smpl. wt	Cruc. + dev. smpl.wt	Moist.	Vols.	t_i
(sec)	(mg)	(mg)	(mg)	(mg)	(g/g dry coal)	(g/g dry coal)	(s)
5	10941	11407	11179	11058	0.94	0.50	-
5	10937	11379	11165	11044	0.96	0.54	-
5	10938	11333	11145	11037	0.91	0.52	-
5	10938	11384	11167	11050	0.93	0.50	-
5	10172	10456	10172	10021	0.90	0.48	-
10	11828	12245	12061	11944	0.76	0.48	-
10	10465	10838	10667	10560	0.86	0.54	-
10	11822	12201	12029	11927	0.79	0.47	-
10	10027	10414	10241	10236	0.80	0.46	-
10	10941	11310	11182	11054	0.54	0.54	-
20	9873	10119	10022	9952	0.59	0.43	-
20	11826	12361	12141	11987	0.66	0.46	-
20	9864	10435	10206	10034	0.65	0.48	-
20	11826	12216	12067	11949	0.58	0.46	-
20	10470	10779	10661	10565	0.60	0.48	-
25	9974	10254	10148	10070	0.53	0.39	-
20	10465	10745	10646	10562	0.49	0.42	-
20	9977	10313	10194	10093	0.49	0.42	-
20	11826	12010	11946	11888	0.50	0.45	-
20	11823	12167	12047	11936	0.51	0.47	-
25	10473	10778	10678	10582	0.44	0.42	-

25	10939	11174	11100	11021	0.43	0.46	-
25	9871	10273	10140	10006	0.47	0.48	-
25	9982	10249	10154	10075	0.49	0.41	-
25	9980	10254	10159	10064	0.54	0.40	-
35	9868	10110	10065	9976	0.20	0.40	-
35	9977	10128	10096	10050	0.21	0.30	-
35	10466	10682	10651	10572	0.14	0.36	-
35	9980	10296	10244	10122	0.18	0.41	-
35	10936	11110	11076	11024	0.19	0.28	-
40	9981	10111	10104	10063	0.04	0.24	35
40	11829	11952	11944	11898	0.06	0.32	37
40	10466	10630	10621	10562	0.05	0.30	36
40	11826	12008	11990	11931	0.08	0.27	35
40	9867	10046	10031	9969	0.07	0.29	36
50							37
50							36
50							37
50							35
50							37
50	9978	10266	10266	10230	0.00	0.07	
50	11818	12036	12036	12008	0.00	0.07	
0	10467	11164	10799	10626	1.10	0.52	-
0	10461	11208	10807	10620	1.16	0.54	
0	10936	11583	11253	11091	1.04	0.51	-
0	10244	10658	10244	10045	1.08	0.52	-
0	11821	12576	12177	11995	1.12	0.51	-

Temperature: 923 K
Particle size: 5 mm
Initial moisture content: 1.1 g moist./g dry coal
Fluidizing velocity: 1.2 m/s
Estimated Biot number: 2.1
Condition: combustion
1) yellow flame
2) white flame

Time (sec)	Cruc. wt (mg)	Cruc. + smpl. wt (mg)	Cruc. + dry smpl. wt (mg)	Cruc. + dev. smpl.wt (mg)	Moist. (g/g dry coal)	Vols. (g/g dry coal)	t_i (s)
10	10516	11061	10831	10667	0.75	0.53	-
10	10523	10814	10681	10600	0.85	0.52	-
10	10427	10665	10562	10492	0.78	0.53	-
10	10502	10819	10683	10593	0.73	0.49	-
10	10413	10843	10656	10532	0.77	0.51	-
15	10452	10642	10565	10507	0.69	0.52	-
15	10530	10812	10705	10612	0.64	0.52	-
15	10530	10781	10681	10607	0.64	0.47	-
15	10947	11322	11180	11060	0.62	0.52	-
15	10382	10723	10590	10478	0.68	0.54	-
20	10947	11393	11284	11119	0.31	0.47	-
20	10542	11003	10889	10729	0.30	0.42	-
20	10421	10944	10797	10608	0.39	0.50	-
20	10411	10547	10508	10459	0.40	0.50	-
20	10513	10745	10680	10605	0.35	0.40	-
30	10379	10826	10558	10579	0.29	0.45	-
30	10952	11321	11264	11117	0.17	0.44	-
30	10385	10710	10660	10524	0.18	0.48	-
30	10370	10742	10636	10508	0.28	0.45	-
30	10908	11083	11053	10988	0.18	0.40	-
40	10523	10905	10859	10716	0.12	0.36	28

40	10544	10744	10733	10682	0.04	0.18	29
40	10516	10617	10612	10576	0.04	0.29	30
40	10909	10985	10969	10957	0.16	0.12	-
40	10512	10682	10669	10612	0.06	0.28	28
45	10011	10063	10063	10039	0.0	0.04	33
45	10380	10424	10424	10421	0.0	0.04	31
45	10922	10979	10979	10974	0.0	0.05	33
45	10516	10582	10582	10577	0.0	0.04	32
45	10952	11036	11036	11028	0.0	0.05	33
0	10423	10872	10625	10532	1.12	0.50	-
0	10371	10846	10604	10483	1.04	0.52	-
0	10911	11350	11115	11011	1.15	0.51	-
0	10518	11053	10775	10641	1.08	0.52	-
0	10423	10961	10684	10554	1.06	0.5	-

Temperature: 823 K
Particle size: 1.8 mm
Initial moisture content: 1.1 g moist./g dry coal
Fluidizing velocity: 0.5 m/s
Estimated Biot number: 1.1
Condition: combustion
1) yellow flame
2) white flame

Time (sec)	Cruc. wt (mg)	Cruc. + smpl. wt (mg)	Cruc. + dry smpl. wt (mg)	Cruc. + dev. smpl.wt (mg)	Moist. (g/g dry coal)	Vols. (g/g dry coal)	t_i (s)
2.5	10267	10894	10608	10427	0.85	0.53	-
2.5	10245	10750	10532	10391	0.71	0.46	-
2.5	11411	11948	11729	11564	0.66	0.51	-
2.5	9690	10144	9954	9814	0.73	0.53	-
2.5	10422	10963	10733	10565	0.76	0.55	-
7.5	10441	10777	10688	10558	0.36	0.53	-
7.5	11453	11875	11729	11580	0.55	0.55	-
7.5	9929	10362	10220	10080	0.45	0.44	-
7.5	10074	10517	10382	10222	0.43	0.51	-
7.5	10452	10875	10720	10589	0.54	0.45	-
10	11428	11598	11554	11490	0.34	0.51	-
10	10271	10523	10455	10356	0.38	0.54	-
10	9704	9864	9835	9767	0.22	0.52	-
10	10419	10563	10538	10475	0.21	0.53	-
10	10443	10528	10515	10475	0.19	0.54	-
12.5	10441	10810	10743	10589	0.15	0.49	-
12.5	10422	10573	10704	10555	0.17	0.53	-
12.5	9707	9947	9944	9830	0.12	0.44	-
12.5	11425	11686	11684	11549	0.11	0.52	-
12.5	10266	10588	10550	10405	0.13	0.49	-
14	10444	10535	10534	10498	0.01	0.32	-

14	10036	10087	10115	10103	0.0	0.29	-
14	9920	10130	10130	10042	0.0	0.34	-
14	11437	11570	11570	11537	0.0	0.26	-
14	10423	10628	10630	10548	0.0	0.31	-
15	10253	10303	10303	10296	0.0	0.08	14
15	11417	11455	11455	11443	0.0	0.22	13
15	9693	9734	9734	9723	0.0	0.17	13
15	10410	10466	10466	10453	0.0	0.14	13
15	10441	10484	10484	10469	0.0	0.25	13
0	10427	11117	10763	10753	1.05	0.51	-
0	11436	12216	11802	11604	1.13	0.54	-
0	10280	11212	10718	10490	1.11	0.52	-
0	9713	10477	10076	9884	1.10	0.53	-
0	10450	11280	10839	10633	1.13	0.53	-

Temperature: 923 K

Particle size: 1.8 mm

Initial moisture content: 1.1 g moist./g dry coal

Fluidizing velocity: 0.5 m/s

Estimated Biot number: 1.1

Condition: combustion

1) yellow flame

2) white flame

Time (sec)	Cruc. wt (mg)	Cruc. + smpl. wt (mg)	Cruc. + dry smpl. wt (mg)	Cruc. + dev. smpl.wt (mg)	Moist. (g/g dry coal)	Vols. (g/g dry coal)	t_i (s)
5	9940	10358	10215	10080	0.48	0.45	-
5	10084	10486	10323	10199	0.67	0.51	-
5	10466	10671	10596	10526	0.59	0.54	-
5	11461	11952	11680	11570	0.59	0.47	-
5	10458	10646	10580	10510	0.60	0.53	-
7.5	10464	10570	10544	10507	0.28	0.40	-
7.5	11477	11590	11558	11515	0.40	0.53	-
7.5	10476	10702	10630	10548	0.47	0.54	-
7.5	10104	10334	10277	10196	0.29	0.41	-
7.5	9974	10269	10180	10085	0.38	0.40	-
10	10467	10771	10471	10607	0.09	0.46	-
10	11482	11561	11548	11517	0.18	0.42	-
10	10481	10653	10632	10566	0.12	0.37	-
10	10108	10217	10204	10160	0.12	0.40	-
10	9968	10167	10147	10070	0.09	0.36	-
12.5	9970	9992	9992	9988	0.0	0.10	8
12.5	10104	10142	10142	10138	0.0	0.06	9
12.5	10469	10518	10518	10509	0.0	0.11	9
12.5	10470	10516	10516	10508	0.0	0.10	8
12.5	10467	10504	10504	10499	0.0	0.07	9
0	9995	10605	10287	10135	1.09	0.52	-

0	10509	11117	10800	10649	1.09	0.52	-
0	10115	10794	10446	10266	1.05	0.54	-
0	11731	12371	12041	11878	1.07	0.53	-
0	10302	10974	10629	10453	1.06	0.54	-

Temperature: 923 K
Particle size: 1.8 mm
Initial moisture content: 0.59 g moist./g dry coal
Fluidizing velocity: 0.5 m/s
Estimated Biot number: 1.1
Condition: combustion
1) white flame
2) yellow flame

Time (sec)	Cruc. wt (mg)	Cruc. + smpl. wt (mg)	Cruc. + dry smpl. wt (mg)	Cruc. + dev. smpl.wt (mg)	Moist. (g/g dry coal)	Vols. (g/g dry coal)	t_i (s)
2.5	10480	10830	10782	10626	0.16	0.52	-
2.5	9981	10304	10269	10113	0.13	0.54	-
2.5	10114	10532	10472	10285	0.17	0.52	-
2.5	11711	11989	11951	11824	0.16	0.53	-
2.5	10267	10543	10511	10389	0.12	0.52	-
5	10469	10620	10620	10569	0.0	0.24	-
5	10266	10478	10474	10386	0.02	0.35	-
5	11693	11898	11894	11813	0.02	0.32	-
5	10105	10332	10332	10240	0.0	0.32	-
5	9974	10137	10137	10003	0.0	0.28	-
7.5	9973	10020	10020	10016	0.0	0.04	6
7.5	10105	10152	10152	10151	0.0	0.01	6
7.5	11693	11730	11730	11729	0.0	0.01	6
7.5	10264	10327	10327	10326	0.0	0.01	6
7.5	10468	10494	10494	10493	0.0	0.02	6
0	10004	10521	10317	10152	0.68	0.53	-
0	10510	11022	10830	10665	0.60	0.52	-
0	10141	10652	10471	10293	0.55	0.54	-
0	11747	12284	12098	11914	0.53	0.53	-
0	10303	10840	10641	10466	0.59	0.52	-

Temperature: 923 K
Particle size: 1.8 mm
Initial moisture content: 0.0 g moist./g dry coal
Fluidizing velocity: 0.5 m/s
Estimated Biot number: 1.1
Condition: combustion
1) white flame
2) yellow flame

Time (sec)	Cruc. wt (mg)	Cruc. + dry smpl. wt (mg)	Cruc. + dev. smpl.wt (mg)	Vols. (g/g dry coal)	t_i (s)
2.5	10285	10612	10491	0.37	-
2.5	11729	12179	12071	0.38	-
2.5	10112	10514	10346	0.42	-
2.5	10495	10844	10677	0.48	-
2.5	9983	10312	10168	0.44	-
5	11716	12005	11990	0.05	4
5	10496	10667	10660	0.04	4
5	9980	10107	10096	0.09	4
5	10112	10169	10166	0.06	4
5	10280	10399	10392	0.06	4
0	10276	10788	10518	0.53	-
0	11717	12161	11927	0.53	-
0	10118	10642	10364	0.53	-
0	9983	10594	10273	0.52	-
0	10476	10991	10717	0.53	-

Temperature: 1023 K
Particle size: 1.8 mm
Initial moisture content: 1.1 g moist./g dry coal
Fluidizing velocity: 0.5 m/s
Estimated Biot number: 1.2
Condition: combustion
1) white flame
2) yellow flame

Time (sec)	Cruc. wt (mg)	Cruc. + smpl. wt (mg)	Cruc. + dry smpl. wt (mg)	Cruc. + dev. smpl.wt (mg)	Moist. (g/g dry coal)	Vols. (g/g dry coal)	t_i (s)
2.5	10420	10789	10645	10532	0.61	0.48	-
2.5	10260	10679	10509	10383	0.65	0.48	-
2.5	10425	10867	10710	10562	0.54	0.51	-
2.5	11420	11880	11714	11557	0.57	0.54	-
2.5	9699	10031	9912	9799	0.56	0.53	-
5	10431	10896	10746	10588	0.45	0.48	-
5	11420	11823	11712	11557	0.38	0.53	-
5	9701	10135	10029	9858	0.32	0.51	-
5	10260	10659	10553	10398	0.36	0.53	-
5	10422	10823	10719	10565	0.34	0.51	-
7.5	10413	10553	10528	10468	0.22	0.52	7
7.5	10247	10470	10427	10341	0.22	0.43	7
7.5	11404	11691	11639	11533	0.19	0.39	7.5
7.5	10411	10610	10656	10518	0.20	0.40	7.5
7.5	9689	9926	9870	9799	0.24	0.39	7.5
10	9669	9817	9817	9769	0.0	0.13	7.5
10	10249	10370	10370	10356	0.0	0.06	8
10	10413	10516	10516	10505	0.0	0.06	7
10	10409	10497	10497	10488	0.0	0.05	7
10	11403	11546	11546	11520	0.0	0.11	7.5
0	9692	10248	9973	9827	0.98	0.52	-

0	11409	12165	11776	11585	1.06	0.52	-
0	10411	11347	10855	10620	1.10	0.53	-
0	10252	11089	10643	10436	1.14	0.53	-
0	10417	11208	10799	10593	1.07	0.54	-

SHRINKAGE EXPERIMENTS

Temperature: 423 K

Particle size: 10 mm

Initial moisture content: 1.1 g moist./g dry coal

Fluidizing velocity: 4.2 m/s

Condition: pyrolysis

estimation of shrinkage

Time (sec)	Cruc. wt (mg)	Cruc. + smpl. wt (mg)	Cruc. + dry smpl. wt (mg)	Cruc. + dev. smpl.wt (mg)	Moist. (g/g dry coal)	Vols. (g/g dry coal)	d (mm)
100	15194	15637	15461	15322	0.660	0.52	9.8
100	15274	15773	15559	15408	0.750	0.529	9.7
300	14307	14771	14608	14452	0.542	0.518	9.6
300	13642	14124	13953	13789	0.549	0.527	9.6
800	14372	14709	14649	14505	0.216	0.52	9.2
800	11887	12266	12201	12038	0.207	0.52	9.2
1200*	13794	14047	14026	13905	0.09	0.52	8.8
1200	10973	11338	11317	11137	0.06	0.523	8.9
1500*	14725	14875	14870	14796	0.03	0.51	7.8
1500*	13700	13950	13945	13818	0.02	0.52	8.2
0	9013	9622	9303	9150	1.1	0.527	10.
0	10422	11094	10747	10578	1.069	0.52	10.

* fractured

Temperature: 823 K
Particle size: 10 mm
Initial moisture content: 1.1 g moist./g dry coal
Fluidizing velocity: 4.2 m/s
Condition: pyrolysis
estimation of shrinkage

Time (sec)	Cruc. wt (mg)	Cruc. + smpl. wt (mg)	Cruc. + dry smpl. wt (mg)	Cruc. + dev. smpl.wt (mg)	Moist. (g/g dry coal)	Vols. (g/g dry coal)	d (mm)
20	10721	11218	11015	10862	0.690	0.520	9.9
20	9934	10474	10246	10090	0.700	0.479	9.8
40	12869	13356	13185	13021	0.539	0.517	9.6
40	13255	13677	13540	13392	0.479	0.517	9.5
60	15010	15430	15296	15150	0.458	0.500	9.2
60	14605	14995	14884	14739	0.397	0.518	9.3
90	15024	15403	15325	15169	0.258	0.515	8.9
90	15106	15385	15333	15220	0.218	0.475	8.8
120	13066	13309	13279	13188	0.118	0.357	8.4
120	15346	15562	15546	15450	0.074	0.442	8.5
0	11309	11980	11623	11460	1.136	0.52	10.
0	10274	10891	10571	10416	1.077	0.522	10.

Temperature: 1023 K
Particle size: 10 mm
Initial moisture content: 1.1 g moist./g dry coal
Fluidizing velocity: 4.2 m/s
Condition: pyrolysis
estimation of shrinkage

Time (sec)	Cruc. wt (mg)	Cruc. + smpl. wt (mg)	Cruc. + dry smpl. wt (mg)	Cruc. + dev. smpl.wt (mg)	Moist. (g/g dry coal)	Vols. (g/g dry coal)	d (mm)
20	13909	14403	14195	14047	0.722	0.514	9.7
20	14959	15481	15268	15102	0.713	0.530	9.6
40	9983	10364	10244	10119	0.423	0.440	9.2
40	10941	11356	11218	11078	0.482	0.489	9.2
60	9446	9762	9680	9565	0.330	0.463	9.0
60	13305	13637	13553	13441	0.296	0.394	8.9
80	14129	14357	14327	14243	0.126	0.353	8.7
80	14243	14484	14464	14376	0.072	0.317	8.8
100	15139	15338	15339	15261	0.0	0.306	8.5
100	14877	15087	15087	15008	0.0	0.289	8.6
0	13726	14404	14045	13917	1.12	0.52	10.
0	12551	13187	12857	12697	1.08	0.522	10.

Temperature: 423 K

Particle size: 5 mm

Initial moisture content: 1.1 g moist./g dry coal

Fluidizing velocity: 1.2 m/s

Condition: pyrolysis
estimation of shrinkage

Time (sec)	Cruc. wt (mg)	Cruc. + smpl. wt (mg)	Cruc. + dry smpl. wt (mg)	Cruc. + dev. smpl.wt (mg)	Moist. (g/g dry coal)	Vols. (g/g dry coal)	d (mm)
30	13794	14233	13929	13914	0.76	0.52	4.9 4.9 4.9 4.9 4.9 4.9
60	14262	14580	14509	14381	0.287	0.52	4.8 4.7 4.8 4.8 4.9 4.7
90	12302	12635	12585	12438	0.180	0.52	4.7 4.6 4.7 4.7 4.7 4.6 4.6
120*	14631	14881	14859	14738	0.096	0.53	4.6 4.7 4.6 4.5 4.4 4.5
180*	13700	13878	13873	13785	0.03	0.51	4.5 4.6
0	15192	15793	15524	15055	1.10	0.52	5.0

*fractured

Temperature: 823 K

Particle size: 5 mm

Initial moisture content: 1.1 g moist./g dry coal

Fluidizing velocity: 1.2 m/s

Condition: pyrolysis
estimation of shrinkage

Time (sec)	Cruc. wt (mg)	Cruc. + smpl. wt (mg)	Cruc. + dry smpl. wt (mg)	Cruc. + dev. smpl.wt (mg)	Moist. (g/g dry coal)	Vols. (g/g dry coal)	d (mm)
10	14127	14342	14244	14183	0.838	0.522	5.0 4.9 4.9 4.9 4.8
20	13698	13989	13879	13787	0.592	0.495	4.7 4.7 4.7 4.7 4.7
40	15145	15447	15380	15260	0.279	0.500	4.6 4.6 4.6 4.7 4.5 4.5
60	13847	13972	13963	13909	0.070	0.417	4.4 4.5 4.5 4.5
0	14878	15472	15162	15014	1.09	0.521	5.0

Temperature: 1023 K

Particle size: 5 mm

Initial moisture content: 1.1 g moist./g dry coal

Fluidizing velocity: 1.2 m/s

Condition: pyrolysis

estimation of shrinkage

Time (sec)	Cruc. wt (mg)	Cruc. + smpl. wt (mg)	Cruc. + dry smpl. wt (mg)	Cruc. + dev. smpl.wt (mg)	Moist. (g/g dry coal)	Vols. (g/g dry coal)	d (mm)
10	12553	12995	12828	12687	0.592	0.500	4.9 5.0 5.9 4.9 4.9 4.9 5.0
20	14963	15265	15198	15080	0.272	0.479	4.7 4.8 4.9 4.8 4.8 4.7 4.9
30*	13914	14092	14082	14005	0.052	0.402	4.7 4.8 4.7 4.7 4.7 4.7
40*	13730	13869	13869	13811	0.0	0.340	4.5 4.6 4.5
0	12552	13211	12866	12701	1.10	0.525	5.0

*fractured

VOLATILE SPECIES EVOLUTION EXPERIMENTS

Temperature: 623 K

Particle size: 5 mm

Initial moisture content: 0.0 g/g dry coal

Flow rate: 2.2 l/min.

Conditions: Pyrolysis

Response factors: CO_2 0.92

time	Column 2	
(min.)	CO_2	CO_2*f
00:30	0.243	0.223
00:30	0.242	0.220
00:40	0.375	0.345
00:50	0.420	0.386
1:00	0.444	0.408
2:00	0.180	0.166
2:00	0.179	0.164
2:30	0.116	0.107
2:30	0.128	0.118
3:00	0.134	0.123
4:00	0.126	0.116
5:00	0.054	0.049
6:00	0.062	0.057

Temperature: 623 K
Particle size: 5 mm
Initial moisture content: 1.1 g/g dry coal
Flow rate: 2.2 l/min.
Conditions: Pyrolysis
Response factors: CO_2 0.92

time	Column 2	
(min.)	CO_2	CO_2*f
4:00	0.186	0.171
4:00	0.237	0.218
4:40	0.464	0.427
5:00	0.856	0.787
5:20	0.489	0.449
6:00	0.135	0.124
6:00	0.105	0.097
8:00	0.115	0.124
8:00	0.079	0.073

Temperature: 773 K
Particle size: 5 mm
Initial moisture content: 0.0 g/g dry coal
Flow rate: 2.2 l/min.
Conditions: Pyrolysis
Response factors: CO_2 0.9
CH_4 1.15
C_2H_4 1.0
C_2H_6 0.94

time	Column 1	
(min.)	CH_4	CH_4*f
00:30	0.2	0.23
00:30	0.2	0.23
1:00	0.44	0.51
1:00	0.45	0.52
1:30	0.27	0.31
1:30	0.25	0.29
2:00	0.09	0.10
2:00	0.08	0.09
2:30	0.11	0.13
2:30	0.12	0.14
3:00	0.08	0.09
3:00	0.09	0.10
3:30	0.07	0.078
3:30	0.07	0.08
4:00	0.06	0.07
4:00	0.05	0.06
4:30	0.05	0.06
4:30	0.05	0.06
5:00	0.05	0.06
5:00	0.05	0.06
5:30	0.05	0.06
5:30	0.03	0.03

6:00	0.02	0.02
6:00	0.03	0.03

time			Column 2			
(min.)	CO_2	CO_2*f	C_2H_4	C_2H_4*f	C_2H_6	C_2H_6*f
00:30	1.269	1.142	0.004	0.004	0.005	0.005
00:30	1.323	1.191	0.003	0.003	0.003	0.003
1:00	1.316	1.184	0.01	0.01	0.01	0.009
1:00	1.367	1.23	0.008	0.008	0.009	0.008
1:30	0.668	0.601	0.01	0.01	0.011	0.010
1:30	0.686	0.617	0.09	0.09	0.01	0.009
2:00	0.261	0.235	0.003	0.003	0.002	0.002
2:00	0.247	0.222	0.003	0.003	-	-
2:30	0.243	0.219	0.005	0.005	0.006	0.006
2:30	0.250	0.225	0.003	0.003	0.003	0.003
3:00	0.154	0.139	0.002	0.002	0.003	0.003
3:00	0.165	0.149	0.003	0.003	0.003	0.003
3:30	0.137	0.123	0.002	0.002	0.003	0.003
3:30	0.129	0.116	0.002	0.002	0.002	0.002
4:00	0.093	0.084	0.001	0.001	0.003	0.003
4:00	0.089	0.080	-	-	-	-
4:30	0.085	0.077	0.002	0.002	-	-
4:30	0.092	0.083	0.002	0.002	-	-
5:00	0.078	0.070	-	-	0.001	0.001
5:00	0.077	0.069	-	-	-	-
5:30	0.072	0.065	-	-	-	-
5:30	0.088	0.079	-	-	-	-
6:00	0.063	0.057	-	-	-	-
6:00	0.076	0.068	-	-	-	-

Temperature: 773 K
Particle size: 5 mm
Initial moisture content: 1.1 g/g dry coal
Flow rate: 2.2 l/min.
Conditions: Pyrolysis

Response factors:		
	CO_2	0.92
	CH_4	1.15
	C_2H_4	1.0
	C_2H_6	0.94

time	Column 1	
(min.)	CH_4	CH_4*f
3:00	0.056	0.064
3:20	0.024	0.028
3:40	0.028	0.032
4:00	0.023	0.026
4:30	0.019	0.022
5:10	0.013	0.015
5:30	0.011	0.012

time	Column 2					
(min.)	CO_2	CO_2*f	C_2H_4	C_2H_4*f	C_2H_6	C_2H_6*f
2:00	0.209	0.192	-	-	-	-
3:00	0.850	0.640	0.03	0.03	-	-
3:20	0.32	0.28	0.021	0.021	0.029	0.027
3:40	0.203	0.178	0.005	0.005	0.026	0.024
4:00	0.129	0.11	0.005	0.005	0.008	0.008
4:30	0.097	0.085	0.003	0.003	0.006	0.0056
5:10	0.072	0.063	0.003	0.003	0.004	0.0037
5:30	0.051	0.044	0.002	0.002	0.003	0.0028
6:00	0.18	0.16	-	-	-	-
6:00	0.16	0.14	-	-	-	-

Temperature: 873 K
Particle size: 5 mm
Initial moisture content: 0.0 g/g dry coal
Flow rate: 2.2 l/min.
Conditions: Pyrolysis

Response factors:		
	CO_2	0.92
	CO	0.96
	CH_4	1.15
	C_2H_4	1.0
	C_2H_6	0.94

time	Column 1			
(min.)	CH_4	CH_4*f	CO	CO*f
00:15	0.021	0.024	0.057	0.055
00:15	0.118	0.136	0.046	0.044
00:25	0.066	0.076	0.188	0.180
00:35	0.063	0.072	0.194	0.186
00:45	0.207	0.238	0.988	0.95
00:45	0.22	0.253	0.99	0.95
00:55	0.232	0.267	0.473	0.454
1:05	0.244	0.281	1.078	1.03
1:10	0.031	0.036	0.35	0.336
1:30	-	-	0.046	0.044

time	Column 2					
(min.)	CO_2	CO_2*f	C_2H_4	C_2H_4*f	C_2H_6	C_2H_6*f
00:10	0.823	0.757	0.003	0.003	0.003	0.0028
00:15	1.12	1.03	0.002	0.002	0.003	0.003
00:15	0.88	0.809	0.001	0.001	0.002	0.002
00:20	0.943	0.8687	0.008	0.008	0.012	0.011
00:25	0.712	0.655	0.009	0.009	0.012	0.012
00:35	0.727	0.669	0.049	0.049	0.063	0.06
00:45	1.831	1.65	0.037	0.037	0.06	0.058
00:55	0.556	0.52	0.041	0.041	0.067	0.064
1:05	0.426	0.392	0.055	0.055	0.077	0.074

1:10	0.059	0.054	-	-	0.002	0.002s

Temperature: 873 K
Particle size: 5 mm
Initial moisture content: 1.1 g/g dry coal
Flow rate: 2.2 l/min.
Conditions: Pyrolysis

Response factors:		
	CO_2	0.92
	CO	0.96
	CH_4	1.15
	C_2H_4	1.0
	C_2H_6	0.94

time	Column 1			
(min.)	CH_4	CH_4*f	CO	CO*f
1:00	-	-	-	-
1:20	-	-	0.032	0.031
1:20	-	-	0.026	0.025
1:30	0.025	0.028	0.077	0.074
1:40	0.041	0.047	0.119	0.114
1:50	0.081	0.093	0.69	0.794
2:00	0.143	0.164	0.297	0.285
2:10	0.35	0.403	0.235	0.226
2:20	0.179	0.206	0.2	0.192
2:30	0.126	0.145	0.082	0.079
3:00	-	-	-	-

time	Column 2					
(min.)	CO_2	CO_2*f	C_2H_4	C_2H_4*f	C_2H_6	C_2H_6*f
1:00	0.394	0.362	0.02	0.02	0.005	0.0047
1:20	0.689	0.634	0.1	0.1	0.016	0.015
1:30	0.927	0.853	0.17	0.17	0.024	0.023
1:40	1.149	1.06	0.12	0.12	0.017	0.016
1:50	1.254	1.154	0.17	0.17	0.025	0.024
2:00	1.515	1.39	0.3	0.3	0.047	0.044
2:10	1.486	1.367	0.22	0.22	0.034	0.032
2:20	0.961	0.88	0.34	0.34	0.055	0.052

2:30	0.29	0.267	0.032	0.032	0.052	0.049
3:00	0.052	0.048	-	-	-	-

Temperature: 873 K
Particle size: 10 mm
Initial moisture content: 0.0 g/g dry coal
Flow rate: 2.2 l/min.
Conditions: Pyrolysis

Response factors:		
	CO_2	0.92
	CO	0.96
	CH_4	1.15
	C_2H_4	1.0
	C_2H_6	0.96

time	Column 1			
(min.)	CH_4	CH_4*f	CO	CO*f
00:30	-	-	-	-
1:00	-	-	0.59	0.57
1:20	0.046	0.053	0.94	0.9
1:40	0.067	0.077	1.29	1.24
2:00	0.088	0.101	1.61	1.55
2:20	0.097	0.11	1.66	1.59
2:40	0.107	0.123	1.36	1.31
3:00	0.102	0.117	1.198	1.14
3:30	0.08	0.092	0.076	0.073
4:00	0.076	0.086	0.053	0.051
4:30	0.057	0.066	-	-
5:00	0.024	0.028	-	-

time	Column 2					
(min.)	CO_2	CO_2*f	C_2H_4	C_2H_4*f	C_2H_6	C_2H_6*f
00:30	0.296	0.272	-	-	-	-
1:00	0.954	0.878	0.005	0.007	0.007	0.007
1:20	1.119	1.029	0.008	0.008	0.011	0.011
1:40	1.2	1.104	0.012	0.012	0.017	0.016
2:00	1.15	1.058	0.015	0.015	0.023	0.022
2:20	0.952	0.876	0.013	0.013	0.021	0.02
2:40	0.897	0.825	0.035	0.035	0.045	0.043

3:00	0.687	0.632	0.014	0.014	0.024	0.023
3:30	0.468	0.431	0.012	0.012	0.02	0.019
3:30	0.384	0.353	0.005	0.005	0.01	0.01
4:00	0.315	0.289	0.009	0.009	0.016	0.0154
4:30	0.255	0.234	0.007	0.007	0.012	0.012
4:30	0.094	0.086	0.003	0.003	0.005	0.005
5:00	0.02	0.018	-	-	-	-

Temperature: 873 K
Particle size: 10 mm
Initial moisture content: 1.1 g/g dry coal
Flow rate: 2.2 l/min.
Conditions: Pyrolysis

Response factors:		
	CO_2	0.92
	CO	0.96
	CH_4	1.15
	C_2H_4	1.0
	C_2H_6	0.96

time	Column 1			
(min.)	CH_4	CH_4*f	CO	CO*f
3:10	0.012	0.014	0.11	0.106
3:30	0.073	0.084	0.34	0.33
3:50	0.055	0.063	0.45	0.43
4:20	0.074	0.085	0.47	0.45
4:40	0.072	0.083	0.43	0.41
5:10	0.052	0.06	0.33	0.317

time	Column 2					
(min.)	CO_2	CO_2*f	C_2H_4	C_2H_4*f	C_2H_6	C_2H_6*f
3:10	0.215	0.198	0.003	0.003	0.004	0.004
3:30	0.343	0.316	0.005	0.005	0.007	0.007
3:50	0.517	0.476	0.019	0.019	0.016	0.015
4:20	0.708	0.651	0.03	0.03	0.041	0.039
4:40	0.335	0.310	0.03	0.03	0.041	0.039
5:10	0.159	0.146	0.009	0.009	0.016	0.015

APENDIX B

PROGRAM NAME: VCFB.FOR

SYSTEM: VAX-VMS (FORTRAN 4.4)

COMMENTS:

This program calculates the volatile combustion of a single coal particle in a fluidized bed. It is assumed, that the coal particle is alternatively in the bubble and emulsion phase. The characteristic frequency describing this particle mobility between phases as well as the relative amounts of time spent in each phase for the bubble emulsion-cycle can be calculated using FREQ.FOR and APQ.FOR respectively. It is assumed that homogeneous ignition takes place when the coal particle is in the bubble phase and approximately 5% of the volatiles are released. The flame temperature has been calculated using a modified Shwab-Zeldovich approach to the fuel droplet problem. The particle temperature can be obtained using unsteady state heat conduction equation and convective boundary condition. The initial condition for the temperature profile for each change of phase is the temperature profile at the end of residence time at the previous phase. Devolatilization is modelled using DAE kinetic model as developed by Anthony and Howard. The order of the Gaussian quadrature is chosen as 36 for all steps. Lower order results in oscillations of the results. The program is interactive and the input parameters are asked when running the program.

```
C*********************************VCFB.FOR************************************
C  FORTRAN PROGRAMM FOR DEVOLATILIZATION AND COMBUSTION OF VOLATILES
C  IN FLUIDIZED BED ASSUMING THAT THE PARTICLE LOCATION CHANGES FROM
C  EMULSION TO BUBBLE PHASE AND VIS VERSA.
C  IGNITION IS ASSUMED TO OCCUR THE FIRST TIME WHEN 5% VOLATILES
C  RELEASED.
C  VOLUME INTEGRATION OF ANTHONY HOWARD KINETICS MODEL
      EXTERNAL FUNC1
       REAL NF1,NF2
      DIMENSION B(15),BFL(15),BVAL(15),RNI(15),RNJ(15)
      COMMON/ABC/ TA,T0,B,RP,ALPA,E0,SIGMA,PI,XL2,XU2,XL3,XU3,RDUM,EDUM
      COMMON/IKAC/ NG2,NG3,BFL
      COMMON/COM/ RNTM,TSTAR,TF,BFO,RNI,RNJ,IW,NF,TS,NC
      COMMON/BIOT/BVAL
      TYPE*,' ENTER AMBIENT TEMPERATURE TA (K)'
      READ*,TA
      DELH=10300
      TYPE*,' ENTER YOA '
      READ*,YOA
      TYPE*,' ENTER CPG '
      READ*,CPG
      F=0.3
      TF=0.95*DELH*F*YOA/CPG+TA
      T0=283.00
      TV2=1000.0
      TE=373.0
      TYPE*,' ENTER BIOT NUMBER BI '
      READ*,BI
      RIF=2.
      CALL BITC(BI)
      DO 999 I=1,15
999   B(I)=BVAL(I)
      BFO=RIF*BI
      CALL BITC(BFO)
      DO 888 I=1,15
888   BFL(I)=BVAL(I)
      TYPE*,' ENTER PARTICLE DIAMETER RP (mm) '
      READ*,RP
      ALPA=0.100
      TYPE*,' ENTER ACTIVATION ENERGY E0 (kJ/mol)'
      READ*,E0
      SIGMA=40.00
      PI=3.14159
      XL1=0.0
      XU1=RP
      NG1=12
      NG2=12
      NG3=12
      XL2=E0 - 3.*SIGMA
      XU2=E0 + 3.*SIGMA
      XL3=0.0
      TYPE*,' ENTER FREQUENCY FOR BUBBLE PHASE '
      READ*,NF1
      TYPE*,' ENTER FREQUENCY FOR EMULSION PHASE '
      READ*,NF2
      TYPE*,' ENTER TIME INTERVAL FOR PYROLYSIS RTM '
      READ*,RTM
      TYPE*,' ENTER TIME FREQUENCY RNTM '
      READ*,RNTM
      TYPE*,' ENTER NUMBER OF INTERVALS BUBBLE PHASE '
```

```
      READ*,BU
      TYPE*,' ENTER NUMBER OF INTERVALS EMULSION PHASE '
      READ*,E
      WRITE(6,5005)RP,BI
      WRITE(7,5005)RP,BI
5005  FORMAT(X,'PARTICLE RADIUS = ',F5.3,'MM',10X,'BIOT NUMBER = ',F6.3)
      WRITE(6,5006)TF,TA
      WRITE(7,5006)TF,TA
5006  FORMAT(X,'FLAME TEMP. = ',F8.3,'K',10X,'BED TEMP. = ',F8.3,'K')
      WRITE(6,5007)E0,SIGMA
      WRITE(7,5007)E0,SIGMA
5007  FORMAT(X,'E0 = ',F8.2,10X,'SIGMA = ',F8.2)
      WRITE(6,2005)
      WRITE(7,2005)
2005  FORMAT(2X,'-------------------------------------------------------')
      WRITE(6,2008)
      WRITE(7,2008)
2008  FORMAT(8X,'TIME(SEC)',7X,'VOL.RETAINED',8X,'TS(K)')
        WRITE(8,1111)BI,RP,E0,TA
        WRITE(8,1112)NF1,NF2,RNTM
1111  FORMAT(X,'BI=',F5.2,5X,'RP=',F5.2,5X,'E0=',F7.2,5X,'TA=',F7.2)
1112  FORMAT(X,'NF1=',F5.2,5X,'NF2=',F5.2,5X,'RNTM=',F7.3)
      WRITE(6,3001)NF1,NF2,RNTM
      WRITE(7,3001)NF1,NF2,RNTM
3001  FORMAT(1X,'NF1= ',F6.4,5X,'NF2= ',F6.4,5X,'RNTM =',F7.3)
        NF=0
        DO 10 I=2,50
       TM=RTM *FLOAT(I-1)
0
       XU3=TM
       IW=2
       CALL CGQA(FUNC1,XL1,XU1,NG1,ANS)
       IW=1
       ANS=3.0*ANS/RP**3
       ADS=1.0-ANS
       R20=RP
       CALL TEMP(TT,TM)
       TS=TT
       WRITE(6,1089)R20,TS
       WRITE(7,1089)R20,TS
       IW=3
       CALL TEMP(TT,TM)
       CALL TEMP(TT,TM)
       T175=TT
       WRITE(6,1089)RDUM,T175
       WRITE(7,1089)RDUM,T175
       IW=4
       CALL TEMP(TT,TM)
       T150=TT
       WRITE(6,1089)RDUM,T150
       WRITE(7,1089)RDUM,T150
       IW=5
       CALL TEMP(TT,TM)
       T125=TT
       WRITE(6,1089)RDUM,T125
       WRITE(7,1089)RDUM,T125
       IW=6
       CALL TEMP(TT,TM)
       T100=TT
       WRITE(6,1089)RDUM,T100
```

```
      WRITE(7,1089)RDUM,T100
      IW=7
      CALL TEMP(TT,TM)
      T075=TT
      WRITE(6,1089)RDUM,T075
      WRITE(7,1089)RDUM,T075
      IW=8
      CALL TEMP(TT,TM)
      T050=TT
      WRITE(6,1089)RDUM,T050
      WRITE(7,1089)RDUM,T050
      IW=9
      CALL TEMP(TT,TM)
      T025=TT
      WRITE(6,1089)RDUM,T025
      WRITE(7,1089)RDUM,T025
      IW=10
      CALL TEMP(TT,TM)
      T001=TT
      WRITE(6,1089)RDUM,T001
      WRITE(7,1089)RDUM,T001
1089  FORMAT(X,'R = ',F5.2,5X,'T = ',F7.2)
       WRITE(8,1113)TM,ANS
1113  FORMAT(2(X,E15.5))
      WRITE(6,2009)TM,ANS,TS
      WRITE(7,2009)TM,ANS,TS
2009  FORMAT(2X,3(2X,E15.5))
      IF (ANS.LT.0.95) GOTO 110
10    CONTINUE
110   TSTAR = TM
      TMT=TSTAR
      WRITE(6,2010)TSTAR
      WRITE(7,2010)TSTAR
2010  FORMAT(2X,'COMBUSTION BEGINS AFTER',F6.2,' SECS')
      TMB=RNTM*NF1/BU
      TME=RNTM*NF2/E
50    CONTINUE
      TIME=TMT
      DO 60 NB=1,BU
      TMT = TIME + TMB*(FLOAT(NB))
      TM=TMB*(FLOAT(NB))
      XU3 = TM
      NF=1
      IW=2
      CALL CGQA(FUNC1,XL1,XU1,NG1,ANS)
      IW=1
      ANS=3.0*ANS/(RP**3.0)
      ADS=1.0-ANS
      R20=RP
      CALL TEMPC(TT,TM)
      TS=TT
       WRITE(6,1089)R20,TS
       WRITE(7,1089)R20,TS
      IW=3
      CALL TEMPC(TT,TM)
      T175=TT
       WRITE(6,1089)RDUM,T175
       WRITE(7,1089)RDUM,T175
      IW=4
      CALL TEMPC(TT,TM)
```

```
      T150=TT
       WRITE(6,1089)RDUM,T150
       WRITE(7,1089)RDUM,T150
      IW=5
      CALL TEMPC(TT,TM)
      T100=TT
       WRITE(6,1089)RDUM,T100
       WRITE(7,1089)RDUM,T100
      IW=6
      CALL TEMPC(TT,TM)
      T125=TT
       WRITE(6,1089)RDUM,T125
       WRITE(7,1089)RDUM,T125
      IW=7
      CALL TEMPC(TT,TM)
      T075=TT
       WRITE(6,1089)RDUM,T075
       WRITE(7,1089)RDUM,T075
      IW=8
      CALL TEMPC(TT,TM)
      T050=TT
       WRITE(6,1089)RDUM,T050
       WRITE(7,1089)RDUM,T050
      IW=9
      CALL TEMPC(TT,TM)
      T025=TT
       WRITE(6,1089)RDUM,T025
       WRITE(7,1089)RDUM,T025
      IW=10
      CALL TEMPC(TT,TM)
      T001=TT
       WRITE(6,1089)RDUM,T001
       WRITE(7,1089)RDUM,T001
       WRITE(8,1113)TMT,ANS
      WRITE(6,2009)TMT,ANS,TS
      WRITE(7,2009)TMT,ANS,TS
      IF (ANS .LT. 0.05) GOTO 99
60    CONTINUE
C
      TIME=TMT
      DO 70 NE=1,E
      TMT=TIME + TME*(FLOAT(NE))
      TM=TME*(FLOAT(NE))
      XU3=TM
      IW=2
      NF=2
      CALL CGQA(FUNC1,XL1,XU1,NG1,ANS)
      ANS=3*ANS/RP**3.
      ADS=1.0-ANS
      IW=1
      R20=RP
      CALL TEMPP(TT,TM)
      TS=TT
       WRITE(6,1089)R20,TS
       WRITE(7,1089)R20,TS
      IW=3
      CALL TEMPP(TT,TM)
      T175=TT
       WRITE(6,1089)RDUM,T175
       WRITE(7,1089)RDUM,T175
```

```
      IW=4
      CALL TEMPP(TT,TM)
      T150=TT
       WRITE(6,1089)RDUM,T150
       WRITE(7,1089)RDUM,T150
      IW=5
      CALL TEMPP(TT,TM)
      T125=TT
       WRITE(6,1089)RDUM,T125
       WRITE(7,1089)RDUM,T125
      IW=6
      CALL TEMPP(TT,TM)
      T100=TT
       WRITE(6,1089)RDUM,T100
       WRITE(7,1089)RDUM,T100
      IW=7
      CALL TEMPP(TT,TM)
      T075=TT
       WRITE(6,1089)RDUM,T075
       WRITE(7,1089)RDUM,T075
      IW=8
      CALL TEMPP(TT,TM)
      T050=TT
       WRITE(6,1089)RDUM,T050
       WRITE(7,1089)RDUM,T050
      IW=9
      CALL TEMPP(TT,TM)
      T025=TT
       WRITE(6,1089)RDUM,T025
       WRITE(7,1089)RDUM,T025
      IW=10
      CALL TEMPP(TT,TM)
      T001=TT
       WRITE(6,1089)RDUM,T001
       WRITE(7,1089)RDUM,T001
       WRITE(8,1113)TMT,ANS
      WRITE(6,2009)TMT,ANS,TS
      WRITE(7,2009)TMT,ANS,TS
      IF (ANS .LT. 0.05) GOTO 99
70    CONTINUE
      IF (ANS .LT. 0.05) THEN
      GOTO 99
      ELSE
      GOTO 50
      END IF
99    STOP
      END
C
      FUNCTION FUNC1(R)
      DIMENSION B(15),BFL(15),BVAL(15),RNI(15),RNJ(15)
      EXTERNAL FUNC2
     COMMON/ABC/ TA,T0,B,RP,ALPA,E0,SIGMA,PI,XL2,XU2,XL3,XU3,RDUM,EDUM
     COMMON/IKAC/ NG2,NG3,BFL
     COMMON/COM/ RNTM,TSTAR,TF,BFO,RNI,RNJ,IW,NF,TS,NC
     COMMON/BIOT/BVAL
      RDUM=R
      CALL CGQB(FUNC2,XL2,XU2,NG2,ANS2)
      FUNC1=ANS2*R*R
      RETURN
      END
```

```
C
      FUNCTION FUNC2(E)
      DIMENSION B(15),BFL(15),BVAL(15),RNI(15),RNJ(15)
      EXTERNAL FUNC3
     COMMON/ABC/ TA,TØ,B,RP,ALPA,EØ,SIGMA,PI,XL2,XU2,XL3,XU3,RDUM,EDUM
     COMMON/IKAC/ NG2,NG3,BFL
     COMMON/COM/ RNTM,TSTAR,TF,BFO,RNI,RNJ,IW,NF,TS,NC
     COMMON/BIOT/BVAL
      EDUM=E
      CALL CGQC(FUNC3,XL3,XU3,NG3,ANS3)
      A=ANS3*1.67E13
      IF(A.GT.5Ø)GO TO 11
      A=EXP(-A)
      GO TO 12
11    A=Ø.Ø
12    FE=EXP((-(E-EØ)**2)/(2.*(SIGMA**2)))
      FE=FE/(SIGMA*SQRT(2.Ø*PI))
      FUNC2=FE*A
      RETURN
      END
C
      FUNCTION FUNC3(T)
      DIMENSION B(15),BFL(15),BVAL(15),RNI(15),RNJ(15)
     COMMON/ABC/ TA,TØ,B,RP,ALPA,EØ,SIGMA,PI,XL2,XU2,XL3,XU3,RDUM,EDUM
     COMMON/IKAC/ NG2,NG3,BFL
     COMMON/COM/ RNTM,TSTAR,TF,BFO,RNI,RNJ,IW,NF,TS,NC
     COMMON/BIOT/BVAL
     IW=2
     IF (NF .EQ. Ø) GOTO 1
     IF (NF.EQ. 1) GOTO 2
     CALL TEMPP(TT,T)
     GOTO 3
1    CALL TEMP(TT,T)
     GOTO 3
2    CALL TEMPC(TT,T)
3    RT = 8.315E-Ø3
     EB=(EDUM/(RT*TT))
     IF(EB.GT.5Ø.Ø)GO TO 2Ø
     FUNC3=EXP(-EB)
     GO TO 21
2Ø   FUNC3=Ø.Ø
21   RETURN
     END

C
      SUBROUTINE TEMP(TT,T)
      DIMENSION B(15),BFL(15),BVAL(15),RNI(15),RNJ(15)
     COMMON/ABC/ TA,TØ,B,RP,ALPA,EØ,SIGMA,PI,XL2,XU2,XL3,XU3,RDUM,EDUM
     COMMON/IKAC/ NG2,NG3,BFL
     COMMON/COM/ RNTM,TSTAR,TF,BFO,RNI,RNJ,IW,NF,TS,NC
     COMMON/BIOT/BVAL
       IF (IW .EQ. 1) RDUM=RP
       IF (IW .EQ. 3) RDUM=3.5Ø
       IF (IW .EQ. 4) RDUM=3.ØØ
       IF (IW .EQ. 5) RDUM=2.5Ø
       IF (IW .EQ. 6) RDUM=2.ØØ
       IF (IW .EQ. 7) RDUM=1.5Ø
       IF (IW .EQ. 8) RDUM=1.ØØ
       IF (IW .EQ. 9) RDUM=Ø.5Ø
       IF (IW .EQ.1Ø) RDUM=Ø.Ø1
```

```
      SUM1=Ø.Ø
      SUM2=Ø.Ø
      DO 1Ø I=1,1Ø
      Y=B(I)
      AØ=SIN(Y)-Y*COS(Y)
      A1=Y-SIN(Y)*COS(Y)
      A2=AØ/A1
      A3=SIN(Y*RDUM/RP)
      A4=Y*RDUM/RP
      A5=A3/A4
      A6=Y**2*ALPA*T/RP**2
      IF(A6 .GT. 5Ø.Ø) GOTO 11
      A6= EXP(-A6)
      GOTO 12
11    A6= Ø.Ø
12    A7=A2*A5*A6*2.Ø*(TA-TØ)
      A8=A2*A6*2.Ø*(TA-TØ)
      IF (IW .GT. 1) GOTO 1Ø
      RNI(I)=A8
1Ø    SUM1=SUM1+A7
      RNI(11)=Ø.Ø
      RNI(12)=Ø.Ø
      RNI(13)=Ø.Ø
      RNI(14)=Ø.Ø
      RNI(15)=Ø.Ø
         TT= TA - SUM1
      RETURN
      END
C
       SUBROUTINE TEMPP(TT,T)
       DIMENSION B(15),BFL(15),BVAL(15),RNI(15),RNJ(15)
      COMMON/ABC/ TA,TØ,B,RP,ALPA,EØ,SIGMA,PI,XL2,XU2,XL3,XU3,RDUM,EDUM
      COMMON/IKAC/ NG2,NG3,BFL
      COMMON/COM/ RNTM,TSTAR,TF,BFO,RNI,RNJ,IW,NF,TS,NC
      COMMON/BIOT/BVAL
      IF (IW .EQ. 1)RDUM=RP
      IF (IW .EQ. 3)RDUM=3.5Ø
      IF (IW .EQ. 4)RDUM=3.ØØ
      IF (IW .EQ. 5)RDUM=2.5Ø
      IF (IW .EQ. 6)RDUM=2.ØØ
      IF (IW .EQ. 7)RDUM=1.5Ø
      IF (IW .EQ. 8)RDUM=1.ØØ
      IF (IW .EQ. 9)RDUM=Ø.5Ø
      IF (IW .EQ.1Ø)RDUM=Ø.Ø1
      SUM3=Ø.Ø
      C14=Ø.Ø
     DO 1Ø I=1,15
      C1=B(I)
      C2=SIN(C1)
      C3=COS(C1)
      C4=C1-C2*C3
      C5=C2-C1*C3
      C5=2.Ø*(TA-TF)*C5
      C5=C5/C4
      SUM1=Ø.Ø
     DO 2Ø J=1,15
      U1=BFL(J)
      U2=U1+C1
      U3=U1-C1
      U4=SIN(U2)/U2
```

```
          U5=SIN(U3)/U3
          U6=-U4+U5
          U7=((C1**2)/U1)*RNJ(J)*U6
20        SUM1=SUM1+U7
          C6= SUM1/C4+C5
          C7=(C1*RDUM/RP)
          C8=SIN(C7)/C7
          C9=C1*C1*ALPA*T/(RP*RP)
          IF (C9 .GT. 50.0) GOTO 13
          C10=EXP(-C9)
          GOTO 14
13        C10=0.0
14        C11=C8*C10
          C12=C11*C6
          IF (IW .GT. 1) GOTO 10
          RNI(I)=C6*C10
10        SUM3=SUM3+C12
             TT=TA-SUM3
        RETURN
        END
C
        SUBROUTINE TEMPC(TT,T)
        DIMENSION B(15),BFL(15),BVAL(15),RNI(15),RNJ(15)
        COMMON/ABC/ TA,T0,B,RP,ALPA,E0,SIGMA,PI,XL2,XU2,XL3,XU3,RDUM,EDUM
        COMMON/IKAC/ NG2,NG3,BFL
        COMMON/COM/ RNTM,TSTAR,TF,BF0,RNI,RNJ,IW,NF,TS,NC
        COMMON/BIOT/BVAL
          IF(IW .EQ. 1 ) RDUM=RP
          IF(IW .EQ. 3)RDUM=3.50
          IF(IW .EQ. 4)RDUM=3.00
          IF(IW .EQ. 5)RDUM=2.50
          IF(IW .EQ. 6)RDUM=2.00
          IF(IW .EQ. 7)RDUM=1.50
          IF(IW .EQ. 8)RDUM=1.00
          IF(IW .EQ. 9)RDUM=0.50
          IF(IW .EQ.10)RDUM=0.01
          SUM1=0.0
          DO 20 J=1,15
          U1=BFL(J)
          U2=SIN(U1)
          U3=COS(U1)
          U4=U1-U2*U3
          U5=U2-U1*U3
          U5=2.0*(TF-TA)*U5
          U5=U5/U4
          SUM2=0.0
          DO 30 I=1,15
          A1=B(I)
          A2=A1+U1
          A3=A1-U1
          A4=SIN(A2)/A2
          A5=SIN(A3)/A3
          A6=-A4+A5
          A7=((U1**2)/A1)*RNI(I)*A6
30        SUM2=SUM2+A7
          U6=SUM2/U4+U5
          U7=U1*RDUM/RP
          U8=SIN(U7)/U7
          U9=U1*U1*ALPA*T/(RP*RP)
          IF(U9 .GT. 50.0) GOTO 23
```

```
        U10=EXP(-U9)
        GOTO 24
23      U10=0.0
24      U11=U6*U10*U8
        IF (IW .GT. 1) GOTO 20
        RNJ(J)=U6*U10
20      SUM1=SUM1+U11
           TT=TF-SUM1
        RETURN
        END
C
      SUBROUTINE BITC(BI)
      DIMENSION BVAL(15)
      COMMON/BIOT/BVAL
      BE = 0.001
      N = 0
2     FBE = 1.0 - BI-BE*COS(BE)/SIN(BE)
      IF(ABS(FBE).LT.0.01)GO TO 1
      BE = BE + 0.00005
      IF(BE.GT.500.0)GOTO 3
      GO TO 2
1     N = N+1
      IF(N.GE.16) GOTO 3
      BVAL(N) = BE
      BE = BE + 2.2
      GO TO 2
3     RETURN
      END
C
C
C**********************************************************************
C********************** SUBROUTINE CGQA ***********************************
C**********************************************************************
C
      SUBROUTINE CGQA(CF,XL,XU,N,CVAL)
C
C        PERFORMS INTEGRATION OF A FUNCTION OF A SINGLE VARIABLE
C        BY GAUSSIAN QUADRATURE.
C
C        N = ORDER OF GUASSIAN QUADRATURE APPROXIMATION. VALUE MAY BE ON
C            (1,2,4,8,10,12,16,32).  IF N=1, CGQA PERFORMS A ONE-POINT
C            RECTANGULAR RULE INTEGRATION.
C        CF = EXTERNALLY SUPPLIED FUNCTION....MUST BE FUNCTION OF ONE
C             VARIABLE FOR CQG1.
C        XL = LOWER BOUND OF VARIABLE
C        XU = UPPER BOUND OF VARIABLE
C        CVAL = RESULTING VALUE OF THE INTEGRATION
C
C       NOTE:  CF MUST BE LISTED IN AN EXTERNAL STATEMENT IN THE
C                CALLING ROUTINE
C
      DIMENSION Q1(52),Q2(24),Q3(32),NQ(8),NS(8),QG(108)
      EQUIVALENCE (Q1(1),QG(1)),(Q2(1),QG(53)),(Q3(1),QG(77))
      DATA Q1
     $                /.28867513459481288E0,0.5E0,.43056815579702629E0,
     $.17392742256872693E0,.16999052179242813E0,.32607257743127307E0,
     $ 0.48014492824876812E0,.50614268145188130E-1,.39833238706813370E0,
     $.11119051722668724E0,.26276620495816449E0,.15685332293894364E0,
     $.91717321247824906E-1,.18134189168918099E0,.48695326425858586E0,
     $.33335672154344070E-1,.43253168334449225E0,.74725674575290 3E-1,
```

```
     $.3397047841496122E0,.1095431812579910ZE0,.2166976970646236E0,
     $.1346333596549981ØE0,.7443716949081560ØE-1,.1477621123573764ØE0,
     $Ø.4907803171233596ØE0,.2358766819325591ØE-1,.4520586281852374ØE0,
     $.5346966299765921ØE-1,.3849513370971523ØE0,.8003916427167311E-1,
     $.2936589771433087ØE0,.1015837133615329ØE0,.1839157494990901ØE0,
     $.1167462682691774ØE0,.6261670425573445ØE-1,.1245735229067013ØE0,
     $.4947004674958249ZE0,.1357622970587704ZE-1,.4722875115366162ØE0,
     $.3112676196932394ØE-1,.4328156011939158ZE0,.4757925584124639ZE-1,
     $.3777022041775015ZE0,.6231448562776693ØE-1,.3089381222013218ZE0,
     $.7479799440828837E-1,.2290083888286136ØE0,.8457825969750127E-1,
     $.1408017753896294ØE0,.9130170752246179E-1,.4750625491881872ØE-1,
     $.9472530522753425E-1 /
      DATA Ø2
     $                / Ø.4975936099985106ØE+Ø   ,Ø.6170614899993599ØE-2 ,
     *              Ø.4873642779856547ØE+Ø    ,    Ø.1426569431446683ØE-1 ,
     *              Ø.4691372760013663ØE+Ø    ,    Ø.2213871940870990ZE-1 ,
     *              Ø.4432077635022005ZE+Ø    ,    Ø.2964929245771889ØE-1 ,
     *              Ø.4100009929869514ØE+Ø    ,    Ø.3667324070554015ZE-1 ,
     *              Ø.3700620957892771ØE+Ø    ,    Ø.4309508076597663ØE-1 ,
     *              Ø.3240468259684877ØE+Ø    ,    Ø.4880932605205694ØE-1 ,
     *              Ø.2727107356944197ZE+Ø    ,    Ø.5372213505792817E-1 ,
     *              Ø.2168967538130225ZE+Ø    ,    Ø.5775283402686280ØE-1 ,
     *              Ø.1575213398480816ØE+Ø    ,    Ø.6083523646390169ØE-1 ,
     *              Ø.9555943373680815ØE-1    ,    Ø.6291872817341414ØE-1 ,
     *              Ø.3202844643130281ZE-1    ,    Ø.6396909767337607ØE-1 /
      DATA Ø3
     $                /Ø.4986319309247407ØE+Ø ,    Ø.3509305004735048ZE-2 ,
     *              Ø.4928057557726341ZE+Ø    ,    Ø.8137197365452835ØE-2 ,
     *              Ø.4823811277937532ZE+Ø    ,    Ø.1269603265463103ØE-1 ,
     *              Ø.4674530379688698ZE+Ø    ,    Ø.1713693145651071ZE-1 ,
     *              Ø.4481605778830260ZE+Ø    ,    Ø.2141794901111334ØE-1 ,
     *              Ø.4246838068662849ZE+Ø    ,    Ø.2549902963118808ØE-1 ,
     *              Ø.3972418979839712ØE+Ø    ,    Ø.2934204673926774E-1 ,
     *              Ø.3660910593701448ZE+Ø    ,    Ø.3291111138818092ZE-1 ,
     *              Ø.3315221334651076ØE+Ø    ,    Ø.3617289705442425ZE-1 ,
     *              Ø.2933578786203811ZE+Ø    ,    Ø.3909694789353515ZE-1 ,
     *              Ø.2534499544661147ØE+Ø    ,    Ø.4165596211347337ØE-1 ,
     *              Ø.2106756380653176ZE+Ø    ,    Ø.4382604650220190ZE-1 ,
     *              Ø.1659343011410638ZE+Ø    ,    Ø.4558693934788194ZE-1 ,
     *              Ø.1196436811260685ZE+Ø    ,    Ø.4692219954040228ZE-1 ,
     *              Ø.7223598079139825ØE-1    ,    Ø.4781936003963743ØE-1 ,
     *              Ø.2415383284386915ØE-1    ;    Ø.4827004425736390ØE-1 /
     $,NQ/2,4,8,10,12,16,24,32/,
     $ NS/1,3,7,15,25,37,53,77/
       IF(N .EQ. 1) GO TO 200
       DO 300 L=1,8
       IF(N.EQ.NQ(L)) GO TO 301
  300  CONTINUE
 9001    WRITE(5,905) N
   905 FORMAT('Ø CALLING PARAMETER =',I5,'   INTEGRATION NOT POSSIBLE'//)
       RETURN
   200 AX=Ø.5*(XU+XL)
       CVAL=CF(AX)*(XU-XL)
       RETURN
  301  CONTINUE
       NP=NS(L)
       NE=NP+N-1
       AX=Ø.5*(XU+XL)
       BX=XU-XL
       CVAL=Ø.
```

```
      DO 350 J=NP,NE,2
      DX=QG(J)*BX
      CVAL=CVAL+QG(J+1)*(CF(AX+DX)+CF(AX-DX))
 350  CONTINUE
      CVAL=CVAL*BX
      RETURN
      END
C*******************************************************************************
C********************* SUBROUTINE CGQB ******************************************
C*******************************************************************************
C
      SUBROUTINE CGQB(CF,XL,XU,N,CVAL)
C
C         PERFORMS INTEGRATION OF A FUNCTION OF A SINGLE VARIABLE
C         BY GAUSSIAN QUADRATURE.
C
C         N = ORDER OF GUASSIAN QUADRATURE APPROXIMATION. VALUE MAY BE ON
C              (1,2,4,8,10,12,16,32).  IF N=1, CGQB PERFORMS A ONE-POINT
C              RECTANGULAR RULE INTEGRATION.
C         CF = EXTERNALLY SUPPLIED FUNCTION....MUST BE FUNCTION OF ONE
C               VARIABLE FOR CQG1.
C         XL = LOWER BOUND OF VARIABLE
C         XU = UPPER BOUND OF VARIABLE
C         CVAL = RESULTING VALUE OF THE INTEGRATION
C
C       NOTE:  CF MUST BE LISTED IN AN EXTERNAL STATEMENT IN THE
C                CALLING ROUTINE
C
      DIMENSION Q1(52),Q2(24),Q3(32),NQ(8),NS(8),QG(108)
      EQUIVALENCE (Q1(1),QG(1)),(Q2(1),QG(53)),(Q3(1),QG(77))
      DATA Q1
     $                /.28867513459481288ZE0,0.5E0,.43056815579702629E0,
     $.17392742256872693E0,.16999052179242813E0,.32607257743127307E0,
     $ 0.48014492824876812E0,.50614268145188130E-1,.39833238706813372E0,
     $.11119051722668724E0,.26276620495816449E0,.15685332293894364E0,
     $.91717321247824906-1,.18134189168918099E0,.48695326425858586E0,
     $.33335672154344072-1,.43253168334449225E0,.74725674575290JE-1,
     $.33970478414961226E0,.10954318125799102E0,.21669769706462J6E0,
     $.13463335965499818E0,.74437169490815605E-1,.14776211235737644E0,
     $0.49078031712335963E0,.23587668193255914E-1,.45205862818523743E0,
     $.53469662997659215E-1,.38495133709715234E0,.80039164271673J1E-1,
     $.29365897714330872E0,.10158371336153296E0,.18391574949909010E0,
     $.11674626826917740E0,.62616704255734456E-1,.12457352290670139E0,
     $.49470046749582497E0,.13576229705877047E-1,.47228751153661629E0,
     $.31126761969323946E-1,.43281560119391587E0,.47579255841246392E-1,
     $.37770220417750152E0,.62314485627766936E-1,.30893812220132187E0,
     $.74797994408288J7E-1,.22900838882861369E0,.84578259697501J7E-1,
     $.14080177538962946E0,.91301707522461J9E-1,.47506254918818720E-1,
     $.94725305227534J5E-1 /
      DATA Q2
     $              / 0.49759360999851068E+0   ,0.61706148999935998E-2 ,
     *           0.48736427798565475E+0   ,    0.14265694314466832E-1 ,
     *           0.46913727600136638E+0   ,    0.22138719408709903E-1 ,
     *           0.44320776350220052E+0   ,    0.29649292457718890E-1 ,
     *           0.41000099298695146E+0   ,    0.36673240705540153E-1 ,
     *           0.37006209578927718E+0   ,    0.43095080765976638E-1 ,
     *           0.32404682596848778E+0   ,    0.49809326052056944E-1 ,
     *           0.27271073569441977E+0   ,    0.53722135057982817E-1 ,
     *           0.21689675381302257E+0   ,    0.57752834026862801E-1 ,
     *           0.15752133984808169E+0   ,    0.60835236463901696E-1 ,
```

```
     *            Ø.9555943373680815ØE-1    ,     Ø.6291872817341414ØE-1 ,
     *            Ø.32028446431302813E-1    ,     Ø.6396909767337607ØE-1 /
      DATA Q3
     $              /Ø.4986319309247407ØE+Ø ,     Ø.3509305004735Ø483E-2 ,
     *            Ø.4928Ø5755772634Ø7E+Ø    ,     Ø.8137197365452835ØE-2 ,
     *            Ø.4823811277937532ØE+Ø    ,     Ø.1269603265463103ØE-1 ,
     *            Ø.4674530379688698ØE+Ø    ,     Ø.1713693145651Ø717E-1 ,
     *            Ø.4481605778830260ØE+Ø    ,     Ø.2141794901111334ØE-1 ,
     *            Ø.4246838068662849ØE+Ø    ,     Ø.2549Ø29631188Ø88E-1 ,
     *            Ø.3972418979839712ØE+Ø    ,     Ø.2934204673926777ØE-1 ,
     *            Ø.3660910593701448ØE+Ø    ,     Ø.3291111138818Ø923E-1 ,
     *            Ø.3315221334651076ØE+Ø    ,     Ø.3617289705442425ØE-1 ,
     *            Ø.2938578786203811ØE+Ø    ,     Ø.3909694789353515ØE-1 ,
     *            Ø.2534499544661147ØE+Ø    ,     Ø.4165596211347337ØE-1 ,
     *            Ø.2106756380653176ØE+Ø    ,     Ø.4382604650220190ØE-1 ,
     *            Ø.1659343011410638ØE+Ø    ,     Ø.4558693934788194ØE-1 ,
     *            Ø.1196436811260685ØE+Ø    ,     Ø.4692219954040228ØE-1 ,
     *            Ø.7223598079139825ØE-1    ,     Ø.4781936003963743ØE-1 ,
     *            Ø.2415383284386915ØE-1    ,     Ø.4827004425736390ØE-1 /
     $,NQ/2,4,8,1Ø,12,16,24,32/,
     $ NS/1,3,7,15,25,37,53,77/
      IF(N .EQ. 1) GO TO 2ØØ
      DO 3ØØ L=1,8
      IF(N.EQ.NQ(L)) GO TO 3Ø1
 3ØØ  CONTINUE
9ØØ2   WRITE(5,9Ø5) N
  9Ø5 FORMAT('Ø CALLING PARAMETER =',I5,'   INTEGRATION NOT POSSIBLE'//)
      RETURN
  2ØØ AX=Ø.5*(XU+XL)
      CVAL=CF(AX)*(XU-XL)
      RETURN
 3Ø1  CONTINUE
      NP=NS(L)
      NE=NP+N-1
      AX=Ø.5*(XU+XL)
      BX=XU-XL
      CVAL=Ø.
      DO 35Ø J=NP,NE,2
      DX=QG(J)*BX
      CVAL=CVAL+QG(J+1)*(CF(AX+DX)+CF(AX-DX))
 35Ø  CONTINUE
      CVAL=CVAL*BX
      RETURN
      END
C*********************************************************************
C********************* SUBROUTINE CGQC ***********************************
C*********************************************************************
C
      SUBROUTINE CGQC(CF,XL,XU,N,CVAL)
C
C        PERFORMS INTEGRATION OF A FUNCTION OF A SINGLE VARIABLE
C        BY GAUSSIAN QUADRATURE.
C
C        N = ORDER OF GUASSIAN QUADRATURE APPROXIMATION. VALUE MAY BE ON
C            (1,2,4,8,1Ø,12,16,32).  IF N=1, CGQC PERFORMS A ONE-POINT
C            RECTANGULAR RULE INTEGRATION.
C        CF = EXTERNALLY SUPPLIED FUNCTION....MUST BE FUNCTION OF ONE
C             VARIABLE FOR CQG1.
C        XL = LOWER BOUND OF VARIABLE
C        XU = UPPER BOUND OF VARIABLE
```

```
C         CVAL = RESULTING VALUE OF THE INTEGRATION
C
C       NOTE:  CF MUST BE LISTED IN AN EXTERNAL STATEMENT IN THE
C                CALLING ROUTINE
C
      DIMENSION Q1(52),Q2(24),Q3(32),NQ(8),NS(8),QG(108)
      EQUIVALENCE (Q1(1),QG(1)),(Q2(1),QG(53)),(Q3(1),QG(77))
      DATA Q1
     $                 /.28867513459481288ZE0,Ø.5E0,.43056815579702629E0,
     $.17392742256872693E0,.16999052179242813E0,.32607257743127307E0,
     $ Ø.48014492824876812E0,.50614268145188130E-1,.39833323870681337E0,
     $.11119051722668724E0,.26276620495816449E0,.15685332293894364E0,
     $.91717321247824900E-1,.18134189168918099E0,.48695326425858586E0,
     $.33335672154344Ø7E-1,.43253168334449225E0,.74725674575290ZE-1,
     $.33970478414961Z2E0,.10954318125799102E0,.21669769706462Z6E0,
     $.13463335965499818E0,.74437169490815605E-1,.14776211235737644E0,
     $Ø.49078031712335963E0,.23587668193255914E-1,.45205862818523743E0,
     $.53469662997659215E-1,.38495133709715234E0,.80039164271673ll E-1,
     $.29365897714330872E0,.10158371336153296E0,.18391574949909010E0,
     $.11674626826917740E0,.62616704255734458E-1,.12457352290670139E0,
     $.49470046749582497E0,.13576229705877047E-1,.47228751153661629E0,
     $.31126761969323946E-1,.43281560119391587E0,.47579255841246392E-1,
     $.37770220417750152E0,.62314485627766936E-1,.30893812220132187E0,
     $.74797994408288Z7E-1,.22900838882861369E0,.84578259697501Z7E-1,
     $.14080177538962946E0,.91301707522461Z9E-1,.47506254918818720E-1,
     $.94725305227534Z5E-1 /
      DATA Q2
     $                / Ø.49759360999851068E+Ø   ,Ø.61706148999935998E-2 ,
     *              Ø.48736427798565475E+Ø   ,    Ø.14265694314466832E-1 ,
     *              Ø.46913727600136636E+Ø   ,    Ø.22138719408709903E-1 ,
     *              Ø.44320776350220052E+Ø   ,    Ø.29649292457718890E-1 ,
     *              Ø.41000099298695146E+Ø   ,    Ø.36673240705540153E-1 ,
     *              Ø.37006209578927718E+Ø   ,    Ø.43095080765976638E-1 ,
     *              Ø.32404682596848778E+Ø   ,    Ø.48809326052056944E-1 ,
     *              Ø.27271073569441977E+Ø   ,    Ø.53722135057982817E-1 ,
     *              Ø.21689675381302257E+Ø   ,    Ø.57752834026862801E-1 ,
     *              Ø.15752133984808169E+Ø   ,    Ø.60835236463901696E-1 ,
     *              Ø.95559433736808150E-1   ,    Ø.62918728173414148E-1 ,
     *              Ø.32028446431302813E-1   ,    Ø.63969097873376078E-1 /
      DATA Q3
     $                /Ø.49863193092474078E+Ø ,    Ø.35093050047350483E-2 ,
     *              Ø.49280575577263417E+Ø   ,    Ø.81371973654528350E-2 ,
     *              Ø.48238112779375322E+Ø   ,    Ø.12696032654631030E-1 ,
     *              Ø.46745303796886984E+Ø   ,    Ø.17136931456510717E-1 ,
     *              Ø.44816057788302606E+Ø   ,    Ø.21417949011113340E-1 ,
     *              Ø.42468380686628499E+Ø   ,    Ø.25499029631188088E-1 ,
     *              Ø.39724189798397120E+Ø   ,    Ø.29342046739267774E-1 ,
     *              Ø.36609105937014484E+Ø   ,    Ø.32911111388180923E-1 ,
     *              Ø.33152213346510760E+Ø   ,    Ø.36172897054424253E-1 ,
     *              Ø.29385787862038116E+Ø   ,    Ø.39096947893535153E-1 ,
     *              Ø.25344995446611470E+Ø   ,    Ø.41655962113473378E-1 ,
     *              Ø.21067563806531767E+Ø   ,    Ø.43826046502201906E-1 ,
     *              Ø.16593430114106382E+Ø   ,    Ø.45586939347681942E-1 ,
     *              Ø.11964368112606854E+Ø   ,    Ø.46922199540402283E-1 ,
     *              Ø.72235980791398250E-1   ,    Ø.47819360039637430E-1 ,
     *              Ø.24153832843869158E-1   ,    Ø.48270044257363900E-1 /
     $,NQ/2,4,8,10,12,16,24,32/,
     $ NS/1,3,7,15,25,37,53,77/
      IF(N .EQ. 1) GO TO 200
      DO 300 L=1,8
```

```
      IF(N.EQ.NQ(L)) GO TO 301
  300 CONTINUE
 9003  WRITE(5,905) N
  905 FORMAT('0 CALLING PARAMETER =',I5,'   INTEGRATION NOT POSSIBLE'//)
      RETURN
  200 AX=0.5*(XU+XL)
      CVAL=CF(AX)*(XU-XL)
      RETURN
  301 CONTINUE
      NP=NS(L)
      NE=NP+N-1
      AX=0.5*(XU+XL)
      BX=XU-XL
      CVAL=0.
      DO 350 J=NP,NE,2
      DX=QG(J)*BX
      CVAL=CVAL+QG(J+1)*(CF(AX+DX)+CF(AX-DX))
  350 CONTINUE
      CVAL=CVAL*BX
      RETURN
      END
```

```
C*********************************FREQ.FOR*************************************
C       CALCULATION OF FREQUENCY BETWEEN BUBBLE AND EMULSION PHASE P/Q
        DIMENSION Z(11)
        TYPE*,' ENTER DELU'
        READ*,DELU
        TYPE*,' ENTER DBØ '
        READ*,DBØ
        Z(1)=5.
        Z(2)=1Ø.
        Z(3)=2Ø.
        Z(4)=3Ø.
        Z(5)=4Ø.
        Z(6)=5Ø.
        Z(7)=6Ø.
        Z(8)=7Ø.
        Z(9)=8Ø.
        Z(1Ø)=9Ø.
        Z(11)=1ØØ.
        DO 1Ø I=1,11
        H=Z(I)
        A = (H**(Ø.6))/(3.*8.2)
        B = 22.26*SQRT(DBØ)/8.2
        C = H**(Ø.2)/8.2
        D = SQRT(22.26*SQRT(DBØ))/(8.2*SQRT(8.2))
        E = H**(Ø.2)*SQRT(8.2/(22.26*SQRT(DBØ)))
        F =(DELU*5.*(A-B*(C-D*ATAN(E))))/H
        WRITE(6,1ØØØ)F,DELU,H,DBØ
1ØØØ  FORMAT(X,'F=',F9.3,X,'DELU=',F7.3,X,'H=',F7.3,X,'DBØ=',F9.5)
1Ø      CONTINUE
        STOP
        END
```

```
C**********************************APQ.FOR*********************************
C       CALCULATION OF FREQUENCY P/Q
        DIMENSION U(12)
        TYPE*,' ENTER BED HEIGHT (cm) '
        READ*,H
        U(1)=1.
        U(2)=5.
        U(3)=10.
        U(4)=20.
        U(5)=25.
        U(6)=40.
        U(7)=50.
        U(8)=60.
        U(9)=70.
        U(10)=80.
        U(11)=90.
        U(12)=100.
        DO 10 I=1,12
        DELU=U(I)
        DB0=0.00376*(DELU**2.)
        A=5*DELU
        B=H**0.6/(3.*8.2)
        C=22.26*SQRT(DB0)/8.2
        D=H**0.2/8.2
        E=(SQRT(22.26*SQRT(DB0)))/(8.2*SQRT(8.2))
     1    *ATAN(H**0.2*SQRT(8.2/(22.26*SQRT(DB0))))
        F=A*(B-C*(D-E))/H
        WRITE(6,1000)F,DELU,H
!       WRITE(7,1000)F,DELU,H
!       WRITE(11,1001)F,DELU
1000    FORMAT(X,'F=',F9.5,5X,'DELU=',F7.2,5X,'H=',F8.5)
1001    FORMAT(X,F9.5,X,F7.2)
10      CONTINUE
        STOP
        END
```

```
C**********************************PQL.FOR************************************
C       CALCULATION OF LOCAL FREQUENCES P/Q
        DIMENSION Z(12)
        Z(1)=1.
        Z(2)=5.
        Z(3)=10.
        Z(4)=20.
        Z(5)=30.
        Z(6)=40.
        Z(7)=50.
        Z(8)=60.
        Z(9)=70.
        Z(10)=80.
        Z(11)=90.
        Z(12)=100.
        TYPE*,' ENTER DELU (CM) '
        READ*,DELU
        DO 10 I=1,12
        H=Z(I)
        DB0=0.00376*DELU**2.
        F=DELU/(22.26*SQRT(DB0)+8.2*H**0.4)
        WRITE(6,1000)F,H,DELU
        WRITE(9,1000)F,H,DELU
       'WRITE(20,1001)F,H
1000    FORMAT(X,'F=',F9.5,5X,'H=',F7.2,5X,'DELU=',F7.2)
1001    FORMAT(X,F9.5,X,F7.2)
10      CONTINUE
        STOP
        END
```

```
C*********************************OSCLO.FOR*********************************
C       CALCULATION OF FREQUENCY OF OSCILLATION LOCAL
        DIMENSION Z(12)
        Z(1)=1.
        Z(2)=5.
        Z(3)=10.
        Z(4)=20.
        Z(5)=30.
        Z(6)=40.
        Z(7)=50.
        Z(8)=60.
        Z(9)=70.
        Z(10)=80.
        Z(11)=90.
        Z(12)=100.
        TYPE*,' ENTER COAL PARTICLE DIAMETER (CM) '
        READ*,DC
        TYPE*,' ENTER DELU '
        READ*,DELU
        DB0=0.00376*DELU**2.
        DO 10 I=1,12
        H=Z(I)
        A=(SQRT(DB0)+0.37*H**0.4)**4.*(H**0.6)
        F=10.3*(DC**2.)/A
        WRITE(6,1000)F,H,DC,DB0
        WRITE(30,1000)F,H,DC,DB0
        WRITE(31,1001)F,H
1000  FORMAT(X,'F=',F9.3,X,'H=',F7.3,X,'DC=',F5.2,X,'DB0=',F9.4)
1001    FORMAT(X,F9.3,X,F7.2)
10      CONTINUE
        STOP
        END
```

PROGRAM NAME: DVCOMB.FOR

SYSTEM: IBM-XT MS-DOS (Microsoft FORTRAN 4.0)

COMMENTS:

This program calculates the coupled drying and devolatilization characteristics of a single coal particle under combustion conditions. Drying is modelled from the transient drying model using a moving wet core radius. The computed temperature profiles are used to determine the devolatilization behaviour of the coal particle. Devolatilization is modelled using the DAE model as developed by Anthony and Howard. It is assumed ignition takes place when 5% of volatiles are released. The flame temperature is calculated using a modified Shwab-Zeldovic approach to the fuel droplet problem. The drying time is adjusted for combustion conditions. After drying is completed, the temperature profile (at the end of drying) is used as an initial condition in the transient heat conduction equation with a convective boundary condition. The temperature profiles computed are used to characterize the devolatilization behaviour. The numerical integrations are performed using a Gaussian quadrature procedure (subroutine CGQA). The program is interactive and the input parameters are asked when running the program.

```
C*******************************DVCOMB.FOR*********************************
C  FORTRAN PROGRAMM FOR COUPLED DRYING AND DEVOLATILIZATION OF A SINGLE
C  COAL PARTICLE UNDER COMBUSTION CONDITIONS
$ STORAGE:2
      REAL KG,KS,NUS
      EXTERNAL FUNC1
      EXTERNAL FUNC4
      EXTERNAL CF
      DIMENSION D(5),DVAL(5)
      COMMON/ABC/ TA,TØ,RP,ALPA,EØ,SIGMA,PI,XL2,XU2,XL3,XU3,RDUM,EDUM,TF
      COMMON/IKAC/ NG2,NG3,IND,CP,CØ,TE,P,PS,BI,TDRY,BVAL,DR,TM,TTR,RE
      COMMON/FGH/ D,SPHIG
      COMMON/GH/ TTM,ADS,BIF,TAUS,DPHI,BVALF,DRF,TTRF,NW,TPHIG,TAUCOM
      COMMON/BIOT/DVAL
C    INPUT PARAMETER
      WRITE(*,*)' ENTER TIME INTERVAL RTM'
      READ(*,*)RTM
      WRITE(*,*)' ENTER AMBIENT TEMPERATURE [K]'
      READ(*,*)TA
      WRITE(*,*)' ENTER PARTICLE RADIUS [mm]'
      READ(*,*)RP
      WRITE(*,*)' ENTER ALPA [mm2/s]'
      READ(*,*)ALPA
      WRITE(*,*)' ENTER EØ [kJ/mol]'
      READ(*,*)EØ
      WRITE(*,*)' ENTER SIGMA [kJ/mol]'
      READ(*,*)SIGMA
      WRITE(*,*)' ENTER DENSITY OF COAL [kg/m3]'
      READ(*,*)PS
      WRITE(*,*)' ENTER SPECIFIC HEAT OF COAL [cal/gK]'
      READ(*,*)CP
      WRITE(*,*)' ENTER ORIGINAL MOISTURE CONTENT OF THE COAL [g/g]'
      READ(*,*)CØ
      WRITE(*,*)' ENTER GAS VELOCITY [m/s]'
      READ(*,*)U
      WRITE(*,*)' ENTER RADIATION FACTOR [-]'
      READ(*,*)FRAD
      WRITE(*,*)' ENTER THERMAL CONDUCTIVITY OF GAS [W/mK]'
      READ(*,*)KG
      WRITE(*,*)' ENTER VISCOSITY OF GAS AT TA [m2/s]'
      READ(*,*)RNU
      WRITE(*,*)' ENTER YOA'
      READ(*,*)YOA
      WRITE(*,*)' ENTER SPECIFIC HEAT OF GAS'
      READ(*,*)CPG
      WRITE(*,*)' ENTER BIOT NUMBER OR Ø.Ø IF NOT KNOWN'
      READ(*,*)BI
C  CALCULATION OF FLAME TEMPERATURE
      DELH=10300.
      COE=-.17
      F=Ø.3
      TF=Ø.95*(DELH*F*YOA/CPG+TA)*(1.+CØ)**COE
C  CALCULATION OF BIOT NUMBER
      IF (BI.GT.Ø.Ø) GOTO 150
      DI=2.*RP
      REN=DI*U*1.E-3/RNU
      PR=Ø.73
      NUS=2.+Ø.6*(PR**(1./3.))*(REN**Ø.5)
      KS=CP*PS*ALPA*4.18
      BI=(KG/KS)*NUS*FRAD
```

```
150       BIR=BI/2.
          BIF=2.*BI
          BIFR=BIF/2.
          PI=3.14159
C   CALCULATION OF ROOTS
          CALL BITC(BIR)
          DO 1 I=1,5
1         D(I)=DVAL(I)
C   INTEGRATION BOUNDARIES
          IND=0
          XU1=RP
          NG1=12
          NG2=12
          NG3=12
          XL2=E0 - 3.*SIGMA
          XU2=E0 + 3.*SIGMA
          XL3=0.0
C   PHYSICAL PARAMETERS
          TE=373.0
          PW=1.
          PSW=PW/PS
          T0=283.
          RLAT=570.0
          RLAT=RLAT+(TE-T0)*(1.0+(CP/C0))
          P=RLAT*C0/CP
C   OUTPUT
          OPEN(UNIT=60,FILE='OUTPUT.DAT')
          WRITE(*,2005)
          WRITE(60,2005)
          WRITE(*,2001)
          WRITE(60,2001)
2001      FORMAT(10X,'PHYSICAL PROPERTIES OF THE COAL')
          WRITE(*,2002)CP,ALPA
          WRITE(60,2002)CP,ALPA
2002      FORMAT(2X,'SPECIFIC HEAT =',F5.3,'CAL/G DEGREE K',5X,'THERMAL DIF
         1FUSIVITY = ',F5.3,'SQ. MM/SEC')
          WRITE(*,2003)PS,RP
          WRITE(60,2003)PS,RP
2003      FORMAT(2X,'DENSITY SOLID=',F5.3,5X,'PARTICLE RADIUS =',F7.4,'MM')
          WRITE(*,2004)C0
          WRITE(60,2004)C0
2004      FORMAT(2X,'INITIAL MOISTURE CONTENT OF THE COAL =',F7.4,'G MOISTU
         1RE/G DRY COAL')
          WRITE(*,2008)TF
          WRITE(60,2008)TF
2008      FORMAT(2X,'FLAME TEMPERATURE =',F10.3,'DEGREE K')
          WRITE(*,2005)
          WRITE(60,2005)
2005      FORMAT(2X,'-------------------------------------------------------
         1-----------------------------------')
          WRITE(*,2006)
          WRITE(60,2006)
2006      FORMAT(5X,'SYSTEM PROPERTIES')
          WRITE(*,2007)BI,TA
          WRITE(60,2007)BI,TA
2007      FORMAT(2X,'HEAT-TRANSFER BIOT NO. =',F10.3,5X,'BED/AMBIENT TEMPER
         1ATURE = ',F10.3,'DEGREE K')
          WRITE(*,2005)
          WRITE(60,2005)
C
```

```
C  TRIAL AND ERROR PROCEDURE FOR CALCULATION OF DRYING TIME TAU UNDER
C  PYROLYSIS CONDITIONS
C
       NE=0
        IF (BI .LT. 5000) THEN
       TAUS=(2./3.+BI/6.)/(TA-TE)
       TAUS=TAUS*RP*RP*P/(ALPA*BI)
       CALL TTRCAL(BI,TAUS,TA,TE,P,TC1,B1,DPHI1,NE,ALPA,RP)
       TTR=TC1
       BVAL=B1
       DR=DPHI1
       TDRY=TTR*TAUS
       TAU1=TAUS
        ELSE
       BMN=5000.0
       NE=1
       TAUSL=RP*RP*P/(6.*(TA-TE)*ALPA)
       CALL TTRCAL(BMN,TAUSL,TA,TE,P,TC2,B2,DPHI2,NE,ALPA,RP)
       TAU2=TC2*TAUSL
       TTR=TC2
       BVAL=B2
       DR=DPHI2
       TDRY=TTR*TAUSL
        END IF
       WRITE(*,2020)
       WRITE(60,2020)
2020   FORMAT(2X,'CHEMICAL KINETIC PARAMETERS OF THE COAL')
       WRITE(*,2005)
       WRITE(60,2005)
       WRITE(*,2030)E0,SIGMA
       WRITE(60,2030)E0,SIGMA
2030   FORMAT(2X,'MEAN ACTIVATION ENERGY=',E15.5,'KJ/MOL',5X,'STANDARD D
     1EVIATION=',E15.5,'KJ/MOL')
       WRITE(*,2005)
       WRITE(60,2005)
       WRITE(*,2040)TDRY
       WRITE(60,2040)TDRY
2040   FORMAT(2X,'TOTAL DRYING TIME PYROLYSIS COND.=',E15.5,'SEC')
       WRITE(*,2005)
       WRITE(60,2005)
       WRITE(*,2010)
       WRITE(60,2010)
C
610     CONTINUE
       WRITE(*,1100)
       WRITE(60,1100)
1100   FORMAT(2X,'STAGE I/II, DRYING AND DEVOLATILIZATION')
       IFLAG1=0
       ADS = 0.0
       NW=0
       DO 10 I=2,100
       TM=RTM*(FLOAT(I-1))
       TMDR=TM/TDRY
       IW=1
       T1=TM
C
       IF (ADS .GE. 0.05) GOTO 111
       CALL WETTEM(T1,IW)
       DTH=TM/TAUS
       IF(T1.LT.0.0.OR.T1.GT.1.0)T1=0.0
```

```
          RE=RP*T1
          PHIM=T1**3.
            XL1=RE
         XU3=TM
         CALL CGQA(FUNC1,XL1,XU1,NG1,ANS)
2010     FORMAT(5X,'TIME(SECS)',10X,'MOISTURE',10X,'VOLATILES')
         ANS=(PHIM) + (3.0*ANS/(RP**3.))
         ADS=1.0-ANS
         WRITE(*,2011)TM,PHIM,ANS
         WRITE(60,2011)TM,PHIM,ANS
2011     FORMAT(2X,F10.4,5X,E15.5,5X,E15.5)
          IF (PHIM .LE. 0.02) GOTO 32
10       CONTINUE
C
111      CONTINUE
          TIG=TM-RTM
          DTHI=TIG/TAUS
          CALL PHICAL(DTHI,BI,SPHIG,IFLAG)
          ATIG=SPHIG*(TA-TE)*BI/(2.*SPHIG+BI*(1.-SPHIG))
          TSIG=(TA-TE)*BI*(1.-SPHIG)/(2.*SPHIG+BI*(1.-SPHIG))+TE
          TPHIG=PHIM**(1./3.)
          NW=1
C CALCULATION OF ROOTS
         CALL BITC(BIFR)
         DO 2 IN=1,5
2        D(IN) = DVAL(IN)
         IF (IFLAG1.EQ. 1) GOTO 60
         WRITE(*,1200)
         WRITE(60,1200)
1200     FORMAT(2X,'STAGE III, DRYING,DEVOL. AND COMBUSTION')
         IFLAG1=1
C         CORRECTION OF DRYING TIME FOR COMBUSTION CONDITIONS
          CON=C0
          RLAT=570.
          RLATN=RLAT+(TE-T0)*(1.0+(CP/CON))
          PN=RLATN*CON/CP
          NE1=0
            IF (BIF .LT. 5000.) THEN
          TAUSC=(2./3.+BIF/6.)/(TF-TE)
          TAUSC=TAUSC*RP**2.*PN/(ALPA*BIF)
          TAUSC=TAUSC*(1.-DTHI)+TIG
          TAUCP=TAUSC/TAUS
          CALL DRYTC(TF,TE,BIF,ATIG,TPHIG,P,TIG,TA,BI,TAUSC,ALPA,A1,
     1 RP,TCF,TPHIC)
          TTRF=TCF
          BVALF=A1
          DRF=TPHIC
            ELSE
          NE1=1
          BFM=5000.
          BM=2500.
          TAUSC=RP**2.*PN/(6.*(TF-TE)*ALPA)*(1.-DTHI)
          TAUSC=TAUSC*TTRF+TIG
          CALL DRYTC(TF,TE,BFM,ATIG,TPHIG,P,TIG,TA,BM,TAUSC,ALPA,A1,
     1 RP,TCF,TPHIC)
          TTRF=TCF
          BVALF=A1
          DRF=TPHIC
            END IF
C           TAUS=TAUSC
```

```
      TAUCOM=TAUSC
C TOTAL DRYING TIME UNDER COMBUSTION CONDITIONS
      TDRYC=TTRF*(TAUSC-TIG)+TIG
       WRITE(*,9001)TDRYC
       WRITE(60,9001)TDRYC
       TDRY=TDRYC
9001   FORMAT (2X,'TOTAL DRYING TIME COMB. COND.= ',E15.5,' SEC')
60     CONTINUE
       WRITE(*,*)' ENTER TIME INTERVAL RTM2'
       READ(*,*)RTM2
       NW=1
       DO 50 I=2,50
       TM=TIG+RTM2*(FLOAT(I-1))
       T1=TM
       IW=1
       IF (TM .GT. TDRYC) GOTO 32
       CALL WETCOM(T1,IW)
       DTH=TM/TAUS
      IF(T1.LT.0.0.OR.T1.GT.1.0)T1=0.0
      RE = RP * T1
      XL1 = RE
      XU1 = RP
      XU3 = TM
      CALL CGQA(FUNC1,XL1,XU1,NG1,ANS)
      PHIM = (T1**3.)
      ANS=(PHIM) + (3.0*ANS/(RP**3.))
      ADS=1.0-ANS
      WRITE(*,2011)TM,PHIM,ANS
      WRITE(60,2011)TM,PHIM,ANS
       IF (PHIM .LE. 0.02) GOTO 32
50     CONTINUE
32     XL1=0.0
       XU1=RP
       WRITE(*,1300)
       WRITE(60,1300)
1300   FORMAT(2X,'STAGE IV, DEVOLATILIZATION AND COMBUSTION')
       WRITE(*,*)' ENTER TIME INTERVAL RTM3'
       READ(*,*)RTM3
       DO 20 J=2,80
       TTM=RTM3*FLOAT(J-1) + TM
       XU3=TTM-TM
       CALL CGQA(FUNC4,XL1,XU1,NG1,ANS)
       PHIM=0.0
       ANS=3.0*ANS/(RP**3.)
       ADS=1.0-ANS
       WRITE(*,2011)TTM,PHIM,ADS
       WRITE(60,2011)TTM,PHIM,ADS
       IF (ANS .LE. 0.02) GOTO 33
20     CONTINUE
33     STOP
       END
C
       FUNCTION FUNC1(R)
       EXTERNAL FUNC2
       DIMENSION D(5),DVAL(5)
      COMMON/ABC/ TA,T0,RP,ALPA,E0,SIGMA,PI,XL2,XU2,XL3,XU3,RDUM,EDUM,TF
      COMMON/IKAC/ NG2,NG3,IND,CP,C0,TE,P,PS,BI,TDRY,BVAL,DR,TM,TTR,RE
      COMMON/FGH/ D,SPHIG
      COMMON/GH/ TTM,ADS,BIF,TAUS,DPHI,BVALF,DRF,TTRF,NW,TPHIG,TAUCOM
      COMMON/BIOT/DVAL
```

```
      RDUM=R
      CALL CGQB(FUNC2,XL2,XU2,NG2,ANS2)
      FUNC1=ANS2*R*R
      RETURN
      END
C
C
      FUNCTION FUNC2(E)
      EXTERNAL FUNC3
      DIMENSION D(5),DVAL(5)
     COMMON/ABC/ TA,TØ,RP,ALPA,EØ,SIGMA,PI,XL2,XU2,XL3,XU3,RDUM,EDUM,TF
     COMMON/IKAC/ NG2,NG3,IND,CP,CØ,TE,P,PS,BI,TDRY,BVAL,DR,TM,TTR,RE
     COMMON/FGH/ D,SPHIG
     COMMON/GH/ TTM,ADS,BIF,TAUS,DPHI,BVALF,DRF,TTRF,NW,TPHIG,TAUCOM
     COMMON/BIOT/DVAL
      EDUM=E
      CALL CGQC(FUNC3,XL3,XU3,NG3,ANS3)
      A=ANS3*1.67E13
      IF(A.GT.6Ø)GO TO 11
      A=EXP(-A)
      GO TO 12
11    A=Ø.Ø
12    FE=EXP((-(E-EØ)**2.)/(2.*(SIGMA**2.)))
      FE=FE/(SIGMA*SQRT(2.Ø*PI))
      FUNC2=FE*A
      RETURN
      END
C
C
      FUNCTION FUNC3(T)
      DIMENSION D(5),DVAL(5)
     COMMON/ABC/ TA,TØ,RP,ALPA,EØ,SIGMA,PI,XL2,XU2,XL3,XU3,RDUM,EDUM,TF
     COMMON/IKAC/ NG2,NG3,IND,CP,CØ,TE,P,PS,BI,TDRY,BVAL,DR,TM,TTR,RE
     COMMON/FGH/ D,SPHIG
     COMMON/GH/ TTM,ADS,BIF,TAUS,DPHI,BVALF,DRF,TTRF,NW,TPHIG,TAUCOM
     COMMON/BIOT/DVAL
      IW=Ø
      T=TM
       IF (NW .EQ. Ø) THEN
      CALL WETTEM(T,IW)
       ELSE
      CALL WETCOM(T,IW)
       END IF
     IF(IND.EQ.1)T=TA
      RT=8.315E-Ø3
      FUNC3=(EDUM/(RT*T))
      IF(FUNC3.GT.6Ø) GO TO 2Ø
      FUNC3=EXP(-FUNC3)
      GO TO 21
2Ø    FUNC3=Ø.Ø
21    RETURN
      END
C
C
C*********************************************************************
C********************* SUBROUTINE CGQA ***********************************
C*********************************************************************
C
      SUBROUTINE CGQA(CF,XL,XU,N,CVAL)
C
```

```
C          PERFORMS INTEGRATION OF A FUNCTION OF A SINGLE VARIABLE
C          BY GAUSSIAN QUADRATURE.
C
C          N = ORDER OF GUASSIAN QUADRATURE APPROXIMATION. VALUE MAY BE ON
C              (1,2,4,8,10,12,16,32).  IF N=1, CGQA PERFORMS A ONE-POINT
C              RECTANGULAR RULE INTEGRATION.
C          CF = EXTERNALLY SUPPLIED FUNCTION....MUST BE FUNCTION OF ONE
C               VARIABLE FOR CQG1.
C          XL = LOWER BOUND OF VARIABLE
C          XU = UPPER BOUND OF VARIABLE
C          CVAL = RESULTING VALUE OF THE INTEGRATION
C
C        NOTE:  CF MUST BE LISTED IN AN EXTERNAL STATEMENT IN THE
C                 CALLING ROUTINE
C
       DIMENSION Q1(52),Q2(24),Q3(32),NQ(8),NS(8),QG(108)
       EQUIVALENCE (Q1(1),QG(1)),(Q2(1),QG(53)),(Q3(1),QG(77))
       DATA Q1
      $                 /.2886751345948128820E0,0.5E0,.4305681557970262 9E0,
      $.1739274225687269 3E0,.1699905217924281 3E0,.3260725774312730 7E0,
      $ 0.4801449282487681 2E0,.5061426814518813 0E-1,.3983332387068133 7E0,
      $.1111905172266872 4E0,.2627662049581644 9E0,.1568533229389436 4E0,
      $.9171732124782490E-1,.1813418916891809 9E0,.4869532642585858 6E0,
      $.3333567215434407E-1,.4325316833444922 5E0,.7472567457529 03E-1,
      $.3397047841496122E0,.1095431812579910 2E0,.2166976970646236E0,
      $.1346333596549981 8E0,.7443716949081560 5E-1,.1477621123573764 4E0,
      $0.4907803171233596 3E0,.2358766819325591 4E-1,.4520586281852374 3E0,
      $.5346966299765921 5E-1,.3849513370971523 4E0,.8003916427167311E-1,
      $.2936589771433087 2E0,.1015837133615329 6E0,.1839157494990901 0E0,
      $.1167462682691774 0E0,.6261670425573445 8E-1,.1245735229067013 9E0,
      $.4947004674958249 7E0,.1357622970587704 7E-1,.4722875115366162 9E0,
      $.3112676196932394 6E-1,.4328156011939158 7E0,.4757925584124639 2E-1,
      $.3777022041775015 2E0,.6231448562776693 6E-1,.3089381222013218 7E0,
      $.7479799440828837E-1,.2290083388286136 9E0,.8457825969750127E-1,
      $.1408017753896294 6E0,.9130170752246179E-1,.4750625491881872 0E-1,
      $.9472530522753425E-1 /
       DATA Q2
      $                / 0.4975936099985106 8E+0   ,0.6170614899993599 8E-2 ,
      *             0.4873642779856547 5E+0   ,    0.1426569431446683 2E-1 ,
      *             0.4691372760013663 8E+0   ,    0.2213871940870990 3E-1 ,
      *             0.4432077635022005 2E+0   ,    0.2964929245771889 0E-1 ,
      *             0.4100009929869514 6E+0   ,    0.3667324070554015 3E-1 ,
      *             0.3700620957892771 8E+0   ,    0.4309508076597663 8E-1 ,
      *             0.3240468259684877 8E+0   ,    0.4880932605205694 4E-1 ,
      *             0.2727107356944197 7E+0   ,    0.5372213505798281 7E-1 ,
      *             0.2168967538130225 7E+0   ,    0.5775283402686280 1E-1 ,
      *             0.1575213398480816 9E+0   ,    0.6083523646390169 6E-1 ,
      *             0.9555943373680815 0E-1   ,    0.6291872817341414 8E-1 ,
      *             0.3202844643130281 3E-1   ,    0.6396909767337607 8E-1 /
       DATA Q3
      $                /0.4986319309247407 8E+0 ,    0.3509305004735048 3E-2 ,
      *             0.4928057557726341 7E+0   ,    0.8137197365452835 0E-2 ,
      *             0.4823811277937532 2E+0   ,    0.1269603265463103 0E-1 ,
      *             0.4674530379688698 4E+0   ,    0.1713693145651071 7E-1 ,
      *             0.4481605778830260 6E+0   ,    0.2141794901111334 0E-1 ,
      *             0.4246838068662849 9E+0   ,    0.2549902963118808 8E-1 ,
      *             0.3972418979839712 0E+0   ,    0.2934204673926777 4E-1 ,
      *             0.3660910593701448 4E+0   ,    0.3291111138818092 3E-1 ,
      *             0.3315221334651076 0E+0   ,    0.3617289705442425 3E-1 ,
      *             0.2938578786203811 6E+0   ,    0.3909694789353515 3E-1 ,
```

```
     *            0.25344995446611470E+0   ,     0.41655962113473378E-1 ,
     *            0.21067563806531767E+0   ,     0.43826046502201906E-1 ,
     *            0.16593430114106382E+0   ,     0.45586939347881942E-1 ,
     *            0.11964368112606854E+0   ,     0.46922199540402283E-1 ,
     *            0.72235980791398250E-1   ,     0.47819360039637430E-1 ,
     *            0.24153832843869158E-1   ,     0.48270044257363900E-1 /
     $,N0/2,4,8,10,12,16,24,32/,
     $ NS/1,3,7,15,25,37,53,77/
      IF(N .EQ. 1) GO TO 200
      DO 300 L=1,8
      IF(N.EQ.N0(L)) GO TO 301
 300  CONTINUE
9001   WRITE(5,905) N
  905 FORMAT('0 CALLING PARAMETER =',I5,'   INTEGRATION NOT POSSIBLE'//)
      RETURN
  200 AX=0.5*(XU+XL)
      CVAL=CF(AX)*(XU-XL)
      RETURN
 301  CONTINUE
      NP=NS(L)
      NE=NP+N-1
      AX=0.5*(XU+XL)
      BX=XU-XL
      CVAL=0.
      DO 350 J=NP,NE,2
      DX=QG(J)*BX
      CVAL=CVAL+QG(J+1)*(CF(AX+DX)+CF(AX-DX))
 350  CONTINUE
      CVAL=CVAL*BX
      RETURN
      END
C*******************************************************************************
C********************* SUBROUTINE CGQB *****************************************
C*******************************************************************************
C
      SUBROUTINE CGQB(CF,XL,XU,N,CVAL)
C
C        PERFORMS INTEGRATION OF A FUNCTION OF A SINGLE VARIABLE
C        BY GAUSSIAN QUADRATURE.
C
C        N = ORDER OF GUASSIAN QUADRATURE APPROXIMATION. VALUE MAY BE ON
C            (1,2,4,8,10,12,16,32).  IF N=1, CGQB PERFORMS A ONE-POINT
C            RECTANGULAR RULE INTEGRATION.
C        CF = EXTERNALLY SUPPLIED FUNCTION....MUST BE FUNCTION OF ONE
C             VARIABLE FOR CQG1.
C        XL = LOWER BOUND OF VARIABLE
C        XU = UPPER BOUND OF VARIABLE
C        CVAL = RESULTING VALUE OF THE INTEGRATION
C
C       NOTE:  CF MUST BE LISTED IN AN EXTERNAL STATEMENT IN THE
C                CALLING ROUTINE
C
      DIMENSION Q1(52),Q2(24),Q3(32),N0(8),NS(8),QG(108)
      EQUIVALENCE (Q1(1),QG(1)),(Q2(1),QG(53)),(Q3(1),QG(77))
      DATA Q1
     $                /.28867513459481288E0,0.5E0,.43056815579702629E0,
     $.17392742256872693E0,.16999052179242813E0,.32607257743127307E0,
     $ 0.48014492824876812E0,.50614268145188130E-1,.39833323870681337E0,
     $.11119051722668724E0,.26276620495816449E0,.15685332293894364E0,
     $.91717321247824906E-1,.18134189168918099E0,.48695326425858586E0,
```

```
     $.3333567215434407E-1,.4325316833444922SE0,.7472567457529Ø3E-1,
     $.3397047841496122E0,.1095431812579910ZE0,.2166976970646236E0,
     $.1346333596549981ØE0,.7443716949081560SE-1,.1477621123573764ØE0,
     $Ø.4907803171233596ØE0,.2358766819325591ØE-1,.4520586281852374ØE0,
     $.5346966299765921SE-1,.3849513370971523ØE0,.8003916427167311E-1,
     $.2936589771433087ØE0,.1015837133615329ØE0,.1839157494990901ØE0,
     $.1167462682691774ØE0,.6261670425573445ØE-1,.1245735229067013ØE0,
     $.4947004674958249ZE0,.1357622970587704ZE-1,.4722875115366162ØE0,
     $.3112676196932394ØE-1,.4328156011939158ZE0,.4757925584124639ZE-1,
     $.3777022041775015ZE0,.6231448562776693ØE-1,.3089381222013218ZE0,
     $.7479799440828837E-1,.2290083888286136ØE0,.8457825969750127E-1,
     $.1408017753896294ØE0,.9130170752246179E-1,.4750625491881872ØE-1,
     $.9472530522753425E-1 /
      DATA Ø2
     $              / Ø.4975936099985106ØE+Ø   ,Ø.6170614899993599ØE-2 ,
     *            Ø.4873642779856547ØE+Ø   ,  Ø.1426569431446683ØE-1 ,
     *            Ø.4691372760013663ØE+Ø   ,  Ø.2213871940870990ZE-1 ,
     *            Ø.4432077635022005ZE+Ø   ,  Ø.2964929245771889ØE-1 ,
     *            Ø.4100009929869514ØE+Ø   ,  Ø.3667324070554015ZE-1 ,
     *            Ø.3700620957892771ØE+Ø   ,  Ø.4309508076597663ØE-1 ,
     *            Ø.3240468259684877ØE+Ø   ,  Ø.4880932605205694ØE-1 ,
     *            Ø.2727107356944197ZE+Ø   ,  Ø.5372213505798281ZE-1 ,
     *            Ø.2168967538130225ZE+Ø   ,  Ø.5775283402686280ZE-1 ,
     *            Ø.1575213398480816ZE+Ø   ,  Ø.6083523646390169ØE-1 ,
     *            Ø.9555943373680815ØE-1   ,  Ø.6291872817341414ØE-1 ,
     *            Ø.3202844643130281ZE-1   ,  Ø.6396909767337607ØE-1 /
      DATA Ø3
     $              /Ø.4966319309247407ØE+Ø  ,  Ø.3509305004735048ZE-2 ,
     *            Ø.4928057557726341ZE+Ø   ,  Ø.8137197365452835ØE-2 ,
     *            Ø.4823811277937532ZE+Ø   ,  Ø.1269603265463103ØE-1 ,
     *            Ø.4674530379688698ØE+Ø   ,  Ø.1713693145651071ZE-1 ,
     *            Ø.4481605778830260ØE+Ø   ,  Ø.2141794901111334ØE-1 ,
     *            Ø.4246838066662849ZE+Ø   ,  Ø.2549902963118808ØE-1 ,
     *            Ø.3972418979839712ØE+Ø   ,  Ø.2934204673926777ØE-1 ,
     *            Ø.3660910593701448ØE+Ø   ,  Ø.3291111138818092ZE-1 ,
     *            Ø.3315221334651076ØE+Ø   ,  Ø.3617289705442425ZE-1 ,
     *            Ø.2938578786203811ØE+Ø   ,  Ø.3909694789353515ZE-1 ,
     *            Ø.2534499544661147ØE+Ø   ,  Ø.4165596211347337ØE-1 ,
     *            Ø.2106756380653176ZE+Ø   ,  Ø.4382604650220190ØE-1 ,
     *            Ø.1659343011410638ZE+Ø   ,  Ø.4558693934768194ZE-1 ,
     *            Ø.1196436811260685ØE+Ø   ,  Ø.4692219954040228ZE-1 ,
     *            Ø.7223598079139825ØE-1   ,  Ø.4781936003963743ØE-1 ,
     *            Ø.2415383284386915ØE-1   ,  Ø.4827004425736390ØE-1 /
     $,NQ/2,4,8,10,12,16,24,32/,
     $ NS/1,3,7,15,25,37,53,77/
      IF(N .EQ. 1) GO TO 200
      DO 300 L=1,8
      IF(N.EQ.NQ(L)) GO TO 301
  300 CONTINUE
 9002   WRITE(5,905) N
  905 FORMAT('Ø CALLING PARAMETER =',I5,'   INTEGRATION NOT POSSIBLE'//)
      RETURN
  200 AX=Ø.5*(XU+XL)
      CVAL=CF(AX)*(XU-XL)
      RETURN
  301 CONTINUE
      NP=NS(L)
      NE=NP+N-1
      AX=Ø.5*(XU+XL)
      BX=XU-XL
```

```
      CVAL=0.
      DO 350 J=NP,NE,2
      DX=QG(J)*BX
      CVAL=CVAL+QG(J+1)*(CF(AX+DX)+CF(AX-DX))
 350  CONTINUE
      CVAL=CVAL*BX
      RETURN
      END
C*******************************************************************************
C********************** SUBROUTINE CGQC ****************************************
C*******************************************************************************
C
      SUBROUTINE CGQC(CF,XL,XU,N,CVAL)
C
C         PERFORMS INTEGRATION OF A FUNCTION OF A SINGLE VARIABLE
C         BY GAUSSIAN QUADRATURE.
C
C         N = ORDER OF GUASSIAN QUADRATURE APPROXIMATION. VALUE MAY BE ON
C             (1,2,4,8,10,12,16,32).  IF N=1, CGQC PERFORMS A ONE-POINT
C             RECTANGULAR RULE INTEGRATION.
C         CF = EXTERNALLY SUPPLIED FUNCTION....MUST BE FUNCTION OF ONE
C              VARIABLE FOR CQG1.
C         XL = LOWER BOUND OF VARIABLE
C         XU = UPPER BOUND OF VARIABLE
C         CVAL = RESULTING VALUE OF THE INTEGRATION
C
C       NOTE:  CF MUST BE LISTED IN AN EXTERNAL STATEMENT IN THE
C                CALLING ROUTINE
C
      DIMENSION Q1(52),Q2(24),Q3(32),NQ(8),NS(8),QG(108)
      EQUIVALENCE (Q1(1),QG(1)),(Q2(1),QG(53)),(Q3(1),QG(77))
      DATA Q1
     $                 /.2886751345948128S2E0,Ø.5E0,.43056815579702629E0,
     $.17392742256872693E0,.16999052179242813E0,.32607257743127307E0,
     $ Ø.48014492824876812E0,.50614268145188130E-1,.39833323870681337E0,
     $.11119051722668724E0,.26276620495816449E0,.15685332293894364E0,
     $.91717321247824Ø0E-1,.18134189168918099E0,.48695326425858586E0,
     $.33335672154344Ø7E-1,.43253168334449225E0,.74725674575290Ø3E-1,
     $.33970478414961Ø2E0,.10954318125799102E0,.21669769706462Ø6E0,
     $.13463335965499818E0,.74437169490815605E-1,.14776211235737644E0,
     $Ø.49078031712335963E0,.23587668193255914E-1,.45205862818523743E0,
     $.53469662997659215E-1,.38495133709715234E0,.80039164271673Ø1E-1,
     $.29365897714330872E0,.10158371336153296E0,.18391574949909010E0,
     $.11674626826917740E0,.62616704255734458E-1,.12457352290670139E0,
     $.49470046749582497E0,.13576229705877047E-1,.47228751153661629E0,
     $.31126761969323946E-1,.43281560119391587E0,.47579255841246392E-1,
     $.37770220417750152E0,.62314485627766936E-1,.30893812220132187E0,
     $.74797994408288Ø7E-1,.22900838882861369E0,.84578259697501Ø7E-1,
     $.14088017753896294ØE0,.91301707522461Ø9E-1,.47506254918818720E-1,
     $.94725305227534Ø5E-1 /
      DATA Q2
     $                / Ø.49759360999851068E+0   ,Ø.61706146999935998E-2 ,
     *             Ø.48736427798565475E+0    ,    Ø.14265694314466832E-1 ,
     *             Ø.46913727600136638E+0    ,    Ø.22138719408709903E-1 ,
     *             Ø.44320776350220052E+0    ,    Ø.29649292457718890E-1 ,
     *             Ø.41000099298695146E+0    ,    Ø.36673240705540153E-1 ,
     *             Ø.37006209578927718E+0    ,    Ø.43095080765976638E-1 ,
     *             Ø.32404682596848778E+0    ,    Ø.48809326052056944E-1 ,
     *             Ø.27271073569441977E+0    ,    Ø.53722135057962817E-1 ,
     *             Ø.21689675381302257E+0    ,    Ø.57752834026862801E-1 ,
```

```
     *             0.15752133984808169E+0    ,     0.60835236463901696E-1 ,
     *             0.95559433736808150E-1    ,     0.62918728173414148E-1 ,
     *             0.32028446431302813E-1    ,     0.63969097673376078E-1 /
      DATA Q3
     $               /0.49863193092474078E+0 ,     0.35093050047350483E-2 ,
     *             0.49280575577263417E+0    ,     0.81371973654528350E-2 ,
     *             0.48238112779375322E+0    ,     0.12696032654631030E-1 ,
     *             0.46745303796886984E+0    ,     0.17136931456510717E-1 ,
     *             0.44816057788302606E+0    ,     0.21417949011113340E-1 ,
     *             0.42468380686628499E+0    ,     0.25499029631188088E-1 ,
     *             0.39724189798397120E+0    ,     0.29342046739267774E-1 ,
     *             0.36609105937014484E+0    ,     0.32911111388180923E-1 ,
     *             0.33152213346510760E+0    ,     0.36172897054424253E-1 ,
     *             0.29385787862038116E+0    ,     0.39096947893535153E-1 ,
     *             0.25344995446611470E+0    ,     0.41655962113473378E-1 ,
     *             0.21067563806531767E+0    ,     0.43826046502201906E-1 ,
     *             0.16593430114106382E+0    ,     0.45586939347881942E-1 ,
     *             0.11964368112606854E+0    ,     0.46922199540402283E-1 ,
     *             0.72235980791398250E-1    ,     0.47819360039637430E-1 ,
     *             0.24153832843869158E-1    ,     0.48270044257363900E-1 /
     $,NQ/2,4,8,10,12,16,24,32/,
     $ NS/1,3,7,15,25,37,53,77/
      IF(N .EQ. 1) GO TO 200
      DO 300 L=1,8
      IF(N.EQ.NQ(L)) GO TO 301
 300  CONTINUE
9003   WRITE(5,905) N
  905 FORMAT('0 CALLING PARAMETER =',I5,'   INTEGRATION NOT POSSIBLE'//)
      RETURN
  200 AX=0.5*(XU+XL)
      CVAL=CF(AX)*(XU-XL)
      RETURN
 301  CONTINUE
      NP=NS(L)
      NE=NP+N-1
      AX=0.5*(XU+XL)
      BX=XU-XL
      CVAL=0.
      DO 350 J=NP,NE,2
      DX=QG(J)*BX
      CVAL=CVAL+QG(J+1)*(CF(AX+DX)+CF(AX-DX))
 350  CONTINUE
      CVAL=CVAL*BX
      RETURN
      END
C
C
C
       SUBROUTINE WETTEM(T1,IW)
       DIMENSION D(5),DVAL(5)
      COMMON/ABC/ TA,T0,RP,ALPA,E0,SIGMA,PI,XL2,XU2,XL3,XU3,RDUM,EDUM,TF
      COMMON/IKAC/ NG2,NG3,IND,CP,C0,TE,P,PS,BI,TDRY,BVAL,DR,TM,TTR,RE
      COMMON/FGH/ D,SPHIG
      COMMON/GH/ TTM,ADS,BIF,TAUS,DPHI,BVALF,DRF,TTRF,NW,TPHIG,TAUCOM
      COMMON/BIOT/DVAL
        DTH=T1/TAUS
       CALL PHICAL(DTH,BI,DPHI,IFLAG)
       A5=BI*(1.0-DPHI)
       TS=((TA-TE)*A5/(2.0*DPHI + A5)) + TE
       AT=DPHI*BI*(TA-TE)/(2.*DPHI+A5)
```

```
      PHIST=DPHI
C
C  CALCULATION OF THE CUBIC DRYING EQUATION
C
       A2=BVAL
       E=(TE+P)/2.
       B=PHIST*BI*(TA-TE)
       B=B/(12.Ø*(2.Ø*PHIST+BI*(1.Ø-PHIST)))
       C=(TE+5.Ø*TS)/12.Ø
       D1=(TE+TS)/4.
       F=(PHIST**2.-1.)/(DR*DR-1.Ø)
       G=D1-E-B
       H=C-B-D1
       R=B-C+E-A2*F
       PO=Ø.5
       N=Ø
25     FDRY=B*PO**3.+G*PO**2.+H*PO+R
       DFDRY=3.*B*PO**2.+2.*G*PO+H
       PN=PO-FDRY/DFDRY
       IF (PN.GE.Ø.Ø.AND.PN.LE.1.Ø.AND.ABS(PN-PO).LE.Ø.ØØ5)
     1GOTO 15
       N=N+1
       IF(N.GT.1ØØ) GOTO 14
       PO=PN
       GOTO 25
14     IFLAG=Ø
       GOTO 16
C
C  CALCULATION OF TEMPERATURE (TRANSIENT AND P.S.S MODELS)  .
C
15     IFLAG=1
       GOTO 16
16    IF (IW .EQ. 1) GOTO 17
      GOTO 18
17    T1=PN
      GOTO 19
18    RW=RDUM/RP
      PHI=(RW-PN)/(1.Ø-PN)
       A3=(1.Ø-PN)*PHIST*BI*(TA-TE)
       A3=A3/(2.*PHIST + BI*(1.Ø - PHIST))
        T1=TE+(TS-TE)*(2.Ø*PHI-PHI*PHI)+A3*(PHI*PHI-PHI)
        IF (T1.LE.TE)T1 = TØ
19      RETURN
        END
C
C  SUBROUTINE PHICAL IS BASED ON THE PSEUDO STEADY STATE MODEL .
C
       SUBROUTINE PHICAL(THETA,BI,PHI,IFLAG)
       PO=Ø.5
2Ø     FP=(3.*BI/(BI+4.))*PO*PO-((BI-2.)/(BI+4.))*2.*PO*PO*PO+THETA-1.Ø
       DFP=(3.*BI/(BI+4.))*2.*PO-((BI-2.)/(BI+4.))*6.*PO*PO
       PN=PO-FP/DFP
       IF(PN.GE.Ø.Ø.AND.ABS(PN-PO).LT.Ø.ØØ1)GO TO 3Ø
       PO=PN
       GO TO 2Ø
3Ø     IF(PN.LE.Ø.Ø)IFLAG=1
       IF(PN.LE.Ø.Ø)GO TO 4Ø
       IFLAG=Ø
4Ø     PHI=PN
       RETURN
```

```
      END
C
C  THIS SUBROUTINE CALCULATES THE DRYING TIME RATIO BETWEEN TRANSIENT
C  AND PSEUDO STEADY STATE MODELS
C
      SUBROUTINE TTRCAL(BI,TAU,TA,TE,P,TC,B,DPHI,NE,ALPA,RP)
      CONV=Ø.ØØØ5
      TC=Ø.5
1     DTH=TC
      CALL PHICAL(DTH,BI,DPHI,IFLAG)
      A1=BI*(1.Ø-DPHI)
      TST=((TA-TE)*A1/(2.Ø*DPHI+A1)) + TE
      IF(TST.LE.TE)TST=TE
      B=(TE+P)*Ø.5 - ((TE+5.*TST)/12.)
      B=B+BI*DPHI*(TA-TE)/(12.*(2.Ø*DPHI + A1))
      IF(NE.EQ.1)GO TO 2
      Z=(ALPA*BI*(TA-TE)*TAU)*(1.Ø-DPHI*DPHI)*(3./(BI+4.))
      GO TO 3
2     Z=ALPA*(TC+2.-2.*DPHI*DPHI*DPHI)*(TA-TE)*TAU
3     Z=Z/(RP*RP)
      IF((ABS(B-Z)/B).GE.Ø.ØØ2Ø)GO TO 4
      GO TO 6
4     TC=TC+CONV
      IF(TC.GT.1.Ø)GO TO 5
      GO TO 1
5     CONV=CONV/4.Ø
      TC=Ø.2
      GO TO 1
6     RETURN
      END
C
C  SUBROUTINE PHICOM IS BASED ON THE PSEUDO STEADY STATE MODEL COMBUST.
C  COONDITIONS.
C
       SUBROUTINE PHICOM(THETA,BIF,BI,PHI,TAUCP,TF,TA,TE,SPHIG)
       PO=SPHIG
       CONV=Ø.ØØØ5
       FP1=(TA-TE)/(TF-TE)*(BI/BIF)
2Ø     FP=FP1/(BI+4.)*(3.*BIF*PO**2.-2.*(BIF-2.)*PO**3.)
       FP=FP+THETA-TAUCP
       IF(ABS(FP).LE.Ø.ØØØ5) GOTO 1Ø
       PO=PO-CONV
       GOTO 2Ø
1Ø     PN=PO
       IF(PN.LE.Ø.Ø) PN=Ø.Ø
       PHI=PN
       RETURN
       END
C
C  SUBROUTINE CALCULATES DRYING TIME RATIO BETWEEN TRANSIENT
C  AND PSEUDO STEADY STATE MODELS COMBUSTION CONDITION
C
      SUBROUTINE DRYTC(TF,TE,BIF,ATIG,PHIG,P,TIG,TA,BI,TAUS,
     1  ALPA,A1,R,TC,PHIC)
       TC=Ø.5
       TCO=TAUS-TIG
       CONV=Ø.ØØØ5
1      CALL PHICAL(TC,BIF,PHIC,IFLAG)
       TSC=(TF-TE)*BIF*(1.-PHIC)/(2.*PHIC+BIF*(1.-PHIC))+TE
       ATC=PHIC*BIF*(TF-TE)/(2.*PHIC+BIF*(1.-PHIC))
```

```
      B1=ATIG/12.*(1.-PHIG)*(1.-PHIG**2.)
      B2=(TE+5*TSIG)/12.*(1.-PHIG)
      B3=(TE+TSIG)/4.*PHIG*(1.-PHIG)
      B4=ATC/12.*PHIG**3.
      B5=(TE+5.*TSC)/12.*PHIG**2.
      B6=(TE+P)/2.
      A1=B1-B2-B3+B4-B5+B6
      A2=BIF*(TF-TE)/(BIF+4.)*TCO+BI*(TA-TE)/(BI+4.)*TIG
      A2=A2*3.*ALPA/(R**2.)*(1.-PHIC**2.)
      IF((ABS(A1-A2)/A1) .GE. 0.002) GOTO 4
      GOTO 6
4     TC=TC+CONV
      IF (TC .GT. 1.0) GOTO 5
      GOTO 1
5     CONV=CONV/4.
      TC=0.1
      GOTO 1
6     RETURN
      END
C
C
C  WETCOM CALCULATES DRYING EQUATION AND TEMPERATURE PROFILE TRANSIENT
C  EQUATION UNDER COMBUSTION CONDITIONS
C
      SUBROUTINE WETCOM(T1,IW)
      DIMENSION D(5),DVAL(5)
     COMMON/ABC/ TA,T0,RP,ALPA,E0,SIGMA,PI,XL2,XU2,XL3,XU3,RDUM,EDUM,TF
     COMMON/IKAC/ NG2,NG3,IND,CP,C0,TE,P,PS,BI,TDRY,BVAL,DR,TM,TTR,RE
     COMMON/FGH/ D,SPHIG
     COMMON/GH/ TTM,ADS,BIF,TAUS,DPHI,BVALF,DRF,TTRF,NW,TPHIG,TAUCOM
     COMMON/BIOT/DVAL
      DTH=T1/TAUS
      TAUCP=TAUCOM/TAUS
      CALL PHICOM(DTH,BIF,BI,PHI,TAUCP,TF,TA,TE,SPHIG)
      TSC=(TF-TE)*(BIF*(1.-PHI))/(2.*PHI+BIF*(1.-PHI))+TE
      ATC=BIF*(TF-TE)*PHI/(2.*PHI+BIF*(1.-PHI))
      A2=BVALF
      E=(TE+P)/2.
      C=(TE+5.*TSC)/12.
      D1=(TE+TSC)/4.
      G=ATC/12.
      F=(PHI**2.-1.)/(DRF**2.-1.)
      H=C*TPHIG-D1*TPHIG-G*TPHIG**2.
      R=G*TPHIG-D1+E
      P0=0.5
      N=0
25    FDRY=H*P0-R*P0**2.+G*P0**3.-A2*(F-1.)
      DFDRY=H-2.*R*P0+3.*G*P0**2.
      PN=P0-FDRY/DFDRY
      IF(PN.GE.0.0.AND.PN.LE.1.0.AND.ABS(PN-P0).LE.0.005)
     1GOTO 15
      N=N+1
      IF(N.GT.100) GOTO 14
      P0=PN
      GOTO 25
14    IFLAG=0
      GOTO 16
C
C CALCULATION OF TEMPERATURE PROFILE
C
```

```
15      IFLAG=1
        GOTO 16
16      IF(IW .EQ. 1.) GOTO 17
        GOTO 18
17      T1=PN
        GOTO 19
18      RW=RDUM/RP
        PHIØ=(RW-PN)/(1.-PN)
        A3=(1.Ø-PN)*PHIST*BIF*(TF-TE)
        A3=A3/(2.*PHIST+BIF*(1.-PHIST))
        T1=TE+(TSC-TE)*(2*PHIØ-PHIØ**2.)+A3*(PHIØ**2.-PHIØ)
        IF (T1 .LE. TE) T1=TØ
19      DPHI=PHI
        RETURN
        END
C
C
       FUNCTION FUNC4(R)
       EXTERNAL FUNC5
       DIMENSION D(5),DVAL(5)
      COMMON/ABC/ TA,TØ,RP,ALPA,EØ,SIGMA,PI,XL2,XU2,XL3,XU3,RDUM,EDUM,TF
      COMMON/IKAC/ NG2,NG3,IND,CP,CØ,TE,P,PS,BI,TDRY,BVAL,DR,TM,TTR,RE
      COMMON/FGH/ D,SPHIG
      COMMON/GH/ TTM,ADS,BIF,TAUS,DPHI,BVALF,DRF,TTRF,NW,TPHIG,TAUCOM
      COMMON/BIOT/DVAL
       RDUM=R
       CALL CGQB(FUNC5,XL2,XU2,NG2,ANS2)
       FUNC4=ANS2*R*R
       RETURN
       END
C
C
       FUNCTION FUNC5(E)
       EXTERNAL FUNC6
       DIMENSION D(5),DVAL(5)
      COMMON/ABC/ TA,TØ,RP,ALPA,EØ,SIGMA,PI,XL2,XU2,XL3,XU3,RDUM,EDUM,TF
      COMMON/IKAC/ NG2,NG3,IND,CP,CØ,TE,P,PS,BI,TDRY,BVAL,DR,TM,TTR,RE
      COMMON/FGH/ D,SPHIG
      COMMON/GH/ TTM,ADS,BIF,TAUS,DPHI,BVALF,DRF,TTRF,NW,TPHIG,TAUCOM
      COMMON/BIOT/DVAL
       EDUM=E
       CALL CGQC(FUNC6,XL3,XU3,NG3,ANS3)
DRV05940
       A=ANS3*1.67E13
       IF(A.GT.6Ø) GOTO 11
       A=EXP(-A)
       GOTO 12
11     A=Ø.Ø
12     FE=EXP((-(E-EØ)**2.)/(2.*(SIGMA**2.)))
       FE=FE/(SIGMA*SQRT(2.Ø*PI))
       FUNC5=FE*A
       RETURN
       END
C
C
       FUNCTION FUNC6(T)
       DIMENSION D(5),DVAL(5)
      COMMON/ABC/ TA,TØ,RP,ALPA,EØ,SIGMA,PI,XL2,XU2,XL3,XU3,RDUM,EDUM,TF
      COMMON/IKAC/ NG2,NG3,IND,CP,CØ,TE,P,PS,BI,TDRY,BVAL,DR,TM,TTR,RE
      COMMON/FGH/ D,SPHIG
```

```
      COMMON/GH/ TTM,ADS,BIF,TAUS,DPHI,BVALF,DRF,TTRF,NW,TPHIG,TAUCOM
      COMMON/BIOT/DVAL
      IF (T .GE. TDRY) GOTO 30
      IW=0
      TT=T
      CALL WETCOM(TT,IW)
      GOTO 40
30    THETA=TM/TAUS
      TAUCP=TAUCOM/TAUS
      CALL PHICOM(THETA,BIF,BI,PHI,TAUCP,TF,TA,TE,SPHIG)
      C1=BF*(1.-PHI)
      C2=((TF-TE)*C1)/(2.*PHI+C1)
      C3=PHI*BIF*(TF-TE)
      C3=C3/(2.*PHI+C1)
      SUM=0.0
      SUM1=0.0
      DO 10 I=1,5
       Y=D(I)
       C4=SIN(Y)
       C5=COS(Y)
       C6=(TF-TE)*(C4-Y*C5)
       C6=C6-(2.*C2-C3)*(C5*((2./Y)-Y)+2.*C4-(2./Y))
       C6=C6-(C3-C2)*(C5*((6./Y)-Y)+3.*C4*(1.-(2./(Y*Y))))
       C6=2.*C6/(Y-C4*C5)
       TER=Y*Y*ALPA*(T-TDRY)/(RP*RP)
       IF (TER.GT.60.0) GOTO 1
       TER=EXP(-TER)
       GOTO 2
1      TER=0.0
2      TES=TER*(SIN(Y))/Y
       SUM1=SUM+C6*TES
       TS=TA-SUM1
       TER=TER*(SIN(Y*RDUM/RP))/(Y*RDUM/RP)
       SUM=SUM+C6*TER
10     CONTINUE
       TT=TA-SUM
40     IF(IND.EQ.1) TT=TA
       RT=8.315E-03
       FUNC6=(EDUM/(RT*TT))
       IF (FUNC6.GT.60.0) GOTO 20
       FUNC6=EXP(-FUNC6)
       GOTO 21
20     FUNC6=0.0
21     RETURN
       END
C
C
       SUBROUTINE BITC(BI)
       DIMENSION D(5),DVAL(5)
       COMMON/BIOT/DVAL
       BE=.001
       N=0
2      FBE=1.0-BI-BE*COS(BE)/SIN(BE)
       IF(ABS(FBE).LE.0.01) GOTO 1
       BE=BE+0.00005
       IF(BE.GT.50.00) GOTO 3
       GOTO 2
1      N=N+1
       IF(N.GE.6) GOTO 3
       DVAL(N)=BE
```

```
      BE=BE+2.2
      GOTO 2
3     RETURN
      END
```

PROGRAM NAME: DSV.FOR

SYSTEM: VAX-VMS (FORTRAN 4.4)

COMMENTS:

This program calculates the coupled drying and devolatilization characteristics of a single coal particle under pyrolysis conditions. Drying is modelled from the transient drying model using a moving wet core radius and it also includes a moving particle diameter due to shrinkage. The computed temperature profiles are used to determine the devolatilization behaviour of the coal particle. Devolatilization is modelled using the DAE model as developed by Anthony and Howard. After drying is completed, the temperature profile (at the end of drying) is used as an initial condition in the transient heat conduction equation with a convective boundary condition. The temperature profiles computed are used to characterize the devolatilization behaviour. The numerical integrations are performed using a Gaussian quadrature procedure (subroutine CGQA). The program is interactive and the input parameters are asked when running the program.

```
C*********************************DSV.FOR*************************************
C  FORTRAN PROGRAMM FOR COUPLED DRYING AND DEVOLATILIZATION OF A SINGLE
C  PARTICLE SHRINKAGE INCLUDED
C
      INTEGER N,ITMAX,IER
      REAL KG,KS,NUS
      REAL WK1(22),PHIS(1),PAR1(3),FNORM1
      REAL WK2(22),PHIT(1),PAR2(7),FNORM2
      DIMENSION D(5),DVAL(5)
       EXTERNAL PHISM
       EXTERNAL PHITM
       EXTERNAL FUNC1
       EXTERNAL FUNC4
       COMMON/ABC/ TA,TØ,RP,ALPA,EØ,SIGMA,PI,XL2,XU2,XL3,XU3,RDUM,EDUM
      COMMON/IKAC/ NG2,NG3,IND,CP,CØ,TE,P,PS,BI,TDRY,BVAL,DR,TM,TTR,RE
      COMMON/FGH/ D
      COMMON/GH/ TTM,TAUS,XFS
      COMMON/BIOT/DVAL
C  INPUT PARAMETER
        TYPE*,' ENTER TIME INTERVAL NTM [-]'
        READ*,NTM
        TYPE*,' ENTER AMBIENT TEMPERATURE [K]'
        READ*,TA
        TYPE*,' ENTER PARTICLE RADIUS [mm]'
        READ*,RP
        TYPE*,' ENTER ALPA [mm2/s]'
        READ*,ALPA
        TYPE*,' ENTER EØ [kJ/mol]'
        READ*,EØ
        TYPE*,' ENTER SIGMA [kJ/mol]'
        READ*,SIGMA
        TYPE*,' ENTER DENSITY OF THE COAL [g/cm3]'
        READ*,PS
        TYPE*,' ENTER SPECIFIC HEAT OF COAL [cal/g K]'
        READ*,CP
        TYPE*,' ENTER ORIGINAL MOISTURE CONTENT OF THE COAL [g/g]'
        READ*,CØ
        TYPE*,' ENTER GAS VELOCITY [m/s]'
        READ*,U
        TYPE*,' ENTER SHRINKAGE FACTOR [-]'
        READ*,FS
        TYPE*,' ENTER RADIATION FACTOR [-]'
        READ*,FRAD
        TYPE*,' ENTER THERMAL CONDUCTIVITY OF GAS [W/mK]'
        READ*,KG
        TYPE*,' ENTER VISCOSITY OF GAS AT TA [m2/s]'
        READ*,RNU
C  INTEGRATIONS BOUNDARIES
       XU1=RP
       NG1=12
       NG2=12
       NG3=32
       XL2=EØ - 3.*SIGMA
       XU2=EØ + 3.*SIGMA
       XL3=Ø.Ø
       IND=Ø
C  CALCULATION OF THE ROOTS
       PI=3.14159
       BIR=BI/2.
       CALL BITC(BIR)
```

```
      DO 999 I=1,5
999   D(I)=DVAL(I)
C  PHYSICAL PARAMETERS
      TE=373.00
      PW=1.0
      PSW=PW/PS
      T0=283.00
      RLAT=570.0
      RLAT=RLAT + (TE-T0)*(1.0+(CP/C0))
      P=RLAT*C0/CP
      KS=CP*PS*ALPA*4.18
      XV=(C0/PW)/(1./PS+C0/PW)
C     CALCULATION OF BIOT NUMBER
      DI=2.*RP
      REN=DI*U*1.E-3/RNU
      PR=0.73
      NUS=2.+0.6*(PR**(1./3.))*(REN**0.5)
      BI=(KG/KS)*NUS*FRAD
C  OUTPUT
      WRITE(6,2005)
      WRITE(60,2005)
      WRITE(6,2001)
      WRITE(60,2001)
2001  FORMAT(10X,'PHYSICAL PROPERTIES OF THE COAL')
      WRITE(6,2002)CP,ALPA
      WRITE(60,2002)CP,ALPA
2002  FORMAT(2X,'SPECIFIC HEAT =',F5.3,'cal/g degree K', 5X,'THERMAL DIF
     1FUSIVITY = ',F5.3,'mm2/s')
      WRITE(6,2003)PS,RP
      WRITE(60,2003)PS,RP
2003  FORMAT(2X,'DENSITY SOLID=',F5.3,5X,'PARTICLE RADIUS =',F7.4,'mm')
      WRITE(6,2004)C0
      WRITE(60,2004)C0
2004  FORMAT(2X,'INITIAL MOISTURE CONTENT OF THE COAL =',F7.4,'g MOISTU
     1RE/g DRY COAL')
      WRITE(6,2005)
      WRITE(60,2005)
2005  FORMAT(2X,'-------------------------------------------------------
     1-------------------------------------')
      WRITE(6,2006)
      WRITE(60,2006)
2006  FORMAT(5X,'SYSTEM PROPERTIES')
      WRITE(6,2007)BI,TA
      WRITE(60,2007)BI,TA
2007  FORMAT(2X,'HEAT-TRANSFER BIOT NO. =',F10.3,5X,'BED/AMBIENT TEMPER
     1ATURE = ',F10.3,'K')
      WRITE(6,2005)
      WRITE(60,2005)
C
C  CALCULATATION OF DRYING TIME
C
      XFS=XV*FS
      XFS13=(1.-XFS)**(1./3.)
      XFS23=(1.-XFS)**(2./3.)
      IF(BI .LT. 5000) THEN
       TAUS=RP**2.*P/(BI*(TA-TE)*ALPA)
       TAUS=TAUS*(2./XFS*(1.-XFS13)-BI/(2.*XFS)*(1.-XFS23)+BI/2.)
       CALL DRYTIME(XFS,BI,TA,TE,P,ALPA,TAUS,A1,TC,C,RP)
       C1=C
       BVAL=A1
```

```
         DR=C1
         TTR=TC
        ELSE
         BI=5000.
         TAUSL=RP**2.*(P/((TA-TE)*ALPA)*(1./2.-1./(2.XFS)*(1.-XFS23))
         CALL DRYTIME(XFS,BI,TA,TE,P,ALPA,TAUSL,A1,TC,C,RP)
         C1=C
         BVAL=A1
         DR=C1
         TTR=TC
        END IF
         TDRY=TC*TAUS

C  OUTPUT
        WRITE(6,2020)
        WRITE(60,2020)
2020    FORMAT(2X,'CHEMICAL KINETIC PARAMETERS OF THE COAL')
        WRITE(6,2005)
        WRITE(60,2005)
        WRITE(6,2030)E0,SIGMA
        WRITE(60,2030)E0,SIGMA
2030    FORMAT(2X,'MEAN ACTIVATION ENERGY=',E15.5,'kJ/mol',5X,'STANDARD D
      1EVIATION=',E15.5,'kJ/mol')
        WRITE(6,2005)
        WRITE(60,2005)
        WRITE(6,2040)TDRY
        WRITE(60,2040)TDRY
2040    FORMAT(2X,'TOTAL DRYING TIME=',E15.5,'s')
        WRITE(6,2005)
        WRITE(60,2005)
        WRITE(6,2010)
        WRITE(60,2010)
C
C  CALCULATION OF MOISTURE AND VOLATILE CONTENT
C
        DO 10 IN=1,NTM
        TM=TDRY/(FLOAT(NTM))*FLOAT(IN)
        IW=1
        T1=TM
        CALL DRYEQ(T1,IW)
        IF(T1.LT.0.0.OR.T1.GT.1.0)T1=0.0
        RE=RP*T1
        RPS=RP*(1.-XFS*(1.-T1**3.))**(1./3.)
        WRITE(6,3000)RPS,RE
3000    FORMAT(2X,'RPS= ',E15.5,5X,'RE= ',E15.5)
        XL1=RE
        XU3=TM
        CALL CGQA(FUNC1,XL1,XU1,NG1,ANS)
        PHIM=(T1**3.)
2010   ,FORMAT(5X,'TIME(SECS)',10X,'MOISTURE',10X,'VOLATILES')
        ANS=(PHIM) + (3.0*ANS/(RP**3.))
        ADS=1.0-ANS
        FO=ALPA*TM/RP**2.
        WRITE(*,2011)TM,PHIM,ANS
        WRITE(60,2011)TM,PHIM,ANS
2011    FORMAT(2X,F10.4,5X,E15.5,5X,E15.5)
10      CONTINUE
        XL1=0.0
        XU1=RP
         TYPE(*,*)' ENTER TIME INTERVAL NTM1 '
```

```
      READ(*,*)NTM1
C
C  CALCULATION OF VOLATILE CONTENT WHEN DRYING IS COMPLETED
C
      DO 20 J=1,500
      TTM=NTM1*FLOAT(J-1) + TDRY
      XU3=TTM
      CALL CGQA(FUNC4,XL1,XU1,NG1,ANS)
      PHIM=0.0
      ANS=3.0*ANS/(RP**3.)
      ADS=1.0-ANS
      FO=ALPA*TM/RP**2.
      WRITE(*,2011)TTM,PHIM,ANS
      WRITE(60,2011)TTM,PHIM,ANS
20    CONTINUE
33    STOP
      END
C
C
C
C  SUBROUTINES AND FUNCTIONS
C
C
C  THIS SUBROUTINE CALCULATES THE ROOTS
C
      SUBROUTINE BITC(BI)
      DIMENSION DVAL(5)
      COMMON/BIOT/DVAL
      BE=0.001
      N=0
2     FBE=1.0-BI-BE*COS(BE)/SIN(BE)
      IF(ABS(FBE).LT.0.01) GOTO 1
      BE=BE+0.00005
      IF(BE.GT.500.0) GOTO 3
      GOTO 2
1     N=N+1
      IF(N.GE.6) GOTO 3
      DVAL(N)=BE
      BE=BE+2.2
      GOTO 2
3     RETURN
      END
C
C  THIS SUBROUTINE CALCULATES THE DRYING TIME RATIO BETWEEN TRANSIENT
C  AND PSEUDO STEADY STATE MODELS
C
      SUBROUTINE DRYTIME (XFS,BI,TA,TE,P,ALPA,TAUS,A1,TC,C,RP)
      INTEGER N,ITMAX,IER
      REAL WK1(22),PHIS(1),PAR1(3),FNORM1
      EXTERNAL PHISM
      N=1
      ITMAX=100
      NSIG=5
      CONV=0.005
      TC=0.5
1     PAR1(1)=TC
      PAR1(2)=XFS
      PAR1(3)=BI
      PHIS(1)=0.5
C  CALCULATION OF PHIS (PSEUDO STEADY STATE EQUATION) USING ISML
```

```
C  SUBROUTINE ZSCNT
       CALL ZSCNT (PHISM,NSIG,N,ITMAX,PAR1,PHIS,FNORM1,WK1,IER)
C  CALCULATION OF A1 FOR TRIAL AND ERROR
       SPHI=PHIS(1)
       XSS=(1.-XFS*(1.-SPHI**3.))
       XSS13=XSS**(1./3.)
       XSS23=XSS**(2./3.)
       AT=BI*SPHI*(TA-TE)
       AT=AT/(12.*(2.*SPHI-BI*XSS13*(SPHI-XSS13)))*(1.-XFS)
       TS=(TA-TE)*BI*XSS23*(1.-SPHI/(XSS13))
       TS=TS/(2.*SPHI-BI*XSS13*(SPHI-XSS13))+TE
       A1=AT-(TE+5.*TS)/12.*(1.-XFS)**(2./3.))+(P+TE)/2.
       A1=A1-TS*(1.-(1.-XFS)**(2./3.))/2.
C  CALCULATION OF A2 FOR TRIAL AND ERROR
       XFS13=(1.-XFS)**(1./3.)
       XFS23=(1.-XFS)**(2./3.)
       BK=2./XFS*(1.-XFS13)-BI/(2.*XFS)*(1.-XFS23)+BI/2.
       A2=ALPA*TAUS*(TA-TE)*BI/(RP**2.*BK*2.)
       C5=(1.-SPHI**2.)
       A2=A2*C5
       C=SPHI
       IF ((ABS(A1-A2)/A1 .GT. 0.005) GOTO 2
       GOTO 4
2      TC=TC+CONV
       IF (TC .GT. 0.99) GOTO 3
       GOTO 1
3      CONV=CONV/4.
       TC=0.2
       GOTO 1
4      RETURN
       END
C
C  THIS SUBROUTINE CALCULATES THE STEADY STATE DRYING EQUATION
C
       SUBROUTINE PHISM(PHIS,F,N,PAR1)
       REAL PHIS(1),F(1),PAR1(3)
       A1=(1.-PAR1(2))**(1./3.)
       A2=(1.-PAR1(2))**(2./3.)
       A3=(1.-PAR1(2)*(1.-PHIS(1)**3.))**(1./3.)
       A4=(1.-PAR1(2)*(1.-PHIS(1)**3.))**(2./3.)
       F1=(2./(PAR1(2)))*(1.-A3)
       F2=(PAR1(3)/(2.*PAR1(2)))*(1.-A4)
       F3=PAR1(3)/2.*(1.-PHIS(1)**2.)
       FUNC1=F1-F2+F3
       F4=(2./(PAR1(2)))*(1.-A1)
       F5=(PAR1(3)/(2.*(PAR1(2)))*(1.-A2)
       F6=PAR1(3)/2.
       FUNC2=F4-F5+F6
       F(1)=(FUNC1/FUNC2)-PAR1(1)
       RETURN
       END
C
C  THIS SUBROUTINE CALCULATES THE TRANSIENT DRYING FUNCTION
C
       SUBROUTINE PHISTM(PHIT,FCT,N,PAR2)
       REAL PHIT(1),FCT(1),PAR2(7)
       IF (PHIT(1) .LE. 0.0001) PHIT(1)=0.0001
       XFT=(1.-PAR2(7)*(1.-PHIT(1)**3.))
       XFT13=XFT**(1./3.)
       XFT23=XFT**(2./3.)
```

```
      B1=PAR2(1)*(XFT-PHIT(1)*XFT23-PHIT(1)**2.*XFT13+PHIT(1)**3.)
      B2=(PAR2(2)+5.*PAR2(3))/12.*(XFT23-PHIT(1)*XFT13)
      B3=(PAR2(2)+PAR2(3))/4.*(PHIT(1)*XFT13-PHIT(1)**2.)
      B4=(PAR2(4)+PAR2(2))/2.*(1.-PHIT(1)**2.)
      B5=PAR2(3)*(1.-XFT23)/2.
      FCT(1)=B1-B2-B3+B4-B5-PAR2(5)*PAR2(6)
      RETURN
      END
C
C THIS SUBROUTINE CALCULATES THE TRANSIENT DRYING EQUATION
C
      SUBROUTINE DRYEQ(T1,IW)
     COMMON/ABC/ TA,T0,RP,ALPA,E0,SIGMA,PI,XL2,XU2,XL3,XU3,RDUM,EDUM
     COMMON/IKAC/ NG2,NG3,IND,CP,C0,TE,P,PS,BI,TDRY,BVAL,DR,TM,TTR,RE
     COMMON/FGH/ D
     COMMON/GH/ TTM,TAUS,XFS,C1
     COMMON/BIOT/DVAL
      INTEGER N,ITMAX,IER
      REAL WK1(22),PHIS(1),PAR1(3),FNORM1
      REAL WK2(22),PHIT(1),PAR2(7),FNORM2
      EXTERNAL PHISM
      EXTERNAL PHITM
      THETA=TM/TAUS
      PAR1(1)=THETA
      PAR1(2)=XFS
      PAR1(3)=BI
      N=1
      NSIG=5
      ITMAX=100
      PHIS(1)=0.5
      CALL ZSCNT(PHISM,NSIG,N,ITMAX,PAR1,PHIS,FNORM1,WK1,IER)
      SPHI=PHIS(1)
      PHIT(1)=0.5
      XSS=(1.-XFS*(1.-SPHI**3.))
      XSS13=XSS**(1./3.)
      XSS23=XSS**(2./3.)
      AT=BI*SPHI*(TA-TE)
      AT=AT/(12.*(2.*SPHI-BI*XSS13*(SPHI-XSS13)))
      TS=(TA-TE)*BI*XSS23*(1.-SPHI/XSS13)
      TS=TS/(2.*SPHI-BI*XSS13*(SPHI-XSS13))+TE
      PAR2(1)=AT
      PAR2(2)=TE
      PAR2(3)=TS
      PAR2(4)=P
      PAR2(5)=BVAL
      PAR2(6)=(SPHI**2.-1.)/(C1**2.-1.)
      PAR2(7)=XFS
      PHIT(1)=0.5
C  CALCULATION OF PHIT (TRANSIENT MODEL) USING IMSL SUBROUTINE
C  ZSCNT
      CALL ZSCNT(PHITM,NSIG,N,ITMAX,PAR2,PHIT,FNORM2,WK2,IER)
      PN=PHIT(1)
      IF (IW .EQ. 1) GOTO 10
      GOTO 20
10    T1=PHIT(1)
      GOTO 30
20    RPS=RP*(1.-XFS*(1.-PN**3.))**(1./3.)
      RW=RDUM/RPS
      PNS=PN*RP/RPS
      PHI=(RW-PNS)/(1.-PNS)
```

```
      A3=12.*AT*(1.-PNS)*RPS/RP
      T1=TE+(TS-TE)*(2.*PHI-PHI**2.)+A3*(PHI**2.-PHI)
      IF (T1 .LE. TE) T1=T0
30    RETURN
      END
C
C  FUNCTIONS FOR NUMERICAL INTEGRATIONS
C
      FUNCTION FUNC1(R)
      EXTERNAL FUNC2
      COMMON/ABC/ TA,T0,RP,ALPA,E0,SIGMA,PI,XL2,XU2,XL3,XU3,RDUM,EDUM
     COMMON/IKAC/ NG2,NG3,IND,CP,C0,TE,P,PS,BI,TDRY,BVAL,DR,TM,TTR,RE
     COMMON/GH/ TTM,TAUS
      RDUM=R
      CALL CGQB(FUNC2,XL2,XU2,NG2,ANS2)
      FUNC1=ANS2*R*R
      RETURN
      END
C
C
      FUNCTION FUNC2(E)
      EXTERNAL FUNC3
      COMMON/ABC/ TA,T0,RP,ALPA,E0,SIGMA,PI,XL2,XU2,XL3,XU3,RDUM,EDUM
     COMMON/IKAC/ NG2,NG3,IND,CP,C0,TE,P,PS,BI,TDRY,BVAL,DR,TM,TTR,RE
     COMMON/GH/ TTM,TAUS
      EDUM=E
      CALL CGQC(FUNC3,XL3,XU3,NG3,ANS3)
      A=ANS3*1.67E13
      IF(A.GT.60.)GO TO 11
      A=EXP(-A)
      GO TO 12
11    A=0.0
12    FE=EXP((-(E-E0)**2.)/(2.*(SIGMA**2.)))
      FE=FE/(SIGMA*SQRT(2.0*PI))
      FUNC2=FE*A
      RETURN
      END
C
C
      FUNCTION FUNC3(T)
      COMMON/ABC/ TA,T0,RP,ALPA,E0,SIGMA,PI,XL2,XU2,XL3,XU3,RDUM,EDUM
     COMMON/IKAC/ NG2,NG3,IND,CP,C0,TE,P,PS,BI,TDRY,BVAL,DR,TM,TTR,RE
     COMMON/GH/ TTM,TAUS
      IW=0
      TT=T
      CALL WETTEM(TT,IW)
     IF(IND.EQ.1)TT=TA
      RT=8.315E-03
      FUNC3=(EDUM/(RT*TT))
      IF(FUNC3.GT. 60.) GOTO 20
      FUNC3=EXP(-FUNC3)
      GO TO 21
20    FUNC3=0.0
21    RETURN
      END
C*********************************************************************
C********************* SUBROUTINE CGQA ***********************************
C*********************************************************************
C
      SUBROUTINE CGQA(CF,XL,XU,N,CVAL)
```

```
C
C       PERFORMS INTEGRATION OF A FUNCTION OF A SINGLE VARIABLE
C       BY GAUSSIAN QUADRATURE.
C
C       N = ORDER OF GUASSIAN QUADRATURE APPROXIMATION. VALUE MAY BE ON
C           (1,2,4,8,10,12,16,32).  IF N=1, CGQA PERFORMS A ONE-POINT
C           RECTANGULAR RULE INTEGRATION.
C       CF = EXTERNALLY SUPPLIED FUNCTION....MUST BE FUNCTION OF ONE
C            VARIABLE FOR CQG1.
C       XL = LOWER BOUND OF VARIABLE
C       XU = UPPER BOUND OF VARIABLE
C       CVAL = RESULTING VALUE OF THE INTEGRATION
C
C     NOTE:  CF MUST BE LISTED IN AN EXTERNAL STATEMENT IN THE
C              CALLING ROUTINE
C
      DIMENSION Q1(52),Q2(24),Q3(32),NQ(8),NS(8),QG(108)
      EQUIVALENCE (Q1(1),QG(1)),(Q2(1),QG(53)),(Q3(1),QG(77))
      DATA Q1
     $                /.28867513459481288ZE0,0.5E0,.43056815579702629E0,
     $.17392742256872693E0,.16999052179242813E0,.32807257743127307E0,
     $ 0.48014492824876812E0,.50614268145188130E-1,.39833323870681337E0,
     $.11119051722668724E0,.26276620495816449E0,.15685332293894364E0,
     $.91717321247624906-1,.18134189168918099E0,.48695326425858586E0,
     $.33335672154344072-1,.43253168334449225E0,.74725674575290JE-1,
     $.33970478414961226E0,.10954318125799102E0,.21669769706462J6E0,
     $.13463335965499818E0,.74437169490815605E-1,.14776211235737644E0,
     $0.49078031712335963E0,.23587668193255914E-1,.45205862818523743E0,
     $.53469662997659215E-1,.38495133709715234E0,.80039164271673J1E-1,
     $.29365897714330872E0,.10158371336153296E0,.18391574949909010E0,
     $.11674626826917740E0,.62616704255734458E-1,.12457352290670139E0,
     $.49470046749582497E0,.13576229705877047E-1,.47228751133661629E0,
     $.31126761969323946E-1,.43291566119391507E0,.47579255841246392E-1,
     $.37770220417750152E0,.62714485627766936E-1,.30893612220132187E0,
     $.74797994403288J7E-1,.22900838882861369E0,.84572259697501277E-1,
     $.14080177538962946E0,.91301707522486179E-1,.47506254918818720E-1,
     $.94725305227534256-1 /
      DATA Q2
     $                / 0.49759360999851068E+0   ,0.61706148999935976E-2 ,
     *             0.48736427798565475E+0   ,    0.14265943144668J2E-1 ,
     *             0.46913772780013666J8E+0   ,    0.22138719408709903E-1 ,
     *             0.44320776350220052E+0   ,    0.29649292457718890E-1 ,
     *             0.41000099298695146E+0   ,    0.36673240705540153E-1 ,
     *             0.37006209578927718E+0   ,    0.43095080765976638E-1 ,
     *             0.32404682596849778E+0   ,    0.48809326052056944E-1 ,
     *             0.27271073569441977E+0   ,    0.53722135057982817E-1 ,
     *             0.21689675381302257E+0   ,    0.57752834026862801E-1 ,
     *             0.15752133984008169E+0   ,    0.60835236463901696E-1 ,
     *             0.95559433736809150E-1   ,    0.62918728173414148E-1 ,
     *             0.32028446431302813E-1   ,    0.63969097673376078E-1 /
      DATA Q3
     $              /0.49863193092474078E+0 ,    0.35093050047350483E-2 ,
     *             0.49280575577263417E+0   ,    0.81371973654528350E-2 ,
     *             0.48238112779375322E+0   ,    0.12696032654631030E-1 ,
     *             0.46745037796886984E+0   ,    0.17136931456510717E-1 ,
     *             0.44816057788302606E+0   ,    0.21417949011113340E-1 ,
     *             0.42468380686628499E+0   ,    0.25499029631188088E-1 ,
     *             0.39724189798397120E+0   ,    0.29342046739267774E-1 ,
     *             0.36609105937014484E+0   ,    0.32911111388180923E-1 ,
     *             0.33152213346510760E+0   ,    0.36172897054424253E-1 ,
```

```
     *             0.29385787862038116E+0   ,     0.39096947893535153E-1 ,
     *             0.25344995446611470E+0   ,     0.41655962113473378E-1 ,
     *             0.21067563806531767E+0   ,     0.43826046502201906E-1 ,
     *             0.16593430114106382E+0   ,     0.45586939347881942E-1 ,
     *             0.11964368112606854E+0   ,     0.46922199540402283E-1 ,
     *             0.72235980791398250E-1   ,     0.47819360039637430E-1 ,
     *             0.24153832843869158E-1   ,     0.48270044257363900E-1 /
     $,NQ/2,4,8,10,12,16,24,32/,
     $ NS/1,3,7,15,25,37,53,77/
      IF(N .EQ. 1) GO TO 200
      DO 300 L=1,8
      IF(N.EQ.NQ(L)) GO TO 301
  300 CONTINUE
 9001   WRITE(5,905) N
  905 FORMAT('0 CALLING PARAMETER =',I5,'   INTEGRATION NOT POSSIBLE'//)
      RETURN
  200 AX=0.5*(XU+XL)
      CVAL=CF(AX)*(XU-XL)
      RETURN
  301 CONTINUE
      NP=NS(L)
      NE=NP+N-1
      AX=0.5*(XU+XL)
      BX=XU-XL
      CVAL=0.
      DO 350 J=NP,NE,2
      DX=QG(J)*BX
      CVAL=CVAL+QG(J+1)*(CF(AX+DX)+CF(AX-DX))
  350 CONTINUE
      CVAL=CVAL*BX
      RETURN
      END
C*******************************************************************************
C********************* SUBROUTINE CGQB *****************************************
C*******************************************************************************
C
      SUBROUTINE CGQB(CF,XL,XU,N,CVAL)
C
C        PERFORMS INTEGRATION OF A FUNCTION OF A SINGLE VARIABLE
C        BY GAUSSIAN QUADRATURE.
C
C        N = ORDER OF GUASSIAN QUADRATURE APPROXIMATION. VALUE MAY BE ON
C            (1,2,4,8,10,12,16,32).  IF N=1, CGQB PERFORMS A ONE-POINT
C            RECTANGULAR RULE INTEGRATION.
C        CF = EXTERNALLY SUPPLIED FUNCTION....MUST BE FUNCTION OF ONE
C             VARIABLE FOR CGG1.
C        XL = LOWER BOUND OF VARIABLE
C        XU = UPPER BOUND OF VARIABLE
C        CVAL = RESULTING VALUE OF THE INTEGRATION
C
C      NOTE: CF MUST BE LISTED IN AN EXTERNAL STATEMENT IN THE
C                CALLING ROUTINE
C
       DIMENSION Q1(52),Q2(24),Q3(32),NQ(8),NS(8),QG(108)
       EQUIVALENCE (Q1(1),QG(1)),(Q2(1),QG(53)),(Q3(1),QG(77))
       DATA Q1
      $                /.28867513459481288E0,.5E0,.43056815579702629E0,
      $.17392742256872693E0,.16999052179242813E0,.32607257743127307E0,
      $ 0.48014492824876812E0,.50614268145188130E-1,.39833323870681337E0,
      $.11119051722668724E0,.26276620495816449E0,.15685332293894364E0,
```

```
     $.9171732124782490E-1,.1813418916891809 9E0,.4869532642585858 6E0,
     $.3333567215434407E-1,.4325316833449225E0,.747256745752903E-1,
     $.3397047841496122E0,.1095431812579910 2E0,.2166976970646236E0,
     $.1346333596549981 8E0,.7443716949081560 5E-1,.1477621123573764 4E0,
     $0.4907803171233596 3E0,.2358766819325591 4E-1,.4520586281852374 3E0,
     $.5346966299765921 5E-1,.3849513370971523 4E0,.8003916427167311E-1,
     $.2936589771433087 2E0,.1015837133615329 6E0,.1839157494990901 0E0,
     $.1167462682691774 0E0,.6261670425573445 8E-1,.1245735229067013 9E0,
     $.4947004674958249 7E0,.1357622970587704 7E-1,.4722875115366162 9E0,
     $.3112676196932394 6E-1,.4328156011939158 7E0,.4757925584124639 2E-1,
     $.3777022041775015 2E0,.6231448562776693 6E-1,.3089381222013218 7E0,
     $.7479799440828837E-1,.2290083888286136 9E0,.8457825969750127E-1,
     $.1408017753896294 6E0,.9130170752246179E-1,.4750625491881872 0E-1,
     $.9472530522753425E-1 /
      DATA 02
     $                / 0.4975936099985106 8E+0    ,0.6170614899993599 8E-2 ,
     *              0.4873642779856547 5E+0    ,     0.1426569431446683 2E-1 ,
     *              0.4691372760013663 8E+0    ,     0.2213871940870990 3E-1 ,
     *              0.4432077635022005 2E+0    ,     0.2964929245771889 0E-1 ,
     *              0.4100009929869514 6E+0    ,     0.3667324070554015 3E-1 ,
     *              0.3700620957892771 8E+0    ,     0.4309508076597663 8E-1 ,
     *              0.3240468259684877 8E+0    ,     0.4880932605205694 4E-1 ,
     *              0.2727107356944197 7E+0    ,     0.5372213505796281 7E-1 ,
     *              0.2168967538130225 7E+0    ,     0.5775283402686280 1E-1 ,
     *              0.1575213398480816 9E+0    ,     0.6083523646390169 6E-1 ,
     *              0.9555943373680815 0E-1    ,     0.6291872817341414 8E-1 ,
     *              0.3202844643130281 3E-1    ,     0.6396909767337607 8E-1 /
      DATA 03
     $                /0.4986319309247407 8E+0 ,     0.3509305004735048 3E-2 ,
     *              0.4928057557726341 7E+0    ,     0.8137197365452835 0E-2 ,
     *              0.4823811277937532 2E+0    ,     0.1269603265463103 0E-1 ,
     *              0.4674503037968869 4E+0    ,     0.1713693145651071 7E-1 ,
     *              0.4481605778830260 6E+0    ,     0.2141794901111333 0E-1 ,
     *              0.4246838068662849 9E+0    ,     0.2549902963118808 8E-1 ,
     *              0.3972418979839712 0E+0    ,     0.2934204673926777 4E-1 ,
     *              0.3660910593701448 4E+0    ,     0.3291111138818092 3E-1 ,
     *              0.3315221334651076 0E+0    ,     0.3617289705442425 3E-1 ,
     *              0.2938578786203811 6E+0    ,     0.3909694739353515 3E-1 ,
     *              0.2534499544661147 0E+0    ,     0.4165596211347337 8E-1 ,
     *              0.2106756380653176 7E+0    ,     0.4382604650220190 6E-1 ,
     *              0.1659343011410638 2E+0    ,     0.4558693934788194 2E-1 ,
     *              0.1196436811260685 4E+0    ,     0.4692219954040228 3E-1 ,
     *              0.7223598079139825 0E-1    ,     0.4781936003963743 0E-1 ,
     *              0.2415383294386915 8E-1    ,     0.4827004425736390 0E-1 /
     $,NQ/2,4,8,10,12,16,24,32/,
     $ NS/1,3,7,15,25,37,53,77/
       IF(N .EQ. 1) GO TO 200
       DO 300 L=1,8
       IF(N.EQ.NQ(L)) GO TO 301
  300  CONTINUE
 9002   WRITE(5,905) N
   905 FORMAT('0 CALLING PARAMETER =',I5,'    INTEGRATION NOT POSSIBLE'//)
       RETURN
   200 AX=0.5*(XU+XL)
       CVAL=CF(AX)*(XU-XL)
       RETURN
  301  CONTINUE
       NP=NS(L)
       NE=NP+N-1
       AX=0.5*(XU+XL)
```

```
      BX=XU-XL
      CVAL=0.
      DO 350 J=NP,NE,2
      DX=QG(J)*BX
      CVAL=CVAL+QG(J+1)*(CF(AX+DX)+CF(AX-DX))
  350 CONTINUE
      CVAL=CVAL*BX
      RETURN
      END
C*******************************************************************************
C********************* SUBROUTINE CGQC *****************************************
C*******************************************************************************
C
      SUBROUTINE CGQC(CF,XL,XU,N,CVAL)
C
C        PERFORMS INTEGRATION OF A FUNCTION OF A SINGLE VARIABLE
C        BY GAUSSIAN QUADRATURE.
C
C        N = ORDER OF GUASSIAN QUADRATURE APPROXIMATION. VALUE MAY BE ON
C            (1,2,4,8,10,12,16,32).  IF N=1, CGQC PERFORMS A ONE-POINT
C            RECTANGULAR RULE INTEGRATION.
C        CF = EXTERNALLY SUPPLIED FUNCTION...MUST BE FUNCTION OF ONE
C             VARIABLE FOR CQG1.
C        XL = LOWER BOUND OF VARIABLE
C        XU = UPPER BOUND OF VARIABLE
C        CVAL = RESULTING VALUE OF THE INTEGRATION
C
C       NOTE:  CF MUST BE LISTED IN AN EXTERNAL STATEMENT IN THE
C                CALLING ROUTINE
C
      DIMENSION Q1(52),Q2(24),Q3(32),NQ(8),NE(8),QG(108)
      EQUIVALENCE (Q1(1),QG(1)),(Q2(1),QG(53)),(Q3(1),QG(77))
      DATA Q1
     $                 /.7811[illegible]2E0,.5E0,.4305681557970262 9E0,
     $.1774274302937693E0,.1699905217924281 3E0,.3260725774312730 7E0,
     $.4328353169294748 2E0,.5061426614518813 0E-1,.3983332387068133 7E0,
     $.1117505172266873 4E0,.2627662049581644 9E0,.1560533229389436 4E0,
     $.9171732124782490 E-1,.1813418916891809 9E0,.4869532642505858 6E0,
     $.3033567215434407 E-1,.4325316633444922 5E0,.7472567457529033 E-1,
     $.3397047641496122 E0,.1095431812579910 2E0,.2166976970646236 E0,
     $.1346333596549981 8E0,.7443716949081560 5E-1,.1477621123573764 4E0,
     $0.4907803171233596 3E0,.2358766819325591 4E-1,.4520598231852374 3E0,
     $.5346966299765921 5E-1,.3849513370971523 4E0,.3003916427167311 E-1,
     $.2936589771433087 2E0,.1015837133615329 6E0,.1839157494990901 0E0,
     $.1167462682691774 0E0,.6716170425573445 8E-1,.1245735229067013 9E0,
     $.4947004674958249 7E0,.1357622970587704 7E-1,.4722875115366162 9E0,
     $.3112676196932394 6E-1,.4320156011939158 7E0,.4757925584124639 2E-1,
     $.3777022041775015 2E0,.6231448562776693 6E-1,.3089381222013218 7E0,
     $.7479799440828837 E-1,.2290083888286136 9E0,.8457825969750127 E-1,
     $.1403017753996294 6E0,.9130170752246179 E-1,.4750625491881872 0E-1,
     $.9472530522753425 E-1 /
      DATA Q2
     $                / 0.4975936099985106 8E+0    ,0.6170614899993599 8E-2 ,
     *              0.4873642779856547 5E+0    ,    0.1426569431446683 2E-1 ,
     *              0.4691372760013663 8E+0    ,    0.2213871940870990 3E-1 ,
     *              0.4432077635022005 2E+0    ,    0.2964929245771889 0E-1 ,
     *              0.4100009929869514 6E+0    ,    0.3667324070554015 3E-1 ,
     *              0.3700620957892771 8E+0    ,    0.4309508076597663 8E-1 ,
     *              0.3240468259684877 8E+0    ,    0.4880932605205694 4E-1 ,
     *              0.2727107356944197 7E+0    ,    0.5372213505798281 7E-1 ,
```

```
     *             0.21689675381302257E+0   ,     0.57752834026862801E-1 ,
     *             0.15752133984808169E+0   ,     0.60835236463901696E-1 ,
     *             0.95559433736808150E-1   ,     0.62918728173414148E-1 ,
     *             0.32028446431302813E-1   ,     0.63969097673376078E-1 /
      DATA Q3
     $               /0.49863193092474078E+0 ,    0.35093050047350483E-2 ,
     *             0.49280575577263417E+0   ,     0.81371973654528350E-2 ,
     *             0.48238112779375322E+0   ,     0.12696032654631030E-1 ,
     *             0.46745303796886984E+0   ,     0.17136931456510717E-1 ,
     *             0.44816057788302606E+0   ,     0.21417949011113340E-1 ,
     *             0.42468380686628499E+0   ,     0.25499029631188088E-1 ,
     *             0.39724189798397120E+0   ,     0.29342046739267774E-1 ,
     *             0.36609105937014484E+0   ,     0.32911111388180923E-1 ,
     *             0.33152213346510760E+0   ,     0.36172897054424253E-1 ,
     *             0.29385787862038116E+0   ,     0.39096947893535153E-1 ,
     *             0.25344995446611470E+0   ,     0.41655962113473378E-1 ,
     *             0.21067563806531767E+0   ,     0.43826046502201906E-1 ,
     *             0.16593430114106382E+0   ,     0.45586939347881942E-1 ,
     *             0.11964368112606854E+0   ,     0.46922199540402283E-1 ,
     *             0.72235980791398250E-1   ,     0.47819360039637430E-1 ,
     *             0.24153832843869158E-1   ,     0.48270044257363900E-1 /
     $,NQ/2,4,8,10,12,16,24,32/,
     $ NS/1,3,7,15,25,37,53,77/
      IF(N .EQ. 1) GO TO 200
      DO 300 L=1,8
      IF(N.EQ.NQ(L)) GO TO 301
  300 CONTINUE
 9003  WRITE(5,905) N
  905 FORMAT('0 CALLING PARAMETER =',I5,'   INTEGRATION NOT POSSIBLE'//)
      RETURN
  200 AX=0.5*(XU+XL)
      CVAL=CF(AX)*(XU-XL)
      RETURN
  301 CONTINUE
      NP=NS(L)
      NE=NP+N-1
      AX=0.5*(XU+XL)
      BX=XU-XL
      CVAL=0.
      DO 350 J=NP,NE,2
      DX=QG(J)*BX
      CVAL=CVAL+QG(J+1)*(CF(AX+DX)+CF(AX-DX))
  350 CONTINUE
      CVAL=CVAL*BX
      RETURN
      END
C
C
C
C  NUMERICAL INTEGRATIONS
       FUNCTION FUNC4(R)
       EXTERNAL FUNC5
       COMMON/ABC/ TA,T0,RP,ALPA,E0,SIGMA,PI,XL2,XU2,XL3,XU3,RDUM,EDUM
      COMMON/IKAC/ NG2,NG3,IND,CP,C0,TE,P,PS,BI,TDRY,BVAL,DR,TM,TTR,RE
      COMMON/GH/ TTM,TAUS
       RDUM=R
       CALL CGQB(FUNC5,XL2,XU2,NG2,ANS2)
       FUNC4=ANS2*R*R
       RETURN
       END
```

```
C
C
      FUNCTION FUNC5(E)
      EXTERNAL FUNC6
      COMMON/ABC/ TA,T0,RP,ALPA,E0,SIGMA,PI,XL2,XU2,XL3,XU3,RDUM,EDUM
      COMMON/IKAC/ NG2,NG3,IND,CP,C0,TE,P,PS,BI,TDRY,BVAL,DR,TM,TTR,RE
      COMMON/FGH/ D
      COMMON/GH/ TTM,TAUS,XFS,C1
      COMMON/BIOT/DVAL
      EDUM=E
      CALL CGQC(FUNC6,XL3,XU3,NG3,ANS3)
      A=ANS3*1.67E13
      IF(A.GT.60.) GOTO 11
      A=EXP(-A)
      GO TO 12
11    A=0.0
12    FE=EXP((-(E-E0)**2.)/(2.*(SIGMA**2.)))
      FE=FE/(SIGMA*SQRT(2.0*PI))
      FUNC5=FE*A
      RETURN
      END
C
C
      FUNCTION FUNC6(T)
      DIMENSION D(5)
      COMMON/ABC/ TA,T0,RP,ALPA,E0,SIGMA,PI,XL2,XU2,XL3,XU3,RDUM,EDUM
      COMMON/IKAC/ NG2,NG3,IND,CP,C0,TE,P,PS,BI,TDRY,BVAL,DR,TM,TTR,RE
      COMMON/FGH/ D
      COMMON/GH/ TTM,TAUS,XFS,C1
      COMMON/BIOT/DVAL
        REAL WK1(22),PHIS(1),PAR1(3),FNORM1
        REAL WK2(22),PHIT(1),PAR2(7),FNORM2
        IF (T .GE. TDRY) GOTO 30
        IW=0
        TT=T
        CALL DRYEQ(TT,IW)
        GOTO 40
30    SPHI=C1
      XSS=(1.-XFS*(1.-SPHI**3.))
      XSS13=XSS**(1./3.)
      XSS23=XSS**(2./3.)
      C2=(TA-TE)*BI*XSS23*(1.-SPHI)
      C2=C2/(2.*SPHI-BI*XSS13*(SPHI-XSS13))
      C3=BI*XSS23*SPHI*(TA-TE)
      C3=C3/(2.*SPHI-BI*XSS13*(SPHI-XSS13))
      RP=(1.-XFS)**(1./3.)
      SUM=0.0
       SUM1=0.0
      DO 10 I=1,5
      Y=D(I)
       C4=SIN(Y)
       C5=COS(Y)
       C6=(TA-TE)*(C4-Y*C5)
       C6=C6-(2.0*C2-C3)*(C5*((2.0/Y)-Y)+2.0*C4-(2.0/Y))
       C6=C6-(C3-C2)*(C5*((6.0/Y)-Y)+3.0*C4*(1.0-(2.0/(Y*Y))))
       C6=2.0*C6/(Y-C4*C5)
       TER=Y*Y*ALPA*(T-TDRY)/(RP*RP)
       IF(TER.GT.60.0)GOTO 1
       TER=EXP(-TER)
       GO TO 2
```

```
1          TER=Ø.Ø
2         TES=TER*(SIN(Y))/Y
          SUM1=SUM1+C6*TES
          TS=TA-SUM1
          TER=TER*(SIN(Y*RDUM/RP))/(Y*RDUM/RP)
          SUM=SUM+C6*TER
1Ø        CONTINUE
          TT=TA-SUM
C         WRITE(*,1999)TT,RDUM
C         WRITE(6Ø,1999)TT,RDUM
1999      FORMAT(2X,F1Ø.4,2X,F1Ø.4)
4Ø       IF(IND.EQ.1)TT=TA
         RT=8.315E-Ø3
         FUNC6=(EDUM/(RT*TT))
         IF(FUNC6.GT.6Ø.) GOTO 2Ø
         FUNC6=EXP(-FUNC6)
         GO TO 21
2Ø       FUNC6=Ø.Ø
21       RETURN
          END
```